Universidade do Minho
Escola de Engenharia

Filomena Cristina Pinto e Costa

Bioremoval and biodegradation of organic solvents in aqueous solutions

June 2016

Universidade do Minho
Escola de Engenharia

Filomena Cristina Pinto e Costa

Bioremoval and biodegradation of organic solvents in aqueous solutions

Thesis submitted in fulfilment of the requirements for the degree of Ph.D. in Chemical and Biological Engineering

Work developed under supervision of:

Doctor Maria Teresa de Jesus Simões Campos Tavares

June 2016

DECLARATION

I hereby declare having conducted my thesis with integrity. I confirm that I have not used plagiarism or any form of falsification of results in the process of the thesis elaboration.

I further declare that I have fully acknowledged the Code of Ethical Conduct of the University of Minho.

University of Minho, Juner 30rd 2016

Full name: Filomena Cristina Pinto e Costa

Signature: _____

Aos Chicos,

Minha fonte de inspiração e motivação.

AGRADECIMENTOS / ACKNOWLEDGEMENTS

Obrigado a todos aqueles que me acompanharam e ajudaram ao longo desta jornada!

The research work presented was financially supported by the Portuguese Foundation for Science and Technology (FCT) under the scope of the strategic funding of UID/BIO/04469/2013 unit and COMPETE 2020 (POCI-01-0145-FEDER-006684) through the research grant SFRH/BD/77666/2011.

ABSTRACT

The interest in environmental technologies has been increasing during the past few decades, due to the continuous and growing degradation of this crucial and indispensable natural resource. With this in mind, and because the detection of organic compounds in water has increased, the study and development of ecological, low-cost alternative technologies of easy operation and maintenance able to remove volatile organic compounds from complex water bodies is the main objective of the research work described in this thesis.

The ability of two contaminating fungi from a bioreactor containing diethylketone and *Streptococcus equisimilis*, posteriorly identified as belonging to the genera *Penicillium*, and *Alternaria*, to degrade diethylketone solutions (0.5 g/L to 4 g/L) was described in Chapter 2. Both fungi proved to be capable of biodegrading high concentrations of diethylketone, reaching biodegradation percentages higher than 95 %. Although both fungi present similar performances, *Penicillium* sp. is capable of degrading diethylketone faster than *Alternaria* sp.

In Chapter 3 the ability of two fungi (*Penicillium* sp., *Alternaria* sp.) and a gram-positive bacteria (*Streptococcus equisimilis*) to decontaminating tertiary solutions composed of diethylketone (4 g/L), nickel (1 mg/L to 20 mg/L) and cadmium (1 mg/L to 20 mg/L) was assessed. Previous studies stablished the toxicity of each metal (5 mg/L to 100 mg/L) towards each microorganism was conducted. It was possible to observe on those experiments that the growth of both fungi is positively stimulated by nickel and adversely affected by cadmium, when present in initial concentrations higher than 40 mg/L. The growth of the bacterium *S. equisimilis* is inhibited by the presence of both metals when in concentrations above 5 mg/L. Despite this behavior, the bacterium *S. equisimilis* presents the best results in terms of removal and uptake, thus justifying its selection for subsequent experiments.

The ability of a biofilm of *S. equisimilis* supported on different masses of clay (vermiculite, bentonite, kaolinite, or sepiolite) to remove diethylketone from aqueous solutions, as well as the interactions between the microbial culture and the clays were evaluated in Chapter 4. The results showed that all the systems tested show similar performances in terms of removal efficiency (> 98%) and in terms of uptake (1.67 mg/g to 0.11 mg/g), differing only in the minimum time required to reach similar removal percentages. The system using *S. equisimilis* supported on vermiculite proved to be the most efficient. During these experiments the formation of several metabolites was detected and they disappeared at the end of the tests, proving not only the ability of the system to remove diethylketone from aqueous solutions but also the metabolites formed during the biodegradation process. This ability is an advantage since it is known that the degradation of certain chemical compounds may lead to the formation of intermediate compounds (metabolites) more toxic than the parent compound and more difficult to biodegrade.

After selecting the microorganism and the clay that present the best performance, several set of different experiments were described in Chapter 5. Different masses of vermiculite were exposed to singular and binary solutions composed by diethylketone, diethylketone and nickel and diethylketone and cadmium. These experiments indicated that when vermiculite is used as the only sorbent it is capable of efficiently sorb those two metals. However, when exposed to binary solutions composed by nickel and diethylketone, the sorption of these two pollutants increases revealing a synergistic interaction between the two of them, as opposite to what happens when vermiculite is exposed to binary solutions

composed by diethylketone and cadmium. In a second stage, a *S. equisimilis* biofilm supported in different masses of vermiculite was exposed to binary solutions of diethylketone and nickel and diethylketone and cadmium. The use of biofilm supported into vermiculite has proven, as expected, to be an advantage, since it increased the removal efficiency for both pollutants. Such behavior can be explained by the occurrence of two distinct processes: one dependent on cellular metabolism, responsible for the pollutants biodegradation and intracellular accumulation, and the other independent on cellular metabolism and responsible for the sorption processes accomplished either by the microbial surface or by the clay surface.

In Chapter 6, the effect of the pH on the sorption capacity of vermiculite when exposed to aqueous solutions containing nickel and cadmium was determined. These experiments showed that the sorption of both metals increases with increasing mass of vermiculite and with increasing initial pH. The maximum sorption values, 86.5 % for cadmium and 86.1 % for nickel were obtained for assays conducted with an initial pH of 8 and 4 g of vermiculite. These results, associated with the optimum pH for *S. equisimilis* growth (pH of 7.4) established a range of optimum pH (6 to 8) for the biodegradation and/or sorption of diethylketone, nickel and cadmium through the combined use of *S. equisimilis* and vermiculite. In this chapter, the system developed at laboratory scale and used in batch mode was applied at pilot scale and in close loop and aimed to treat big volumes of diethylketone and metal (nickel or cadmium) solutions. The results demonstrated not only the excellent ability of this joint system to biodegrade the diethylketone while sorbing metals, but also that the removal of both pollutants is continuous and tends to increase along time, even after successive replacements of the initial solution by new solutions with identical composition.

In Chapter 7 the capacity of the joint system, *S. equisimilis* –vermiculite, studied in Chapter 6 at pilot-scale, to treat solutions composed by diethylketone, aluminium, nickel, cadmium and manganese was studied. The results obtained corroborate once again the ability of this joint system to completely biodegrade high concentrations of diethylketone in the presence of high concentrations of metals and reveal that, with the exception of aluminium, the sorption of the remaining metals increases over time, even after replacing the initial solution by new solutions with identical composition.

The main conclusions concerning the results achieved in this thesis are described in Chapter 8. Briefly, the systems applied either at laboratory and pilot-scale have proven to be able not only to efficiently remove diethylketone from singular and complex aqueous solutions, but also to sorb nickel, cadmium and manganese. In Chapter 8 is also presented some future perspectives concerning the biodegradation or organic compounds.

SUMÁRIO

Nas últimas décadas, a tecnologia ambiental aplicada aos sistemas aquáticos, tem sido alvo de crescente interesse, dada a contínua e crescente degradação deste muito importante e indispensável recurso natural. Neste sentido, o trabalho desenvolvido ao longo desta tese de doutoramento apresenta uma abordagem alternativa, ecológica, de custo reduzido e de fácil operação e manutenção que permite o tratamento simultâneo de águas contaminadas com dietilcetona e metais, através da ação combinada de microrganismos e argilas.

No Capítulo 2 foi estudada a capacidade de dois fungos contaminantes e identificados como pertencentes ao género *Penicillium* e *Alternaria*, em degradar soluções de dietilcetona (0.5 g/L a 4 g/L). Ambos os fungos demonstraram ser capazes de degradar elevadas concentrações de dietilcetona, apresentando percentagens de biodegradação superiores a 95 %. O fungo *Penicillium* sp. é capaz de degradar a dietilcetona de forma mais rápida, tornando mais vantajosa e atrativa a sua utilização, em detrimento da utilização de outras culturas microbianas, que apesar de apresentaram capacidades de degradação similares, apresentam um tempo necessário superior. No Capítulo 3 comparou-se a capacidade de dois fungos (*Penicillium* sp. e *Alternaria* sp.) e duma bactéria gram-positiva (*Streptococcus equisimilis*) em descontaminar soluções compostas por dietilcetona (4 g/L), níquel (1 mg/L a 20 mg/L) e cádmio (1 mg/L a 20 mg/L). Nesse sentido foram previamente realizados ensaios de toxicidade com os três microrganismos relativamente a cada metal, cuja concentração inicial variou entre 5 mg/L e 100 mg/L. Foi possível concluir que o crescimento de ambos os fungos é positivamente estimulado pela presença de níquel e negativamente afetado pela presença de cádmio, quando em concentrações iniciais superiores a 40 mg/L, enquanto que o crescimento da bactéria *S. equisimilis* é inibido pela presença de ambos os metais quando em concentrações superiores a 5 mg/L. Apesar deste comportamento, a bactéria *S. equisimilis* apresenta os melhores resultados em termos de remoção e uptake, justificando assim a sua seleção para os ensaios posteriores.

No Capítulo 4, é descrita a capacidade de um sistema composto por uma cultura de *S. equisimilis* suportada em diferentes massas de argila (vermiculite, bentonite, caulino ou sepiolita) em descontaminar soluções de dietilcetona, bem como as interações entre a cultura microbiana e as argilas. Os resultados obtidos revelaram que todas as combinações de sistemas utilizadas apresentam performances semelhantes, quer em termos de remoção (> 98 %) quer em termos de uptake (1.67 mg/g a 0.11 mg/g), diferindo apenas no tempo mínimo necessário para alcançar as mesmas percentagens de remoção. O sistema composto por um biofilme de *S. equisimilis* suportado em vermiculite revelou-se mais eficiente. No decurso destes ensaios verificou-se a formação de vários metabolitos que desapareceram no final dos mesmos, demonstrando não só a capacidade do sistema em remover elevadas concentrações de dietilcetona, mas também os seus metabolitos. Esta capacidade constitui uma vantagem, uma vez que a degradação de certos compostos químicos pode levar à formação de compostos intermediários (metabolitos) com propriedades tóxicas e de difícil degradação.

No Capitulo 5, após a seleção do microrganismo e da argila que apresentam melhores resultados, foram realizados diversos ensaios com diferentes massas de vermiculite expostas a soluções singulares e binárias, compostas por dietilcetona, dietilcetona e níquel ou dietilcetona e cádmio. Estes ensaios permitiram inferir que, quando a vermiculite é

utilizada como único sorbente é capaz de reter de forma eficiente aqueles dois metais. Quando exposta a soluções binárias compostas por dietilcetona e níquel a sorção destes dois poluentes aumenta de forma significava, revelando uma interação sinérgica entre os dois sorbatos, ao contrário do que acontece quando a vermiculite é exposta a soluções de dietilcetona e cádmio. Numa segunda fase, foram realizados ensaios nos quais um biofilme *de S. equisimilis* suportado em diferentes massas de vermiculite foi exposto a soluções binários de dietilcetona e níquel e de dietilcetona e cádmio. A utilização do biofilme associado à argila, constitui como esperado uma mais-valia, uma vez que aumentou a eficiência do processo de descontaminação das soluções a tratar. Tal comportamento pode ser explicado pela ocorrência de dois processos distintos, um dependente do metabolismo celular e responsável pelo processo de biodegradação e acumulação intracelular dos poluentes e outro independente do metabolismo celular, responsável pelos processos de sorção realizados quer pela cultura microbiana quer pela argila.

No Capítulo 6, foi estudado o efeito do pH na capacidade de sorção da vermiculite relativamente a soluções aquosas contendo níquel e cádmio. Estes ensaios permitiram concluir que a sorção de ambos os metais aumenta com o aumento da massa de vermiculite utilizada e com o aumento do pH inicial. Os valores máximos de sorção, 86.5 % para o cádmio e 86.1 % para o níquel, foram obtidos para os ensaios realizados com um pH inicial de 8 e com 4 g de vermiculite. Estes resultados, associados ao valor de pH ótimo para o crescimento da bactéria *S. equisimilis* (7.4) permitiram estabelecer uma gama de pH ótima (6 a 8) para a realização de processos de biodegradação e sorção de dietilcetona, níquel e cádmio recorrendo à utilização combinada de *S. equisimilis* e vermiculite. Neste capítulo, o sistema desenvolvido à escala laboratorial e utilizado em modo *batch* foi testado à escala-piloto e em circuito fechado visando assim a descontaminação de volumes elevados de soluções binárias de dietilcetona e metal (níquel ou cádmio). Os resultados obtidos nestes ensaios demonstraram não só a excelente capacidade deste sistema conjunto em biodegradar a dietilcetona ao mesmo tempo que retém os metais, mas também que a remoção dos poluentes é contínua e crescente ao longo do tempo e após sucessivas reposições da solução contaminante por novas soluções. No Capítulo 7 foi avaliada a capacidade do sistema conjunto *S. equisimilis*-vermiculita à escala-piloto definido no Capítulo 6, em degradar de forma contínua e eficiente soluções de dietilcetona, alumínio, níquel, cádmio e manganês. Estes ensaios têm como objetivo estudar o comportamento do biofilme *S. equisimilis* quando exposto a soluções de maior complexidade, como serão os efluentes reais. Estes resultados comprovaram a capacidade do sistema conjunto *S. equisimilis*-vermiculite em biodegradar totalmente, concentrações relevantes de dietilcetona na presença de concentrações elevadas de diferentes metais (alumínio, níquel, cádmio e manganês). Foi também demonstrado que, com exceção do alumínio a sorção dos metais aumentou ao longo do tempo e após substituição da solução inicial por novas soluções de igual composição.

As principais conclusões obtidas a partir dos ensaios desenvolvidos no âmbito desta tese de doutoramento encontram-se descritas no Capítulo 8. De forma sucinta, os sistemas desenvolvidos, quer à escala laboratorial quer à escala-piloto, demonstraram ser capazes não só de remover de forma eficaz e eficiente, concentrações elevadas de dietilcetona a partir de soluções aquosas simples ou complexas, mas também de reter de forma contínua e crescente níquel, cádmio e manganês. Neste capítulo são apresentadas algumas perspetivas futuras relativamente à biodegradação de compostos orgânicos.

RESEARCH MOTIVATION, SCOPE AND AIMS

The contamination of water and soils with hazardous substances has attracted growing attention, all over the world in the past few years. The discharge of effluents with organic solvents and metals from different industrial processes into wastewater systems or directly into the environment may cause and/or enhance the development of severe health disorders, especially due to their carcinogenic, mutagenic and toxic properties, their capacity to produce hazardous intermediates, persist in the environment and to be bio-accumulated via food chain.

In the past years, biological processes, such as biodegradation and biosorption have gained importance, not only due to the economic advantages they present, but also due to their high efficiency, low maintenance requirements, eco-friendly character and absence of solid wastes and greenhouse emissions (nitrous oxides). These advantages are more significant for small industrial units, since they operate on tight budgets, far from centers of technological innovation where the processes of reducing emissions are developed.

Several microorganism such as bacteria and fungi, have been found not only to be able to efficiently treat contaminated water with organic solvents and metals but also to be selective for specific compounds and metals of interest. In the treatment of aqueous solutions contaminated with organic compounds or heavy metals, microorganisms have been used either in suspension, due to the ability to degrade, fix and/or entrap pollutants from aquatic environment, a direct consequence of the presence of numerous chemical on the biomass surface, or supported on low-cost sorbents, such as mineral clays that are known to have a large specific surface area, excellent physical and chemical stability and high cation exchange capacity.

Although organic compounds and metals appear together in wastewater from different industries (metal refining, paint manufacturing, etc.) there are very few published works concerning the treatment of water contaminated simultaneous with this kind of chemicals. With this in mind, the development of techniques able to simultaneously remove different contaminants from large volumes of effluents becomes urgent.

The present thesis aims therefore to explore and assess the development of a robust, economically viable and environmental friendly system, able to degrade volatile organic compounds with high efficiency rates in the presence or absence of other pollutants such as metals. In this work a joint

clay-microorganism system, that combines the biodegradation and biosorption properties of microorganisms, with the sorbing capacity of clays, is proposed to treat singular, binary and multi-component solutions, specifically solutions containing high concentrations of diethylketone, aluminium, nickel, cadmium and manganese.

In order to expose the development of the research work, and the achievements within the mentioned objectives, the thesis is based on the author's original articles, as shown in the following subsection.

THESIS OUTLINE

The present thesis is structured in eight chapters, in order to provide a comprehensive report of the progress achieved during the PhD work. Chapter 1 and chapter 8 correspond respectively, to the general introduction and to the main conclusions. The main body of the text (Chapter 2 to Chapter 7) is based on 6 scientific papers, two of which are already published by an international refereed journal, while the others are under review.

In Chapter 1 a general introduction and state-of-the-art revision mainly centered on the biodegradation processes of volatile organic compounds, eventually with simultaneous biosorption of metals, by microorganisms supported on clays is presented.

During the biodegradation assays conducted with *Streptococcus equisimilis* and diethylketone, successive fungal contamination were detected. The fungi were isolated, characterized at molecular level and subsequently identified. Pure cultures of each fungi were exposed to diethylketone solutions and their ability to degrade this compound was discussed in Chapter 2.

Since wastewater is composed by several kinds of pollutants the ability of the bacterium *S. equisimilis* and of the two fungi identified in Chapter 2, as belonging to the *Alternaria* and *Penicillium* genera, to biodegrade diethylketone in the presence of nickel and cadmium is assessed in Chapter 3 The biosorption capacity of these three microorganisms towards nickel and cadmium, as well as the effect of the initial concentration of nickel and cadmium on the microorganism's growth are also explored, allowing to select the best performing microorganism.

Chapter 4 focuses mainly on a *Streptococcus equisimilis* culture, supported by four different clays to decontaminate aqueous solutions containing diethylketone. The interaction between the *Streptococcus equisimilis* and the clays employed on the removal of diethylketone is presented and the combined system with the best performance is selected for the following experiments.

In Chapter 5, the capacity of a *Streptococcus equisimilis* biofilm supported on vermiculite to decontaminate aqueous solutions containing diethylketone, nickel and/or cadmium, as well as the interaction between the sorbent matrices and the different sorbates, individually and in binary combinations is explored. A possible mechanism for diethylketone biodegradation by *Streptococcus equisimilis* is also forwarded.

The effect of pH on the sorption capacity of vermiculite towards nickel and cadmium in batch systems is also evaluated in Chapter 6. The capacity of a pilot-scale bioreactor filled with a *Streptococcus equisimilis* biofilm supported on vermiculite, to treat large volumes of aqueous solutions containing relevant concentrations of diethylketone, nickel and/or cadmium is also explored.

The ability of a *Streptococcus equisimilis* biofilm supported on vermiculite to biodegrade diethylketone, in the presence of different metals (Al^{3+}, Cd^{2+}, Ni^{2+} and Mn^{2+}), at lab and pilot scale is explored in Chapter 7 in order to simulate the behavior of *S. equisimilis* when exposed to complex solutions, such as wastewater.

Finally, Chapter 8 presents the main conclusions of the present thesis and proposes suggestions for future work.

This PhD thesis was carried out at the Centre of Biological Engineering, at the Department of Biological Engineering of the University of Minho. The FTIR analysis were performed at the Centre of Chemistry at the Department of Chemistry of the University of Minho. The SEM and XRD analysis were performed at the Earth Science Department of the University of Minho.

SCIENTIFIC OUTPUT

The overall work developed during this PhD thesis originated the following publications, as well as the participation in several scientific meetings.

BOOK AND CHAPTERS

Costa F., Silva B., Tavares T. Bioprocesses, Bioreactors and Controls *In:* Pandey A. (Eds.) Current Developments in Biotechnology & Bioengineering. Elsevier, *in print*.

Costa F., Silva B., Tavares T. Suitability of nickel resistant microbes for the use in enhanced nickel bioremediation *In:* Das S., Dash H. R. (Eds.) Metal-Microbe interactions and bioremediation: Principle and applications for toxic metals. Taylor & Francis (CRC Press), *in print.*

Silva B., Costa F., Neves I. C., Tavares T. 2015. Psychiatric Pharmaceuticals as Emerging Contaminants in Wastewater. Springer International Publishing (ISBN: 978-3-319-20492-5).

Costa F., Silva B., Tavares T. 2015. The effect of a joint clay-microorganism system to treat Ni and diethylketone solutions *In:* Vilarinho C., Castro F., Russo M. (Eds.) WASTES: solutions, treatments and opportunities, London: Taylor & Francis Group, pp. 61-66 (ISBN: 978-1-138-02882-1).

PAPERS IN INTERNATIONAL SCIENTIFIC PERIODICALS WITH REFEREES

Quintelas C., Costa F., Tavares T. 2013. Bioremoval of diethylketone by the synergistic combination of microorganisms and clays: uptake, removal and kinetic studies. Environmental Science and Pollution Research 20 (3), 1374-1383.

Costa F., Neto M., Nicolau A., Tavares T. 2015. Biodegradation of diethylketone by *Penicillium* sp. and *Alternaria* sp. – A comparative study. Current Biochemical Engineering 2 (1), 81-89.

Ferronato C., Silva B., Costa F., Tavares T. 2016. Vermiculite bio-barriers for Cu and Zn remediation: an eco-friendly approach for freshwater and sediments protection. International Journal of Environmental Science and Technology 13 (5), 1219-1228

PAPERS IN CONFERENCE PROCEEDINGS

Costa F., Quintelas C., Tavares T. Biodegradation of diethylketone by *S. equisimilis*. Conference Abstracts Book of the 7th International Conference on Environmental Engineering and Management - ICEEM 2013, 18-23 September 2013, Vienna, Austria. 257-258 (ISBN: 978-973-621-418-9).

Costa F., Silva B., Tavares T. Study of Ni (II) and diethylketone removal from aqueous solutions using a biofilm of *Streptococcus equisimilis* supported on vermiculite. Book of Extended Abstracts of the 12nd International Chemical and Biological Engineering Conference – CHEMPOR 2014, 10-12 September 2014, Porto, Portugal (ISBN: 978-972-752-170-8).

Ferronato C., Silva B., Costa F., Antisari L. V., Tavares T. Biorecovery of heavy metals using vermiculite for sediment and water protection. Book of Extended Abstracts of the 12nd International Chemical and Biological Engineering Conference – CHEMPOR 2014, 10-12 September 2014, Porto, Portugal (ISBN: 978-972-752-170-8).

PAPERS SUBMITTED TO PUBLICATION

Costa F., Tavares T. Biosorption of nickel and cadmium in the presence of diethylketone by a *Streptococcus equisimilis* biofilm supported on vermiculite. Submitted to publication (2016).

Costa F., Tavares T. Pilot scale sorption studies of diethylketone in the presence of Cd and Ni. Submitted to publication (2016).

Costa F., Tavares T. Bioremoval of Ni and Cd in the presence of diethylketone by fungi and bacteria – A comparative study. Submitted to publication (2016).

Costa F., Tavares T. Sorption studies of diethylketone in the presence of Al^{3+}, Cd^{2+}, Ni^{2+} and Mn^{2+}, from lab-scale to pilot scale. Submitted to publication (2016).

COMMUNICATIONS IN SCIENTIFIC MEETING

Oral Communications

Costa F., Quintelas C., Tavares T. Biodegradation of diethylketone by *S. equisimilis*. ICEEM 2013, 7th International Conference on Environmental Engineering and Management, 18-23 September 2013, Vienna, Austria.

Costa F., Neto M.M., Nicolau A., Tavares T. Biodegradation of diethylketone by two fungi. IWA 2014, IWA World Water Congress & Exhibition, 21-26 September 2014, Lisbon, Portugal.

Silva B., Costa F., Figueiredo H., Soares O. S. G. P., Pereira M. F. R., Figueiredo J. L., Lewandowska A. E., Bañares M. A., Neves I. C., Tavares T. Biorecovery of Cr(VI) from wastewater and its catalytic reutilization. IWA 2014, IWA World Water Congress & Exhibition, 21-26 September 2014, Lisbon, Portugal.

Costa F., Silva B., Tavares T. Biosorption of diethylketone and Cd using a *Streptococcus equisimilis* biofilm supported on vermiculite: kinetics and equilibrium studies. WMESS 2015, The World Multidisciplinary Earth Sciences Symposium, 7-11 September 2015.

Costa F., Silva B., Tavares T. The effect of a joint clay-microorganism system to treat Ni and diethylketone solutions. WASTES 2015, 3rd International Conference - WASTES: solutions, treatments and opportunities, 14-16 September 2015, Viana do Castelo, Portugal.

Silva B., Tuuguu E., Costa F., Tavares T. Application of vermiculite and zeolite in water remediation using a permeable barrier. EWaS 2016, 2nd International Conference - Efficient & Sustainable Water Systems Management toward Worth Living Development, 1-4 June 2016, Chania, Crete, Greece.

P**oster Presentations**

Costa F., Silva B., Tavares T. Study of Ni (II) and diethylketone removal from aqueous solutions using a biofilm of *Streptococcus equisimilis* supported on vermiculite. CHEMPOR 2014, 12nd International Chemical and Biological Engineering Conference, 10-12 September 2014, Porto, Portugal.

Ferronato C., Silva B., Costa F., Antisari L. V., Tavares T. Biorecovery of heavy metals using vermiculite for sediment and water protection. CHEMPOR 2014, 12nd International Chemical and Biological Engineering Conference, 10-12 September 2014, Porto, Portugal.

Ferraz A., Costa F., Tavares T., Teixeira J. A. Mechanisms of Cr(III) biosorption onto residual brewer's yeast. IWA 2014, IWA World Water Congress & Exhibition, 21-26 September 2014, Lisbon, Portugal.

TABLE OF CONTENTS

LIST OF FIGURES

CHAPTER 1

CHAPTER 2

CHAPTER 3

CHAPTER 4

CHAPTER 5

CHAPTER 6

CHAPTER 7

LIST OF TABLES

CHAPTER 2

CHAPTER 3

CHAPTER 4

CHAPTER 5

CHAPTER 6

CHAPTER 7

LIST OF ABBREVIATIONS

Abbreviation	Description
BC	Biomass concentration
BET	Brunauer-Emmett-Teller
BHI	Brain heart infussion
CEC	Cation exchange capacity
DEK	Diethylketone
D-R	Dubinin-Radushkevich
DRBC	Dichloran rose bengal chloramphenicol
EC	Exchangeable cations
EEA	European environment agency
EPA	Environmental protection agency
EPS	Exopolysaccharides
EU	European union
FTIR	Fourier Transform infrared
GAC	Granular activated carbon
GC	Gas chromatography
ICP-OES	Inductively coupled plasma optical emission spectrometry
ITS	Internal transcribe sequences
LSU	Large subunit-coding sequence
MBK	Methyl butyl ketone
MC	Microbial control
MEA	Malt extract agar
MEK	Methyl ethyl ketone

Abbreviation	Description
MIBK	Methyl isobutyl ketone
MIPK	Methyl isopropyl ketone
MPK	Methyl propyl ketone
MS	Mass spectrometry
NECD	National emission ceilings directive
NMVOC	Non-methane volatile organic compounds
NPL	National priorities list
OD	Optical density
OSHA	Occupational Safety and Health Hazards
PCR	Polymerase chain reaction
$PM_{2.5}$	Fine particulate matter
PVC	Poly(vinyl chloride)
PZC	Point of zero charge
SEM	Scanning electron microscopy
SSU	Small subunit-coding sequence
TEM-EDS	Yransmission electron microscopy and energy dispersive x-ray spectroscopy
US EPA	United states environmental protection agency
VOC	Volatile organic compound
XRD	X-ray diffraction

LIST OF SYMBOLS

Abbreviation	Description	Units
μ	Specific growth	h^{-1}
μ_{max}	Maximum specific growth rate	h^{-1}
A	maximum biomass reached in terms of OD_{620}	g/L
B	BET constant	
B_D	Mean free energy of sorption per gram of the sorbate	mol^2/J^2
C_0	Influent sorbate concentration	mg/g
C_b	Sorbate concentration in solution inside the column	mg/L
C_e	Equilibrium solute concentration in solution	mg/L
C_{max}	Maximum concentrations of biomass	g/L
C_S	Saturation concentration of the adsorbed component	mg/L
$C_{S.1}$	Solute concentration at the solid/liquid interface	mg/L
C_t	Effluent sorbate concentration	mg/g
D	Axial diffusion coefficient	cm^2/h
E_D	Energy of adsorption	
K_0	Zero order kinetic constant	g/Lh^{-1}
K_1	Self-inhibition constant	g/L
$K_{1.1}$	Pseudo-first order kinetic constant	
K_2	Pseudo-second order kinetic constant	
K_{31}	First three and half order constant	
K_{32}	Second three and half order constant	

Abbreviation	Description	Units
k_{AB}	Adams-Bohart kinetic constant	L/mgh
K_S	Substrate affinity constant	g/L
k_{YN}	Yoon and Nelson kinetic coefficient	h^{-1}
m	Maintenance rate	
n	Luong positive integer number.	
N_0	Maximum sorption capacity per unit of volume of column sorbent	
P	Formation of CO_2	
q	Concentration of sorbate in the solid phase, inside the column at time t	mg/L
q_D	Theoretical saturation capacity of the monolayer	mg/g
q_e	Amount of pollutant removed till equilibrium is achieved	mg/g
q_e cal	Calculated amount of pollutant removed till equilibrium is achieved	mg/g
q_{max}	Maximum sorption capacity	mg/g
q_t	Amount of pollutant removed at time t	mg/g
R	Universal gas constant	
R^2	Correlation coefficients	
R_W	Approaching equilibrium factor	
S	Substrate concentration	g/L
S_0	Substrate initial concentration	g/L
S_{crit}	Critical concentration	g/L
S_m	Substrate inhibitory effect	g/L

Abbreviation	Description	Units
S_{min}	Maintenance threshold	g/L
t	Time	h
T	Temperature	K
U_0	Linear velocity of influent	cm/h
v	Interstitial velocity	cm/h
Z	Bed depth of column	cm
β_a	Kinetic coefficient of the external mass transfer	h^{-1}
λ	Lag time	h
$\mu_{exp,}$	Experimental specific growth rates	h^{-1}
$\mu_{predicted}$	Predicted values of specific growth rate	h^{-1}
τ	Time needed to reach 50 % of the sorbate breakthrough	h

CHAPTER 1

General Introduction

The purpose of this introductory chapter is to provide a short review of the main subjects regarding the areas focused in this thesis: biodegradation of volatile organic compounds (VOC) eventually with concomitant biosorption of metals, performed by microorganisms supported on clays. In the first part of this chapter, the environmental problematic concerning the contamination of wastewater with volatile organic compounds, as well as the hazardous effects caused by its discharge into the aquatic matrices is discussed. Special emphasis is given to diethylketone environmental impact, due to its extensive use, toxicity and reduced number of studies concerning its biodegradability in the environment. In the second part of this chapter, special attention is given to the environmental problems resulting from the discharge of metals, namely nickel, cadmium, aluminium and manganese, into water bodies due not only to their particular chemistry, toxicity, extensive use and persistence in the environment but also because effluents do not contain only one pollutant, but a cocktail of pollutants. In the third part of this chapter a short survey of the techniques available and usually employed to treat wastewater are focused and discussed in detail.

The main contamination sources of VOC and metals for aquatic systems, as well as the European legislation currently applied in the environmental field, are also discussed.

1.1| VOLATILE ORGANIC COMPOUNDS (VOC): RELEASE AND IMPACT

Volatile organic compounds are currently acknowledged as some of the major contributors for air and water pollution, through their large release into the environment, their human toxicity, their ability to act as precursors in the formation of ozone and other components of the photochemical smog, and their susceptibility to persist and migrate within the different matrices, eventually ending up contaminating air, soil, ground-water and drinking water supply (Lam et al. 2012). VOC are release into the atmosphere from natural and from anthropogenic sources and include a broad variety of substances such as aromatic compounds (benzene, toluene, cresol, phenol, etc.) (Vijayara-ghavan et al. 1995; Shim and Yang, 1999; Cinar, 2004; Gemini et al. 2005; Chen et al. 2006; Juang and Tsai, 2006; Sahinkaya and Dilek, 2007; Alexieva et al. 2008; Pamukoglu and Kargi, 2008; Li et al. 2009; Zheng et al. 2009; Aresta et al. 2010), aliphatic compounds such as hydrocarbons (kerosene and pristane) (Sharma and Pant, 2000; Ghazali et al. 2004), ketones (diethylketone, methyl-isobutyl ketone, methyl-terc-butylketone, methyl ethyl ketone) (Agathos et al. 1997; Geoghegan et al. 1997; Przybulewska and Wieczorek, 2009; Chan and Lai, 2010; Raghuvanshi and Babu, 2010), halogenated compounds (1,2-dichloroethane, 2,4-dichlorophenol, 2,4,6-trichlorophenol esters (phthalates) and aldehydes (Zeng et al. 2004; Zhang et al. 2008; Kocamemi and Çeçen, 2009).

Several definitions of volatile organic compounds (VOC) can be found. According to the European Solvent Emissions Directive, Directive 1999/13/EC of 11th March 1999, volatile organic compounds can be functionally defined as organic compounds having at 293.15 K (i.e. 20°C) a vapour pressure of 0.01 kPa or more, or have a corresponding volatility, under particular conditions of use. Other definition is given by the United States Environmental Protection Agency (US EPA) where VOC mean any compound of carbon, excluding carbon monoxide, carbon dioxide, carbonic acid, metallic carbides or carbonates and ammonium carbonate, which participates in atmospheric photochemical reactions, except those designated by Environmental Protection Agency (EPA) as having negligible photochemical reactivity.

Since volatile organic compounds participate in the physical and chemical atmospheric reactions, they are therefore co-responsible for the formation and development of the existent ozone on the tropospheric layer, as well as for the formation of other photochemical oxidants, so the control of their emissions into the atmosphere becomes crucial. VOC are known to react with hydroxyl radicals (-OH) leading to the production of ozone and other components of the photochemical smog in urban

areas (Lam et al. 2012) and also with nitrogen oxides (NO_x) in the presence of sunlight, leading to the production *in situ* of ozone at ground level. High concentrations of ozone near the tropospheric layer (ground level) are known to cause and/or aggravate several health problems in the respiratory system (irritation of the respiratory system, chest discomfort, thoracic pain, premature aging of the lungs, increased risk of respiratory infections, aggravation of asthma, emphysema and other respiratory diseases). Several factors may influence the health impacts caused by high concentrations of ozone at ground level, including the exposure time, the ventilation rate and the length of intervals between short-term exposures (Ackermann et al. 1999).

The harmful properties and effects of volatile organic compounds and the continuous increase of their emission into the environment through different sectors (Figure 1.1) have led to the development and implementation of increasingly strict laws and regulations. According to the European Environment Agency (EEA), the anthropogenic emissions of the main air pollutants decreased significantly in most EEA-33 member countries between 1990 and 2013. Nitrogen oxides (NO_x) emissions decreased by 49 % (54 % in the EU-28), sulphur oxides (SO_x) emissions decreased by 80 % (87 % in the EU-28), non-methane volatile organic compounds (NMVOC) emissions decreased by 57 % (59 % in the EU-28), ammonia (NH_3) emissions decreased by 15 % (27 % in the EU-28), and fine particulate matter ($PM_{2.5}$) emissions decreased by 34% (34 % in the EU-28) (Figure 1.2). The reduction in emissions since 1990 was due to a combination of measures, such as a) major economic structural alterations from newer member states of the European Union which led to a general and significant decline of certain industrial activities, known to contribute to the total emissions of air pollutants and to the closure of older, less efficient power installations; b) the introduction of limits on the maximum volatility of petrol that can be sold in the EU member states, as established in fuel quality directives combined with the introduction of carbon canisters and three way catalytic converters on petrol-fuelled cars; c) implementation of numerous directives within the European Union (EU) limiting the content of sulphur on fuel transport; d) reduction in livestock numbers and changes in the treatment and management of organic, natural and synthetic fertilizers.

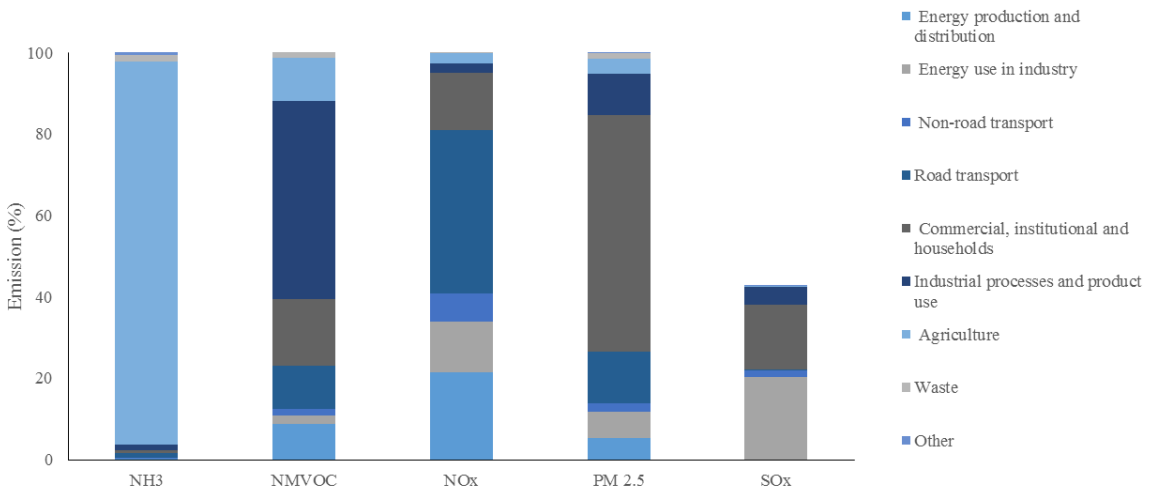

Figure 1.1. Contribution of different sectors to the emission of the main air pollutants. NH_3 – Ammonia; NMVOC - Non-methane volatile organic compounds; NO_x - Nitrogen oxides compounds (NO and NO_2); $PM_{2.5}$ - Particular matter, fine particles with a diameter equal or inferior than 2.5 micrometres; SO_x - Sulphur oxides compounds (SO, SO_2, SO_3, S_7O_2, S_6O_2, etc.) (adapted from the European Environment Agency, NEC Directive status report 2014, reported by Member States under Directive 2001/81/EC of the European Parliament and of the Council of 23 October 2001 on national emission ceilings for certain atmospheric pollutants).

In general, the EU-28 Member States have made a good effort to reduce the emissions of NO_x SO_x, NH_3 and NMVOC below the legal established values as specified by the National Emission Ceilings Directive (NECD). However, six member States have reported for NO_x (Belgium, Austria, Germany, France, Ireland and Luxembourg) and for NH_3 (Denmark, Austria, Finland, Netherlands, Germany and Spain) and three for NMVOC (Germany, Denmark and Ireland) emissions above their NECD emission ceilings. Emissions reduction commitments for 2020 have been set under the 2012 amended Gothenburg Protocol for SO_x, NO_x, NMVOC, NH_3, and $PM_{2.5}$.

The reduction of volatile organic compounds emissions can be accomplished in two different stages. The first set of measures involves processes and equipments modification and it is achieved by prevention (for example through the optimization of the operational conditions in order to minimize the development and/or volatilization of organic compounds, by improving and/or modifying the processes and equipments and by selecting the proper raw materials. The enforceability of prevention procedures is limited since it is not possible to adjust and change all the processes, methods and equipment.

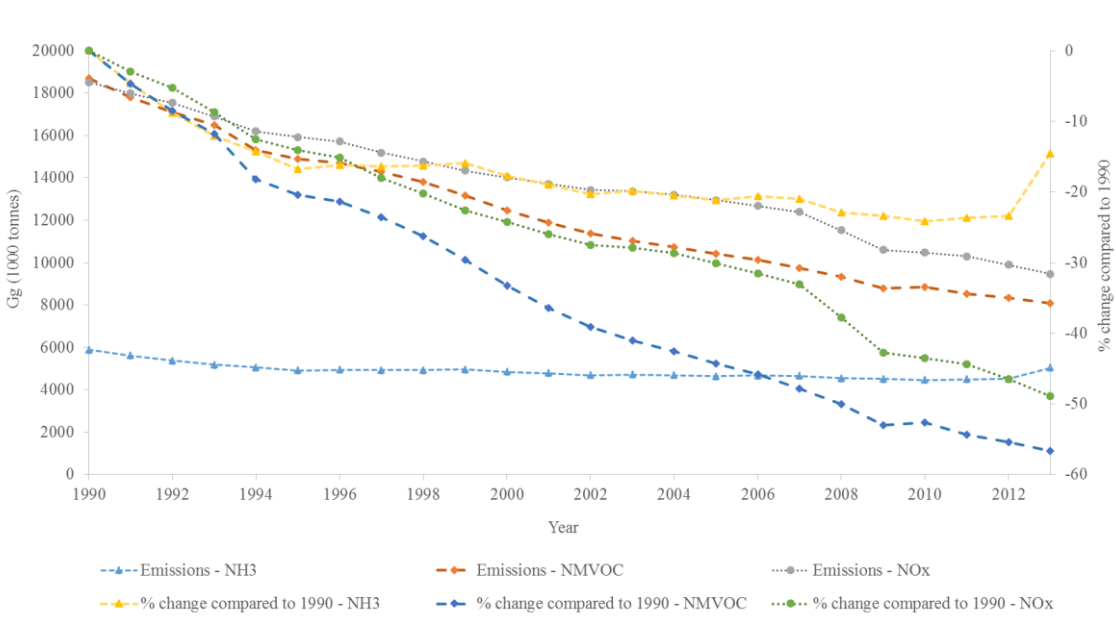

Figure 1.2. Emissions of the main air pollutants across Europe from 1990 to 2013 and their respective variation compared to 1990 (adapted from the European Environment Agency, Technical report nº 8/2015, reported in the European Union emission inventory report 1990 to 2013 under the UNECE Convention on Long-range Transboundary Air Pollution, LRTAP).

The second set of measures involves additional add-on-control techniques and it is usually classified in two distinct groups: recovery and destruction. Recovery methods comprise condensation, adsorption, membrane separation and absorption processes, in which volatile organic compounds are relocated without chemical transformation to a solid or liquid phase. Destruction methods such as catalytic oxidation, thermal oxidation, biodegradation and biofiltration, transform volatile organic compounds into different compounds, inert or less harmful (Días et al. 2005). The selection of the most indicated method to remove volatile organic compounds from environment is intrinsically associated with and dependent of the characteristics of the effluent to be treated (concentration and nature of the volatile organic compounds, gas flow rate and cost effectiveness (Khan and Ghoshal, 2000).

The toxicity of diethylketone will be discussed in detail in the following section as well as the current national legislation on solutions containing diethylketone.

1.1.1| Diethylketone

Diethylketone ($CH_3CH_2C(=O)CH_2CH_3$) also known as 3-pentanone, propione, dimethyl acetone, methacetone and pentan-3-one, is a simple symmetric dialkyl ketone that is naturally produced and released into nature by several biogenic sources such as plants, (*Betula pendula*, *Larix decidua*, *Abies alba*, *Pinus sylvestrisi* and *Pinus sibirica*, for example) fruits (kiwis and nectarines) and by several industrial activities such as electronics, paints, plastics, rubbers, lubricants, food additives and pharmaceuticals industries (Geoghegan et al. 1997; Quintelas et al. 2012). Diethylketone (DEK) is a colourless liquid with a characteristic pungent odour, a boiling point of 101.7 °C, a melting point of -39.8 °C and a density of 0.814 g/cm^3 at 20°C. It is soluble in alcohol and acetone and slightly soluble in water (Patnaik, 2007). When in the atmosphere, diethylketone can react with OH radicals promoting the formation of ozone and other components of the photochemical smog in urban areas (Lam et al. 2012).

Despite its intensive use and environmental impact, diethylketone has not been subjected to extensive studies on its removal from the different environmental matrices, especially by biological processes such as biodegradation and biosorption.

1.1.1.1| Diethylketone Toxicity

Regardless its physical state, exposure to diethylketone presents a significant impact on human and animal health, as well as on aquatic and terrestrial ecosystems. According to Occupational Safety and Health Hazards (OSHA) of United States Department Labor (https://www.osha.gov), dry skin, eyes irritation, mucous membrane, onset of cough, drowsiness or dizziness, chapped and red eyes, dyspnoea, tachycardia, faintness, coma and even death, are some of the symptoms caused by acute and chronic exposure to diethylketone.

According to several studies conducted in aquatic ecosystems, when exposed to concentrations in the range of 259 mg/L to 2300 mg/L during 96 hours, fish begin to rise to the surface, with clear signs of depression and loss of balance followed by death (http://www.inchem.org). With regard to terrestrial ecosystems, according to Tani and Hewitt (2009), the C_4-C_6 ketones are absorbed by plants

leaves and can enter the food chain of animals and humans, causing severe consequences on their health.

1.1.1.2| Legislation Applied to Water Contaminated With Diethylketone

The widespread use of organic solvents resulted in their accumulation in aquatic and terrestrial matrices. In order to minimize, control or even to prevent the pollution caused by the discharge of organic solvents in nature, as well as to protect and improve the quality of the environment, strict environmental laws and directives were enacted in most countries.

In Portugal, the emission limits concerning the discharge of wastewater are set in order to protect the aquatic environment and improve the water quality in function of its main purposes. The Decree-Law nº. 236/98 of 1st August 1998, transposed from the European Directive 80/778/EEC establishes the maximum permissible concentration in fresh surface water intended for human consumption, for chlorides, fluorides, nitrates, phenolic compounds and aromatic hydrocarbons, the values of 200 mg/L, 1.5 mg/L, 50 mg/L, 0.001 mg/L and 0.2 mg/L, respectively. The emissions limit values for aldehydes, nitrates, phenols, oils and fats in wastewaters discharges are 1 mg/L, 50 mg/L, 0.5 mg/L and 15 mg/L, respectively.

The Decree-Law nº. 306/07 of 27th August 2007 revises the Decree-Law nº 243/01 of 5th September 2001, which results from the transposition of the European Directive 98/83/EC into national law and defines the water quality requirements for human consumption, provided by public water supply systems, distribution networks. The maximum permissible value for phenolic compounds, fluorides, nitrates polycyclic aromatic hydrocarbons (PAH), in water intended for human consumption is 0.5 µg/L, 1.5 µg/L, 50 µg/L, 0.10 µg/L, respectively.

The Decree-Law nº. 178/06 of 5th September 2006 frames the general residues system and results from the transposition of the Directive no. 2006/12/EC of the European Parliament and European Council of 5th April and from the Directive nº. 91/689/EEC of the same Council, of 12th December, into national law and applies to waste management operations, including any and every operation of collection, transport, storage, triage, treatment, recovery and disposal of wastes, as well as soil decontamination operations and monitoring of disposal sites, after the closure of their facilities. The

Decree-Law nº. 242/01 of 31st August 2001, aims to reduce the direct and indirect effects of the emissions of volatile organic compounds into the environment, as a result of the application of organic solvents in certain activities and installations, as well as the potential risks of these same emissions to human health and to the environment, transposing into national law the Directive nº. 1999/13/EC of the European Council of 11th March.

The Decree-Law nº. 78/04 of 3rd April 2004, determines the regimen of prevention and control of the pollutants emissions into the atmosphere, setting the principles, the main goals and the appropriate instruments, to guarantee natural air resource protection, as well as the measures, procedures and obligations of plant operators included, in order to prevent or reduce to acceptable levels the atmospheric pollution caused by these same facilities.

1.2| METALS IN WASTEWATER: RELEASE, TRANSPORT, FATE AND IMPACT

The increasing and continuous contamination of water systems with toxic and dangerous compounds in the past few decades, simultaneously with the increased attention on the ecological and health hazards caused by the discharge of different pollutants into water systems, has resulted on a continuous and worldwide effort to develop eco-friendly techniques and processes able to efficiently decontaminate aqueous solutions with different classes and concentrations of pollutants. The release of metals and volatile organic compounds by industrial effluents is considered to be an issue of critical and high concern (Amor et al. 2001; Ogbodu et al. 2015).

In the past few decades, the use of the term *heavy metals* is far from being consensual among the scientific community and thus several different definitions have been proposed based on the atomic number, atomic weight, density, chemical properties and toxicity (Duffus, 2001). According to Lyman (1995), the term *heavy metals* refers to a metal with an atomic number between 21 and 92, whereas for Harrison and Waites (1998) it refers to a collective term used for metals with high atomic mass, particular transition metals which are toxic and cannot be processed by living organism and for Wright (2003) it refers to metallic elements with a relatively high density compared to water (equal to or greater than 6 g/cm^3). Although heavy metals present certain properties in common, each element presents specific characteristics that determine its biological and toxicological properties and how it moves through the different environmental matrices. Therefore, when referring to a specific metal it

is of crucial importance to consider its potential impact on the environment as well as its physicochemical properties.

Metals are naturally occurring elements that are commonly found in the Earth's crust, but the majority of human exposure and environmental contamination results from different anthropogenic activities such mining and smelting operations, domestic and agriculture use of metals and metal-containing products (Nriagu, 1989; Tchounwou et al. 2012). Industrial sources of metal contamination include nuclear power stations and high tension lines, coal burning in power plants, metal processing in refineries, petroleum combustion, plastics, textiles, microelectronics, wood preservation and paper processing plants, (Tchounwou et al. 2012) jewellery, mining, tanneries, textile, batteries, petrochemical and fine chemistry, chemicals production, (Ahmed at al. 1998; Chopra and Pathak, 2010; Merrikhpour and Jalali, 2013), electronic device manufacturing, oil refining, printing, production of dyes, paints, pulp paper (Ogbodu et al. 2015) and health care products (Azeez et al. 2013). Natural phenomena such as volcanic eruptions and weathering have been reported as major contributors to heavy metal pollution (Nriagu 1989; Fergusson, 1990; Bradl, 2002; He et al. 2005). Environmental contamination with metals can also occur through soil and sediments erosion, with consequent leaching of metals, metal corrosion, resuspension of sediments, atmospheric deposition and metal evaporation from aquatic resources to soil and ground water (Tchounwou et al. 2012).

Heavy metal pollution is particularly problematic since unlike organic pollutants, metals are non-biodegradable and therefore able to be bio-accumulated by living organisms via food chain, in living tissues, triggering numerous diseases and health disorders (Ibrahim and Mutawie, 2013; Chaudhuri et al. 2014; Roy et al. 2015) as well as ecological damages. (Wan Ngah and Hanafiah, 2008). For these reasons the Agency for Toxic Substances and Disease Registry, of the U.S. Department of Health and Human Services, has designated heavy metals as priority pollutants. It should be noted, that this is a prioritization of substances based on their frequency, toxicity and potential for human exposure at National Priorities List (NPL) sites. Aluminium, arsenic, cadmium, chromium, lead, manganese, mercury nickel, present in the priority list are commonly found at the NPL installations, and tend to pose the most significant potential threat to human health. Although aluminium (Al^{3+}), nickel (Ni^{2+}) and manganese (Mn^{2+}) are not as toxic as cadmium (Cd^{2+}), chromium (Cr^{6+}) and mercury (Hg^{2+}) their increasing levels in industrial effluents and consequent detection in soils and water (Tam et al. 1989), are of serious concern (Volesky, 1990).

In this thesis, special consideration is given to aluminium, cadmium, nickel and manganese. These four metals will be detailed in the next section.

1.2.1| Aluminium, Cadmium, Nickel and Manganese: A General Overview

Aluminium

Aluminium (Al), with an atomic number of 13, a density of 2.70 g/cm^3 is a metal occurring in the Group 13, Period 3 of the periodic table and its electronic configuration is [Al] 3s^2 3p^1. Although aluminium is the 3rd most abundant metallic element in the Earth's crust (~ 8%) and is present in more than 270 different minerals, its high affinity towards oxygen, as well as the chemical stability of its oxides and silicates have precluded its existence and isolation in pure form (Rabinovich, 2013).

Aluminium is released to the environment through natural processes and through the discharge of effluents from different anthropogenic activities such as construction, automotive, food packaging, food additives industries, pigments and paints production, medical and personal care products (ATSDR, 1992). Aluminium salts are also extensively used in water treatment as a coagulant agent to reduce the organic matter, microorganisms, colour and turbidity levels (WHO, 1998).

Aluminium in water can produce complexes with inorganic ligands such as chloride, fluoride and sulphate and with different organic compounds, such as fulvic or humic acids, most but not all of which are soluble. It can also produce colloidal polymeric solutions, monomeric and polymeric hydroxyl species, precipitates and gels (WHO 1998).

In water the chemistry of aluminium is complex, and numerous chemical parameters, including pH, influence and determine which aluminium oxidation state is present in aqueous systems. The concentration of total dissolved aluminium in pure water is minimal in the pH range between 5.5 and 6, increasing at higher and lower pH values (Figure 1.3) (CCME, 1988; ISO, 1994). Despite aluminium widespread occurrence in drinking water, foods and several antacid formulations (WHO, 1997), the health effects of aluminium exposure on humans are still not definitive and perceived. It is known that people with kidney disorders have less capacity to remove this metal from their body. In this context the Joint Food and Agriculture Organization and the World Health Organization Expert

Committee on Food Additives lowered the allowable intake of aluminium in 2006, from 77/mg/Kg body weight to 1/mg/Kg body weight per week (Bondy et al. 2016).

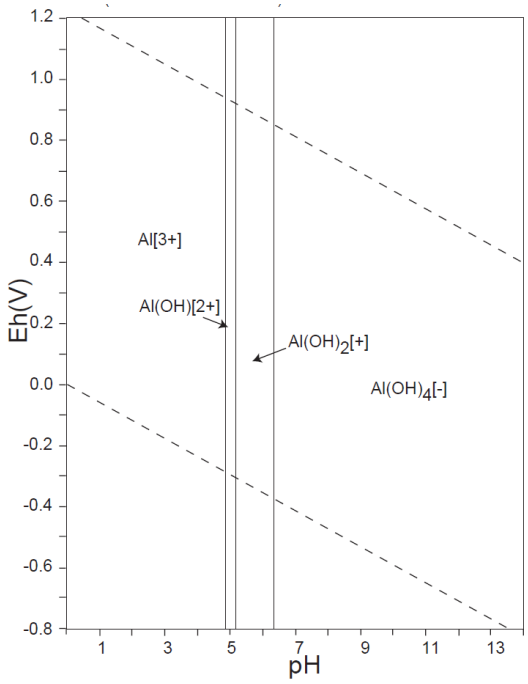

Figure 1.3. Eh-pH diagrams of aluminium species under chemical equilibrium conditions: Al-O-H (2) systems at 25 °C and 1 atm (adapted from Takeno, 2005).

In the past years, several studies have been conducted aiming to understand the effect and impact of aluminium exposure on the human health. It has been conjectured that exposure to aluminium in humans increases the risk to develop or accelerate the outset of Alzheimer disease (Martyn et al. 1989; Flaten, 1990; Michel et al. 1991; Neri & Hewitt, 1991; Wettstein et al. 1991; Jacqmin et al. 1994). Nevertheless, the Environmental Health Criteria document for aluminium (WHO, 1997) concluded that the positive correlation between the presence of aluminium in drinking water and Alzheimer disease, in some of the studies conducted could not be totally dismissed. It is not possible, however, to assume a causal relationship between the presence of aluminium and the development of the Alzheimer disease due to various problems, particularly in quantifying the total aluminium intake from all sources and to methodological limitations (Krewski et al. 2007).

Cadmium

Cadmium (Cd), with an atomic number of 48, a density of 8.7 g/cm^3 is a silver-white, lustrous, ductile and very malleable metal occurring in the Group 12, Period 5 of the period table and its electronic configuration is [Cd] 3d^{10} 3s^2. Cadmium is widely distributed in the Earth's crust with an average concentration of about 10 mg/Kg, although in sedimentary rocks and marine phosphates cadmium concentration can reach 15 mg/L (Tchounwou et al. 2012). In similarity to aluminium, the availability of cadmium in aqueous solutions is also influenced by pH. The total concentration of dissolved cadmium in pure water decreases for pH values higher then 8 (Figure1.4).

Natural emissions of cadmium to the environment can result from forest fires, volcanic eruptions, production of sea salts aerosols (EPA 1985; Shevchenko et al. 2003). Cadmium is released into the environment by anthropogenic sources, through the discharge of wastewater from different industries, such as electronic devices manufacturing, steels, oil refining, printing, dyes, paints, pulp and paper, fertilizers, pesticides (Ogbodu et al. 2015), mining, jewellery, tanneries, batteries, petrochemical, textile, fine chemistry and chemicals (Ahmed et al. 1998; Chopra and Pathak, 2010; Merrikhpour and Jalali, 2013), and health care products (Tam et al. 1989), causing serious environmental and health problems. The most significant use of cadmium is in nickel/cadmium batteries, as secondary or rechargeable power sources, demonstrating long life, low maintenance, high output and high tolerance to physical and electrical stress. It can also be used in alloys and electronic compounds as pigments and PVC stabilizers. Although the use of nickel/cadmium batteries has shown substantial increase over the past years, its commercial use has decayed in developed countries in response to environmental concerns (EPA, 2006).

Cadmium toxicological properties derive from its chemical similarity to zinc (Zn), an essential micronutrient for humans, animals and plants. It is bio-persistent and once absorbed by an organism it usually remains within the organism for several years (over decades for humans) until be eventually excreted.

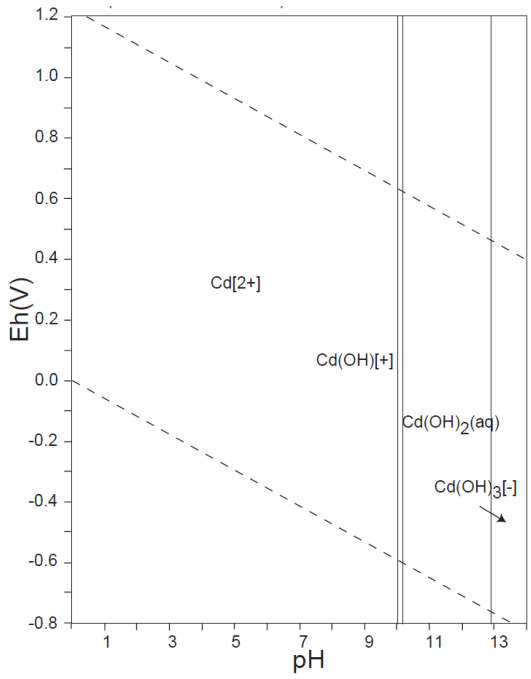

Figure 1.4. Eh-pH diagrams of cadmium species under chemical equilibrium conditions: Cd-O-H (2) systems at 25 °C and 1 atm (adapted from Takeno, 2005.

Besides playing no constructive role in human-metabolism, cadmium is an irritant to the respiratory system and is able to cause anaemia and serious damage in different organs including kidneys, lungs, liver and testis. Chronic inhalation exposure to cadmium particles is usually associated with alterations in chest radiographs and pulmonary function which are consistent with emphysema (Davison et al. 1988). Exposure to airborne cadmium in workplaces has been associated with osteoporosis, with a decrease in bone mineral density (Akesson et al. 2006; Gallagher et al. 2008; Schutte et al. 2008) and olfactory malfunction (Mascagni et al. 2003). Cadmium exposure may also induce infertility (Çelikli and Bozkurt, 2000; Chaudhuri et al. 2014), affect the action of enzymes, impedes respiration and transpiration (Ahmed et al. 1998) and may induce genomic instability through complex and multifactorial mechanisms, including proteinuria, a decrease in glomerular filtration rate and an increase in the frequency of kidney-stone formation, eventually causing certain types of cancer (group B1). In most of the non-smoking population the principal cadmium exposure pathway is through food and drinking water, through the natural and artificial addition of cadmium to agricultural soils (atmospheric deposition and fertiliser application, for example) and through its uptake by food and forage crops. The average daily intake of cadmium for humans is evaluated to

be 1 µg from water and 0.15 µg from air. However smoking people can inhale around 2 to 4 µg of cadmium when smoking a packet of 20 cigarettes. Cadmium exposure is usually assessed by measuring cadmium concentration in blood and urine. The presence of cadmium in the bloodstream is usually indicative of a recent exposure to cadmium, whereas the presence of cadmium in urine (usually adjusted for dilution by calculating the cadmium/creatinine ratio) indicates cadmium accumulation or kidney damage (Jarup et al. 1998; Wittman and Hu, 2002). The simultaneous presence of cadmium in urine and bloodstream is usually higher in cigarette smokers, intermediate in former smokers and lower in non-smokers (Becker et al. 2002; Mannino et al. 2004). Due to the continuous use of cadmium in different industrial activities, the environmental contamination and human exposure to this metal has dramatically increased during the past century (Elinder and Jarup, 1996).

Nickel

Nickel (Ni) has an atomic number of 28, a density of 8.9 g/cm^3 and is a naturally occurring hard, malleable, ductal, lustrous and silvery-white metallic element. Nickel occurs in Group 10, Period 4 of the periodic table and its electronic configuration is [Ni] $3d^8$ $4s^2$. Although nickel occurs extensively in the Earth's crust, most of nickel is inaccessible in the core on the Earth. Nickel is classified as a good thermal and electric conductor. Nickel release into the environment can occur from biogenic sources such as windblown, dust and volcanic eruptions. However most of its release comes from the burning of residual fuel oils from metal refining, municipal incineration, steel production and coal production (Bennet, 1984). Nickel is usually bivalent, though it may assume other valences and form several different complex compounds. In water, the concentration of total dissolved nickel starts to decrease for pH values higher than 8 (Figure 1.5).

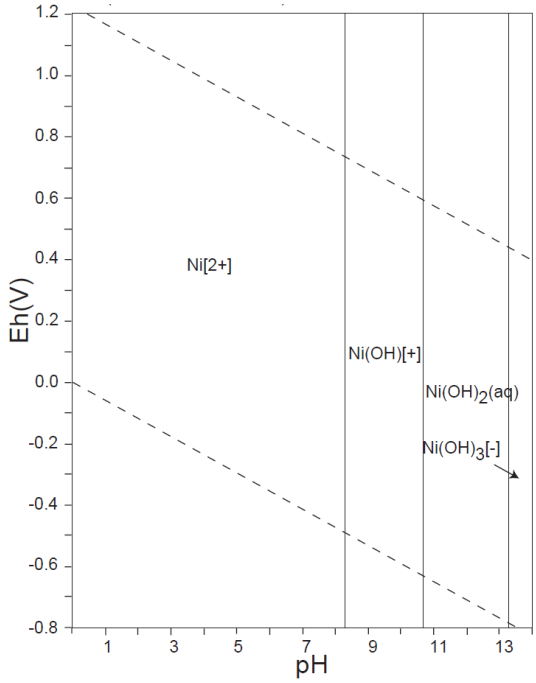

Figure 1.5. Eh-pH diagrams of nickel species under chemical equilibrium conditions: Ni-O-H (2) systems at 25 °C and 1 atm (adapted from Takeno, 2005).

Contrary to what happens with cadmium, nickel plays a constructive role in human-metabolism since it is needed, in small quantities, for the production of haemoglobin. However, when present in excessive quantities for long-term it causes several types of acute and chronic health illnesses, such as dry cough, nausea and vomiting, chest pain, skin dermatitis, lungs and kidney damage, rapid respiration, renal edema, pulmonary fibrosis, cyanosis and extreme weakness (Suazo-Madrid et al. 2011). Nickel is also known for its carcinogenic, embryotoxin and nephrotoxin character. Despite its toxicity and hazardous effects, the environmental Protection Agency (EPA) does not presently control nickel levels in drinking water.

Manganese

Manganese (Mn) with an atomic number of 25, a density of 7.43 g/cm^3 is a silvery metallic metal occurring in Group 7, Period 4 of the periodic table and its electronic configuration is [Mn] 3d^5 4s^2. Manganese is ubiquitous in the Earth's crust and it is present in more than 100 minerals, with soil backgrounds levels ranging between 40 and 900 mg/kg, with an expected average backgrounds

concentration of 330 mg/kg (Barceloux 1999). Manganese release into the environment, and consequent exposure of humans occur from both natural and anthropogenic sources. It can be released into the atmosphere through volcanic eruptions, but almost of 80 % industrial emissions are attributed to steel and iron production facilities, whereas the reaming 20 % are attributed to power plants and coke oven emissions (EPA 2003). Manganese and manganese compounds are extensively used in the manufacture of steel and iron alloys, batteries, glass and fireworks. They are also used as an oxidant for cleaning, bleaching and disinfection purposes, livestock feeding supplements and in fertilizers, fungicides and varnish, (ATSDR, 2000). Their concentration in aqueous solutions is pH dependent (Figure 1.6).

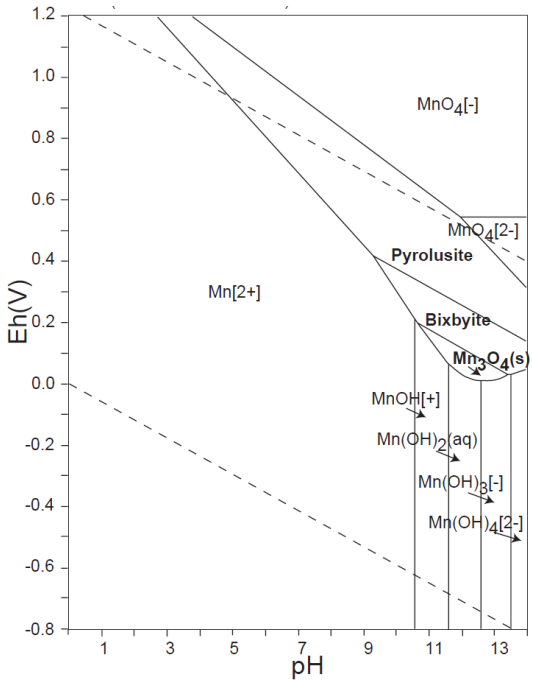

Figure 1.6. Eh-pH diagrams of manganese species under chemical equilibrium conditions: Mn-O-H (2) systems at 25 °C and 1 atm (adapted from Takeno, 2005).

Although toxic when present in high concentrations, manganese is indispensable for the functioning of several cellular enzymes (co-factors, also known as essential metals or micro-nutrients) such as prolidase, an enzyme necessary to produce collagen, urease, hydrogenase, manganese superoxide dismutase, pyruvate carboxylase and for the activation of others enzymes, such as kinases,

decarboxylases, transferases and hydrolases. Overexposure to manganese may occur either orally or by inhalation and can onset a serious of toxic responses. Usually, the primary symptoms are headache, disorientation, anxiety, insomnia, memory loss and lethargy. However, with continued exposure these symptoms can develop and led to motor disturbances, tremors, and difficulty in walking (http://hydratechnm.org).

1.2.2| Legislation Applied to Water Contaminated With Metals

In order to preserve the environment, the Portuguese government has been implementing and developing several environmental policies, specifically European Directives. The Portuguese legislation establishes limits of emission in the discharge of wastewater in order to protect and preserve the aquatic ecosystem, and to improve the water quality, according to its main purposes.

The Decree-Law nº. 238/98 of 1st August 1998 establish the maximum admissible values for fresh water intended for human consumption for several pollutants such as chlorides, fluorides, nitrates, phenolic compounds, aromatic hydrocarbons and cadmium, the values of 200 mg/L, 1.5 mg/L, 50 mg/L, 0.001 mg/L e 0.2 mg/L, 0.005 mg/L, respectively. The emission limit value for the discharge of wastewater for aldehydes is 1 mg/L, for nitrates is 50 mg/L, for phenolic compounds is 0.5 mg/L, for oils and fats is 15 mg/L, for aluminium is 10 mg/L, for manganese is 2 mg/L, for cadmium is 0.2 mg/L and for nickel is 2 mg/L. The Decree-Law nº. 178/06 of 5th September deliberates the general system of wastes, transposing into national law the Directive nº. 2006/12/EC of the Parliament and European Council of 5th of April, and the Directive nº. 91/689/EC of the same Council of 12th of December and applies to the operations concerning waste management and include any operation of collection, transport, storage, triage, treatment, valorization and elimination of residues, and all operation related to soil decontamination and monitoring of disposal sites, after the closure of its facilities.

The appearance and subsequent enforcement of environmental laws and regulations increasingly restrictive, have force the development of new approaches that aim to identify more efficient physico-chemical treatment processes, with lower waste production (Dunn e Bush, 2000; Kim et al. 2008), and the definition of systems capable of removing a wide diversity of pollutant and therefore reduce their concentration in the environment, but also able to recover and reuse them (Quintelas, 2007).

In summary, the environmental policy aims the development of new techniques and processes that are safer, more ecological, effective and economical.

1.3| TECHNOLOGIES APPLIED TO TREAT WATER CONTAMINATED WITH VOC AND/OR METALS

The development and implementation of cost-effective processes for the treatment of aqueous solutions containing organic compounds and metals is crucial to enhance the competitiveness of industrial processes and to reduce the environmental impact of the effluents containing these toxic and hazardous contaminants (Javanbakht et al. 2014). The traditional methods for wastewater treatment are usually based on pollutant concentration and composition, salinity, pH and volume, and they tend to consume too much energy, they are unable to meet the treatment objectives, they produce huge amounts of toxic sludge, that will require an additional treatment and proper disposal, all of this associated with high economical costs, making them unattractive for real applications.

Processes such as chemical precipitation, condensation, thermal degradation, reverse osmosis, ion exchange, adsorption on granular activated carbon (GAC), oxidation and incineration (Costa et al. 2014), sludge separation cementation, coagulation, flocculation, electrochemical treatment, membrane processes and evaporation (Javanbakht et al. 2014) are examples of the traditional techniques usually employed to decontaminate wastewaters. Although the removal of toxic and hazardous compounds by biological materials has received a substantial attention in the last past years, only a small fraction of these studies used growing active microbial biomass.

Although nowadays there are several biological treatment methods available for the decontamination of aquatic and terrestrial systems, taking into consideration the scope of the present thesis, the biodegradation and biosorption are highlighted and discussed in detail.

1.3.1| Biodegradation

In the last few years several studies regarding the biodegradation of organic compounds, such as hydrocarbons, polychlorinated biphenyls (PCBs), polycyclic aromatic hydrocarbons (PAHs),

pharmaceutical substances, have been conducted in order to better understand the microorganisms importance and role in the treatment and/or removal of different pollutants in the different environmental matrices (Agathos et al. 1997, Sharma and Pant, 2000, Ghazali et al. 2004, Zeng et al. 2004, Gemini et al. 2005, Alexieva et al. 2008, Pamukoglu and Kargi, 2008, Zhang et al. 2008, Kocamemi and Çeçen, 2009, Onesios et al. 2009, Zheng et al. 2009, Chan and Lai, 2010; Essam et al. 2010; Quintelas et al. 2010; Raghuvanshi and Babu, 2010).

Currently, due to the technological advances in the fields of biotechnology and molecular biology, it is now possible to perform genomic, metagenomic and proteomic analyses and thus obtain information regarding a) the metabolic and regulating networks, b) the development of the degradation pathways, c) the molecular adaptation strategies caused by changes in the environmental conditions and d) the identification of the microorganisms involved in the biodegradation of the pollutants, with a better understanding of the microbial structure and of the role of the microbial communities in the biodegradation processes (Díaz, 2008).

The biodegradation processes can be either aerobic or anaerobic. Aerobic biodegradation occurs due to the natural occurring biological activity, through enzymatic action, in the presence of oxygen, which creates changes in the chemical structure of the material to be degraded, generating carbon dioxide and stabilised organic matter. Studies conducted by Cinar (2004), allow to infer that the aerobic degradation of the anaerobic central intermediaries (thioester) that results from on the incomplete anaerobic degradation of the aromatic compounds (phenol and *p*-cresol), and usually leads to the formation of the 3, 4- dihydroxybenzoate, the most common intermediate of the aerobic degradation of aromatic compounds. Anaerobic biodegradation, on the other hand, is developed by the natural occurring biological activity, through enzymatic action, in the absence of oxygen or with low oxygen availability, triggering a set of changes on the chemical structure of the material to be degraded, generating mostly methane, stabilised organic matter and carbon dioxide.

The use of microorganism in the form of biofilms in biological processes, namely biodegradation processes to decontaminate aquatic and terrestrial systems have been extensively studied in the last years (Kumer et al. 2009, Hosseini et al. 2010, Chandran and Das, 2011, Sunder et al. 2011). Biofilms are often defined as an accumulation of microbial cells enclosed in a self-produced polymeric matrix with a jelly appearance, adhered to a solid surface (Lewandowski. and Beyenal, 2014). Microalgae, fungi, bacteria and protozoa, are some of the microorganisms commonly found

forming biofilms. The use of bacteria as biodegrading agents presents various advantages, mainly because of their small size, high reproduction rates, high adaptability, resistance to extreme environmental conditions and abundant production of exopolysaccharides (EPS), which protects the biofilm against the hazardous conditions from the surrounding environment (Pereira, 2001).

In the following subsections, the different types of biomass usually employed in biodegradation processes will be discussed.

1.3.1.1| Different Types of Biomass Used in Degradation Systems

Active biomass (living biomass) or inactive biomass (death biomass), in suspension or in the form of biofilm, can be used in biodegradation processes. When using active biomass, the biodegradation of the pollutant may occur either inside or outside de cell and is dependent on several parameters such as metabolic activity and sensitivity of the microorganism towards the pollutants. When using inactive biomass, the removal of the pollutant is achieved by the functional groups present on the cell surfaced.

In the following subsections a brief description of the main biomasses usually employed in biodegradation processes is given.

1.3.1.1.1| Fungi

According to the taxonomy developed by Carolus Linnaeus, the father of modern taxonomy, in the 18th century, fungi comprise a large group of organisms ranked as a kingdom belonging to Eucaryota domain. Abundant in all ecosystems, most fungi are inconspicuous due to their reduced size and their modes of cryptic life in soil, dead matter and as symbionts of plants and animals.

The fungi present fast reproduction cycles, which result in high production of biomass, and are easily manipulated genetically and morphologically. These factors, combined with the fact that many industrial processes generate abundant amounts of fungal biomass as a by-product and with their

ability to remove toxic chemicals such as metal compounds and ketones, make fungi a very attractive kind of biodegrading agent. (Quintelas, 2007; Przybulewska and Wieczorek, 2009).

Studies conducted by Agathos et al. (1997), using *Geotrichum candidum* and *Fusarium oxysporum* species allowed to prove the excellent ability of these two fungi to fully degrade high concentrations of methyl ethyl ketone (3 g/L).

1.3.1.1.1.1| Yeasts

Yeasts are unicellular fungi that can reproduce either sexually or asexually, by budding or splitting, depending on the environmental conditions. They differ from unicellular algae, as they do not perform photosynthesis, from protozoa due to the presence of rigid cell walls and from bacteria due to their larger size and morphological properties (Quintelas, 2007). The cell wall of yeasts possesses several amine groups and presents a microfibrillar structure that is constituted by polysaccharides in more than 90 %. The main existing groups on yeasts walls are amino groups ($-NH_2$), carbonyls (-CO), hydroxides (-OH), sulphates ($-SO^{2-}_4$) and phosphates ($-PO^{3-}_4$) (Mukhopadhyay et al. 2007, Quintelas, 2007).

Geoghegan et al. 1997 investigated the biodegradation capacity of *Hansenula polymorpha*, a methylotrophic yeast, towards mixed media containing glucose and methanol. These authors concluded that a complete and simultaneous degradation of both substrates occurred, even in the stationary phase.

1.3.1.1.2| Algae

Algae comprise several groups of aquatic and autotrophic living organisms. Most algae are unicellular, and even the most complex algae do not possess differentiated tissues, roots, stems or leaves. It should be highlighted that although algae have been considered plants for a long time, only green algae show an evolutionary relationship with terrestrial plants. The remaining algae groups present independent but parallel evolutionary lines to the lines of higher plants (Quintelas, 2007).

1.3.1.1.3| Bacteria

Discovered by Antonie van Leeuwenhoek in 1683, bacteria were initially classified by Linnaeus as plants. In 1866, Ernest Haeckel included them in the Kingdom Protista. Currently, the bacteria comprise one of the three domains of the cladistics classification system. Although archaebacteria constitute a separate domain, the term *bacteria* commonly applies.

The inherent characteristics of bacteria (small size, ubiquity, high reproductive capacity under controlled conditions, and high resilience to a wide range of environmental conditions) have served as the basis for their study and consequent application to the treatment of contaminated aquatic and terrestrial systems.

Shim and Yang (1999) studied the kinetic mechanisms of BTEX (solution composed by benzene, toluene, ethylbenzene and xylene) biodegradation by a co-culture of *Pseudomonas putida* and *Pseudomonas fluorescens*, in hypoxic conditions and in a fixed bed bioreactor. These authors were able to prove the efficient degrading capacity of these two bacteria and to determine a certain resistance of the bacteria towards the toxic effects of benzene. Gemini et al. (2005) studied the aerobic biodegradation mechanisms of *p*-nitrophenol by *Rhodococcus wratislaviensi*, the elimination mechanisms of the nitrite group of *p*-nitrophenol during biodegradation and assessed the level of decontamination. These authors achieved biodegradation performances of 99.8% and obtained specific growth rates of 0.18 h^{-1} and 0.17 h^{-1} for initial concentrations of the substrate of 0.36 mM and 0.72 mM, respectively. These authors also established the ability of *Rhodococcus wratislaviensi* to eliminate the nitrite group during biodegradation.

Numerous biodegradation experiments using *Pseudomonas* bacteria have been reported during the past few years. Among these, the works performed by Chen et al. (2009) and Yongliang et al. (2009), are highlighted. The studies conducted by Chen et al. (2009) aimed to infer about the ability of *Pseudomonas putida* CZ1 and different clays (smectites, goetites, kaolinite and manganite) to remove copper (Cu) and zinc (Zn) from a liquid medium. These authors concluded that when compared to the bacteria used, clays present a higher number of affinity sites towards copper and a lower number of affinity sites for zinc. The analyses carried out using Transmission Electron Microscopy and Energy Dispersive X-ray Spectroscopy (TEM-EDS) revealed that most of the removed zinc was associated in *Pseudomonas putida* CZ1-clay complexes, which in turn corroborates the important role of bacteria on the mobility of metals in soil.

The biodegradation mechanisms and kinetics of *p*-nitrophenol by *Pseudomonas aeruginosa* HS-D38 was studied by Yongliang et al. (2009). This bacterium is able to use *p*-nitrophenol as its sole source of carbon, nitrogen and energy, and mineralizes it, even when a medium containing mineral salt (MSM) was used, at an initial concentration of 500 mg/L, over a 24 hour period. The results obtained showed that the biodegradation follows a first order kinetics with a biodegradation constant of 2.309 $x10^{-2}$ h^{-1}. When ammonia and glucose were added to the system, the biodegradation constant tended to respectively increase (3.603 $x10^{-2}$ h^{-1}) and decrease (9.74 $x10^{-3}$ h^{-1}). The authors established that the addition of ammonia increases the biodegradation efficiency of the *p*-nitrofeneol, while the addition of glucose delayed and inhibited the biodegradation of *p*-nitrofeneol. The chemical analysis carried out, thin layer chromatography, UV-Vis spectroscopy and gas chromatography suggested a conversion of *p*-nitrophenol to hydroquinone, which was subsequently degraded via 1, 2, 4 benzenetriol. Raghuvanshi and Babu (2010) studied the biodegradation capacity of an acclimatized consortium of bacteria from activated sludge towards methyl isobutyl ketone (MIBK). The results accomplished indicated the existence of a direct proportionality between the time required for MIBK consumption and its initial concentration and the maximum specific growth rate obtained was of 0.128 h^{-1} for an initial concentration of MIBK equal to 600 mg/L.

1.3.1.2| Biodegradation Mechanisms

The biodegradation of organic compounds by microorganisms is usually accompanied with the formation of metabolites (intermediates or by-products). Depending on their toxicity and complexity, the metabolites can be degraded by microorganisms or remain unaltered and be gradually accumulated.

Several mechanisms have been proposed to explain the degradation of ketones or ketonic compounds by microorganisms. Schühle and Heider (2011) proposed a catabolic pathway of acetone degradation by bacteria. Acetone is firstly carboxylase to acetoacetate (reaction 1) by acetone carboxylase. Activation of acetoacetate to acetyl-CoS (reaction 2) may be catalysed by either CoA ligase or CoA transferase. Reactions 1 and 2 are proposed to be ATP-dependent. Acetoacetyl-CoA is thiolytically cleaved (reaction 3) by a thiolase to form 2 acetyl-CoA (Figure 1.7).

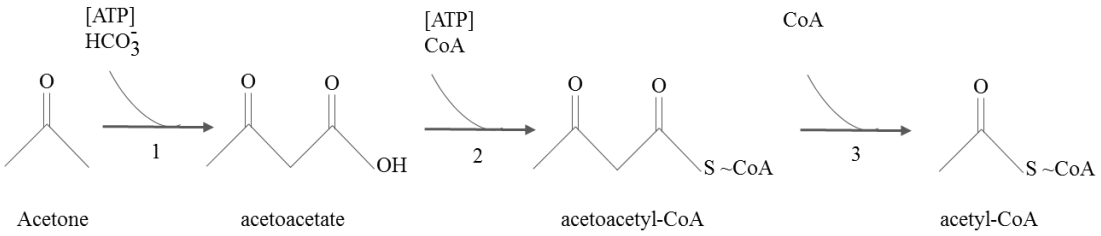

Figure 1.7. Proposed catabolic pathway of acetone degradation by bacteria.

Neilson and Allard (2009) suggest that the anaerobic degradation of ketones occurs by carboxylation followed by hydrolysis (Figure 1.8).

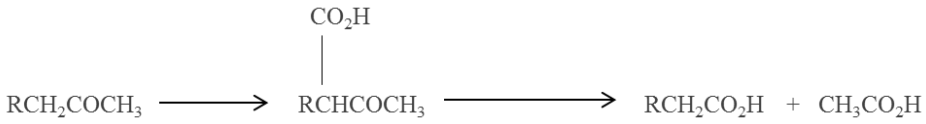

Figure 18. Anaerobic degradation of ketones.

Another mechanism for ketone degradation (methyl ethyl ketone, MEK) is presented in the (Figure 1.9) MEK is carboxilazed by 2-butanone oxidase, originating ethyl acetate. Ethyl acetate is then hydrolyzed by acetylesterase originating acetate and ethanol. Ethanol is finally dehydrogenated by a NADP dependent alcohol dehydrogenase, originating acetaldehyde (www.genome.jp).

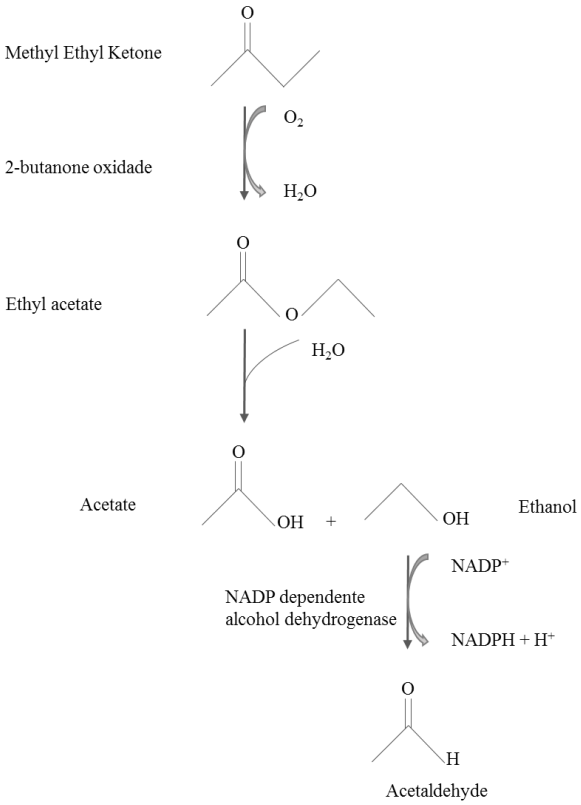

Figure 1.9. Proposed catabolic pathway of methyl ethyl ketone degradation.

1.3.2| Biosorption

Though the ability of active microorganisms to sequester metals from aqueous solutions was explored as early as the XVIII and XIX centuries, it was only in the last 3 decades that active and inactive microorganisms have been used as sorbents for the removal and recovery of different substances from aqueous solutions.

Several definitions of the term biosorption can be currently found. According to Volesky (1990) biosorption can be defined as the different forms of non-active uptake of metals by biological materials (active or inactive biomass) and can occur via complexation, coordination, chelation, ion exchange, adsorption and inorganic microprecipitation. Gadd (1993) defines biosorption as the property of certain biomolecules (or types of biomass) to bind and concentrate selected ions or molecules from aqueous solutions without active uptake. As opposed to a much more complex phenomenon of bioaccumulation based on active metabolic transport, biosorption by inactive biomass (or by some molecules and/or their active groups) is a physiochemical process that occurs

naturally in certain types of biomass and allows them to passively concentrate and bind metals or organic material, even from very dilute aqueous solutions (Volesky 2007; Pina, 2010).

The biosorption processes involve a solid phase, sorbent or biosorbent, and a liquid phase, solvent, usually water, containing the dissolved species to be sorbed, sorbate. Due to higher affinity of the sorbent for the sorbate species, the latter is attracted and bound to it by different mechanisms. The sorption process continues till equilibrium is established between the amount of solid-bound sorbate species and its portion remaining in the solution. The degree of sorbent affinity for the sorbate determines its distribution between the solid and liquid phases. The biosorption mechanisms differ qualitatively and quantitatively according to the species in solution, the biomass used and its processing (Pina, 2010) and may occur by one process or combination of processes, such as: physical adsorption, ionic exchange, complexation, chelation, microprecipitation, intracellular uptake, storage via active transport, among others (Volesky, 1990; Wang and Chen, 2009; Pina 2010). The chemical and biological details of the biosorption processes are very important for the understanding of the role of metallic ions in basic cellular functions and also for the determination of the most effective way to implement these processes on the detoxification of industrial water polluted with heavy metals.

According to the dependence on the cell's metabolism, biosorption mechanism can be classified into metabolism dependent and non-metabolism dependent and considering the location where the metal is retained, biosorption can be classified as extracellular accumulation and/or precipitation, cell surface sorption/ precipitation or intracellular accumulation.

For example, the transport of metal, across the cell membrane leads to an intracellular accumulation, which is dependent on the cell's metabolism. This means that this kind of biosorption, metabolism dependent with intracellular accumulation, may occur only with active cells and it is often associated with an active defence system of the microorganism, in reaction towards presence of toxic metal. For the non-metabolic biosorption, metal uptake may occur by physicochemical interaction between the metal and the functional groups present on the microbial cell surface. This is based on physical adsorption, ion exchange and chemical sorption, which is not dependent on the cells' metabolism. This type of biosorption is relatively rapid and usually reversible (Kuyucak and Volesky, 1988).

The understanding of the biosorption mechanism is fundamental for the development and improvement of wastewater treatment processes (Figure 1.10). A brief description of the main reaction paths concerning metal sorption is given below.

Complexation –formation of molecules or ensembles by the combination of ligands and metal ions. A ligand is either an atom, ion or molecule that bonds to a metal ion, generally involving formal donation of one or more of its electrons. The metal-ligand bonding ranges from covalent to ionic, being the simplest case the complexation by a mono-dentate ligand such RNH_2 and the metal-ligand bond order can range from one to three. The metal removal from solution, after interaction between the metal and the active groups, may also take place by complex formation on the cell surface (Chopra and Pathak, 2010; Tsezos et al. 2006). A significant part of the recent advances in biosorption is based on the classification of elements according to the Pearson's classification (hard-soft acid-base classification). In general, "hard acid" metal ions such as Na^+, K^+, Ca^{2+}, Mg^{2+}, usually essential nutrients for microbial growth, bind preferentially to oxygen-containing "hard bases" ligand such as OH-, HPO_4, CO_3^{2-}, R-COO-, =C=O. "Soft acid" metals such as silver (Ag), gold (Au), platinum (Pt) and palladium (Pd) are bound covalently to the cell wall by "soft bases", ligands containing nitrogen or sulphur (Tsezos et al. 2006).

Although several researchers confirmed that the biosorption of precious metals has a two-step mechanisms comprising first a covalent bonding and then *in situ* reduction (Tsezos et al. 2006; Beveridge and Murray, 1976; Beveridge and Murray, 1980; Remoudaki et al. 1999; Tsezos et al. 1995) the biosorption of calcium, magnesium, cadmium, zinc, copper and mercury by *Pseudomonas syringae* was due only to complexation..

Aksu et al. (1992) hypothesized that biosorption of copper by *Chorella vulgaris* and *Zoogloea ramigera* takes place through both adsorption and coordination bonds between metals and amino and carboxyl groups of the cell wall polysaccharides. Microorganisms may also produce organic acids (citric, oxalic, gluonic, fumaric, lactic and malic acids, for example), which may chelate toxic metals resulting in the formation of metallo-organic molecules (Ahalya et al. 2003).

Coordination – it can be described as any combination of cations with molecules or anions containing free pairs of electrons. Usually, biosorption of toxic metals and radionuclides is based on non-enzymatic processes such as adsorption. Adsorption is due to the non-specific binding of ionic species to polysaccharides and proteins on the cell surface or outside the cell (Tsezos and Volesky,

1981; Mullen et al. 1992). Limited information of surface complexation models, based on the theory of surface co-ordination chemistry is available to describe metal biosorption; however the uniqueness of the metal species should be considered to explain observed metal biosorption capacities and to elucidate biosorption mechanisms (Tsezos et al. 1995; Remoudaki et al. 1999). Bacterial cell walls and envelopes, and the walls of fungi, yeasts and algae, are efficient metal biosorbents that bind charged groups. The cell walls of Gram-positive bacteria bind larger quantities of toxic metals and radionuclides than the envelopes of Gram-negative bacteria.

Chelation - it has been defined as the firm binding of a metal ion to an organic molecule (ligand) to form a ring structure. Organic molecules containing more than one functional group with donor electron pairs can donate these to a metal atom. This can result in the formation of a ring structure involving the metal atom, which protects the metal from participating into specific chemical reactions. In general, since a chelating agent can simultaneously bond to a metal ion in more than one site, chelated compounds are more stable than complexes involving mono-dentate ligands. Chelation stability tends to increase with the number of chelating sites available on the ligand. Thus chelation of metals by donor ligands of biopolymers leads to the formation of stable species (Chopra and Pathak, 2010; Tsezos et al. 2006).

Ion-exchange – metal ions from dilute solutions are exchanged with ions held by electrostatic forces on the exchange resin. Ion exchange is a reversible chemical reaction where an ion in solution is exchanged for a similarly charged ion attached to an immobile solid particle. According to Muraleedharan and Venkobachr (1990) ion exchange reactions are stoichiometric and reversible.

Adsorption – it is based in the principle that a solid or gel in contact with a gaseous or liquid solution, has the tendency to accumulate on its surface solute molecules, due to the unbalance of the existing surface forces. The molecules are attracted to the surface but do not enter the intraparticle minute spaces in the solid as in absorption. This process creates a film of adsorbate on the surface of the adsorbent.

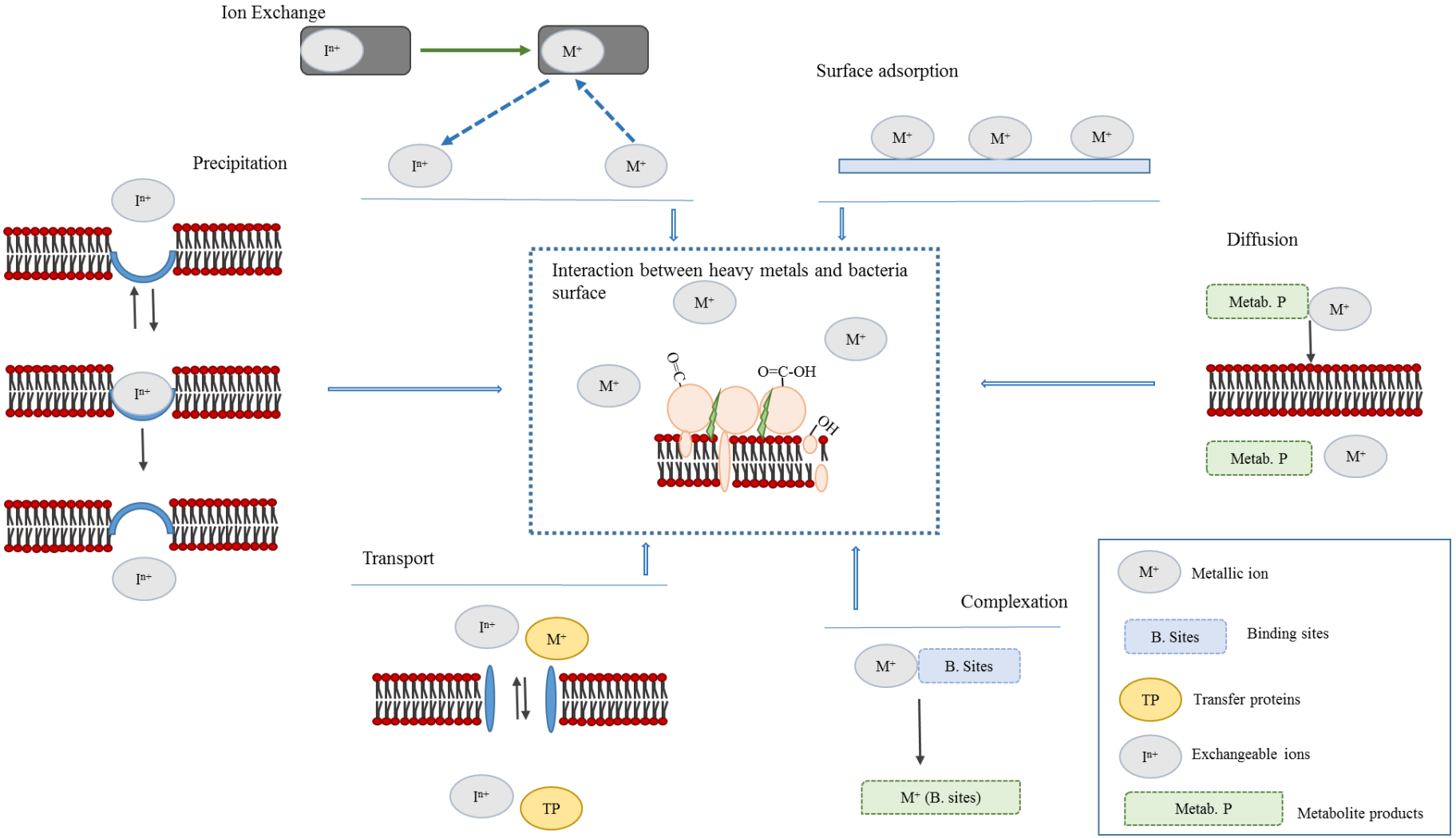

Figure 1.10. Mechanisms for the biosorption of metals (adapted from Hansda et al. 2015)

Precipitation – as previously mentioned, precipitation can be either dependent or independent on the cellular metabolism. In the former case, the metal removal from solution is often associated with active defence system of the microorganisms (Ahalya et al. 2003). The term precipitation refers in most cases to the formation of insoluble inorganic metal precipitates. However, in the case of biosorption by microbial biomass, organic metal precipitates may also be formed due to the binding of metals to the exopolysaccharides, excreted by some prokaryotic (bacteria and archaebacteria) and eukaryotic (algae and fungi) microorganisms (Tsezos et al. 2006).

It is important to highlight that the biosorption mechanisms are complicated and not completely understood yet.

1.3.2.1 | Biological Sorbents

Biological sorbents, usually designated as biosorbents, can be defined as a natural and solid material that will sorb the dissolved species in aqueous solutions and can be classified into low and high cost sorbents.

A wide diversity of microbial cells has been investigated as biosorbents for the removal of different metals and organic compounds. These materials can be classified into the following categories: industrial waste, agriculture wastes, polysaccharide materials, bacteria, fungi, yeast and algae. The first seven materials are considered as low cost biosorbents because they can be collected directly from the environment and its cost is reduced. The last two materials are considered high cost materials, since they are manufactured with a particular purpose (Wang and Chen, 2009; Chopra and Pathak, 2010). Regardless of the category and cost, biosorbents need characteristics suitable for process application such as hardness, porosity, particle size, density, high versatility, metal selectivity and resistance to a broad spectrum of variable solution parameter (temperature, pH and pollutants content, for example) (Volesky, 1990).

1.3.2.1.1| Fungi

Norris and Kelly (1979) studied the extent and selectivity of the uptake of metals ions by different live species of yeast. According to these authors copper was accumulated at a relatively high level in *Rhodotorula mucilaginosa* (014.29 mg/g), whereas *Candida utilities* and three species of *Saccharomyces* exhibited a relatively lower uptake (11.44 mg/gand 1.04 mg/g, respectively). Morley and Gadd (1995) investigated the removal of divalent ions (Cu^{2+}, Cd^{2+} and Zn^{2+}) from pH buffered solutions by the soil fungi *Rhizopus arrizhus* and *Thricoderma viride*. The concentration used by these authors ranged from 0 μM to 1000 μM, in the presence and absence of clay minerals montmorillonite and kaolinite. The uptake of the metals was followed at three different pH values in order to determine the influence of pH on the biosorption process. The results obtained showed that the clays used demonstrated a more rapid uptake of the metal ions with equilibrium being reached in less than 2 minutes compared to 3 hours to 6 hours taken by the fungal biomass. On a dry weight basis the clay minerals took up greater amounts of metal (up 48.89 mg/g for Cd^{2+}, up to 15.57 mg/g for Cu^{2+} and up to 15.63 mg/g for Zn^{2+}) than the fungi (up to 8.77 for Cd^{2+}, up to 2.22 for $Cu^{2+}$and up to 3.07 for Zn^{2+}). However, when the data were expressed in terms of metal bound per unit surface area, the fungi showed much greater sorption capacities (up to 36.6 μmol/m^2) than the clays (up to 3.1 μmol/m^2). Mixtures of montmorillonite and fungal biomass showed reduced uptake of metals, depressed below calculated values by up to 37 % at pH 4, possibly because of masking of exchange sites. Experiments performed by Mukhopadhyay et al. (2007) allowed the determination of the effect of several parameters (pH, initial metal concentration and biomass concentration) on the biodegradation of copper compounds by *Aspergillus niger*. It was observed in these assays that the increase on the initial concentration of metal compound led to higher biodegradation efficiency, whereas an increase on the initial concentration of biomass led to a decrease on the biodegradation efficiency, which may be explained either the fact that when in the presence of highly concentrated solutions, the ratio between the number of available sites and metal ions present is solution is reduced or by the fact that in diluted solutions the number of metal ions is reduced when compared with the number of available binding sites Pipíška et al. (2007) investigated the sorption of cobalt by the foliose lichen *Hypogymnia physodes* from $CoCl_2$ solutions spiked with $^{60}Co^{2+}$. It was also possible to conclude that after 24 hours the biosorption is not pH-dependent within the range of pH 4 to 7, negligible at pH 2 and is not dependent on metabolic activity, and up to 98 % of Co taken up by lichen can be removed by washing with 0.1 M of $NiCl_2$ at 20°C. This means that only a small fraction

of the cobalt is localized intracellularly. Studies conducted by Alexieva et al. (2008) revealed the excellent ability of yeasts belonging to the genera *Trichosporon* to degrade a wide range of toxic compounds such as hydroquinone, catechol and resorcinol, present in industrial effluents. Kapor and Viraraghavan (1998) studied the ability of an acclimatized culture of *Aspergillus niger* to remove cadmium, copper and nickel and the functional groups involved in the biosorption process of those metals.

1.3.2.1.2| Algae

The algae have many features that make them ideal for the selective removal and concentration of metals, which include high tolerance to metals, ability to grow both autographically and heterotrophically, large surface area/volume ratios, phototaxy, phytochelatin expression and potential for genetic manipulation. The use of algae in biosorption is reduced as compared to those using other biomass, mainly fungi and bacteria, and is still lower for multimetallic systems (Chopra and Pathak, 2010). Antunes et al. (2003) investigated the removal of copper ions from aqueous solutions by *Sargassum* sp. in batch conditions and found that the copper uptake capacity (94.05 mg/g) of *Sargassum* sp. proved it to be an excellent biomaterial for accumulating and recovering copper from industrial solutions. The biosorption of lead by the algae *Laminaria japonica*, after being subjected to different pre-treatments, was studied by Luo et al. (2006). *Laminaria japonica* was washed with distilled water and chemically modified by crosslinking with epichlorohydrin (EC_1 – washed with 70 % aqueous 2-propanol and then dry in an oven at 60°C overnight, EC_2 – washed with 20 % aqueous 2-propanol and then dry in an oven at 60°C overnight) or by oxidation with potassium permanganate ($KMnO_4$). The results achieved by these authors showed that the removal capacity of the lead compounds increased over time, when the seaweed undergoes a pre-treatment (EC_1, EC_2 or $KMnO_4$) reaching equilibrium after two hours and that the process is pH dependent. The maximum values for the removal efficiency were obtained for a range of pH between 4.0 and 5.3 when the EC_1 and EC_2 treatment was applied. Maximum removal values were obtained for pH values between 3.0 and 5.3 when the pre-treatment with $KMnO_4$ and distilled water was applied. Omar (2008) carried out a study on biosorption of copper, nickel and manganese using non-living biomass of marine alga, *Ulva lactuca*. The results of this study indicated that the biomass of *Ulva lactuca* is suitable for the development of an efficient metal removal system for the removal of Cu^{2+}, Ni^{2+} and Mn^{2+} from aqueous

solution. Biosorption of these metals on the algal biomass showed a higher affinity for Cu^{2+} compared to Ni^{2+} and Mn^{2+}. Al-fawwaz and Wan Maznah (2008) studied that biosorption of copper using live and dead green microalgae isolated from Penang river, Malaysia. The copper biosorptive capacity of green microalgae (*Chlorella* sp. and *Scenedesmus* sp.) has been studied to find the differences in copper uptake using live and dead microalgae in aqueous solutions. The study indicated that using dead *Chlorella* sp. and *Scenedesmus* sp. was better than using live one and the biosorption efficiency for *Chlorella* sp. was better than *Scenedesmus* sp. Zhou et al. (2012) studied the removal of zinc and copper by two freshwater green microalgae, *Chlorella pyrenoidosa* and *Scenedesmus obliquus*, during 8 days and investigate changes of algal ultra-structure and photosynthetic pigment. The results obtained by these authors revealed that low zinc and copper concentrations induced increase in algal growth, whereas of high zinc and copper concentrations suppressed the growth of both algae. High metal concentrations also decreased the photosynthetic pigments and destroyed algal cell ultra-structure. The zinc removal efficiency by both algae increased rapidly during the first day and thereafter remained nearly constant throughout the experiment. The copper removal efficiency by both algae increased slowly during the whole experimental periods. In all cultures, the quantity of both metals removed intracellularly was much lower than the adsorbed quantity on the cell surface. Non-metabolic adsorption played an important role in the removal of metals by both algae.

1.3.2.1.3| Bacteria

Tornebe and Edwards (1976) described the capacity of *Micrococcus luteus* and *Azotobacter* sp. cells to immobilize 4.9×10^{2} mg and 3.1×10^{2} mg of lead per gram of dry cell weigh, respectively. These authors also confirm that the lead produced no toxic effect on growth of the cells and that about 99% of the metal was found in the cell wall and membrane. Burke and Pfisher (1986) investigated cadmium uptake by a Cd^{2+} sensitive (IAI) and a Cd^{2+} resistant mutant (IAIr) strain of *Bacillus subtilis* using isotopically labelled Cd^{2+}. The resistant mutant strain IAIr, showed lower uptake values, when compared to the values obtained for the sensitive strain IAI. According to Beveridge (1989), bacteria make excellent biosorbents because of their high surface-to-volume ratios and a high content of potentially active chemisorption sites such as on teichoic acid in their cell walls. Churchill et al. (1995) used two Gram-negative strains *Escherichia coli* K-12 and *Pseudomonas aeruginosa* and a Gram-positive strain *Micrococcus luteus* to demonstrate biosorption of Cu^{2+}, Cr^{3+}, Co^{2+} and Ni^{2+}. Their

sorption binding constants suggested that *E. coli* cells were the most efficient at binding copper, chromium and nickel and *M. luteus* sorbed cobalt most efficiently. Silva et al. 2008, investigated the biosorption ability of *Arthrobacter viscosus* in removing hexavalent chromium from contaminated wastewaters. The effect of biomass concentration on Cr(VI) reduction and removal from aqueous solution was studied in the range of 1.2 g/L to 5.3 g/L. The removal of Cr(VI) and total chromium increased linearly with the increase of biomass concentration. The best removal efficiencies of Cr(VI) and total chromium were reached for the highest biomass concentration, 72.2 % and 44.0 %, respectively. The increase in biomass concentration did not produce significant changes in the uptake values. The maximum uptake value, 8.2 mg/g was obtained for a biomass concentration of 2.3 g/L.

1.3.3| Bioaccumulation

Bioaccumulation can be defined as the intracellular accumulation of sorbates (metal or other molecules) in a tissue or a whole organism that results from exposure. It occurs in two phases. The first phase is similar to biosorption whereas the second phase is slower and comprises the transport of the sorbate to the interior of the cells. Bioaccumulation is a non-equilibrium process (Dercová et al. 2005; Hussein et al. 2004) and arises from all different environmental sources including water, air, solid phases (organic and inorganic phases in sediments and soils).

Bioaccumulation holds certain intrinsic disadvantages over other biological processes, such as biosorption especially in terms of versatility, costs, pollutants affinity, uptake capacity, regeneration and reuse capability. The high costs associated with bioaccumulation are usually related to the mandatory nutrient and cultivation requirements, whereas the lower uptake capacity is influenced by the toxicity of the pollutant and is related to the fact that intracellular accumulation is time consuming. Consequently, bioaccumulation can succeed only if the selected microorganisms possess outstanding resistance towards the hazardous compounds and are versatile in relation to an extensive range of environmental conditions (Mishra and Malik, 2013).

1.3.4| Bioremediation

The bioremediation process comprise the control and manipulation of biological processes, usually microbiologic and in situ, to degrade the organic pollutants present in soil and sediments in less toxic and/or non-toxic compounds and restrain elements such as metals. The degradation is generally done by biostimulation or bio-addition, whose isolated or combined execution may lead to a rapid and complete pollutant degradation. The biostimulation aims to stimulate and increase the activity of decomposing microorganisms of native communities present in a particular section of the contaminated section, through the addition of nutrients, electron and receptors donors.

Bioaugmentation consists in the addition of new microorganisms, native or non-native (genetically modified or not) with the capability of specifically degrade the pollutant, using it as an energy and carbon source to the existent community (Quintelas, 2007). Bacteria, fungi, plants or any mind-green algae are some of the organism used in bioremediation. The microorganism and treatment selection is determined by the nature, concentration and bioavailability of the toxic material, and by the physical and biological characteristics of the system to be treated (nutrients composition and microbial population).

1.3.5| Factors Affecting Biological Processes

As previously mentioned, the mechanisms involved in biosorption include several processes such as complexation, coordination, chelation, ion exchange, adsorption and inorganic microprecipitation. It is the combination of some these steps, each functioning independently, that contributes to the overall pollutant uptake. Biosorption is a rather complex process influenced by several parameters such as the types of biomaterials, status of the biomass (active or inactive), chemical properties of the pollutant to be sorbed, initial concentration of the sorbent, biosorbents dosage, ionic strength, chemical properties of the sorbate and its functional groups and environmental conditions like temperature and pH (Javanbakht et al. 2014).

In the past years, biosorption of metals by microbial cells has been recognized as a potential alternative to existing technologies for waste streams, natural waters and contaminated soil, and as a consequence it has been studied extensively. Microorganisms can affect metal and organic

compounds concentrations in the environment since they exhibit a strong ability for the removal of a wide diversity of pollutants from solution through enzymatic or non-enzymatic mechanisms (Volesky, 1990; Wang and Chen, 2009; Chopra and Pathak, 2010).

1.3.5.1 | Cell Wall

The cell wall is usually one of the first cellular structure that comes in contact with the soluble metal species in the extracellular environment. The cell wall is a well-defined polymeric matrix located just outside the plasma membrane of eubacteria, archaebacteria, fungi, algae and plant cells and can be composed by polysaccharides, proteins, lipids or a combination of these same compounds. These molecules have abundant metal binding groups such carboxyl, sulphate, phosphate and amino groups. These molecules have abundant metal binding groups such carboxyl, sulphate, phosphate and amino groups. The cell wall increases the mechanical strength and resistance of the cell, it protects the microorganisms against the hazardous conditions of the environment, controls the fluxes between the cytoplasm and the surrounding environment and determines the shape and the rigidity of the cell (Volesky, 1990; Tsezos et al. 2006).

Fungi

It is generally considered that eukaryotic microorganisms are always of unicellular nature, however, it has to be noticed that vegetative phases of fungi and algae are frequently multicellular. The fungal cells are protected by a true cell wall which is rigid as in bacterial cells, though it has different chemical and structural characteristics. The cell walls of fungi are typically composed by proteins, lipids and others substances and present a multilaminate microfibrilliar structure. Previous studies revealed two phases: an outer layer consisting of glucans, mannans or galactans and an inner microfibrillar layer with crystalline properties which are conferred by the parallel arrangement of chitins chains, and sometimes of cellulose chains (Volesky, 1990).

Algae

The algae cell wall is structurally similar to the fungal cell wall: a multi-layered microfibrillar framework generally composed of cellulose (1 % to 90 % of the wall constituents) and interspersed with amorphous material, such as glycoproteins. Most of the algae are also covered by a mucilaginous layers characterized by a significant metal sorption capacity due to the presence of uronic acids (Volesky, 1990; Tsezos et al. 2006; Wang and Chen, 2009).

Bacteria

Although the walls of all bacteria present common features, such as composition material, the cell structure can vary significantly according to the peptidoglycan percentage allowing their classification into three major groups: the Gram-positive bacteria, the Gram-negative bacteria and the archaebacteria (Figure 1.11). Peptidoglycan is a rigid, porous and amorphous molecule that consists of linear chains of the disaccharide N-acetylglucosamine-β-1, 4-N-acetylmuramic acid (Volesky, 1990; Wang and Chen, 2009). The cell wall of Gram-positive bacteria is 50 nm to 150 nm thick and is mainly composed of several layers of peptidoglycan, which accounts for 40 % to 90 % of the total cell wall material. Peptidoglycan layers have two main constituents covalently attached, the teichoic acid and the teichuronic acids, which contribute to the anionic character of the cell wall. These two acids were proved to participate in the metal trapping, but they are mainly known to play a physiological role specially by supplying magnesium to the plasma membrane (Volesky, 1990; Wang and Chen, 2009).

The cell walls of Gram-negative bacteria are thinner than the cell walls of Gram-positive bacteria. They are usually 30 nm to 80 nm thicker and the peptidoglycan is sandwiched between the plasma membrane and the outer membrane. The peptidoglycan layer is only 15 nm to 20 nm thick and accounts for approximately 10 % of the cell wall material. The outer membrane is composed of an outer layer of phospholipids, proteins and lipopolysaccharides, being the last one, one of the main responsible for the heavy negative surface charge of this kind of bacteria (Volesky, 1990).

The cell walls of archaebacteria lack muramic acid, a typical constituent of the eubacterial cell wall. The archaebacteria classified as Gram-positive archaebacteria have cell walls containing

pseudomurein, methanocondroitin or heteropolysaccharides whereas the archaebacteria classified as Gram-negative archaebacteria are composed of either a single surface layer protein or glycoprotein or a cell envelope layer and the cells are enclosed in a tubular sheath (Volesky, 1990; Wang and Chen, 2009).

Cells of a number of bacterial strains belonging to Gram-positive, Gram-negative and archaebacterial groups are often covered by an additional surface layer non-covalently associated with the underlying cellular wall, the S-layers. These layers are assumed to be of prime importance for the survival of bacteria in the natural environment and it is usually composed of regular arrays of homogeneous polypeptides (mainly acidic amino acids) and sometimes of carbohydrates as a secondary component (Volesky, 1990).

It is possible to conclude that the biomolecules (protein, polysaccharides and EPS), that constitute the cell wall of microorganism, such as bacteria, fungi and algae possess functional groups that have a significant potential for metal binding.

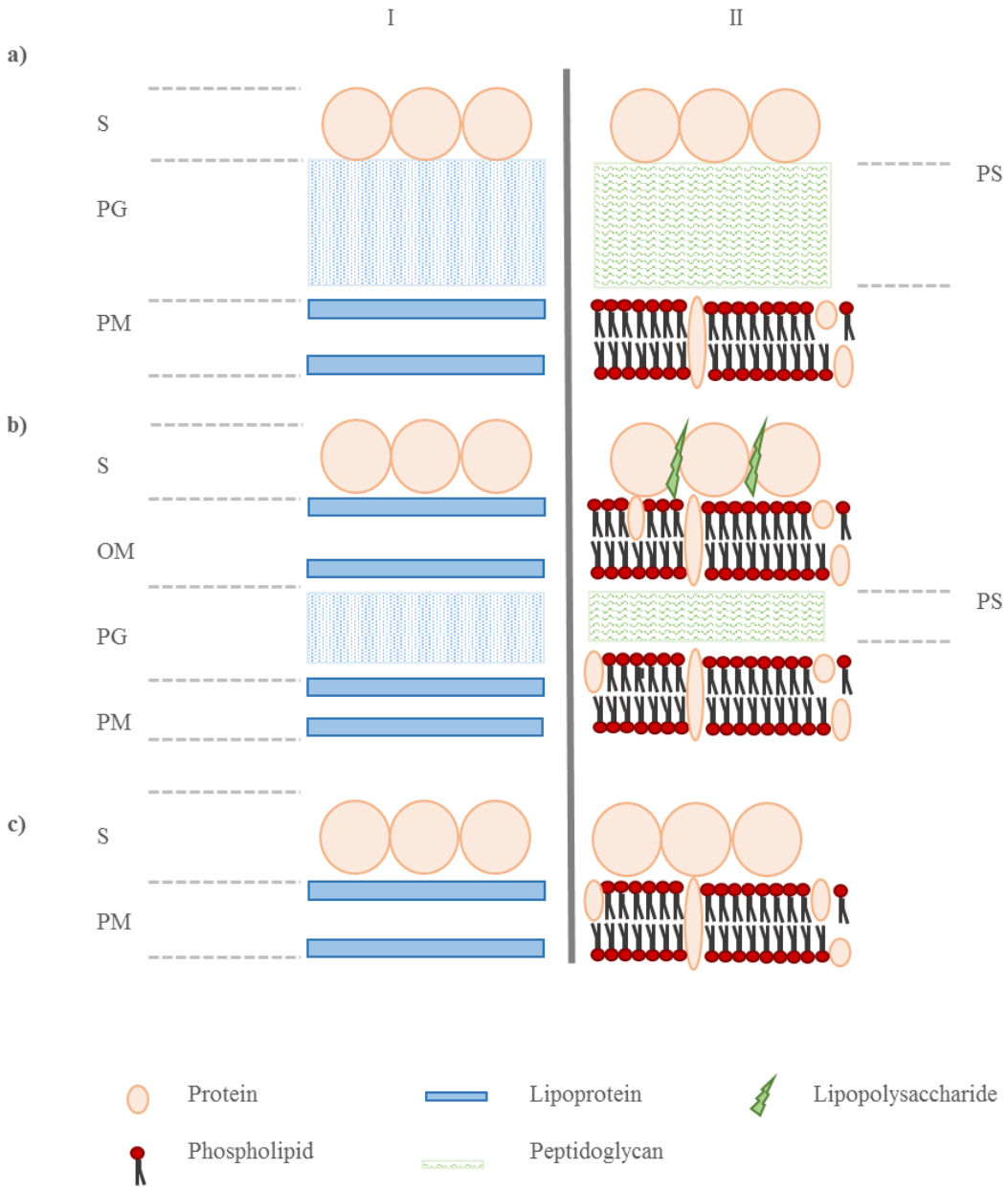

Figure 1.11. Schematic diagram of main categories of bacterial cell walls including regular cell surface layers: (I) thin section profiles, (II) molecular architecture showing major components. **a)** Gram positive cell envelope; **b)** Gram-negative cell envelope; **c)** cell envelope structure that lacks a rigid cell wall component. OM – outer membrane; PG – Peptidoglycan containing layer; PM – Plasma membrane; PS – Periplasmatic space, S – surface layer.

1.3.5.2| Functional Groups on the Surface of Microorganisms

According to Volesky (2007) the main functional groups accountable for sorption processes are the imidazole, hydroxyl phosphonate, sulfonate, amide, phosphodiester, carboxyl and carbonyl groups. Some of these functional groups detected by infrared spectroscopy (phosphate bands at 1237 cm^{-1} and carbohydrate bands at 1070 cm^{-1} next to hydrocarbon sorption bands in the wavelength region between 3000 cm^{-1} and 2800 cm^{-1}) (Van der Mei et al. 1996) are known to be present on the *Streptococcus* sp. surface and be responsible for the removal of toxic compounds such as diethylketone (Costa et al. 2014). Studies conducted by Zvinowanda et al. (2010) indicated that the hydroxyl (-OH) and the amino groups ($-NH_2$) identified on the surface of *Zea mays* tassel powder, by the Fourier transform infrared (FTIR) spectroscopy are responsible for the uptake of lead (PB) on the tassel.

FTIR analyses conducted by Hasan et al. (2009) have also indicated the participation of carboxyl (-COOH), hydroxyl (-OH), and amine (-NH2) groups present on the biomass surface of *Aeromonas hydrophila* in the sorption of Pb(II). Studies conducted by Shraboni et al. (2008) revealed the presence of amino ($-NH_2$), carboxyl (-COOH), and phosphate ($-PO_4H_2$) groups on the surface of *Mucor rouxii*.

1.3.5.3| Operational Parameters: pH, Temperature, Biosorbents Dosage and Sorbate Initial Concentration

The pH is one of the parameters that affect more significantly the efficiency of the biological treatments of contaminated soil and aquatic systems. It strongly influences not only the solution chemistry: complexation by organic and/or inorganic ligands, precipitation, hydrolysis, redox reactions, the speciation and biosorption availability of the metals, but also the activity of the functional groups (Choudhary and Sar, 2009). The pH influences the global electric charge of the biosorbents, by either protonation or deprotonation of the metals binding sites. It is commonly recognized that the uptake capacity of metals cations such as Al^{2+}, Ni^{2+}, Cd^{2+} and Mn^{2+} by biosorption, increases with the increasing of the pH values and decreases with the decreasing of the pH values. At lower pH values, the actives sites of the biosorbents are protonated and became positively charged, hence producing an electrostatic repulsion with the metals cations and competition between

metal cations and protons for the active sites occurs. It is important to highlight that, despite the biosorption of the cationic metal is enhanced with the increase of pH, the formation of metal hydroxides may occur, which due to its reduced solubility may precipitate (Naja et al. 2010). As opposed to cationic metals, the uptake of anionic metals is favored at lower pH, since the functional groups present on the sorbent surface became positively charged, thus increasing the electrostatic forces between the sorbate and the sorbent surface and the uptake. It is important to highlight that as the pH increase, the surface becomes negative and the biosorption capacity decreases (Wang and Chen, 2006)

The temperature also exerts influence on the biosorption processes, but in a more restricted way (within the range from 20 °C to 35 °C). Usually, at higher temperatures, the sorption processes are enhanced by the increase on the kinetic energy of the sorbate and by the surface activity. Nevertheless, extreme temperatures can cause irreversible physiological damages to the biosorbents (Sag and Kutsal, 2000).

Concerning the effect of the initial sorbate concentration on the uptake, if the biosorbent dosage is kept constant, the uptake is expected to increase with the increase of the initial sorbate concentration. Since the uptake is inversely proportional to the biosorbent concentration, when the biosorbent concentration is small it is expected to have higher uptakes and lower removal efficiencies, whereas when the biosorbent concentration is higher, the amount of sorbate sorbed is also higher due to the increased surface area of the biosorbent, which in turn increases the number of actives sites available for sorption.

1.3.6| Sorption Using Mineral Clays

Natural adsorbents such as mineral clays have been used with success, for the decontamination of wastewaters contaminated with metals and organic compounds. The large surface area of natural clays particles, the competitive prices, the chemical and mechanical stability and the high cation-exchange capacity account for the outstanding aptitude of the clays to sorb different type of sorbates (Quintelas et al. 2010, 2013).

Although the term clay has been revised several times, without changing the fundamental characteristics involving particle size, plasticity and hardening on fire. The term clays usually denotes to a naturally occurring material composed primarily of fine-grained minerals, that will harden when dried or fired and that present plastic properties in the presence of appropriate water contents. The clay-size fraction of soils consists of mineral particles, usually planar arrays of Sio_4 structural units and countless structural hydroxyls and water units and with an equivalent diameter less than 2 μm. Clay-minerals present usually an equivalent diameter lower than 2 μm and tend to crystallize in the aqueous environment at the Earth's surface from the ions released by the weathering process of primary minerals, such as quartz, olivine, feldspars, pyroxenes, micas and other clay minerals formed under extreme pressure and hot conditions. Most of the chemical and physical characteristics and properties of soil (soil mitigation capacity towards a specific pollutant, capacity to fix phosphorous fertilizers and how it will reflect on its availability to crops, shrink-swell properties and cation exchange capacity) are influenced by the molecular-scale differences in soil clay-minerals.

Within the crystalline structure of soil clay minerals it is possible to distinguish two distinct structures arrangements. The first structural arrangement (tetrahedron) consists of three O^{2-} ions organized in a triangle and a fourth O^{2-} ion occupying the hollow formed by the other three ions. The centres of the four O^{2-} ions form the vertices of a regular tetrahedron and the reduce space located in the centre is named tetrahedral sites. The cations placed in these tetrahedral sites are in tetrahedral and fourfold coordination, since they are enclosed by and bounded to four O^{2-} ions. The second structural arrangement (octahedron) consists of six O^{2-} ions thoroughly packed, three of which are organized in one plane, forming a triangle, where the other three O^{2-} ions are also organized in the form of a triangle, with a rotation of 60 ° in relation to the first three O^{2-} ions and in a second plane so that the two triangles interconnect. The centres of the six O^{2-} ions origin the vertices of a regular octahedron, where the small central space is named octahedral site. The cations placed at the octahedral site are six fold or octahedral coordination, since they are enclosed by and bonded to six three O^{2-} ions (Schulze, 2005)

Clays usually possess trivial amounts of impurities such as calcium, potassium, sodium, iron or magnesium and are the result of chemical weathering of other silicates minerals at the Earth surface (Guggenheim and Martin, 1995). The retention capacity of clays is a consequence of the presence of unbalance electrical charges existing on the surface of the clay particles. The electrical charge on the clay surface is considered unbalance since some regions of the clay surface are positively

charged, thus attracting anionic species, whereas other regions of the clay surface are negatively charged, and therefore able to attract cationic species. When immersed in water, clays tend to form colloidal suspensions, but when dried clays become rigid and lose their malleability, being thus easily moulded to the form that they will retain when dried.

Clays properties include colour after firing, contraction under air drying and firing, cohesion, fineness of grain, plasticity in the presence of water and rigidity when dried. Taking these properties into account it is possible to classify clays in two groups, the residual and the transported clays. Residual clays are found in the place of origin and are usually produced by surface weathering, whereas the transported clays (also known as sedimentary clays) consist in clays removed from the place of origin by an erosion agent and posteriorly deposited in a new place.

The majority of clay minerals are defined as hydrous aluminium silicates that are structurally composed of planes of cations organized in tetrahedral or octahedral sheets, coordinated with oxygen. These tetrahedral or octahedral sheets are organized into layers often described as 1:1 – and 2:1- type minerals. Based on the number of tetrahedral and octahedral sheets composing the layer structure. The 1:1 layer structure comprises a unit composed by one tetrahedral and one octahedral sheet with the apical O^{2-} ion being shared with the octahedral sheet. In 1:1 layers there are three planes of anions, one plane comprises the basal O^{2-} ions of the tetrahedral sheet, the second plane consists of O^{2-} ions common to both the octahedral and the tetrahedral sheets (with the hydroxyl group (OH-) belonging to the octahedral sheet) and the third plane comprise only, the hydroxyl group (OH-) belonging to the octahedral sheet. The 2:1 layers are structurally more diverse than the 1:1 layers and consists of two tetrahedral sheets, one of which is connected to each side of the octahedral sheets. The 2:1 layers possess four planes of anions (two outer planes and two inner planes. The two outer planes comprise the basal O^{2-} ions of the two tetrahedral sheets, whereas the two inner planes comprise the hydroxyl group (OH-) belonging to the octahedral sheet, plus the O^{2-} ions common to the two tetrahedral sheets and the octahedral sheet. Furthermore some 2:1 clay minerals possess interlayers sites between consecutive 2:1 units, which can be occupied by interlayer cations often hydrated (Schulze, 2005).

In this project four clays, vermiculite, bentonite, sepiolite and kaolinite, were tested with the primary purpose of selecting the clay with the best support characteristic for the biofilm formation and secondly evaluated their sorption capacity.

1.3.6.1 | Vermiculite

Vermiculite has a 2:1 layers structure and presents a layer charge of 0.9 to 0.6 per formula unit and includes hydrated exchangeable cations in the interlayers, essentially Ca^{2+} and Mg^{2+} (Figure 1.12). The idealized formula of vermiculite weathered from muscovite is $EC^{+}_{0.75}Al_2(Si_{3.25}Al_{0.75})O_{10}(OH)_2$ where EC denotes the exchangeable cations. The high cation exchange capacity and the high affinity for weakly hydrated cations of vermiculite is caused by the high charge per formula unit (Schulze, 2005).

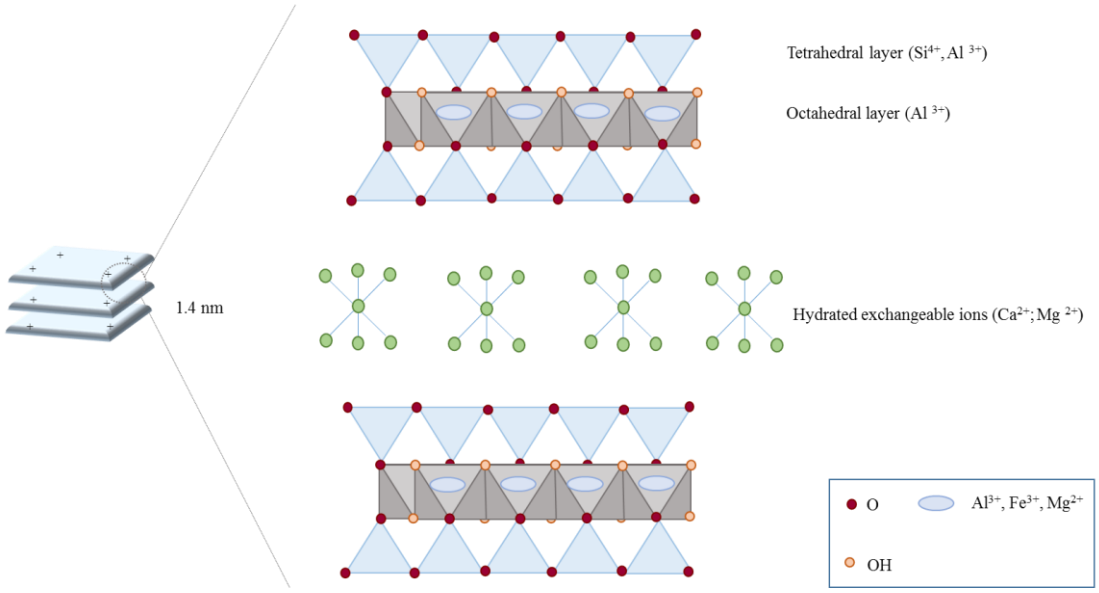

Figure 1.12. Vermiculite crystalline structure

The weathering of pyroxene, mica, chlorite or other similar minerals (Brown 1961) to vermiculite, a hydrated magnesium aluminium silicate, usually occurs due to replacement of the K^+ ions present in the interlayer sites of vermiculite by hydrated exchangeable cations. The positive charge deficiency of vermiculite is caused by the tetrahedral replacement of Al and Fe(III) by Si and is usually compensated by the presence of interlayer cations. This high charge deficiency is accountable for the capacity of vermiculite to adsorb either metals or organic compounds between its layers. From the catalytic point of view, vermiculite is a very interesting material due to the thermal resistance and the number of tetrahedral replacements, which guarantee the presence of a larger number of

Brønsted-type acid sites. Vermiculite presents a high cation exchange capacity (CEC) from 100 meq/100 g to 150 meq/100 g.

1.3.6.2| Bentonite

Bentonite is an aluminium phyllosilicate montmorillonite clay that consists of two tetrahedral layers and one octahedral layer (2:1) (Figure 1.13). Despite sharing a common elementary structure, the numerous types of bentonite are very different regarding to their chemical composition and to physical state of their components, which are responsible for bentonite different properties and define its technological applications.

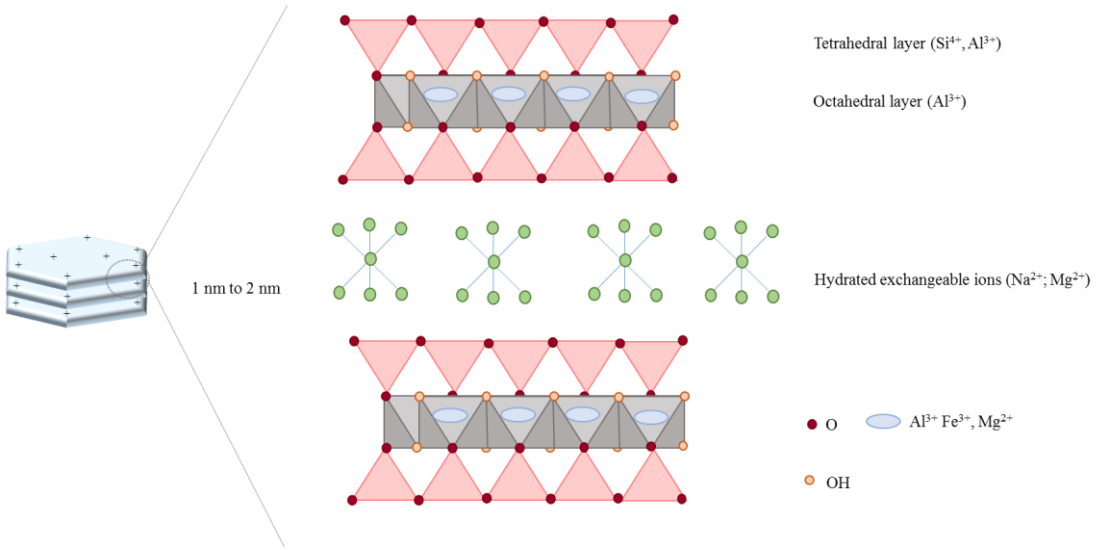

Figure 1.13. Bentonite crystalline layer structure

Montmorillonite is a cluster of lamellar platelets, assembled together by electrochemical forces and containing interposition water. Each platelet comprises three sandwich-arranged layers: a central octahedral alumina (Al_2O_3) layer and two tetrahedral silica (SiO_2) layers. The silicon ion and the aluminium ion often experience isomorphs substitutions by lower valence metals, such as iron and magnesium, which lead to an unbalanced charge, compensated by water molecules bonded together

by ion-dipole forces and exchangeable cations, in particular magnesium (Mg^{2+}) calcium (Ca^{2+}) and sodium (Na^{+}) ions. These ions, without further place inside the reticular structure, migrate to the outer silica layers and are responsible for hydration in the crystal structure.

Every clay has a constant maximum amount of exchangeable cations, as specified by its CEC assessed in milliequivalents per gram (meq/g) or more often per 100 grams (meq/100 g). Bentonite cation exchange capacity varies according on the level of isomorphs substitutions occurred within the lattice (Contreras, 2014).

1.3.6.3| Kaolinite

Kaolinite is a 1:1 aluminium phyllosilicate mineral which chemical structure contains Si^{4+} in the tetrahedral sites bonded to the Al^{3+} in the octahedral sites by the sharing of oxygen atoms between Si^{4+} and Al^{3+} in adjacent sheets (Figure 1.14) (Turan et al. 2007).

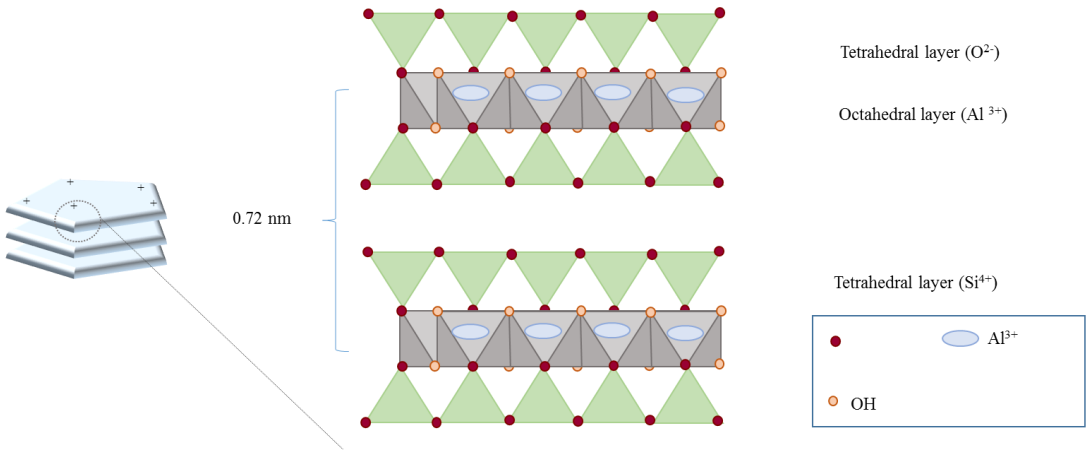

Figure 1.14. Kaolinite crystalline layer structure.

Kaolinite's 1:1 layers are electrically neutral due to the extremely reduced number of substitutions, consequently the area surface and the cation exchange capacity is naturally reduced. The adjacent layers of 1:1 kaolinite are kept together through the bounding of the hydroxyls (OH) of the exterior plane of the adjacent octahedral sheet with the hydrogen (H^{+}) of the basal O^{2-} ions of the tetrahedral

sheet (Schulze, 2005). Kaolinite is a common component of soils and sediments and the exchange sites are found on the surface of kaolinit with no interlayer exchange sites. According to Sari et al. (2007), the sorption properties of kaolinite are influenced by the nature of its surface and edges. The variable charge of kaolinite can be related to the chemical reactions between the ions present in aqueous solution and the ionisable surface groups present mainly on the edges of the clay surface.

1.3.6.4| Sepiolite

Unlike vermiculite, bentonite and kaolinite, sepiolite has a continuous tetrahedral sheets, however the adjacent tetrahedral groups inside the tetrahedral sheet have opposite directions (Schulze, 2005). This results in a structure that can be described as a quincunx of talc-type sheets separated by parallel channels, which in turn forms needle-like particles instead of plate-like particles (Figure 1.15). Despite of having the highest surface area of all the clay minerals, the negligible negative charge existent on the silicate lattice makes the cation exchange capacity very small. The high surface area and porosity, as well as the unusual particle shape of sepiolite are responsible for its excellent sorption capacity and colloidal properties (http://www.ima-europe.eu). Despite of having the highest surface area of all the clay minerals, the negligible negative charge existent on the silicate lattice makes the cation exchange capacity, very small. The high surface area and porosity, as well as the unusual particle shape of sepiolite are responsible for its excellent sorption capacity and colloidal properties (http://www.ima-europe.eu).

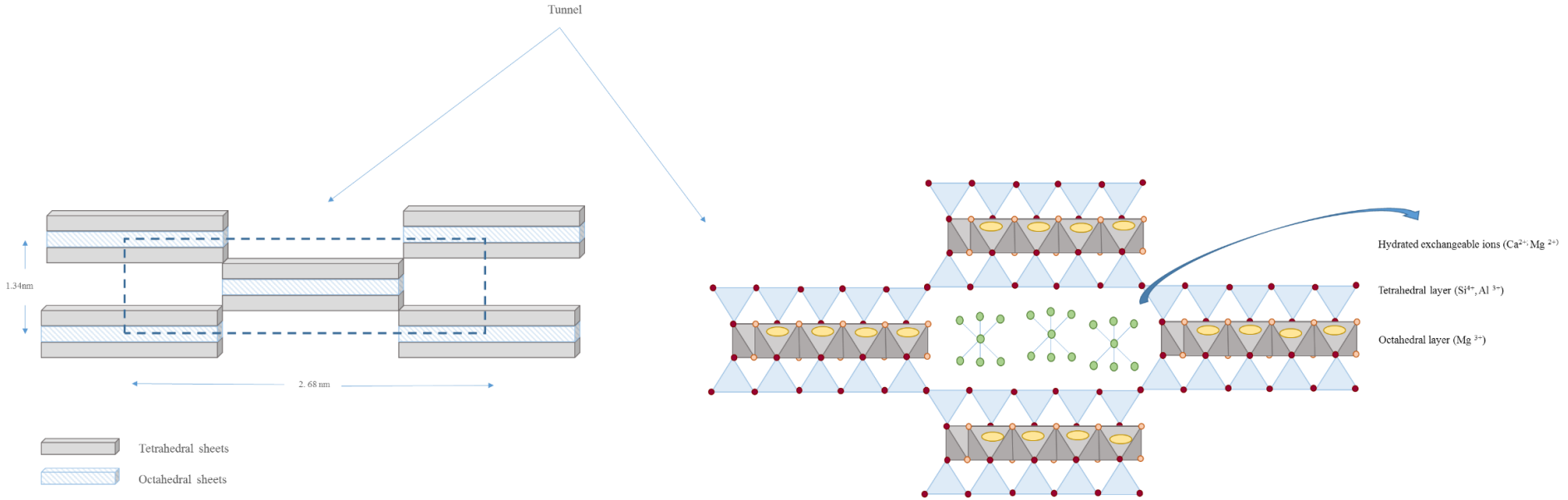

Figure 1.15. Sepiolite crystalline layer structure.

1.3.6.5| Functional Groups on the Surface of Clays

One of the parameters influencing the sorption behaviour of clay minerals besides the existence of electrical charge on the clay surface is the relation between the pH and the point of zero charge (PZC) of the clay (Figure 1.16).

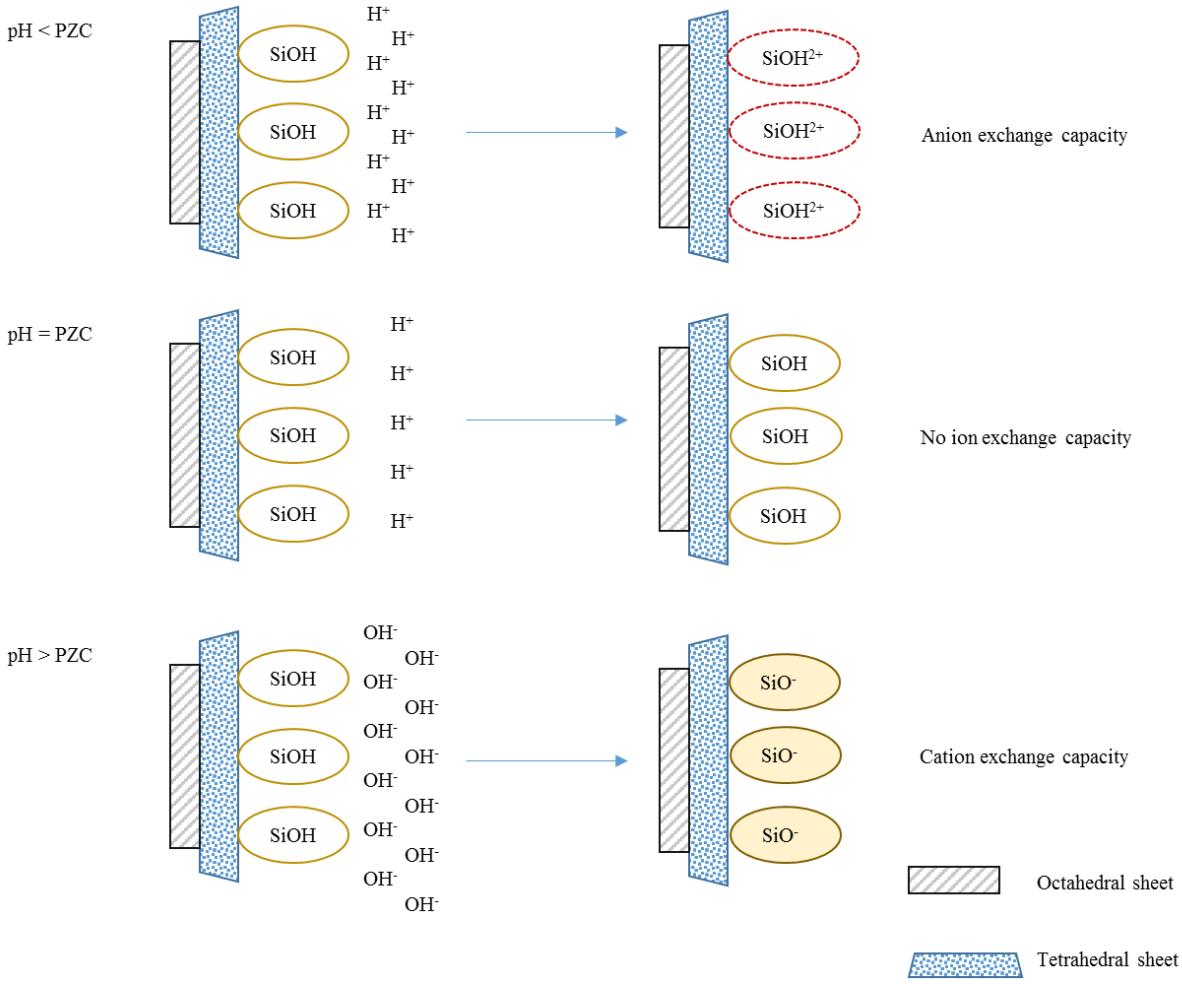

Figure 1.16. Effect of the relationship between the pH and the PZC in the electrical charge of the clays surface.

There are two kinds of electrical charge, the structural charge and the surface charge. Although the structural charge, also known as permanent charge, can be caused by structural flaws, it is usually caused due to ionic substitutions. The substitutions of Al^{3+} for Si^{4+} in the tetrahedral sheets and the substitutions of Al^{3+} for Mg^{2+} or Fe^{2+} in the octahedral sheets, are the cause for most of the permanent

negative charge in smectites, for example. The chemical reactions that occur at the surface of the clay mineral, as well as the adsorption of surfactant ions are responsible for the surface charge and are pH dependent. The surface charge is originated by the hydrolysis of broken Si-O and Al-OH bonds with the surfaces of clay matrices and occurs on the basal surface of both types of sheets in 1:1 clays, and along the edges of both sheets in 1:1 and 2:1 clays (Eslinger and Pevear, 1988).

REFERENCES

Açikel Y.S., Kutsal T. 2000. Determination of the biosorbents activation energies of heavy metals ions on *Zoogloea ramigera* and *Rhizopus arrhizus*. Process Biochemistry 35: 801-807.

Ackermann R., Hughes G., Hanrahan D., Somani A., Aggarwal S., Fitzgerald A., Dixon J., Kunte A., Lovei M., Lvovsky K. 1999. Ground Ozone *In*: Pollution Prevention and Abatement Handbook: Toward Cleaner Production. The World Bank Group, pp. 227-230

Agathos S.N., Hellin E., Ali-Khodja H., Deseveaus S., Vandermesse F. & Naveau H. 1997. Gas-phase methyl ethyl ketone biodegradation in a tubular biofilm reactor: microbiological and bioprocess aspects. Biodegradation 8: 251-264.

Ahalya N., Ramachandra T.V., Kanamadi R.D. 2003. Biosorption of heavy metals. Research Journal of Chemistry and Environment 7: 71- 78.

Ahmed S., Chughtai S., Keane M.A. 1998. The removal of cadmium and lead from aqueous solution by ion exchange with Na-Y zeolites. Separation and Purification Technology 13: 57-64.

Akesson A., Bjellerup P., Lundh T., Lidfeldt J., Nerbrand C., Samsioe G., Staffan S., Vahter m. 2006. Cadmium-induced effects on bone in a population-based study of women. Environmental Health Perspectives 114:830– 834.

Aksu Z., Sag Y., Kutsal T. 1992. The biosorption of Cu (II) by *C. vulgaris* and *Z. ramigera*. Environmental Technology 13: 579-586.

Alexieva Z., Gerginova M., Zlateva P., Manasiev J., Ivanova D., Dimova N. 2008. Monitoring of aromatic pollutants biodegradation. Biochemical Engineering Journal 40: 233-240.

Al-fawwaz A.T., Maznah W.O. 2008. Biosorption of Copper Using Live and Dead Green Microalgae Isolated from Penang Rivers, Malaysia. International Conference on Environmental Research and Technology (ICERT 2008).

Amor L., Kennes C., Veiga M.C. 2001. Kinetics of inhibition in the biodegradation of monoaromatic hydrocarbons in presence of heavy metals. Bioresource & Technology 72:181-185.

Antunes W. M., Aderval S., Luna C. A. H., Antonio C. A. C. 2003. An evaluation of copper biosorption by a brown seaweed under optimized Conditions. Electronic Journal of Biotechnology 6: 174- 184.

Aresta A., Acquaviva M.I., Baruzzi F., Lo Noce R.M., Matarante A., Narracci M., Stabili L., Cavallo A. 2010. Isolation and characterization of polyphenols-degrading bacteria from olive-mill wastewaters polluted soil. World Journal of Microbiology and Biotechnology 26: 639-647.

ATSDR. 1992. Toxicological profile for aluminium. Atlanta, GA, US Department of Health and Human Services, Public Health Service, Agency for Toxic Substances and Disease Registry.

ATSDR. 2000. Toxicological profile for manganese. Atlanta, GA, US Department of Health and Human Services, Public Health Service, Agency for Toxic Substances and Disease Registry.

Azeez L., Adeoye M.D., Lawal A.T., Idris Z.A., Majolagbe T.A., Agbaogun B.K.O., Olaogur M.A. 2013. Assessment of volatile organic compounds and heavy metals concentrations in some Nigerian-made cosmetics. Analytical Chemistry: An Indian Journal 12: 443-483.

Barceloux D.G. 1999. Manganese. Clinical Toxicology 37: 293–307.

Becker K., Kaus S., Krause C, Lepom P., Schulz C., Seiwert M., Seifert B. 2002. German Environmental Survey 1998 (GerES III): environmental pollutants in blood of the German population. International Journal of Hygiene and Environmental Health 205: 297–308.

Bennett, B.G. 1984. Environmental nickel pathways in man *In*: Nickel in the human environment. Proceedings of a joint symposium. IARC scientific publication no. 53. Lyon, France: International Agency for Research on Cancer, pp. 487-495.

Beveridge T.J. 1989. The role of cellular design in bacterial metal accumulation and mineralization. Annual Review of Microbiology 43:147-171.

Beveridge T.J., Murray R.G.E. 1976. Uptake and retention of metals by cell wall of *Bacillus subtilis*. Journal of Bacteriology 127: 1502-1518.

Bondy S.C. 2016. Low levels of aluminum can lead to behavioral and morphological changes associated with Alzheimer's disease and age-related neurodegeneration. Neurotoxicology 52: 222-229.

Bradl H. (Ed.) 2002. Heavy Metals in the Environment: Origin, Interaction and Remediation. London: Academic Press (Vol 6).

Brown B. 1961. The X-Ray identification and crystal structures of clay minerals. Mineralogical Society, London.

Burke B.E., Pfister R. 1986. Cadmium transport by a Cd^{2+}-sensitive and a Cd^{2+}-resistant strain of *Bacillus subtilis*. Canadian Journal of Microbiology 32: 539-542.

CCME. 1988. Canadian Water Quality Guidelines. Ottawa, Ontario, Canadian Council of

Çelekli A., Bozkurt H. 2000. Bio-sorption of cadmium and nickel ions using *Spirulina platensis*: Kinetic and equilibrium studies. Desalination 275. 141-147.

Chan W-C., Lai T-Y. 2010. Compounds interaction on the biodegradation of acetone and methyl ethyl ketone mixture in a composite bead biofilter. Bioresource Technology 101: 126-130.

Chandran P. Das N. 2011. Degradation of diesel oil by immobilized *Candida tropicalis* and biofilm formed on gravels. Biodegradation 22: 1181-1189.

Chaudhuri D., Majumder A., Misra A.K., Bandyopadhyay K. 2014. Cadmium Removal by *Lemna minor* and *Spirodela polyrhiza*. International Journal of Phytoremediation 16: 1119-1132.

Chen H-J., Guo G-L., Tseng D-H., Cheng C-L., Huang S-L. 2006. Growth factors, kinetics and biodegradation mechanism associated with *Pseudomonas nitroreducen*s TX1 grown on octylphenol polyethoxylates. Journal of Environmental Management 80: 279-286.

Chen X.C., Hu S.P., Shen C.F., Dou C.M., Shi J.Y., Chen Y.X. 2009. Interaction of *Pseudomonas* putida CZ1 With clays and ability of the composite to immobilize copper and zinc from solution. Bioresource Technology 100: 330-337.

Chopra A.K., Pathak C. 2010. Biosorption technology for removal of metallic pollutants – An overview. Journal of Applied and Natural Science 2: 318-329.

Choudhary S., Sar P. 2009. Characterization of a metal resistant *Pseudomonas* sp. Isolated from uranium mine for its potential in heavy metal (Ni^{2+}, Co^{2+}, Cu^{2+} and Cd^{2+}) sequestrion. Bioresource Technology 100: 2482-2492.

Churchill S.A., Walters J.V., Churchill P.F. 1995. Sorption of heavy metals by prepared bacterial cell surfaces. Journal of Environmental Engineering 121: 706-711.

Cinar O. 2004. Biodegradation of central intermediate compounds produced from bio-degradation of aromatic compounds. Bioprocess and Biosystems Engineering 26: 341-345.

Contreras J.C.A. 2014. Multi-method approach to study the influence of additives in ternary systems: gypsum, water and impurities Doctoral Thesis Ingeniería Química Administrativva from Mexico City, Faculty of Natural and Materials Sciences, Clausthal University of Technology.

Costa F., Neto M., Nicolau A., Tavares T. 2015. Biodegradation of Diethylketone by *Penicillium* sp. and *Alternaria* sp. – A Comparative Study, Current of Biochemical Engineering 2: 81-89.

Costa F., Quintelas C., Tavares T. 2014. An approach to the metabolic degradation of diethylketone (DEK) by *Streptococcus equisimilis*: Effect of DEK on the growth, biodegradation kinetics and efficiency. Ecological Engineering 70: 183-188.

Davison A.G., Fayers P.M., Taylor A.J., Venables K.M., Darbyshire J., Pickering C.A., Chettle D.R., Franklin D., Guthrie C.J., Scott M.C. 1988. Cadmium fume inhalation and emphysema. Lancet 1: 663–667.

Decree-Law no. 178/06 of 5th September 2006. Journal of the Portuguese Republic.

Decree-Law no. 238/98 of 1st August 1998. Journal of the Portuguese Republic.

Decree-Law no. 306/07 of 1st Agosto de 1998. Journal of the Portuguese Republic.

Decree-Law no. 306/07 of 27th August 2007. Journal of the Portuguese Republic.

Decree-Law no. 78/04 of 3rd April 2004. Journal of the Portuguese Republic.

Dercová K., Makovníková J., Barančíková G., Žuffa J. (2005) Bioremediation of soil and wastewater contaminated with toxic metals. Chemické Listy 99: 682– 693.

Díaz E., Ordóñez S., Vega A., Coca J. 2005. Evaluation of different zeolites in their parent and protonated forms for the catalytic combustion of hexane and benzene. Microporous and Mesoporous Mat 83: 292-300.

Duffus J.H. 2001. Heavy metals a meaningless term. Chemistry International 23: 163-167

Dunn R., Bush G. 2000. Using process integration technology for CLEANER production. Journal of Cleaner Production 9: 1-23.

Elinder C.G., Jarup L. 1996. Cadmium exposure and health risks: Recent findings. Ambio 25: 370-373.

EPA 2003. Health Effects Support Document for Manganese. Environmental Protection Agency (EPA)

EPA. 1985. Cadmium contamination of the environment: An assessment of nationwide risk. Washington, DC: U.S. Environmental Protection Agency, Office of Water Regulations and Standards.

EPA. 2006. Cadmium Compounds. Washington, DC: U.S. Environmental Protection Agency, Office of Water Regulations and Standards.

Eslinger E. 1988. Clay Minerals for Petroleum Geologists and Engineers: SEPM Short Course Notes 22. Sepm Society for Sedimentary.

Essam T., Amim M.A., Tayeb O., Mattiasson B., Guieysse B. 2010. Kinetics and metabolic versatility of highly tolerant phenol degrading *Alcaligenes* strain TW1. Journal of Hazardous Materials 173: 783-788.

Fergusson J.E. (Ed.) 1990. The Heavy Elements: Chemistry, Environmental Impact and Health Effects. Pergamon Press, Oxford.

Flaten T.P. 1990. Geographical associations between aluminium in drinking water and death rates with dementia (including Alzheimer's disease), Parkinson's disease and amyotrophic lateral sclerosis in Norway. Environmental Geochemistry and Health 12: 152-167.

Gadd G.M. 1993. Interactions of fungi with toxic metals. Phytologist 124: 25-60.

Gallagher C.M., Kovach J.S., Meliker J.R. 2008.Urinary cadmium and osteoporosis in U.S. women ≥ 50 years of age: NHANES 1988–1994 and 1999–2004. Environmental Health Perspectives 116: 1338–1343.

Gemini V.L., Gallego A., Oliveira V.M., Gomez C.E., Manfio G.P., Korol S.E. 2005. Biodegradation and detoxification of *p*-nitrophenol by *Rhodococcus wratislaviensis*. International Biodeterioration & Biodegradation 55: 103-108.

Geoghegan D.P., Hamer G., Deshusses M.A. 1997. Effects of unsteady state conditions on the biooxidattion of methyl ethyl and methyl isobutyl ketone in continuous flow liquid phase cultures. Bioprocess Engineering 16: 315-322.

Ghazali F.M., Rahman R.N.Z.A., Salleh A.B., Basri. M. 2004. Biodegradation of hydrocarbons in soil microbial consortium. International Biodeterioration & Biodegradation 54: 61-67.

Guggenheim S., Martin R.T. 1995. Definition of clay and clay mineral: joint report of the AIPEA nomenclature and CMS nomenclature committees. Clays and Clay Minerals 43: 255-256.

Hansdan A. Kumar V. Anshumali 2015. Biosorption of copper and by bacterial adsorbents: a review. Research journal of Environmental Toxicology 9: 45-58.

Harrison P., Waites G. 1998. The Cassell Dictionary of Chemistry, Cassell, London.

Hasan S. H., Srivastava P., Talat M. 2009. Biosorption of Pb(II) from water using biomass of Aeromonas hydrophila: Central composite design for optimization of process variables. Journal of Hazardous Materials 168: 1155–1162.

Haynes W.M. (Ed.). 2014. CRC Handbook of Chemistry and Physics (95th Edition). CRC Press Taylor and Francis Group, Boca Raton, London.

He Z.L., Yang X.E., Stoffella P.J. 2005. Trace elements in agroecosystems and impacts on the environment. Journal of Trace Elements in Medicine and Biology 19:125–140.

Hosseini F., Malekzadeh F., Amirmozafari N., Ghaemi N. 2010. Biodegradation of dodecylbenzene sulfonate sodium by *Stenotrophomonas maltophilia* biofilm African Journal of Biotechnology 9: 55-62.

Hussein H., Ibrahim S.F., Kandeel K., Moawad H. 2004. Biosorption of heavy metals from waste water using *Pseudomonas* sp. Electronic Journal of Biotechnology 7: 38–46.

Ibrahim W.M., Mutawie H.H. 2013. Bioremoval of heavy metals from industrial effluent by fixed-bed column of red macroalgae. Toxicology and Industrial Health 29: 38-42.

ISO. 1994. Water quality - Determination of aluminium: spectrometric method using pyrocatechol violet. Geneva, International Organization for Standardization (ISO 10566:1994 (E)).

Jacqmin H., Commenges D., Letenneur L., Barberger-Gateau P., Dartigues J.F. 1994. Components of drinking water and risk of cognitive impairment in the elderly. American Journal of Epidemiology 139: 48-57.

Jarup L., Berglund M., Elinder C.G., Nordberg G., Vahter M. 1998. Health effects of cadmium exposure-a review of the literature and a risk estimate. Scandinavian Journal of Work, Environment & Health 24: 1-51.

Javanbakht V., Alavi S.A., Zilouei H. 2014. Mechanisms of heavy metal removal using microorganisms as biosorbent. Water Science & Technology 69: 1775-1787.

Juang R-S., Tsai S-Y. 2006. Growth kinetics of *Pseudomonas putida* in the biodegradation of single and mixed phenol and sodium salicylate. Biochemical Engineering Journal 31: 133-140.

Kapor A., Viraraghavan T. 1998. Biosorption of heavy metals on *Aspergillus niger*, effect on pretreatment. Bioresource Technology 70: 94-104.

Khan F.I., Ghoshal A. Kr. 2000. Removal of Volatile Organic Compounds from polluted air. Journal of Loss Prevention in the Process Industries 13: 527-545.

Kim J., Kim J., Kim J., Yoo C.,Moon I. 2008. A simultaneous optimization approach for the design of wastewater and heat exchange networks based on cost estimation. Journal of Cleaner Production 17: 162-171.

Kocamemi B.A., Çecen F. 2009. Biodegradation of 1,2-dichloroethane (1,2-DCA) by cometabolism in a nitrifying biofilm reactor. International Biodeterioration & Biodegradation 63: 717-726.

Krewski D., Yokel R.A., Nieboer E., Borchelt D., Cohen J., Harry J., Kacew S., Lindsay J., Mahfouz A.M., Rondeau V. 2007. Human health risk assessment for aluminium, aluminium oxide, and aluminium hydroxide. Journal of Toxicological and Environmental Health, Part B: Critical Reviews 10: 1–269.

Kumar A., Dewulf J., Van De Wiele T., Van Langenhove H. 2009. Bacterial dynamics of biofilm development during toluene degradation by *Burkholderia vietnamiensis* G4 in a gas phase membrane bioreactor. Journal of Microbiology and Biotechnology 19:1028-1033.

Kuyucak N., Volesky B. 1988. Biosorbents for recovery of metals from industrial solutions. *Biotechnology Letter* 10: 137-142.

Lam K-Y., Davidson F.F., Hanson R.K. 2012. High-Temperature Measurements of the Reactions of OH with a Series of Ketones: Acetone, 2-Butanone, 3-Pentanone, and 2-Pentanone. The Journal of Physical Chemistry 116: 5549-5559.

Lewandowski Z., Beyenal H. 2014. Fundamentals of Biofilm Research. CRC Press Taylor and Francis Group, Boca Raton, London.

Li J., Cai W., Cai J. 2009. The characteristics and mechanisms of pyridine biodegradation by *Streptomyces* sp. Journal of Hazardous Materials 165: 950-954.

Lou F., Liu Y., Li X., Xuan Z., Ma J. 2006. Biosorption of lead ion by chemically-modified biomass of marine brown algae *Laminaria japónica*. Chemosphere 64: 1122-1127.

Lyman W.J. 1995. Transport and transformation processes *In*: Fundamentals of Aquatic Toxicology. Taylor & Francis, Washington..

Mannino D.M., Holguin F., Greves H.M., Savage-Brown A., Stock A.L., Jones R.L. 2004. Urinary cadmium levels predict lower lung function in current and former smokers: data from the Third National Health and Nutrition Examination Survey. Thorax 59: 194–198.

Martyn C.N., Barker D.J. Osmond C., Harris E.C., Edwardson J.A., Lacey R.F. 1989. Geographical relation between Alzheimer's disease and aluminium in drinking water. Lancet 1: 59-62.

Mascagni P., Consonni D., Bregante G., Chiappino G., Toffoletto F. 2003. Olfactory function in workers exposed to moderate airborne cadmium levels. Neurotoxicology. 24: 717–724.

Mascagni P., Consonni D., Bregante G., Chiappino G., Toffoletto F. 2003. Olfactory Function in Workers Exposed to Moderate Airborne Cadmium Levels. NeuroToxicology 24: 717-724.

Merrikhpour H., Jalali M. 2013. Sorption processes of natural Iranian bentonite exchanged with Cd^{2+}, Cu^{2+}, Ni^{2+}, and Pb^{2+} cations. Chemical Engineering Communications 200: 1645-1665.

Michel P., Commenges D., Dartigues J.F., Gagnon M., Barberger-Gateau P., Letenneur L., Paquid Research Group. 1991. Study of the relationship between aluminium concentration in drinking water and risk of Alzheimer's disease *In*: Alzheimer's disease: Basic mechanisms, diagnosis and therapeutic strategies. John Wiley, New York, pp. 387-391.

Mishra A., Malik A. 2012. Recent Advances in Microbial Metal Bioaccumulation. Critical Reviews in Environmental Science and Technology 43: 1162-1222.

Morley G. F., Gadd G.M. 1995. Sorption of toxic metals by fungi and clay minerals. Mycology Research 99: 1429-1438.

Mukhopadhyay M., Noronha S.B., Suraishkumar G.K. 2007. Kinetic modeling for the biosorption of copper by pretreated *Aspergillus niger* biomass. Bioresource Technology 98: 1781-1787.

Mullen M.D., Wolf D.C., Beveridge T.J., Bailey G.W. 1992. Sorption of heavy metals by soil fungi *Aspergillus niger* and *Mucor Rouxii*. Soil Biology & Biochemestry 24: 129-135.

Muraleedharan T.R., Venkobachr, C. 1990. Mechanisms of biosorption of Cu (II) by *Ganoderma lucidum*. Biotechnology and Bioengineering 35: 320-325.

Naja G.M., Murphy V., Volesky B., Flickinger M.Cm. 2010. Biosorption, metals, encyclopedia of industrial biotechnology. Jonh Wiley & Sons, inc.

Neri L.C., Hewitt D. 1991. Aluminium, Alzheimer's disease, and drinking water. Lancet: 338:390.

Nielsen A., Allard A.S. 2009. Chemistry of organic pollutants *In*: Environmental and Ecological Chemistry (Vol 1). EOLSS, pp. 1–424.

Norris P.R., Kelly D.P. 1979. Accumulation of metals by bacteria and yeasts. Developments in Industrial Microbiology 20: 299-308.

Nriagu J.O. 1989. A global assessment of natural sources of atmospheric trace metals. Nature 338: 47–49.

Ogbodu R.O., Omorogie M.O., Unuabonah E., Babalola J.O. 2015. Biosorption of heavy metals from aqueous solutions by *Parkia biglobosa* biomass: Equilibrium, kinetics, and thermodynamic studies. Environmental Progress & Sustainable Energy 34: 1694-1704.

Omar H.H. 2008. Biosorption of copper, nickel and manganese using non-living biomass of marine alga, *Ulva lactuca*. Pakistan Journal of Biological Sciences 11: 964-973.

Onesios K.M., Yu J.T., Bouwer E.J. 2009. Biodegradation and removal of pharmaceuticals and personal care products in treatment systems: a review. Biodegradation 20: 441-466.

Pamukoglu M.Y., Kargi F. 2008. Biodegradation kinetics of 2,4,6-trichlorophenol by *Rhodococcus rhodochrous* in batch culture. Enzyme and Microbial Technology 43: 43-47.

Patnaik P. 2007. A Comprehensive Guide to the Hazardous Properties of Chemical Substances (3rd Edition). Jonh Wiley & Sons, Inc., Hoboken, New Jersey.

Pereira M. 2001. Comparação da Eficácia de Dois Biocidas (carbamato e glutaraldeído) em Sistemas de Biofilme. Tese de Doutoramento, Departamento de Engenharia Biológica, Universidade do Minho.

Pina, F. 2011. Tratamento de águas contaminadas com crómio (VI) por biossorção em algas marinhas. Tese de Mestrado em Engenharia do Ambiente - Ramo de Gestão, Faculdade de Engenharia, Universidade do Porto.

Pipíška M., Horník M., Vrtoch L., Augustín J., Lesný J. 2007. Biosorption of Co^{2+} ions by lichen *Hypogymnia physodes* from aqueous solutions. Biologia 62: 276-282.

Przybulewska K., Wieczorek A. 2009. Biodegradation of methyl isobutyl ketone (MIBK) by *Fusarium solani*. Archives of Environmental Protection 35: 3-10.

Quintelas C. 2007. Implementação e Desenvolvimento de Sistemas de Biossorção para Fixação de Metais Pesados. Tese de Doutoramento, Departamento de Engenharia Biológica, Universidade do Minho.

Quintelas C., Costa F., Tavares T. 2012. Bioremoval of diethylketone by the synergistic combination of microorganisms and clays: Uptake, removal and kinetic studies. Environmental Science and Pollution Research 20: 1374-1383.

Quintelas C., Figueiredo H., Tavares T. 2010. The effect of clay treatment on remediation of diethylketone contaminated wastewater: uptake, equilibrium and kinetic studies. Journal of Hazardous Materials 186: 1241-1248.

Quintelas C., Silva B., Figueiredo H., Tavares T. 2009. Removal of organic com-pounds by a biofilm supported on GAC: modelling of batch and column data. Biodegradation 21 (3): 379-392.

Rabinovich D. 2013. The allure of aluminium. Nature Chemistry 5: 76.

Raghuvanshi S., Babu B.V. 2010. Biodegradation kinetics of methyl iso-butyl ketone by acclimated mixed culture. Biodegradation 21: 31-42.

Remoudaki E., Tezos M., Hatzikioeyian A., Karakoussis V. 1999. Mechanism of palladium biosorption by microbial biomass. The effects of metal ionic speciation and solution co-ions. In: International Biohydrometallurgy Symposium IBS 99: Biohydrometallurgy and the Environment toward the minig of the 21st Century. Elsiever.

Roy A.S., Hazarika J., Manikandan N.A., Pakshirajan K., Syiem M.B. 2015. Heavy metal removal from multicomponent system by the cyanobacterium *Nostoc muscorum*: kinetics and interaction study. Applied Biochemestry and Biotechnology 175: 3863-3874.

Sahinkaya E., Dilek F. Biodegradation kinetic of 2, 4-dichlorophenol by acclimated mixed cultures. Journal of Biotechnology 127: 716-726.

Sari A., Tuzen M., Citak D., Soylak M. 2007. Equilibrium, kinetic and thermodynamic studies of adsorption of Pb(II) from aqueous solution onto Turkish kaolinite clay. Journal of Hazardous Materials 149: 283–291.

Schühle K. Heider J. 2012. Acetone and Butanone Metabolism of the Denitrifying Bacterium "*Aromatoleum aromaticum*" Demonstrates Novel Biochemical Properties of an ATP-Dependent Aliphatic Ketone Carboxylase. Journal of Bacteriology 194: 11-141.

Schulze D.G. 2005. Clay Minerals, Clay Minerals *In*: D. Hillel (editor-in-chief), Encyclopedia of Soils in the Environment., Elsevier / Academic Press, Boston. Vol. 1, pP. 246-254.

Schulze D.G. 2005. Clay Minerals, Clay Minerals *In*: Encyclopedia of Soils in the Environment D. Hillel (editor-in-chief) Elsevier / Academic Press, Boston Vol. 1, pp. 246-254.

Schutte R., Nawrot T.S., Richart T., Thijs L., Vanderschueren D., Kuznetsova T., Van Hecke E., Roels H.A., Staessen J.A. 2008. Bone resorption and environmental exposure to cadmium in women: a population study. Environmental Health Perspectives 116: 777–783.

Sharma S.L., Pant A. 2000. Biodegradation and conversion of alkanes and crude oil by marine *Rhodococcus* sp. Biodegradation 11: 289-294.

Shevchenko V., Lisitzin A., Vinogradova A., Stein R. 2003. Heavy metals in aerosols over the seas of the Russian Arctic. Science of the Total Environment 306:11-25.

Shim H., Yang S-T. 1999. Biodegradation of benzene, toluene, ethylbenzene, and *o*-xylene by a coculture of *Pseudomonas* putida and *Pseudomonas fluorescens* immobilized in a fibrous-bed bioreactoor. Journal of Biotechnology 67: 99-112.

Shim H., Yang S-T. 1999. Biodegradation of benzene, toluene, ethylbenzene, and *o*-xylene by a coculture of *Pseudomonas putida* and *Pseudomonas fluorescens* immobilized in a fibrous-bed bioreactor. Journal of Biotechnology 67: 99-112.

Shraboni S.M., Das S.K., Sah T., Panda G.C., Bandyopadhyoy T., Guha A.K. 2008. Adsorption behavior of copper ions on *Mucor rouxii* biomass through microscopic and FTIR analysis. Colloids and Surfaces B: Biointerfaces 63: 138–145.

Silva B., Figueiredo H., Quintelas C, Neves I., Tavares T. 2008. Proceedings of the 10th International Chemical and Biological Engineering Conference (CHEMPOR 2008).

Suazo-Madrid A., Morales-Barrera L., Aranda-Garcia E., Cristiani-Urbina E. 2011. Nickel (II) biosorption by *Rhodotorula glutinis*. Journal of Industrial Microbiology & Biotechnology 38: 51-64.

Sundar K., Sadiq I. M., Mukherjee A., Chandrasekaran N. 2011. Bioremoval of trivalent chromium using *Bacillus* biofilms through continuous flow reactor. Journal of Hazardous Materials 196: 44-51.

Takeno N. 2005. Atlas of Eh-pH diagrams, Intercomparison of thermodynamic databases, Geological Survey of Japan Open File Report No. 419. National Institute of Advanced Industrial Science and Technology Research Center for Deep Geological Environments.

Tam N.F.Y., Wong Y.S., Wong M.H. 1989. Effects of acidity on acute toxicity of aluminium-waste and aluminium-contaminated soil. Hydrobiology 188/189: 385-395.

Tani A., Hewitt C.N. 2009. Uptake of aldehydes and ketones at typical indoor concentrations by houseplants. Environmental Science & Technology 43: 8338-8843.

Tchounwou P.B., Yedjou C.G., Patlolla A.K., Sutton D.J. 2012. Heavy Metals Toxicity and the Environment. National Institute of Health 101: 133-164

Tornabene T.G., Edwards H.W. 1976. Microbial uptake of lead. Science 196: 1334-1972.

Tsezos M., Remoudaki E., Angelatou V. 1995. A systematic study on equilibrium and kinetics of biosorptive accumulation. The Case of Ag and Ni. International Biodeterioration and Biodegradation 35: 129-153.

Tsezos M., Remoudaki E., Hatzikioseyian A. 2006. Biosorption – Principles and Applications for Metal Immobilization from Waste-Water Streams. Proceedings of EU-Asia Workshop on Clean Production and Nanotechnologies, Seoul, Korea, pp. 23-33.

Tsezos M., Volesky B. 1981 Biosorption of Uranium and thorium. Biotechnology and Bioengeneering 23: 583 – 604.

Turan P., Dogan M., Alkan M. 2007. Uptake of trivalent chromium ions from aqueous solutions using kaolinite, Journal of Hazardous Materials. 148: 56–63.

Van der Mei H.C., Naumann D., Busscher H.J. 1996. Grouping of *Streptococcus mitis* strains grown on different growth media by FT-IR. Infrared Physics & Technology 37: 561–564.

Vijayaraghavan S., Srinivasaraghavan T., Musti S., Kar S., Swaminathan T., Baradarajan A. 1995. Biodegradation of phenol by *Arthrobacter* and modelling of the kinetics. Bioprocess Engineering 12: 227-229.

Volesky B. 1990. Biosorption of heavy metals. CRC press, Boca Raton, Ann Arbor, Boston.

Volesky B. 2007. Biosorption and me. Water Research 41: 4017-4029.

Wan Ngah W.S., Hanafiah M.A.K.M. 2008. Removal of heavy metal ions from wastewater by chemically modified plant wastes as adsorbents: A review. Bioresource Technology 99: 3935-3948.

Wang J. Chen C, 2006. Biosorption of heavy metals by *Saccharomyces cerevisiae*: a review. Biotechnology Advances, 2: 427-451.

Wang J., Chen C. 2009. Biosorbents for heavy metals removal and their future. Biotechnology Advances 27: 195-226.

Wettstein A., Aepple J., Gautschi K., Peters M. 1991. Failure to find a relationship between mnestic skills of octogenarians and aluminium in drinking water. International Archives of Occupational and Environmental Health 63: 97-103.

WHO. 1997. Aluminium. Geneva, World Health Organization, International Programme on Chemical Safety (Environmental Health Criteria 194).

WHO. 1998. Guidelines for drinking-water quality, 2nd ed. Addendum to Vol. 2. Health criteria and other supporting information. World Health Organization, Geneva.

Wittman R., Hu H. 2002. Cadmium exposure and nephropathy in a 28-year-old female metals worker. Environmental Health Perspectives 110: 1261-1266.

Wright J. 2003. Environmental chemistry, heavy metals and pollution of the lithosphere. Taylor and Francis, New York.

Yongliang Z., Deli L., Shiwang L., Shangying X., Yongze Y., Li X. 2009. Kinetics and mechanisms of *p*-nitrophenol biodegradation by *Pseudomonas aeruginosa* HS-D38. Journal of Environmental Sciences 21: 1194-1199.

Zeng F., Cui K., Li X., Fu J., Sheng G. 2004. Biodegradation kinetics of phthalate esters by *Pseudomonas fluoresences* FS1. Process Biochemistry 39: 1125-1129.

Zhang L.-L., Zhu R.Y., Chen J.M., Cai W.M. 2008. Biodegradation of methyl tert-butyl ether as a sole carbon source by aerobic granules cultivated in a sequencing batch reactor. Bioprocess and Biosystems Engineering 31: 527-534.

Zheng Y., Liu D., Xu H., Zhong Y., Yuan Y., Xiong L., Li W. 2009. Biodegradation of *p*-nitrophenol by *Pseudomonas aeruginosa* HS-D38 and analysis of metabolites with HPLC-ESI/MS. International Biodeterioration & Biodegradation 63: 1125-1129.

Zhou G-J., Peng F-Q., Zhang L-J., Ying G-G. 2012. Biosorption of zinc and copper from aqueous solutions by two freshwater green microalgae *Chlorella pyrenoidosa* and *Scenedesmus obliquus*. Environmental Science and Pollution Research 19: 2918-2929.

Zvinowanda C.M., Okonkwo J.O., Agyei N.M., Staden M.V., Jordaan W., Kharebe B.V. 2010. Recovery of lead(II) from aqueous solutions by *Zea mays* tassel biosorption. American Journal of Biochemistry and Biotechnology 6: 1–10.

WEB REFERENCES

http://www.ima-europe.eu

http://www.inchem.org

http://www2.epa.gov

https://www.osha.gov

CHAPTER 2

Biodegradation of diethylketone by *Penicillium* sp. and *Alternaria* sp. – a comparative study

In this chapter, two contaminating fungi from a bioreactor containing diethylketone and *Streptococcus equisimilis* were isolated and characterized at molecular level and identified as belonging to the *Alternaria* and *Penicillium* genera. The biodegradation capacity of these two fungi towards diethylketone, as well as the growth kinetic and biodegradation kinetic parameters were assessed. For both fungi and for all the initials concentrations tested, the biodegradation was found to be almost complete. The experimental results obtained for *Alternaria* sp. and *Penicillium* sp. were found to be best described by, respectively, the Haldane and the Luong growth kinetic models. For *Penicillium* sp. the results obtained for all the concentrations tested are best described by the pseudo-second order model, whereas for *Alternaria* sp. the pseudo-second-order model just describes properly the experiments conducted with initial concentrations of diethylketone higher than 0.5 g/L.

This chapter is based on the following publication: Costa F., Neto M., Nicolau A., Tavares T. 2015. Biodegradation of diethylketone by *Penicillium* sp. and *Alternaria* sp. – a comparative study. Current Biochemical Engineering 2: 81-89.

2.1| INTRODUCTION

The extensive usage of ketones in different anthropogenic activities in the last years has resulted in their increasing release and accumulation in various types of water bodies and locations in the environment (Hernandez et al. 2002; Chan et al. 2010; Datta and Phillip, 2012; Quintelas et al. 2012). Within the several ketones used, diethylketone stands out, not only due its intensive use in several anthropogenic activities as solvent or polymer precursor in industries (Lam et al. 2012), as an intermediate in the synthesis of pharmaceuticals, flavours and pesticides (Quintelas et al. 2012), but also because it can react with OH radicals promoting the formation of ozone and other components of the photochemical smog in urban areas (Lam et al. 2012). Diethylketone is persistence in water, soil and air and possess high mobility (www.cdc.gov) and ability to form toxic and phototoxic intermediates (Costa et al. 2012). It does not bind well to soil and thus pollutes groundwater, causing acute and chronic toxicity to the terrestrial and aquatic life. Diethylketone inhalation may trigger irritation in the eyes, skin, mucous membrane, cough and sneezing according to the Occupational Safety and Health hazards (OSHA) of United States Department Labor (https://www.osha.gov/). Prolonged exposure results in tachycardia, nausea, shortness of breath, dizziness, fainting, coma and even death.

Biological treatments techniques such as biodegradation are considered an attractive approach for decontamination of wastewater from VOC such as diethylketone as compared with some conventional techniques such as adsorption on granular activated carbon (GAC), air-stripping, oxidation, with or without flame, thermal degradation (Costa et al. 2012), condensation and incineration (Raghuvanshi and Babu, 2010). The main disadvantages of these conventional techniques consist on the excessive use of chemicals, generation of contaminated solid waste, emission of nitrogen oxides gases (NOx), which requires additional costs for the secondary treatment, present low efficiency and high costs from operational, maintenance and equipment perspectives (Raghuvanshi and Babu, 2009; Costa et al. 2012).

Studies conducted by different authors demonstrated that biological treatments can efficiently replace the conventional techniques and involve lower investment, in terms of capital and operational costs, present a good operational stability and are environmental friendly as they lead to the formation of less and/or non-dangerous products (Vijayaraghavan et al. 1995; Agathos et al. 1997;

Alexieva et al. 2007; Zhang et al. 2008; Przybulewska and Wieczorek, 2009; Raghuvanshi and Babu, 2009; Essam et al. 2010).

The biodegradation process of hazardous compounds by microorganisms is extremely complex and may result from the combination of several factors such enzymatic degradation, binding by functional groups present on the cell wall or binding by extracellular polymeric substances (EPS). The use of fungi to degrade complex and persistent natural materials and hazardous compounds is well known (Haas et al. 1998; Kim and Rhee, 2003; Atagana, 2004). The cell wall and extracellular exudates of fungi exhibit a variety of Lewis-acid functional groups including amine, carboxyl, phosphoryl, hydroxyl moieties and sulphates, most of which possess a strong binding affinity for cationic aqueous species (Haas et al. 1998). The main structural components of fungal cell walls are chitosan chitin and, comprised of polymerized D-glucosamine and N-acetyl-D-glucosamine, respectively, along with a variety of extracellular polymers including cellulose, α- and β-glucans and a diversity of mannoproteins and glycoproteins (Haas et al. 1998), which have been implicated in the sequestering of metals (Volesky and Holan, 1995).

Fungi are known to be able to produce different enzymes including amylolytic and pectinolytic systems, cellulases, invertases and hemicelullases, proteases, pectinases, laccases, phytases, α-glucuronidases, lipases and mannanases that are involved in the degradation of hazardous substanced (Ayala et al. 2008). Atagana (2004) used indigenous soil fungi present in contaminated soil with creosote to biodegrade phenol, *o*-cresol, *m*-cresol and *p*-cresol. These authors reached degradation yields between 84 % and 100 % for the phenols tested. Chai et al. (2005) investigated the biodegradation of 2,2-bis (4-hydroxyphenyl) propane by 26 fungi belonging to different groups: *Aspergillus*, *Fusarium*, P*enicillium*, *Fungi imperfecti*, *Ascomycetes* and *Zygomycetes*. Among the 26 strains tested, 11 reached biodegradation percentages equal or higher than 50 %. Pipíška et al. (2007) studied the sorption of cobalt by the foliose lichen *Hypogymnia physodes* from $CoCl_2$ solutions spiked with $^{60}Co^{2+}$. The maximum uptake value was achieved within 1 hour. These authors were also able to conclude that after 24 hours biosorption is not pH-dependent within the range of pH 4 to pH 7, is negligible at pH 2 and is not dependent on metabolic activity.

The present work aims the development of an environmental technology applicable to the treatment of aqueous solution contaminated with diethylketone and is focused on the detailed kinetic study for

the biodegradation of diethylketone. The effect of the initial concentration of diethylketone (0.5 g/L to 4 g/L) on the growth of fungi and on the biodegradation process was evaluated.

The information collected from these experimental studies was used to calculate the growth kinetic constants and the degradation kinetic constants from different models, Monod (Monod, 1949), Powell (Powell, 1967), Haldane (Andrews, 1968), Luong (Luong, 1987) and Edwards (Edwards, 1970), reported in literature as models with application in biodegradation of organic pollutants. The intensive modelling effort described herein will allow the definition of general equations to be applied to many other contaminated systems foreseeing the overall efficiency of the biodegradation process while still in the project phase. The importance of this work is notorious because not only it defends a quite straightforward technology to biodegrade high concentrations of diethylketone from contaminated aqueous solutions using microorganisms, but also because up to the present knowledge these two fungi were never used to biodegrade diethylketone.

2.2| MATERIAL AND METHODS

2.2.1| Organisms, Culture Media and Chemicals

The appearance of successive fungi contaminations on different stages of the experiments, in bioreactors employed for the treatment of aqueous solutions with diethylketone (1 g/L to 7.5 g/L) using *S. equisimilis*, promoted the formulation of the hypothesis that those microorganisms could be able to biodegrade diethylketone or at least, their growth would not be inhibited by diethylketone. In order to test this hypothesis, a sample from the contaminated bioreactor was collected and subsequently inoculated in a selective culture media to allow the growth of fungi and inhibit the bacterial growth. For this purpose Dichloran Rose Bengal Chloramphenicol agar (DRBC) with composition described by Ayala et al. (2008) was used for screening and isolation while Malt Extract Agar (MEA) media with composition also described by those authors was used for the maintenance of the two fungi. Brain Heart Infusion (OXOID CM1135) culture medium with the following composition: brain infusion solids (12.5 g/L), beef heart infusion solids (5.0 g/L), proteose peptone (10.0 g/L), glucose (2.0 g/L), sodium chloride (5.0 g/L) and di-sodium phosphate (2.0 g/L),was used for the fungal growth and concentration. Diethylketone was purchased from Acros Organics (98 % pure) and it was diluted in sterilized distilled water.

2.2.2| Isolation of Fungi From Contaminated Bioreactors

A sample of the contaminated bioreactors was aseptically collected and spread directly in a DRBC agar medium, and maintained in the dark, at 37°C for 5 days. The colonies formed were aseptically collected and successively sub-cultured in sterilized DRBC agar medium. This procedure was repeated tenfold in order to ensure the isolation of the culture.

The cultures of each fungal isolate were transferred, sub-cultured aseptically in MEA agar medium at 25°C for 5 days and subsequently stored at -2°C.

2.2.3| Extraction of Fungal DNA

Fungal isolates were inoculated separately into a new fresh MEA liquid medium and maintained at 25°C, 150 rpm for 24 hours. Samples of 2 mL were collected and centrifuged at 13400 rpm for 10 minutes (Eppendorf MiniSpin 9056, F-45-12-11). DNA extraction was performed according to PowerSoil®Dna Isolation Kit, MO Bio Laboratories, Inc.

2.2.4| Molecular Identification of the Two Fungi

DNA extract was used to amplify the Internal Transcribe Sequences (ITS) surrounding the 5.8S-coding sequence, situated between the Small SubUnit-coding sequence (SSU) and the Large SubUnit-coding sequence (LSU) of the ribosomal operon. The ITS region was amplified by PCR using fungal primers ITS1-F 5'-CTTGGTCATTTAGAGGAAGTAA-3' and ITS4 5'-TCCTCCGCTTATTGATATGC-3'. PCR reactions (50 µL) comprised 1 µL of genomic DNA, 35.25 µL of autoclaved ultra-pure water (Millipore Milli-Q Synthesis, 1998), 5 µL of PCR buffer (10x PCR Rxn Buffer, Invitrogen™ Life Technologies), 3 µL of 50 mM $MgCl_2$ (Invitrogen™ Life Technologies), 1 µL of dNTP Mix, 1 µL of forward primer ITS1-F, 1 µL of reverse primer ITS 4 (Invitrogen™ Life Technologies), 0.25 µL of 500 U Taq DNA polymerase recombinant (Invitrogen™ Life Technologies), 2.5 µL of 1 % W-1 solution (Invitrogen™ Life Technologies). Amplifications were carried out in a Bio-Rad MYCYCLER thermal cycler using the following temperature gradient protocol: initial denaturation at 95°C for 3 minutes, followed by 39 cycles of denaturation at 95°C for 30 seconds, annealing at 50.7°C for 30 seconds, extension at

72°C for 36 seconds and final extension 72°C for 5 minutes. PCR amplification products were analyzed by electrophoresis and subsequently purified according to the PCR Clean-up Gel extraction, NucleoSpin®Extract II kit. The sequencing of the PCR purified products were conducted by Eurofins MWG Operon (Ebersberg, Germany) and subjected to a GenBank BLAST in the National Center for Biotechnology Information (NCBI database) search to retrieve sequences of closely related taxa.

2.2.5| Biodegradation Experiments

Each fungal isolate was grown for 24 hours at 37°C and 150 rpm in 0.5 L of a Brain Heart Infusion (BHI) culture medium with the composition described in section 2.2.1. Three sets of 0.15 L of this inoculated medium were transferred to 3 new BHI culture media (1 L). These cultures were grown for 48 hours at 37°C and 150 rpm. After this period, the biomass was recovered on a Sigma 4K15 centrifuge (RCF of 7950) and the supernatant was collected on a sterile bottle for later use. The biomass pellets were re-suspended on a smaller volume of the collected medium, being this volume calculated so that a final biomass concentration in culture between 2 g/L and 3 g/L (Costa et al. 2012) might be obtained.

The experiments were conducted in 0.25 L Erlenmeyer flasks containing 0.15 L of diethylketone solution which were then inoculated with the previous concentrated biomass. The diethylketone concentrations used for these assays were on the range 0.5 g/L to 4 g/L. A sample was taken at different time intervals, centrifuged at 13400 rpm for 10 minutes and the optical density (OD) was measured. The supernatant was used to quantify the concentration of diethylketone.

The assays were conducted in duplicate, during 5 days to 7 days, at 37°C and 150 rpm and the results are an average of both duplicates. The relative standard deviation and relative error of the experimental measurements were less than 2 % and 5 %, respectively.

2.2.6| Analytical Methods

2.2.6.1| Cell Growth Determination

Cell density was monitored spectrophotometrically (PG Instruments T60-UV Visible Spectrophotometer) by measuring the optical density at λ= 620 nm. The OD was then converted to biomass concentration (BC) using the following equations:

For the *Penicillium* sp. fungi,

$$BC = 1.9625\ OD_{620nm} \quad (2.1)$$

For the *Alternaria* sp. fungi,

$$BC = 2.0792\ OD_{620nm} \quad (2.2)$$

2.2.6.2| Gas Chromatography (GC)

Gas chromatography (GC) analyses were performed in order to evaluate the biodegradation capacity of these fungi through the decreasing of diethylketone concentration over time. The GC employed herein was a GC-MS Varian 4000, equipped with a flame ionization detector (FID) and mass spectrometry (MS). The separations were performed using a Meta Wax column (30 m x 0.25 mm x 0.25 μm). The operating conditions were as follows: the column was held initially at a temperature 50°C, then heated at 10°C/minute to 100°C, held at 100°C for 4 minutes, then heated again at 40°C/minute to 200°C and finally held at 200°C for 2 minutes. The temperature of injector and detector were maintained at 250°C. Nitrogen was used as a carrier gas at a flow rate of 30 mL/minute and the injections were performed in the split mode with a split ratio of 1:7. Under these conditions, the retention time for diethylketone was 3.2 minutes.

2.2.7| Data Modelling

2.2.7.1| Growth Kinetics of Fungi

In the present study, the linear and nonlinear growth kinetic models were fitted by linear and nonlinear least squares methods using MATLAB software. The models used were Monod (Monod, 1949), Powell (Powell, 1967), Haldane (Andrews, 1968), Luong (Luong, 1987) and Edwards (Edwards, 1970).

Monod Model

Monod introduced the concept of a growth-limiting or controlling substrate, where the specific growth rate (μ, h^{-1}) can be related with the concentration of a single growth-controlling substrate (S, g/L) via two parameters, the maximum specific growth rate (μ_{max}, h^{-1}) and the substrate affinity constant (K_s, g/L) as given by the equation 2.3.

$$\mu = (\mu_{max} S) / (K_S + S) \quad (2.3)$$

The maximum specific growth rate (μ_{max}) and the substrate affinity constant (K_s) can be determined after linearization of equation 2.3 and application of the method of least squares adjustment, equation 2.4:

$$\mu = (K_s / \mu_{max} S) + (1/\mu_{max}) \quad (2.4)$$

The Monod model is considered a simple model that only describes the dependence of the biodegradation rate on the biomass concentration. One of limitations of the Monod model lies in not taking into account the fact that the microbial growth can be sensible to inhibition caused either by its reaction towards the substrate, as well as the substrate itself when its concentration is above a certain concentration (Molchanov et al. 2007). The original Monod equation was posteriorly modified by Powell, which has considered some of the above limitations.

Powell Model

Powell introduced in the Monod equation the terms of maintenance rate (m) and maintenance threshold (S_{min}, g/L) and can be describe by the equation 2.5.

$$\mu = [((\mu_{max} + m)S_{min}) / (K_S + S_{min})] - m \quad (2.5)$$

where μ_{max} denotes the maximum specific growth rate (h^{-1}), K_S represents the substrate affinity constant (g/L). The three unknown parameters (μ_{max}, K_S, m) can be determined by linear regression of the data obtained for the exponential growth phase.

Haldane Model

Haldane incorporated the substrate inhibition constant (K_1, g/L) into the Monod model considers the existence of substrate inhibitory effect.

$$\mu = (\mu_{max}S) / ((K_S + S + (S^2/K_1)) \quad (2.6)$$

where μ_{max} denotes the maximum specific growth rate (h^{-1}), S represents the substrate concentration (g/L), K_S denotes the substrate affinity constant (g/L) and K_1 denotes the self-inhibition constant (g/L). The bio-kinetic parameters can be determined using the data obtained in the exponential phase. A higher value of K_1 indicate a reduce sensitivity of the microbial culture towards the substrate inhibition effect. When the substrate inhibition effect is verified, it is possible to determine the critical concentration (S_{crit}), above which the substrate removal ceases, equation 2.7.

$$S_{crit} = (K_S + K_1)^{-1/2} \quad (2.7)$$

Luong Model

Luong's model has into account the substrate inhibitory effect (S_m, g/L), from which the microbial growth and biodegradation processes are completely inhibited, equation 2.8.

$$\mu = ((\mu_{max}S) / (K_S + S)) \cdot (1 - (S / S_m))^n \quad (2.8)$$

where μ_{max} denotes the maximum specific growth rate (h^{-1}), S represents the substrate concentration (g/L), K_S denotes the substrate affinity constant (g/L) and n denotes a positive integer number.

Edwards Model

The formation of intermediates or metabolites, the modification, dissociation of one or more enzymes and the formation of metabolic aggregates are some of the examples pointed out for Edwards. The model proposed by Edwards describes the mechanism responsible for the substrate inhibition effect when it is used a broader range of concentrations.

$$\mu = ((\mu_{max}S) / (K_S + S + (1 + S/K)\cdot(S^2 / K_1)) \quad (2.9)$$

where μ_{max} denotes the maximum specific growth rate (h^{-1}), S represents the substrate concentration (g/L), K_S denotes the substrate affinity constant (g/L), K_1 denotes the self-inhibition constant (g/L) and K the Edwards positive constant. The introduction of the term (1+ S/K) represents an improvement on the Haldane model

2.2.7.2| Diethylketone Biodegradation Kinetics

The biodegradation data were analyzed using the linearized form of the zero order, pseudo-first order, pseudo-second order and three-half order models (Brunne and Focht, 1984, Khamis et al. 2009, Saravanan et al. 2009).

Zero-order kinetic model

According to Shoaib et al. (2006) the zero-order model describes the systems wherein the removal of the substrate (pollutant) is independent of its concentration:

$$S = K_0 t \quad (2.10)$$

The linearized form of equation 2.8 is given by equation 2.9:

$$\log S = \log S_0 - (K_0 t / 2.303) \quad (2.11)$$

where S_0 (g/L) represents the substrate initial concentration, S (g/L) denotes the substrate concentration at time t and K_0 represents the zero order kinetic constant (g/Lh^{-1}).

Pseudo-first order kinetic model

The pseudo-first order kinetic model assumes that the interaction rate between the microbial culture and the substrate is limited by a single process or mechanism of a unique class of sorption site, all of which are time dependent (Won et al. 2008), equation 2.12.

$$\log(q_e - q_t) = \log(q_e) - K_{1.1} t \quad (2.12)$$

where q_e (mg/g) correspond to the amount of substrate removed till the equilibrium is achieved, q_t (mg/g) denotes the amount of substrate removed at time t and $K_{1.1}$ represents the pseudo-first order kinetic constant.

Pseudo-second order kinetic model

According to Paris et al. (1981) the pseudo-second order kinetics depends on both the concentration of the substrate as well as the biomass or the substrate concentration and time. Larson (1980) however considers that the concentration of biomass is directly proportional to time, determining a second order differential. Larson does not consider metabolism without the existence of growth. The integrated equation produces a sigmoidal curve equation.

$$(t / q_e) = ((1 / K_2 q_e^2) + (t / q_e) \quad (2.13)$$

In here q_e (mg/g) correspond to the amount of substrate removed till the equilibrium is achieved, q_t (mg/g) denotes the amount of substrate removed at time t and K_2 represents the pseudo-second order kinetic constant.

Three and half o order kinetic model

The three and half order kinetic model is based on the pseudo-first order kinetic model and introduces the term that explains the biomass formation (Raghuvanshi and Babu, 2010). Saravan et al. (2009) used the third and a half kinetic order model to explain the biodegradation of *m*-cresol by a microbial culture (equation 2.12 to equation 2.14).

$$Y = - K_{31} - (K_{32}t/2) \quad (2.14)$$

with

$$Y = (1/t)\cdot(\ln(S_0P + K_0t) / S_0) \quad (2.15)$$

and

$$P = S_0 - S + K_0t \quad (2.16)$$

K_0 denotes for the zero order kinetic constant (g/Lh^{-1}), K_{31} and K_{32} to the first and second three and half order constant. P corresponds to the formation of CO_2, which is directly related with the biomass variation and S_0 represents the initial substrate concentration (g/L).The parameters K_0 and S_0 can be determined from the zero order kinetic model (equation 2.8 and 2.9).

2.3| RESULTS AND DISCUSSION

2.3.1| Isolation and Genetic Identification of Diethylketone Degrading Fungi

Two fungi (one green and the other white) were collected from the contaminated bioreactors working with aqueous solutions of diethylketone and *S. equisimilis*, according to the methods described in section 2.2.2, and differentiated by both macroscopic characteristics when cultured in agar plates (colour, shape, texture) and microscopic ones (cells morphology and Gram staining). The main characteristics of these two fungi are listed in Table 2.1.

The green and white fungi were identified by sequencing the ITS region and possess high homology respectively with the *Alternaria* genera (99 %, accession number KC623563.1) and with the

Penicillium genera (99 %, accession number HQ850362.1). According to Agathos et al. (1997), the appearance and abundance of fungi in the bioreactors is related to the acidic conditions inside the reactor and to their broader tolerance to changes in pH values, concomitant with ketones degradation.

Table 2.1. Characteristics of fungi: growth, front view, back view, characteristics of hyphae and Gram staining of the two fungi.

Fungi	Growth	Front view	Back view	Character of hyphae	Gram
White	Rapid	White with central yellow green powdery appearance	White	Irregular form, with raised elevation and undulate margins	-
Green	Rapid	Olive green with wrinkled appearance	Dark green	Irregular form, with umbonate elevation and entire margins	+

2.3.2| Degradation of Diethylketone by the Two Fungi

In the present study, concentrated biomass of the isolated fungi and initial concentrations of diethylketone of 0.5 g/L, 1 g/L, 2 g/L and 4 g/L were used. Diethylketone was supplied as the only carbon and energy source. The biomass concentration for each isolated fungi was calculated using a calibration curve (optical density versus biomass concentration, equations 2.1 and 2.2) and the measurement of the dry weight. The effect of the initial concentration of diethylketone on the growth of the biomass used and on the biodegradation process was evaluated. In Table 2.2 the maximum concentration of biomass and the specific growth rate for each initial concentration of diethylketone, for *Penicillium* sp. and for *Alternaria* sp. are listed. It is possible to observe from Table 2.2 that the maximum biomass concentration and the maximum specific growth rate of *Penicillium* sp. (0.58 g/L and 9.00×10^{-4} h^{-1}, respectively) are obtained for an initial concentration of diethylketone of 1 g/L and 2 g/L respectively.

For higher concentrations these values start to slightly decrease. For *Alternaria* sp. the highest value of biomass concentration and of specific growth rate (1.07 g/L and 1.90x10^{-3} h^{-1}, respectively) are obtained for an initial concentration of diethylketone of 0.5 g/L. For higher concentrations of diethylketone the biomass concentration and the specific growth rate decrease significantly suggesting that initial concentration of diethylketone higher than 0.5 g/L negatively affects the microbial growth.

Table 2.2. Maximum concentrations of biomass (C_{max}. g/L), experimental specific growth rates (μ_{exp}, h^{-1}) and correlation coefficients (R^2) obtained for the biodegradation assays with the *Penicillium* sp. and *Alternaria* sp. using the method of least-squares fitting.

S (g/L)	C_{max} (g/L)		μ_{exp} (h^{-1})		R^2	
	Penicillium sp.	*Alternaria* sp.	*Penicillium* sp.	*Alternaria* sp.	*Penicillium* sp.	*Alternaria* sp.
0.5	0.52	1.07	4.00x10^{-4}	1.90x10^{-3}	0.68	1.00
1	0.58	0.83	5.00x10^{-4}	4.00x10^{-4}	0.92	0.62
2	0.51	0.87	9.00x10^{-4}	3.00x10^{-4}	0.99	0.76
4	0.48	0.76	8.00x10^{-4}	6.10x10^{-5}	0.98	0.99

2.3.2.1| Biodegradation of Diethylketone by *Penicillium* sp.

Figure 2.1 shows the time profile of *Penicillium* sp. growth and the biodegradation percentage (%) of diethylketone as a function of time, for all the initial concentrations tested using the *Penicillium* sp. as biodegradation agent. The biodegradation of diethylketone is fast in the first 80 hours, after that it slows down until values equal and higher than 99 % are reached (for initial concentrations higher than 0.5 g/L). This initial input is explained by the availability of the biomass and the need of the biomass to consume nutrients such as carbon. After this period of time, the biodegradation rate slows down due the saturation of the biomass (Costa et al. 2012). It is possible to infer from analysis of Figure 2.1 that the biomass grows slightly with the consumption of diethylketone and the biomass growth decreases as the diethylketone disappears. Similar results were also observed by other authors (Alexieva et al. 2007; Costa et al. 2012).

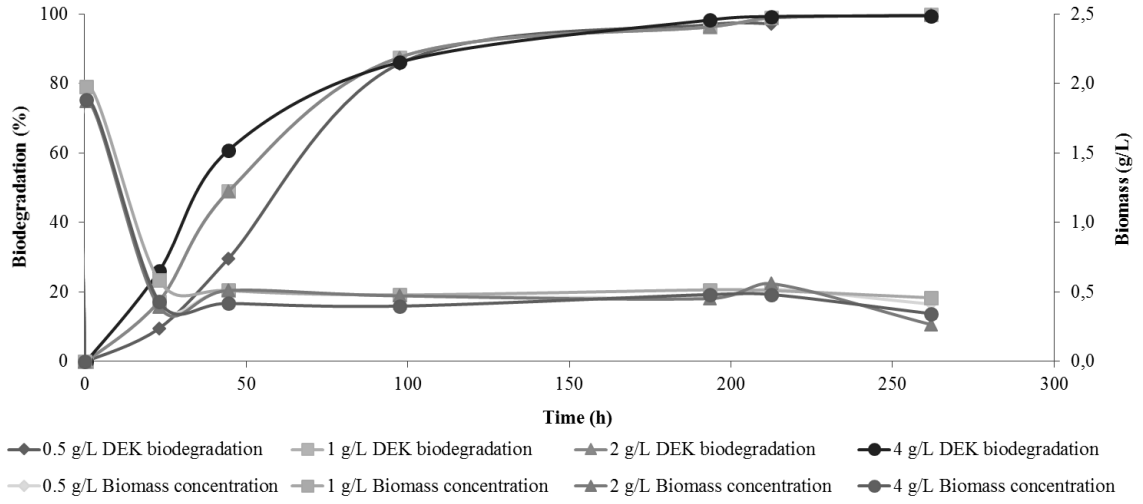

Figure 2.1. Biomass concentration for the *Penicillium* sp. (g/L) and the biodegradation percentage (%) as function of time, for different initial concentrations of diethylketone.

2.3.2.2| Biodegradation of Diethylketone by *Alternaria* sp.

The time profile of biomass concentration and the biodegradation percentage (%) of diethylketone, for all the initial concentrations tested using the *Alternaria* sp. as biodegradation agent are shown in Figure 2.2. The biodegradation of diethylketone is fast in the first 160 hours, after that it slows down until values equal and higher than 95 % are reached. It is possible to observe from analysis of Figure 2.2 that the biomass grows slightly with the consumption of diethylketone and decreases as the diethylketone disappears. It is therefore possible to infer that both fungi are able to efficiently biodegrade diethylketone, however the *Penicillium* sp. biodegrades the ketone faster, making it more attractive and advantageous in these processes.

Lee et al. (2006) reported that the strain *Penicillium* sp. KT-3 is capable of biodegrade small concentrations of several ketones such as diethylketone, methyl ethyl ketone (MEK), methyl propyl ketone (MPK), methyl isopropyl ketone (MIPK), methyl isobutyl ketone (MIBK), methyl butyl ketone (MBK). Alexieva et al. (2007) reported the capacity of *Trichosporon cutaneum* to biodegrade mono hydroxyl derivates of phenol (resorcinol, cathecol and hydroquinone) and 2,6-dinitrophenol, α-methylsterene and acetophenone.

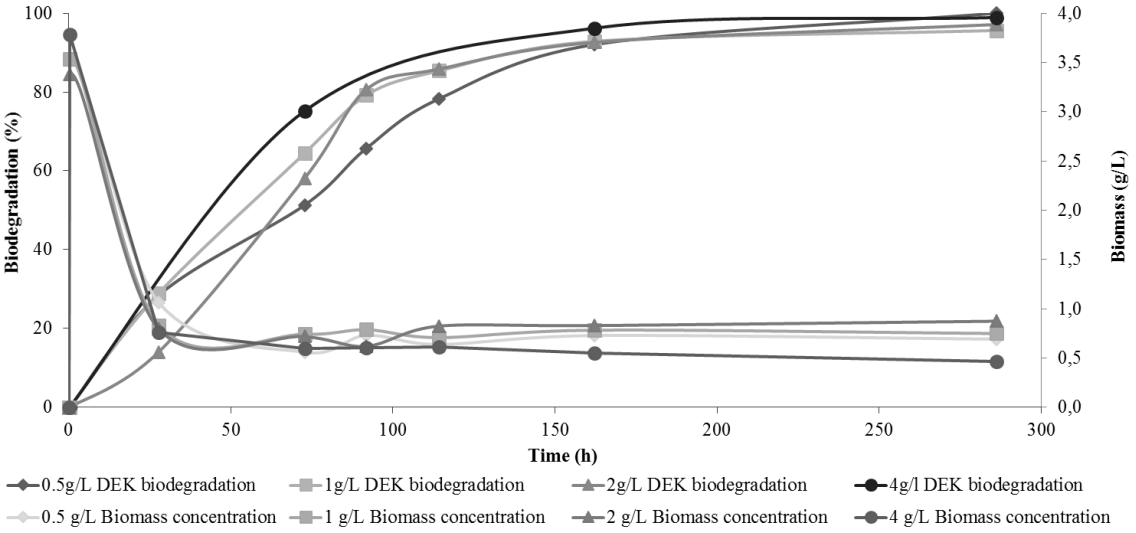

Figure 2.2. Biomass concentration for the *Alternaria* sp. (g/L) and the biodegradation percentage (%) as function of time, for different initial concentrations of diethylketone.

The ability of *Fusarium solani* to biodegrade MIBK was investigated by Przybulewska and Wieczorek (2009). These authors discovered that *Fusarium solani* was able to efficiently degrade MIBK at the rate up to 60 $gm^{-3}h^{-1}$. Costa (2010), reported the excellent capacity of *Streptococcus equisimilis*, a gram-positive bacteria to biodegrade diethylketone solutions. This author discovered that *S. equisimilis* was able to biodegrade relevant concentrations of diethylketone (100 % biodegradation efficiency) in shorter periods of time (< 60 hours).

2.3.3| Modelling of the Growth Kinetics for the Two Fungi

Carbon substrates as ketones are usually used by microorganisms simultaneously as carbon and energy sources under controlled environmental conditions (Quintelas et al. 2009). Since growth is a result of anabolic and catabolic enzymatic activities, these processes (substrate utilization or growth associated to product formation) can also be quantitatively described on the basis of growth models. The specific growth rate (μ) of a population of microorganisms and the substrate concentration (S) can be related by a set of empirically derived rate laws which are considered as theoretical models.

Several theoretical models such as Monod, Powell, Haldane and Luong and kinetic models were used in this study.

2.3.3.1| Modelling of the Growth Kinetics of the *Penicillium* sp. in the Presence of Diethylketone

The comparison between the *Penicillium* sp. experimental and theoretical specific growth rate for the different kinetics models applied in this work is shown in Figure 2.3. For the Monod model the values of maximum substrate concentration (C_{max}) and of the substrate affinity constant (Saravanan et al. 2009) were obtained from the plot of $1/\mu$ versus $1/S$. The values of μ_{max} and K_S obtained were $1.10x10^{-3}$ h^{-1} and 0.81 g/L respectively, indicating that there are no manifest signs of substrate inhibition for the range of concentration of diethylketone used, despite the insignificant growth (Table 2.2) and the fact that this model is not the most appropriate to describe the relation between the specific growth rate and the substrate concentration ($K_S<S_0$). The obtained value for the coefficient of determination (R^2=0.768) corroborate that this model does not fit the experimental data properly.

The experimental and predicted values for the specific growth rate at different substrate concentrations values are given in Table 2.3. For the Powell model, the three kinetic constants (μ_{max}, K_S and m) obtained were respectively $1.10x10^{-4}$ h^{-1}, 0.79 g/L and $6.30x10^{-6}$. The obtained value for the coefficient of determination (R^2=0.931) showed that this model fits better the experimental data than the Monod model. Table 2.3 allows the comparison between experimental data and Powell predicted data. The similarity of the results obtained for the Monod and Powell models is due to the fact that the value of maintenance rate (m) is very small ($6.30x10^{-6}$).

The kinetic parameters for the Haldane model (μ_{max}, K_S and K_I) were respectively $3.50x10^{-2}$ h^{-1}, 51.88 g/L and 0.14. The high value of Ks suggests that the biomass has a low affinity with the substrate used. The value obtained for the coefficient of determination (R^2=0.968) indicates that the predict data for the Haldane model fits better to the data compared to other two models.

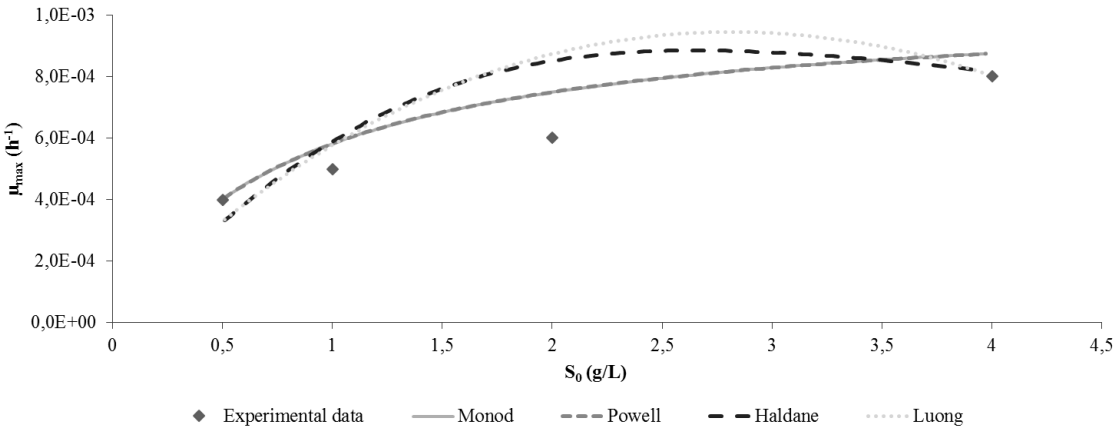

Figure 2.3. Comparison between the experimental results obtained for *Penicillium* sp. and those predicted by the different models at different initial diethylketone concentrations.

For the Luong model the kinetic parameters (μ_{max}, K_S, S_m and n) obtained were respectively 9.60x10^{-2} h^{-1}, 123 g/L, 5.94 g/L and 0.75, indicating the affinity of the substrate and that, above 5.94 g/L the biodegradation and consequently the growth ceases. The coefficient of determination (R^2=0.977) showed that this model fits better the experimental data than the Haldane model.

Table 2.3. Experimental and predicted values of specific growth rate ($\mu_{exp,}$ h^{-1} and $\mu_{predicted,}$ h^{-1}) of *Penicillium* sp. and *Alternaria* sp. fungi using different growth kinetic models.

***Penicillium* sp.**					
S_0 (g/L)	μ_{exp} (h^{-1})	$\mu_{predicted}$ (h^{-1})			
		Monod	**Powell**	**Haldane**	**Luong**
0.5	$4.00x10^{-4}$	$-1.10x10^{-2}$	$-1.70x10^{-2}$	$6.10x10^{-2}$	$-1.10x10^{-2}$
1	$3.10x10^{-4}$	$1.80x10^{-4}$	$2.30x10^{-3}$	$1.30x10^{-3}$	$1.80x10^{-4}$
2	$8.70x10^{-4}$	$1.10x10^{-3}$	$1.30x10^{-3}$	$7.00x10^{-4}$	$1.10x10^{-3}$
4	$7.70x10^{-4}$	$9.00x10^{-4}$	$1.00x10^{-3}$	$5.00x10^{-4}$	$9.00x10^{-4}$
***Alternaria* sp.**					
S_0 (g/L)	μ_{exp} (h^{-1})	$\mu_{predicted}$ (h^{-1})			
		Monod	**Powell**	**Haldane**	**Luong**
0.5	$1.90x10^{-3}$	$1.80x10^{-3}$	$3.70x10^{-3}$	0.00	$1.80x10^{-3}$
1	$4.50x10^{-4}$	$6.00x10^{-4}$	$9.00x10^{-4}$	$5.00x10^{-4}$	$6.00x10^{-4}$
2	$1.20x10^{-4}$	$5.00x10^{-4}$	$6.00x10^{-4}$	$3.00x10^{-4}$	$5.00x10^{-4}$
4	$3.70x10^{-4}$	$4.00x10^{-4}$	$5.00x10^{-4}$	$2.00x10^{-4}$	$4.00x10^{-4}$

2.3.3.2| Modelling of the Growth Kinetics of the *Alternaria* sp. in the Presence of Diethylketone

For the Monod model the value for the μ_{max} and the K_S obtained were $1.80x10^{-4}$ h^{-1} and -0.45 g/L respectively. The small coefficient of determination (R^2=0.701) associated with the negative value obtained for the K_s indicates that this model does not describe the experimental data, reinforcing consequently the need and importance of testing kinetic models accounting inhibition. The experimental and predicted values for the specific growth rate at different substrate concentrations values are given in Table 2.3.

The three kinetic constants of the Powell model, (μ_{max}, K_S and m) obtained were -3.10x10^{-4} h^{-1}, 4.00x10^{-3} g/L and -0.26, respectively. The small value obtained for K_S and the negative values obtained for μ_{max} and m showed that this model does not fit properly to the experimental data. The bad fit obtained with these two models is not unexpected as these models do not consider the inhibition effect detected during the diethylketone biodegradation process. The kinetic parameters for the Haldane model (μ_{max}, K_S and K_1) were respectively 5.40x10^{-4} h^{-1}, 0.57 g/L and 1.16. The high value obtained for K_1 indicates the high sensitivity of the culture towards the substrate inhibition. The value obtained for the coefficient of determination (R^2=0.995) associated with the obtained value for K_1 showed that this model fits properly to the experimental data. For the Luong model the kinetic parameters (μ_{max}, K_S, S_m and n) were obtained as 2.91x10^{-6} h^{-1}, 5.09 g/L, 8.02 g/L and -3.32, respectively. The negative value obtained for the K_S and n showed that the experimental data is not properly described by the Luong model. The bad fit obtained for the Luong model was unexpected because this model takes into consideration the inhibitory effect, which was detected for initial concentrations of diethylketone higher than 0.5 g/L.

The negative value obtained for the K_S and n showed that the experimental data is not properly described by the Luong model. The bad fit obtained for the Luong model was unexpected because this model takes into consideration the inhibitory effect, which was detected for initial concentrations of diethylketone higher than 0.5 g/L.

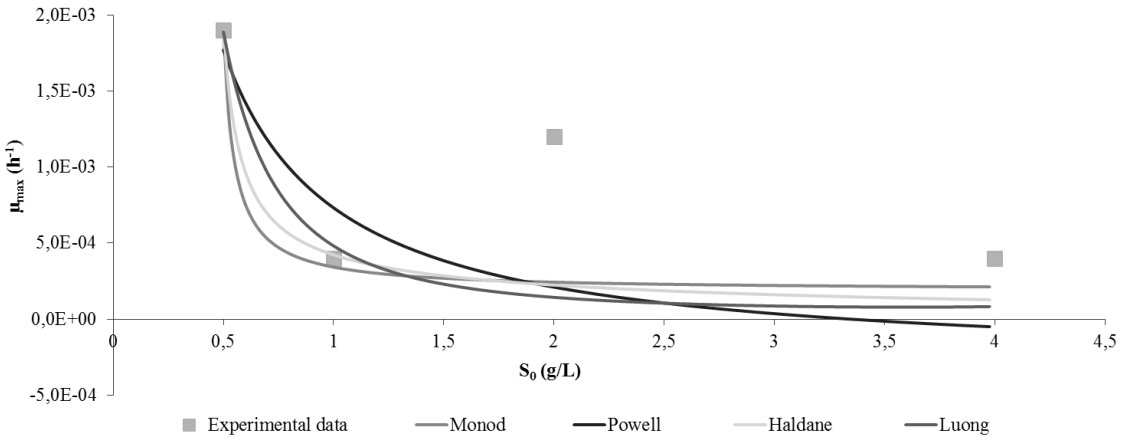

Figure 2.4. Comparison between the experimental results obtained for *Alternaria* sp. and those predicted by the different models at different initial diethylketone concentrations.

2.3.4| Modelling of Diethylketone Biodegradation Kinetics by the Two Isolated Fungi

The biodegradation kinetics is used to describe the transformation rate of organic compounds by suspended microorganism in simpler molecules and it controls the equilibrium reaching time, being therefore an important instrument for the process design and operational control of a biodegradation system. Zero order, pseudo-first order, pseudo-second order and three-half-order rate kinetics were used to describe the biodegradation of diethylketone by the *Penicillium* sp. and *Alternaria* sp.The biodegradation constants for all models were determined and are listed in Table 2.4 and Table 2.5 for the biodegradation experiments with *Penicillium* sp. and *Alternaria* sp., respectively.

2.3.4.1| Modelling of Diethylketone Biodegradation Kinetics by the *Penicillium* sp.

From Table 2.4 it is possible to conclude the best fit for the experimental data was obtained with the pseudo-second order model ($0.980 \leq R^2 \leq 1$) followed by the pseudo-first order ($0.830 \leq R^2 \leq 0.970$), by the zero-order model ($0.720 \leq R^2 \leq 0.990$) and the three-half order ($0.680 \leq R^2 \leq 0.880$). For the zero-order model the values of S_0 and of K_0 although small, increase with the increase of the initial concentration of diethylketone which indicates respectively, that the amount of biodegraded diethylketone and the rate of biodegradation increase with the raising of the initial concentration. For the pseudo-first order, the $K_{1.1}$ constant was found to decrease indicating that the biodegradation rate decreases with the increasing of initial concentration of diethylketone. In the case of the pseudo-second order model, the K_2 constant decrease with the increase of the initial concentration of diethylketone which suggests that the biodegradation of diethylketone decreases over time, which is in agreement with the obtained results. The three-half order model is not able to describe the experimental data for initial diethylketone concentrations of 0.5 g/L and 2 g/L which is unexpected because as previously mentioned this model considers the microbial growth during the biodegradation process. This behaviour may be explained by the reduced values of K_{31} and K_{32} that assume that the biodegradation rate should be extremely slow or even absent (Table 2.4), which was not observed.

Table 2.4. Parameters of zero-order, pseudo-first, pseudo-second and three-half-order kinetic models for different initial diethylketone concentrations and for the biodegradation with *Penicillium* sp.

S (g/L)	Zero order kinetics			Pseudo-first order kinetics	
	K_0	S_0(g/L)	R^2	$K_{1.1}$	R^2
0.5	-0.07	0.77	0.960	$-6.60x10^{-3}$	0.832
1	-0.02	0.53	0.722	$-14.10x10^{-3}$	0.966
2	-0.02	2.29	0.983	$-9.70x10^{-3}$	0.957
4	-0.021	4.236	0.990	$-14.1x10^{-3}$	0.961

S (g/L)	Pseudo-second order kinetics		Three-half order kinetics		
	K_2	R^2	K_{31}	K_{32}	R^2
0.5	$1.20x10^{-5}$	0.984	-	-	-
1	$3.80x10^{-5}$	0.996	$9.90x10^{-3}$	$-6.00x10^{-5}$	0.875
2	$5.40x10^{-6}$	0.985	-	-	-
4	$6.40x10^{-7}$	0.999	$11.20x10^{-1}$	$-8.00x10^{-5}$	0.682

2.3.4.2| Modelling of Diethylketone Biodegradation Kinetics by the *Alternaria* sp.

Table 2.5 shows that the best fit for the experimental data was obtained for the pseudo-second order model ($R^2 \geq 0.990$) for the biodegradations experiments conducted with an initial concentrations of diethylketone higher than 0.5 g/L, followed by the zero-order model ($0.840 \leq R^2 \leq 0.970$). For the zero-order model, S_0 increases with the increase of the initial concentration of diethylketone whereas K_0 remains almost unchanged which indicates respectively that the amount of biodegraded diethylketone increases with the increase of initial concentration of diethylketone and that the rate of biodegradation remains constant. The pseudo-second order constant K_2 tends to decrease with the increase of the initial concentration of diethylketone suggesting that the biodegradation rate decreases over time, which is in agreement with the obtained results. The pseudo-first order and the three-half order models are not able to describe the experimental data for several and different initial concentrations of diethylketone.

Table 2.5. Parameters of zero-order, pseudo-first, pseudo-second and three-half-order kinetic models for different initial diethylketone concentrations and for the biodegradation with *Alternaria* sp.

S_0 (g/L)	Zero order kinetics			Pseudo-first order kinetics	
	K_0	S_0 (g/L)	R^2	$K_{1.1}$	R^2
0.5	-0.02	0.78	0.964	-	-
1	-0.01	1.56	0.941	-0.01	0.972
2	-0.01	1.56	0.941	-	-
4	-0.02	5.28	0.840	-	-
S_0 (g/L)	Pseudo-second order kinetics		Three-half order kinetics		
	K_2	R^2	K_{31}	K_{32}	R^2
0.5	1.20×10^{-5}	0.754	-	-	-
1	1.00×10^{-5}	0.996	0.01	-4.00×10^{-5}	0.824
2	1.00×10^{-6}	0.998	-	-	-
4	1.40×10^{-6}	0.996	0.01	-2.00×10^{-5}	0.928

2.4| CONCLUSIONS

The obtained results showed the potential of two fungi isolated from contaminated reactor with diethylketone and *S. equisimilis*, identified as fungi belonging to the *Penicillium* and *Alternaria* genera, to efficiently biodegrade diethylketone in aqueous solutions (98 % and 99 %, respectively). The growth kinetic model that best describe the growth of *Penicillium* sp. and *Alternaria* sp. are respectively the Luong and the Haldane model. The degradation kinetic model that best fit the results obtained for *Penicillium* sp. is the pseudo-second order whereas for the *Alternaria* sp. the pseudo-second order model only describes adequately the assays with initial concentrations of diethylketone higher than 0.5 g/L.

REFERENCES

Agathos S.N., Hellin E., Ali-Khodja H., Deseveaux S., Vandermesse F., Naveau H. 1997. Gas-phase methyl ethyl ketone biodegradation in a tubular biofilm reactor: Microbiological and bioprocess aspects. Biodegradation 8: 251-264.

Alexieva Z., Gerginova M., Zlateva P., Manasiev J., Ivanova D., Dimova N. 2008. Monitoring of aromatic pollutants biodegradation. Biochemical Engineering Journal 40: 233-240.

Al-Ghouti, M. A. Khraisheh M. A.M., Ahmad M. N.M., Allen S. 2009. Adsorption behaviour of methylene blue onto Jordanian diatomite: A kinetic study. Journal of. Hazardous Materials 165: 589–598.

Andrews J.F. 1968. A mathematical model for the continuous culture of microorganisms utilizing inhibitory substance. Biotechnology and Bioengineering 10: 707-723.

Atagana H.I. 2004. Biodegradation of phenol, *o*-cresol, *m*-cresol and *p*-cresol by indigenous soil fungi in soil contaminated with creosote. World Journal Microbiology and Biotechnology 20: 851-858.

Ayala M., Pickard M.A., Vazquez-Duhalt R. 2008. Fungal enzymes for environmental purposes, a molecular biology challenge. Journal of Molecular Microbiology and Biotechnology 15: 172-180.

Brunner W., Focht D.D. 1984. Deterministic three-half-order kinetic model for microbial degradation of added carbon substrates in soil. Applied and Environmental Microbiology 47: 167-172.

Chai W., Handa Y., Suzuki M., Saito M., Kato N., Horiuchi C.A. 2005.Biodegradation of bisphenol a by fungi. Applied Biochemistry Biotechnology 120: 175-182.

Chan W.C., Lai T.Y. 2010. Interaction of compounds on biodegradation of ketone mixtures in a biofilter. Journal of Chemical Technology and Biotechnology 85: 416-422.

Costa F. 2010. Cinéticas de biodegradação de dietilcetona (3-pentanona) por bactérias. Tese de Mestrado, Departamento de Engenharia Biológica, Universidade do Minho.

Costa F., Quintelas C., Tavares T. 2012. Kinetics of biodegradation of diethylketone *by Arthrobacter viscosus*. Biodegradation 23: 81-92.

Datta A., Philip L. 2012. Biodegradation of volatile organic compounds from paint industries. Applied Biochemistry Biotechnology 167: 564-580.

Edwards V.H. 1970. The influence of high substrate concentrations on microbial kinetics. Biotechnology and Bioenineering 12: 679-712.

Essam T., Amim M.A., El Tayeb O., Mattiasson B., Guieysse B. 2010. Kinetics and metabolic versatility of highly tolerant phenol degrading Alcaligenes strain TW1. Journal of Hazardous Materials 173: 783-788.

Geoghegan D.P., Hamer G., Deshusses M.A. 1997. Effects of unsteady state conditions on the biooxidation of methyl ethyl and methyl isobutyl ketone in continuous flow liquid phase cultures. Bioprocess Engineering 16: 315-322.

Haas J.R., Bailey E.H., William Purvis O. 1998. Bioaccumulation of metals by lichens: Uptake of aqueous uranium by Peltigera membranacea as a function of time and pH. American Minerallogist 83: 1494-1502.

Hernandez R., Zappi M., Colucci J., Jones R. 2002. Comparing the performance of various advanced oxidation processes for treatment of acetone contaminated water. Journal of Hazardous Materials 92: 33-50.

Khamis M, Jumean F, Abdo N., 2009. Speciation and removal of chromium from aqueous solution by white, yellow and red UAE sand. Journal of Hazardous Materials 169, 948–952.

Kim, D.Y., Rhee, Y.H., 2003. Biodegradation of microbial and synthetic polyesters by fungi. Applied Microbiology and Biotechnology 91: 300-308.

Lam K-Y., Davidson D.F., Hanson R.K., 2012. High-Temperature Measurements of the Reactions of OH with a Series of Ketones: Acetone, 2-Butanone, 3-Pentanone, and 2-Pentanone. The Journal of Physical Chemistry A 116: 5549-5559.

Larson R.J. 1980. Role of biodegradation kinetics in predicting environmental fate In: Biotransformation and the fate of chemicals in the aquatic environment. American Society for Microbiology, Washington, pp 67–86.

Lee T.H., Kim J., Kim M-J., Ryo H.W., Cho K-S. 2006. Degradation characteristics of methyl ethyl ketone by *Pseudomonas* sp. KT-3 in liquid culture and biofilter. Chemosphere 63: 315-322.

Leitão A.L. 2009. Potential of *Penicillium* Species in the Bioremediation Field. International Journal of Environmental Research and Public Health 6: 1939-1417.

Luong J.H.T. 1987. Generalization of Monod kinetics for analysis of growth data with substrate inhibition. Biotechnology and Bioengineering 29: 242-248.

Molchanov S., Gendel Y., Ioslvich I., Lahav O. 2007. Experimental and Computational Methodology for Determining the Kinetic Equation and the Extant Kinetic Constants of Fe(II) Oxidation by Acidithiobacillus ferrooxidans. Applied and Environmental Microbiology 73: 1742-1752.

Monod J. 1987. The growth of bacterial cultures. Annual Review of Microbiology 3: 371-394.

Paris D.F., Steen W.C., Baughman G.L., Barnett J.T. Jr. 1981. Second-order model to predict microbial degradation of organic compounds in natural waters. Applied Environmental Microbiology 41: 603–609.

Pipíška M., Horník M., Vrtoch L.u., Augustín J., Lesný J. 2007. Biosorption of Co^{2+} ions by lichen Hypogymnia physodes from aqueous solutions. Biologia 62: 276-282.

Powell E.O. 1967. The growth rate of microorganisms as function of substrate concentration. E. C.G.T., S. R.E. HMSO, London, United Kigndom.

Przybulewska K., Wieczorek A. 2009. Biodegradation of methyl isobutyl ketone (MIBK) by Fusarium solani. Archives of Environmental Protection 35: 3-10.

Quintelas C., Costa F., Tavares T. 2012. Bioremoval of diethylketone by the synergistic combination of microorganisms and clays: Uptake, removal and kinetic studies. Environmental Science and Pollution Research 20: 1374-1383.

Quintelas C., Fonseca B., Silva B., Figueiredo H., Tavares T. 2008. Treatment of chromium (VI) solutions in a pilot-scale bioreactor through a biofilm of *Arthrobacter viscosus* supported on GAC. Bioresource Technology 100: 220-226.

Raghuvanshi S., Babu B.V. 2009a. Biodegradation kinetics of methyl iso-butyl ketone by acclimated mixed culture. Biodegradation 21: 31-42.

Raghuvanshi S., Babu B.V. 2009b. Experimental studies and kinetic modelling for removal of methyl ethyl ketone using biofiltration. Bioresource Technology 100: 3855- 3861.

Raghuvanshi S., Babu B.V. 2010. Biofiltration for removal of methyl isobutyl ketone (MIBK): Experimental studies and kinetic modelling. Environmental Technology 31: 29-40.

Saravanan P., Pakshirajan K., Saha P. 2009. Batch growth kinetics of an indigenous mixed microbial culture utilizing m-cresol as the sole carbon source. Journal of Hazardous Materials 162: 476-481.

Shoiab M.H., Tazeen J., Merchant H.A., Yousuf R.I. 2006. Evaluation of drug release kinetics from ibuprofen matrix tablets using HPMC. Pakistan Journal of Pharmaceutical Sciences 19: 119-124.

Vijayaraghavan S., Srinivasaraghavan T., Musti S., Kar S., Swaminathan T., Baradarajan A., 1995. Biodegradation of phenol by *Arthrobacter* and modelling of the kinetics. . Bioprocess Engineering 12: 227-229.

Volesky B., Holan Z.R. 1995. Biosorption of heavy metals. Biotechnology Progress 11: 235-250.

Won W.S., Han M.H., Yun Y-S. 2008. Different binding mechanisms in biosorption of reactive dyes according to their reactivity. Water Research 42: 4847-4855.

Zhang L.L., Zhu R.Y., Chen J.M., Cai W.M. 2008. Biodegradation of methyl tert-butyl ether as a sole carbon source by aerobic granules cultivated in a sequencing batch reactor. Bioprocess and Biosystems Engineering 31: 527-534.

WEB REFERENCES

http://www.cdc.gov/niosh/npg/npgd0212.html

https://www.osha.gov/

CHAPTER 3

Bioremoval of Ni and Cd in the presence of diethylketone by fungi and by bacteria – A comparative study

This chapter focuses on the study of two fungi (*Alternaria* sp. and *Penicillium* sp.) and one gram-positive bacterium (*Streptococcus equisimilis*) and their ability to remove nickel and cadmium from aqueous solutions in the presence of diethylketone. In a first stage, individual toxicity experiments were performed to evaluate the xenobiotic impact of the initial concentration of nickel and cadmium on the growth of *Alternaria* sp., *Penicillium* sp. and *Streptococcus equisimilis*. In a second stage, biosorption experiments were performed using aqueous solutions containing both metals and diethylketone (mixed solutions) and aimed to infer about the global effect of the initial metal concentration on the growth, on the sorption capacity of the microorganisms and on the interaction between the sorbent matrices. Both sets of experiments aimed to determine which microorganisms have the best features to biologically remove Ni^{2+}, Cd^{2+} and diethylketone. It was found that the growth of both fungi is positively stimulated by the presence of nickel and inhibited for cadmium concentrations higher than 40 mg/L, whereas *S. equisimilis* growth was found to be negatively affected by both metals. Within the group of microorganisms tested, *S. equisimilis* presented higher removal efficiency (%) and uptake. It was demonstrated that despite the fact that the mixed solution exerts a negative effect on the removal process and on the growth of the three microbial cultures, the system is able to decontaminate aqueous solutions with high concentrations of nickel, cadmium and diethylketone.

This chapter is based on the following submitted publication: Costa F., Tavares T. 2016. Bioremoval of Ni and Cd in the presence of diethylketone by fungi and by bacteria – A comparative study

3.1| INTRODUCTION

Many industrial activities have led directly and indirectly to the artificial redistribution of organic and inorganic chemicals into the terrestrial and aquatic environment (Morley and Gadd, 1995). The artificial redistribution of these chemicals has culminated firstly in their increasing release and accumulation in the environment and secondly in the development of environmental and public health problems (Işik, 2008, Fereidouni et al. 2009, Flores-Garnica et al. 2013, Khairy et al. 2014, Costa et al. 2015).

Ketones are extensively used in food, chemicals, electronics, paint, rubbers, lubricants and pharmaceutical industries and are generally released into the environment by petrol and petrochemical industries. Diethylketone as almost all the volatile organic solvents, is dangerous to the aquatic life in high concentrations (Costa et al. 2011; Costa et al. 2015). Diethylketone can react with OH radicals enhancing the production of ozone and other components of the photochemical smog in urban areas (Lam et al. 2012), is persistent in water, soil and air. Chronic exposure to diethylketone may cause tachycardia, nausea, shortness of breath, dizziness, fainting, coma and death (Costa et al. 2015).

Metals are usually found in wastewater from electroplating, mining, metal plating, ceramic, batteries, (Işik, 2008, Flores-Garnica et al. 2013), paint, chemical manufacturing, coating and extractive metallurgy (Khairy et al. 2014). Cadmium, nickel, copper and cobalt are considered within the more dangerous metals and therefore they are included in the U.S. Environmental Protection Agency's (EPA) list of priority pollutants (Arshadi et al. 2014). Nickel is listed as carcinogenic (group 2B) and has been implicated as a nephrotoxin, an embryotoxin and teratogen element. Acute and chronic nickel exposure to nickel can cause several disorders such as tightness cyanosis, chest pain, pulmonary fibrosis and skin dermatitis, (Flores-Garnica et al. 2014). Cd, in addition of not playing any constructive role in human-metabolism, can cause severe damage in different organs including kidneys, lungs, liver and testis. Exposure to cadmium may also lead to infertility (Ahmed et al. 1998, Chaudhuri et al. 2014), impedes respiration, affect the action of enzymes, transpiration (Ahmed et al. 1998) and can induce genomic instability through complex and multifactorial mechanisms, including proteinuria, a decrease in glomerular filtration rate and an increase in the frequency of kidney-stone formation, eventually causing certain types of cancer (group B1) (Khairy et al. 2014). Although there are several methods for the decontamination of different kinds of pollutants (chemical

precipitation, complexation, solvent extraction, membrane processes (Işik, 2008, Fereidouni et al. 2009), adsorption on granular activated carbon (Flores-Garnica et al. 2013, Costa et al. 2015), biological processes present several advantages over those methods (Işik, 2008, Fereidouni et al. 2009, Flores-Garnica et al. 2013, Costa et al. 2015). In this endeavour, biodegradation and biosorption processes have emerged as an attractive, sustainable, inexpensive and eco-friendly alternative for the treatment of contaminated water with organic and inorganic pollutants (Morley et al. 1995, Aksu, 2005, Quintelas et al. 2012).

In the present study *Penicillium* sp., *Alternaria* sp. and *Streptococcus equisimilis* were used to simultaneously decontaminate aqueous solutions containing nickel, cadmium and diethylketone. The effect of the initial metal concentration on the growth, on the biodegradation and/or sorption capacity of these pollutants, as well as on the biological activity after exposure, was evaluated. Diethylketone's toxicity towards *Penicillium* sp., *Alternaria* sp. and *Streptococcus equisimilis* is reported in Costa et al. (2014, 2015). The work presented herein is original and its impact on society and on environment is evident due to the hazardous effects of those pollutants on the health of living beings but also because, up to the present knowledge, these two fungi were never used to remove metals from aqueous solutions.

3.2| MATERIAL AND METHODS

3.2.1| Organisms, Culture Media and Chemicals

The fungi *Penicillium* sp. and *Alternaria* sp. obtained and identified previously (Costa et al. 2015) were used in this work. The bacterium *Streptococcus equisimilis* was obtained from the Spanish Type Culture Collection (University of Valencia). The growth medium employed was Brain Heart Infusion (BHI, OXOID CM1135) with a pH of 7.4. Elementary stock solutions (1 g/L) of cadmium and nickel were prepared by dissolving, respectively, an appropriate amount of $CdSO_4 \bullet 8/3H_2O$ (Riedel-de-Haën) and of $NiCl_2 \bullet 6H_2O$ (Carlo Erba Reagents) in distilled water. All glassware used for experimental purposes was washed with 60 % nitric acid and subsequently rinsed with deionized water to eliminate any possible interference by other metals.

The range of concentrations of each metal used in the toxicological experiments was obtained by dilution of the stock solutions and varied between 5 mg/L and 100 mg/L and the main objective was to infer about the toxic effect of each pollutant on the microbial culture. The biosorption experiments were conducted using a mixture of Ni^{2+} and Cd^{2+} (1 mg/L to 20 mg/L) and diethylketone (4 g/L) and aimed to access the sorption capacity of each microbial culture in respect to each pollutant, as well as to infer about the interaction between biomass-pollutant and pollutant-pollutant, in terms of uptake and removal percentages. At the end of all experiments, viability tests were performed to confirm the death or inactivation of all the microbial cultures.

3.2.2| Toxicological Experiments With Metals

Penicillium sp., *Alternaria* sp. and *S. equisimilis* were inoculated separately into 0.5 L of autoclaved BHI culture medium (24 hours, at 37°C and 150 rpm - Culture 1). The toxicity experiments were carried out for 24 hours at 37 °C and 150 rpm in 0.25 L Erlenmeyer flasks containing 0.125 L of autoclaved BHI culture medium either with Ni^{2+} or Cd^{2+} (5 mg/L to 100 mg/L) and 10 mL of Culture 1. At different time intervals, a sample was collected, centrifuged at 13400 rpm for 10 minutes and the OD was measured at 620 nm. The supernatant was used to quantify the concentration of metal over time, by inductively coupled plasma optical emission spectrometry, ICP-OES. A control with each microorganism (microbial control, MC) suspended just in culture medium was used to access the normal growth behavior of each culture. The assays were conducted during a period of 2 days at 37°C and 150 rpm. The study of the toxic effect of different initial concentrations of diethylketone on the growth of all three microorganisms is reported in Costa et al. (2014, 2015).

3.2.3| Biosorption Experiments With Ni, Cd and DEK

A set of individual experiments were conducted and aimed to infer firstly about the sorption capacity of all three microorganisms towards Ni^{2+}, Cd^{2+} and diethylketone, and secondly about the effect that this mixture of pollutants exerts in its own removal.

The growth of the three microorganisms was promoted individually, inoculating them in 0.5 L of a BHI culture medium for 24 hours at 37°C and 150 rpm. After this period of time, 10 mL of each

biomass was inoculated into Erlenmeyer's flasks (0.25 L) with a final working volume of 0.125 L. Each Erlenmeyer's flask contained an aqueous solution with Ni^{2+} (1 mg/L to 20 mg/L), Cd (1 mg/L to 20 mg/L) and diethylketone (4 g/L). The Erlenmeyer's flasks were rotated at a constant rate of 150 rpm until equilibrium was reached (7 days). Samples of 1 mL were periodically collected, centrifuged at 13400 rpm for 10 minutes and the supernatant was used to determine the pollutants concentration. The samples were analyzed by gas chromatography-mass spectroscopy, GC-MS and by ICP-OES, respectively for diethylketone and for metals. A control with Ni^{2+}, Cd^{2+} and diethylketone was used in order to infer about the influence of the Erlenmeyer flasks walls on the sorption of all pollutants.

3.2.4| Analytical Methods

3.2.4.1| Gas Chromatography (GC)

Gas chromatography with mass spectrometry (GC-MS) was used to assess the concentration of diethylketone in aqueous solution and thereby to evaluate the biodegradation capacity of the microorganisms regarding diethylketone, in the presence of Ni^{2+} and Cd^{2+}. The chromatograph was a Varian 4000, equipped with a flame ionization detector (FID) and mass spectrometry (MS). The separations were performed using a Meta Wax column (30 m x 0.25 mm x 0.25 μm). The operating conditions and the retention time are reported at Costa et al. (2015).

3.2.4.2| Inductively Coupled Plasma Optical Emission Spectrometry (ICP-OES)

The concentration of Ni^{2+} and Cd^{2+} in samples was measured by an ICP-OES (Optima 8000, PerkinElmer). The operating conditions were as follows: RF power: 1300 W, argon plasma flow: 8 L/min, auxiliary gas flow: 0.2 L/min, nebulizer gas flow: 0.5 L/min. For the analysis of nickel concentration, the plasma view was radial and the wavelength used was 221.648 nm, whereas for cadmium, the plasma view was axial and the wavelength used was 226.502 nm. All calibration solutions were prepared from a nickel and from a cadmium stock standard solutions with a concentration of 1 g/L. All samples were acidified with nitric acid before analyses. The instrument response was periodically checked with standard Ni^{2+} and Cd^{2+} solutions and a blank (HNO3 5 %).

3.2.5| Data Modelling

3.2.5.1| Growth Kinetics Modelling

The kinetics of growth of both fungi was analyzed using five different growth kinetic models: Monod (1949), Powell (1967), Haldane (Andrews, 1968), Luong (1987) and Edwards (1970), fitted by linear and nonlinear least squares methods, using MATLAB software (see Chapter 2, section 2.2.7.1).

3.2.5.2| Diethylketone, Ni and Cd Removal Kinetics Modelling

The removal kinetics of all pollutants were analyzed using the linearized form of the zero order, pseudo-first order, pseudo-second order and three-half order models (Brunne and Focht, 1984, Khamis et al. 2009, Saravanan et al. 2009) (see Chapter 2, section 2.2.7.2).

3.3| RESULTS AND DISCUSSION

3.3.1| Toxicological Experiments

Alternaria sp. exhibits similar growth behavior for all the Ni^{2+} concentrations tested (Figure 3.1.a), including the microbial control. Maximum removal percentages ranged between 69 % and 76 % while maximum uptake of 10 mg/g to 254 mg/g were obtained and both tended to increase with the increase of initial concentration of Ni^{2+} (Figure 3.1.b). Although *Alternaria* sp. presents similar growth profiles (short lag and log phase) when exposed to Cd^{2+}, its growth is inhibited for concentrations higher than 40 mg/L (Figure 3.2.a).

Maximum removal percentages of 29 % to 67 % and uptake values of 3 mg/g to 137 mg/g (Figure 3.2.b) were registered. The uptake tended to increase with the increase of Cd^{2+} concentration. The growth results obtained for *Alternaria* sp. with Ni^{2+} and with Cd^{2+} are both best described by the Haldane model (Table 3.1, R^2= 0.966 and R^2=0.822, respectively). This model was originally proposed in 1968 and is used to represent growth kinetics with an inhibitory compound. The critical concentration, S_{crit}, above which the removal rate of the compound decreases due to the self-inhibitory effect (Raghuvanshi and Babu, 2010) was found to be 85.3 mg/L for Ni^{2+} and 87.7 mg/L for Cd^{2+}.

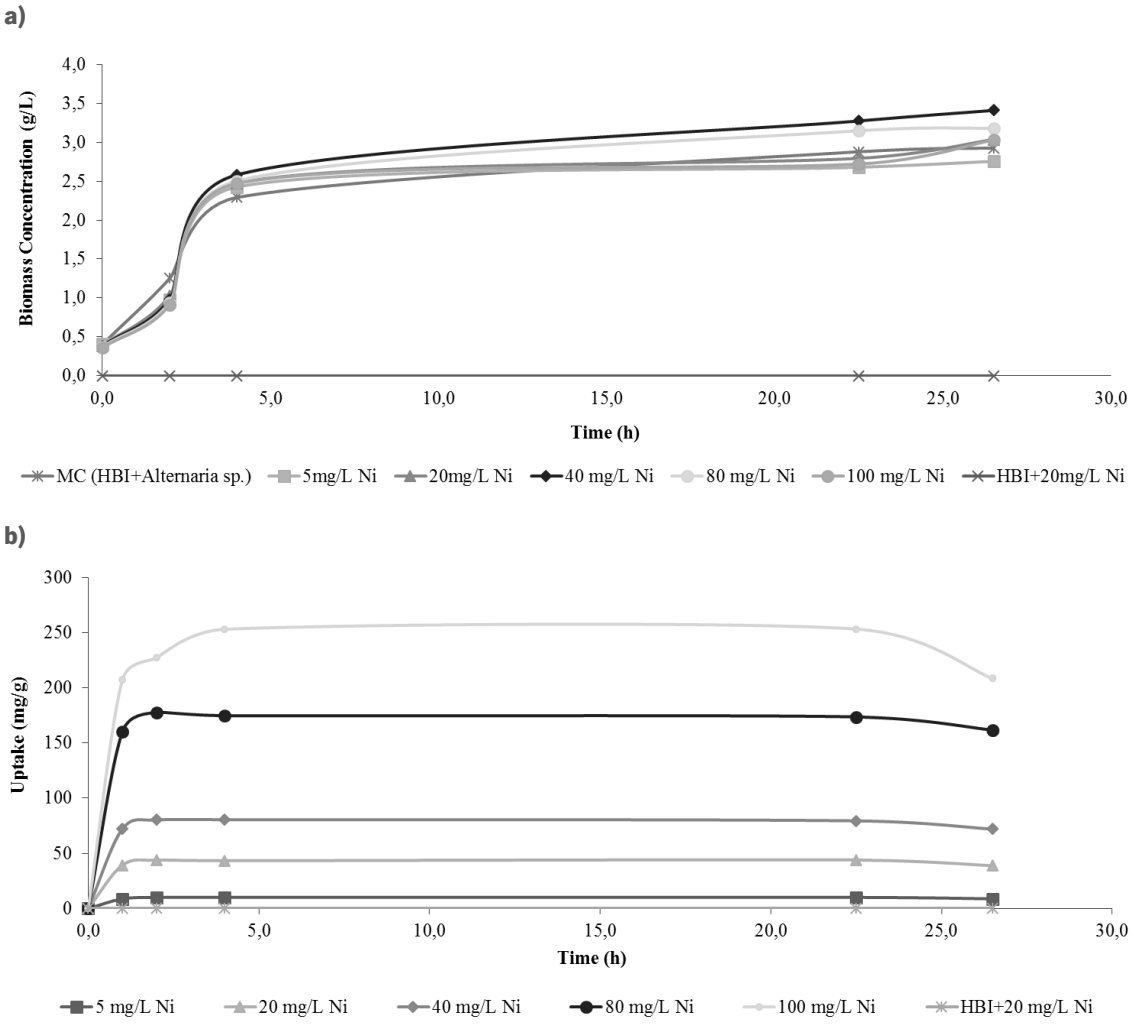

Figure 3.1. a) Growth profile for *Alternaria* sp. (g/L) when exposed to different initial concentrations of Ni^{2+}; **b)** Uptake (mg/g) of Ni^{2+} for different initial concentrations (5 mg/L to 100 mg/L) (37°C, 150 rpm) for the suspended culture of *Alternaria* sp.

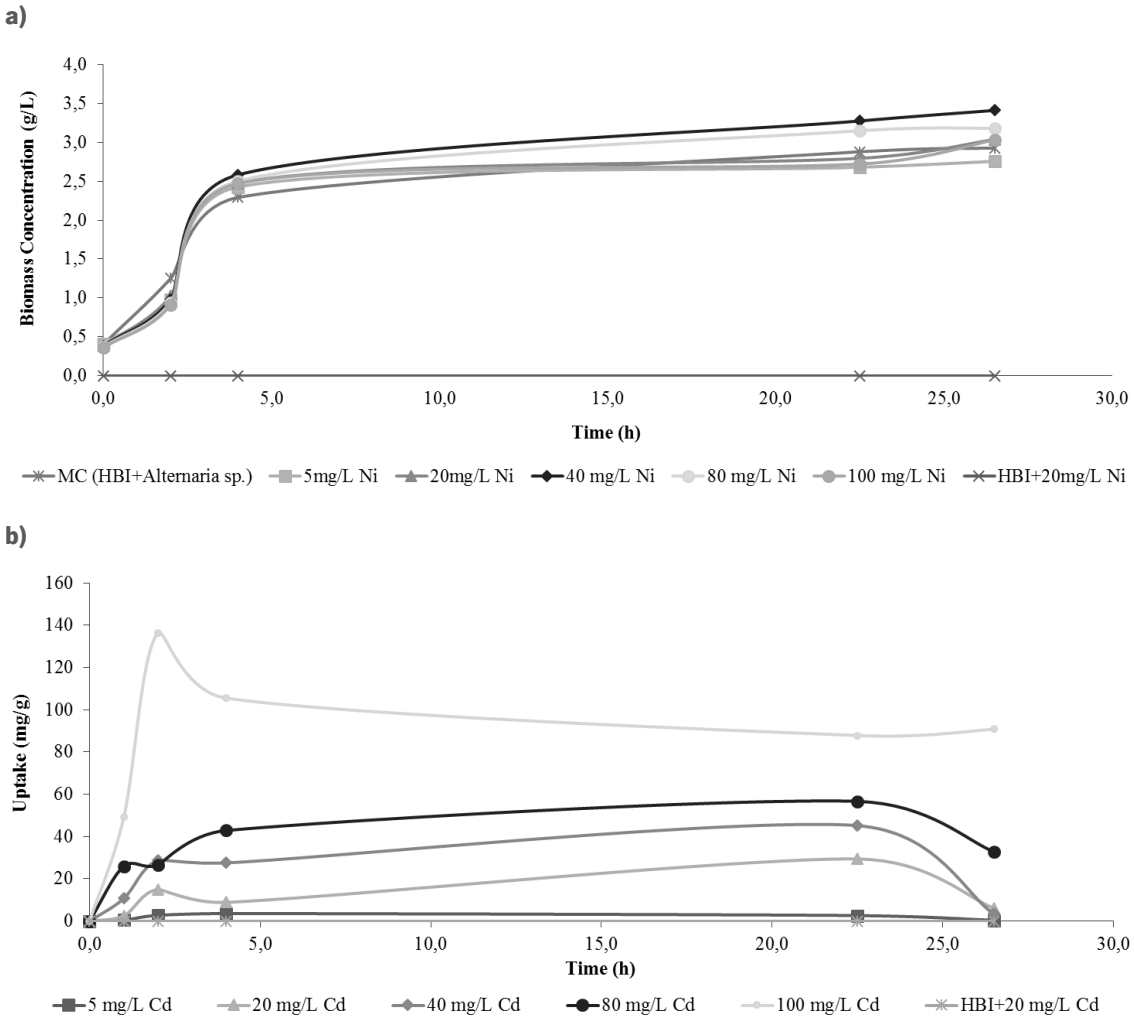

Figure 3.2. a) Growth profile for *Alternaria* sp. (g/L) when exposed to different initial concentrations of Cd^{2+}; **b)** Uptake (mg/g) of Cd^{2+} for different initial concentrations (5 mg/L to 100 mg/L) (37°C, 150 rpm) for the suspended culture of *Alternaria* sp.

The assays conducted with *Penicillium* sp. and Ni^{2+} showed that the growth profile is identical, not only for all the initial concentrations tested, but also to the growth profile obtained for *Alternaria* sp. when exposed to Ni^{2+}. Figure 3.3.a shows that, as the concentration of Ni^{2+} increases, the maximum concentration of biomass obtained decreases, always being higher than the one obtained with MC. Maximum removal percentages of 33 % to 71 % and maximum uptake of 7.2 mg/g to 86 mg/g were obtained. The maximum removal percentage tended to decrease with the increase of Ni^{2+} concentration, whereas the uptake tended to increase during the first 22.5 hours (Figure 3.3.b).

When exposed to Cd^{2+}, the growth profile of *Penicillium* sp. changed dramatically (Figure 3.4.a). For initial concentrations of 20 mg/L and 40 mg/L this fungus growth is faster than the growth in MC. However, when exposed to initial concentrations equal to 5 mg/L, 80 mg/L and 100 mg/L, its growth is significantly inhibited, which may be explained by the fact that 5 mg/L of Cd^{2+} may not exercise any positive effect on the growth mechanisms, whereas for concentrations higher than 80 mg/L, Cd^{2+} may exhibit a xenobiotic behavior.

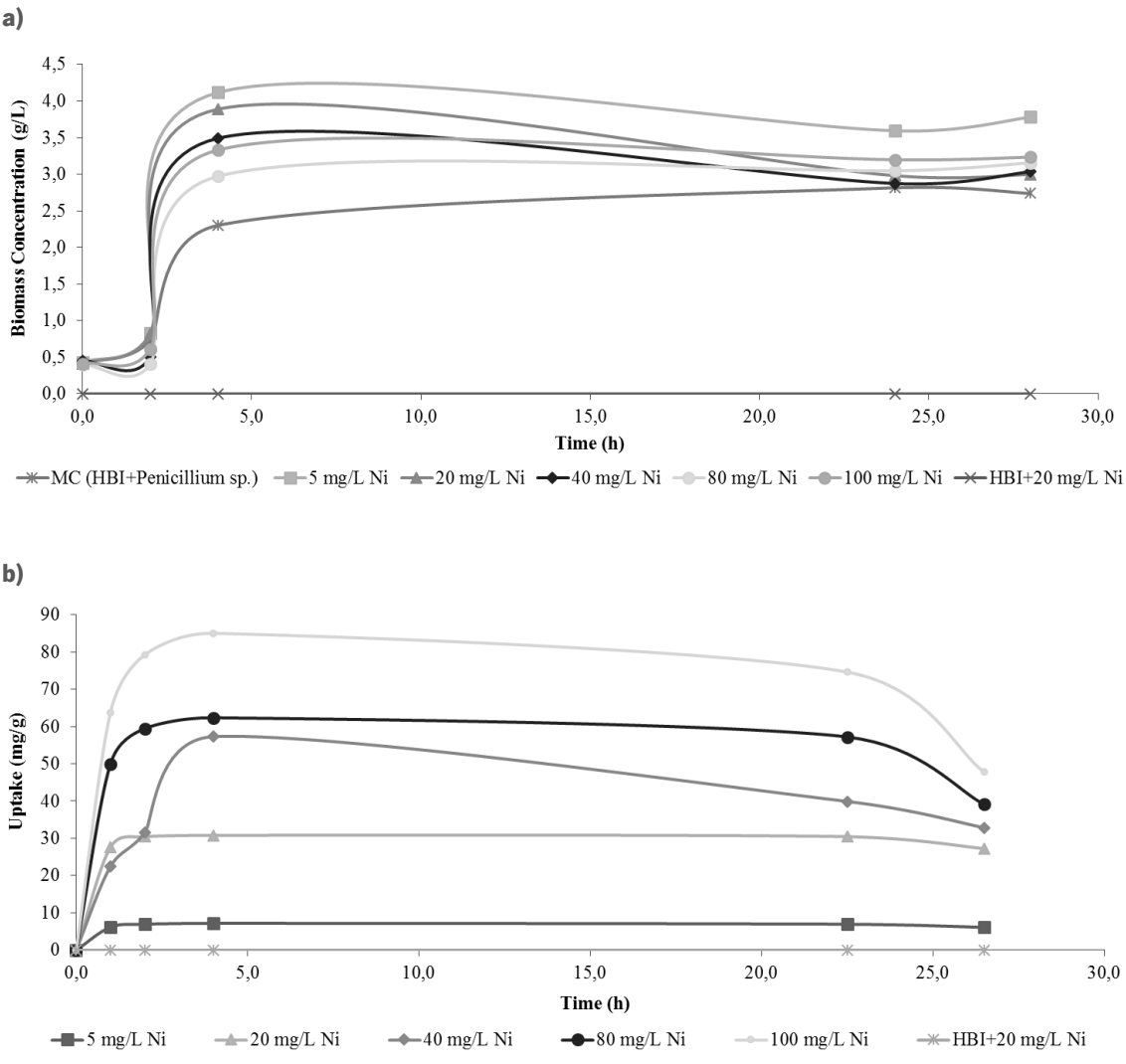

Figure 3.3 .a) Growth profile for *Penicillium* sp. (g/L) when exposed to different initial concentrations of Ni^{2+}; **b)** Uptake (mg/g) of Ni^{2+} for different initial concentrations (5 mg/L to 100 mg/L) (37°C, 150 rpm) for the suspended culture of *Penicillium* sp.

Maximum removal percentages of 16 % to 52 % and uptake of 6.2 mg/g and 80 mg/g were observed (Figure 3.4.b). The maximum removal percentage was obtained for an initial concentration of 5 mg/L of Cd^{2+} and the uptake tended to increase with the increase of Cd^{2+} concentration and through time.

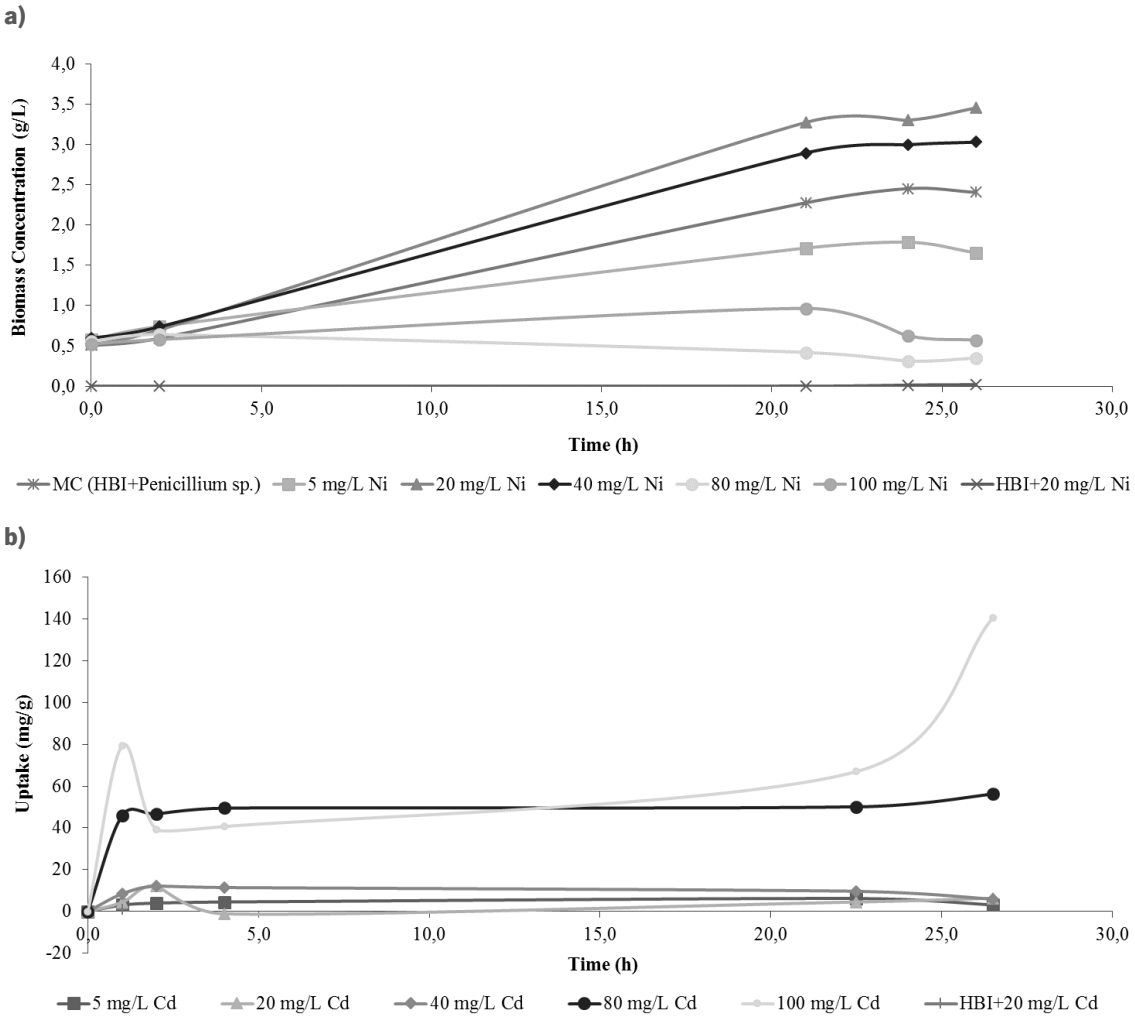

Figure 3.4. a) Growth profile for *Penicillium* sp. (g/L) when exposed to different initial concentrations of Cd^{2+}; **b)** Uptake (mg/g) of Cd^{2+} for different initial concentrations (5 mg/L to 100 mg/L) (37°C, 150 rpm) for the suspended culture of *Penicillium* sp.

S. equisimilis growth (Figure 3.5.a and 3.6.a) is significantly inhibited when exposed to initial concentrations higher than 5 mg/L of either Ni^{2+} or Cd^{2+}, decreasing to values of about half of those obtained with the MC.

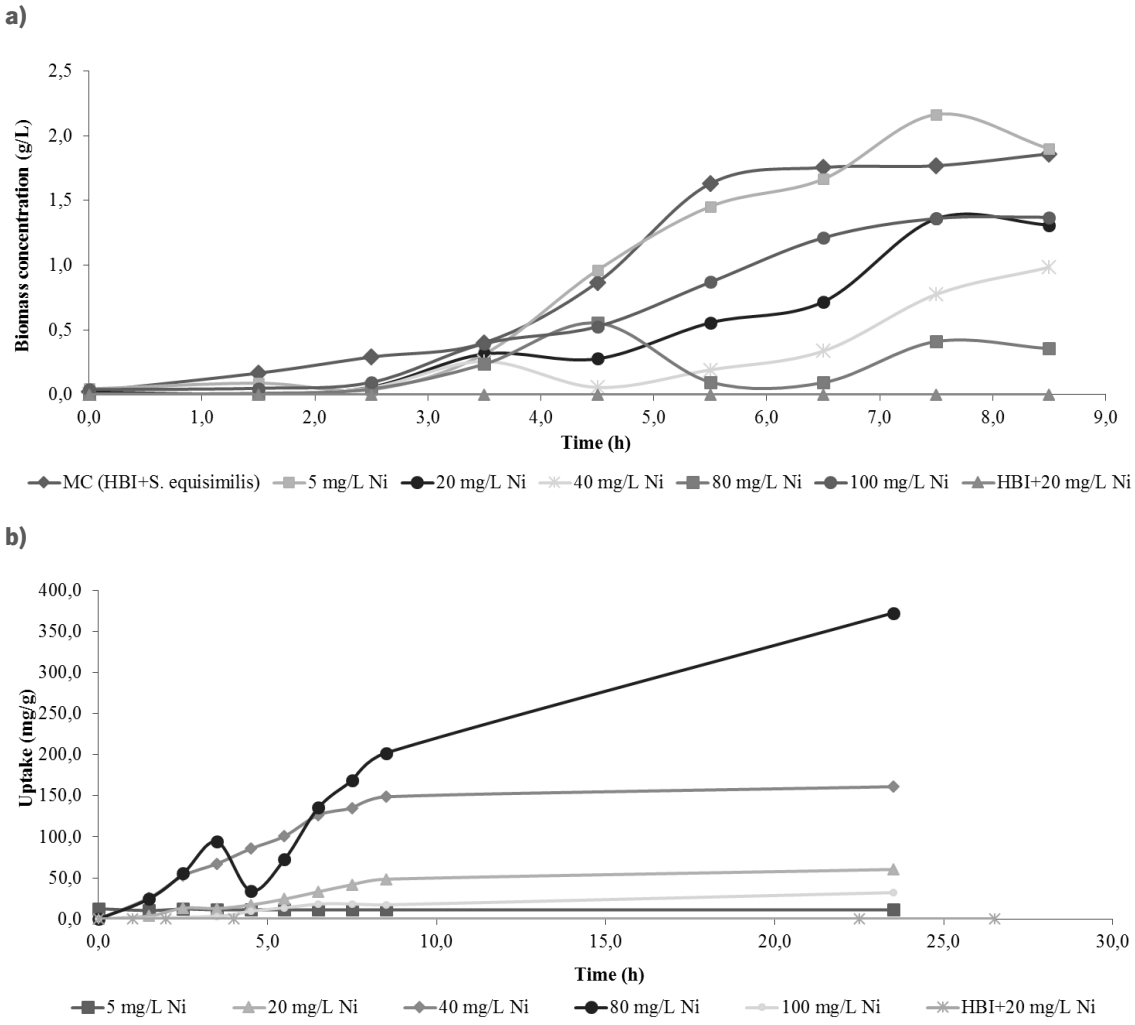

Figure 3.5. a) Growth profile for S. *equisimilis* (g/L) when exposed to different initial concentrations of Ni^{2+}; **b)** Uptake (mg/g) of Ni^{2+} for different initial concentrations (5 mg/L to 100 mg/L) (37°C, 150 rpm) for the suspended culture of *S. equisimilis.*

Ni^{2+} maximum removal percentages ranged between 43 % and 94 %, and the uptake ranged from 3 mg/g to 373 mg/g. For Cd^{2+}, the maximum removal percentages ranged between 61 % and 88 % and the uptake varied between 3.6 mg/g and 155 mg/g. For both metals, the maximum removal percentage tends to decrease with the increase of initial concentration, whereas the uptake tends to increase (Figure 3.5.b and 3.6.b).

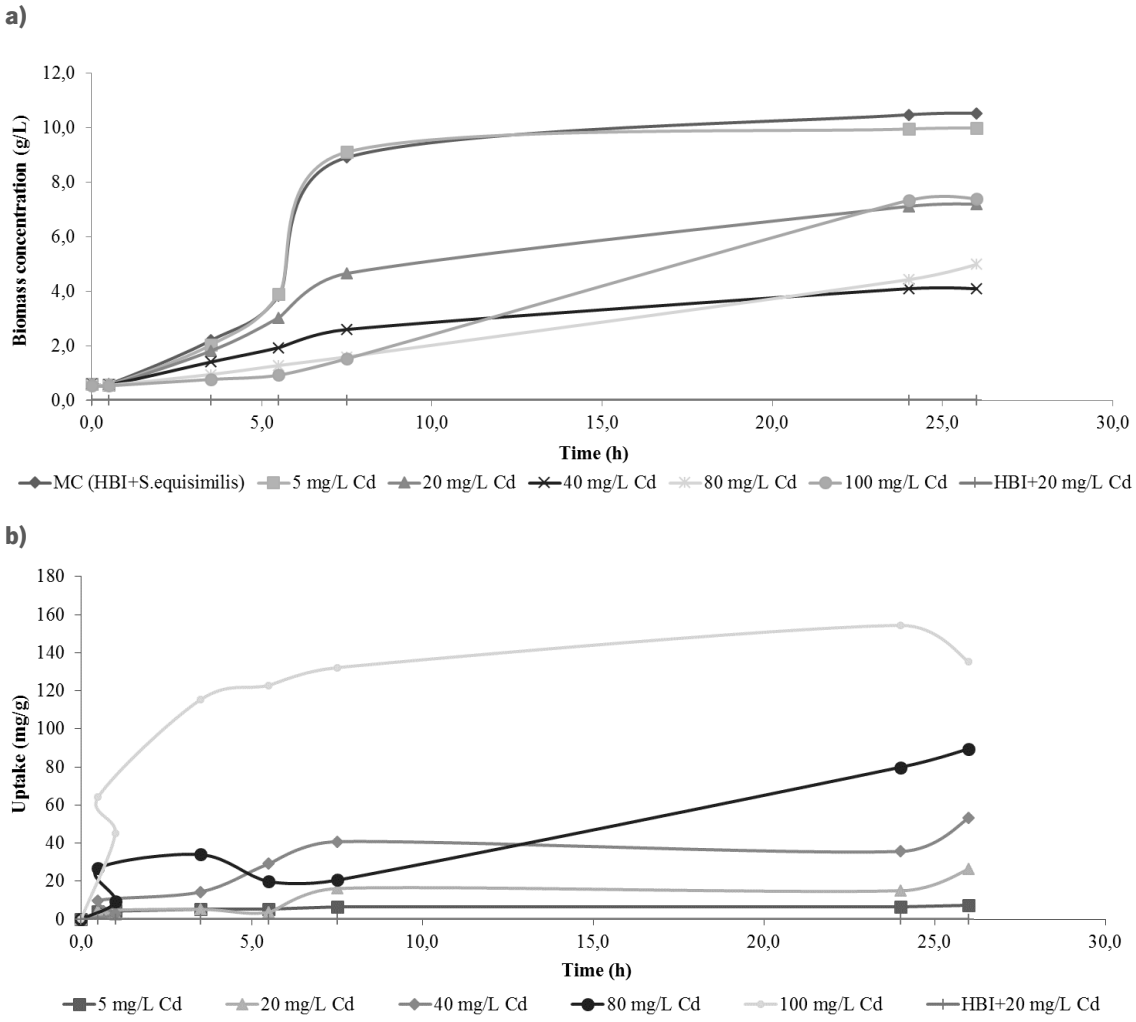

Figure 3.6. a.) Growth profile for *S. equisimilis* (g/L) when exposed to different initial concentrations of Cd^{2+}; **b)** Uptake (mg/g) of Cd^{2+} for different initial concentrations (5 mg/L to 100 mg/L) (37°C, 150 rpm) for the suspended culture of *S. equisimilis*.

The growth results obtained for Ni^{2+} and Cd^{2+} are respectively best described by the Edwards model (R^2= 0.970) and by the Haldane model (R^2=0.999) (Table 3.1).

Table 3.1. Growth kinetic parameters obtained by modelling for *Alternaria* sp., *Penicillium* sp. and *S. equisimilis* in the presence of Ni^{2+} or Cd^{2+}.

Microorganisms/ Metal	Model	μ_{max} (h^{-1})	K_s (g/L)	K_i (g/L)	K	R^2
***Alternaria* sp. (Ni^{2+})**	Haldane	0.53	0.28	26492	-	0.966
***Alternaria* sp. (Cd^{2+})**	Haldane	0.11	13.67	562.70	-	0.822
***Penicillium* sp. (Ni^{2+})**	Haldane	0.85	0.45	530.400	-	0.936
***Penicillium* sp. (Cd^{2+})**	Haldane	0,29	21.92	15.100	-	0.890
***S. equisimilis* (Ni^{2+})**	Edwards	0.78	0.17	492.200	$1.41x10^{15}$	0.970
***S. equisimilis* (C^{2+})**	Haldane	0.37	12.68	20	-	0.999

This corroborates the xenobiotic effect of these metals over the microbial growth. Edwards's model admits the existence of an inhibitory effect which may be caused by the formation of toxic metabolites or by-products, dissociation and/or alteration in the activity of one or more enzymes and development of metabolic aggregates (Raghuvanshi and Babu, 2010). The Scrit obtained for Cd^{2+} is 15.9 mg/L.

Sargassum angustifolium was exposed to Ni and Zn in the assays performed by Ahmady-Asbchin and Jafari et al. (2013). These authors obtained maximum uptake capacities of 0.0417 g/g and 0.0608 g/g dry *S. angustifolium* for Ni and Zn, respectively. Assays conducted by Chaudhuri et al. (2014) with Cd (0.5 mg/L to 3.0 mg/L) achieved maximum removal percentages of 77.07 % and 74.47 % when using *Lemna minor* and *Spirodela polyrhiz*a respectively, as biosorbents. Comparatively, the efficiency of the biosorption matrices herein described appears to be more interesting for the decontamination of Ni^{2+} and Cd^{2+} aqueous solutions.

The kinetic data obtained respectively for the removal of Ni^{2+} and Cd^{2+} were best described by the pseudo-second order model ($R^2 > 0.985$ and $R^2 > 0.899$ for *Alternaria* sp., $R^2 > 0.927$ and $R^2 > 0.940$ for *Penicillium* sp., $R^2 > 0.927$ and $R^2 > 0.865$ for *S. equisimilis*). This model assumes that the rate limiting step of the overall mechanism is the surface chemisorption, a physicochemical interaction between the two phases and it is usually represented by its linear form, as shown in Figure 3.7 to

Figure 3.9. The results obtained indicate that, under these experimental conditions, the rate-limiting step for Ni^{2+} sorption is the surface chemisorption. The straight-line of t/Qt (time / amount of substrate removed at time t) versus t plots indicated the good ability of this model to describe the kinetic data.

a)

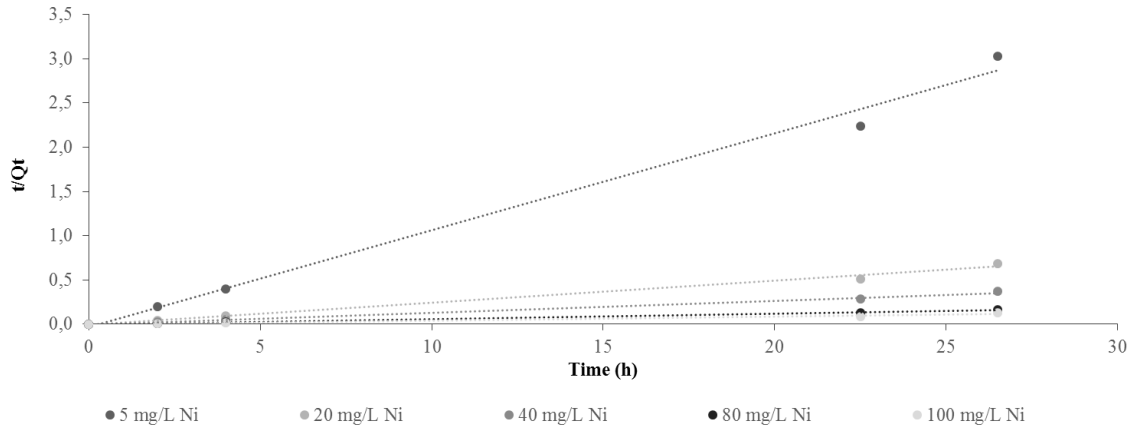

b)

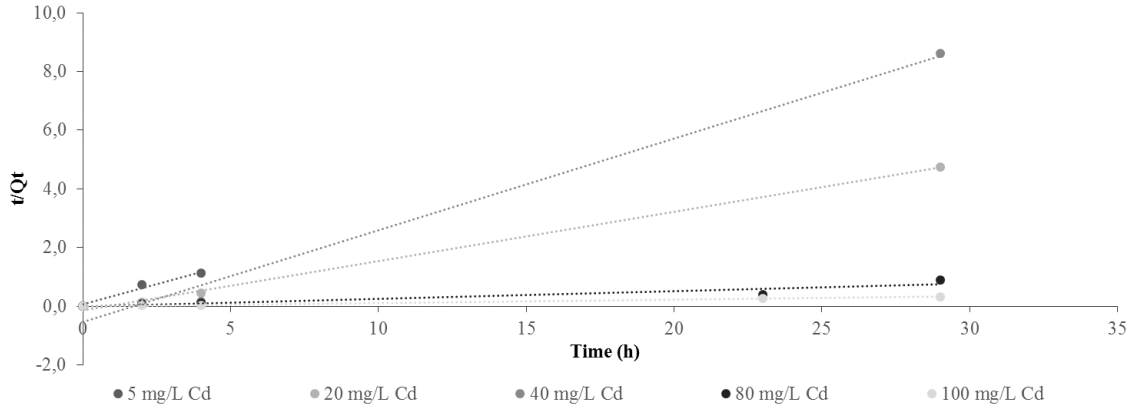

Figure 3.7. a) *Alternaria* sp. kinetic model for the sorption of **a)** Ni^{2+} (5 mg/L and 100 mg/L); **b)** Cd^{2+} (5 mg/L and 100 mg/L).

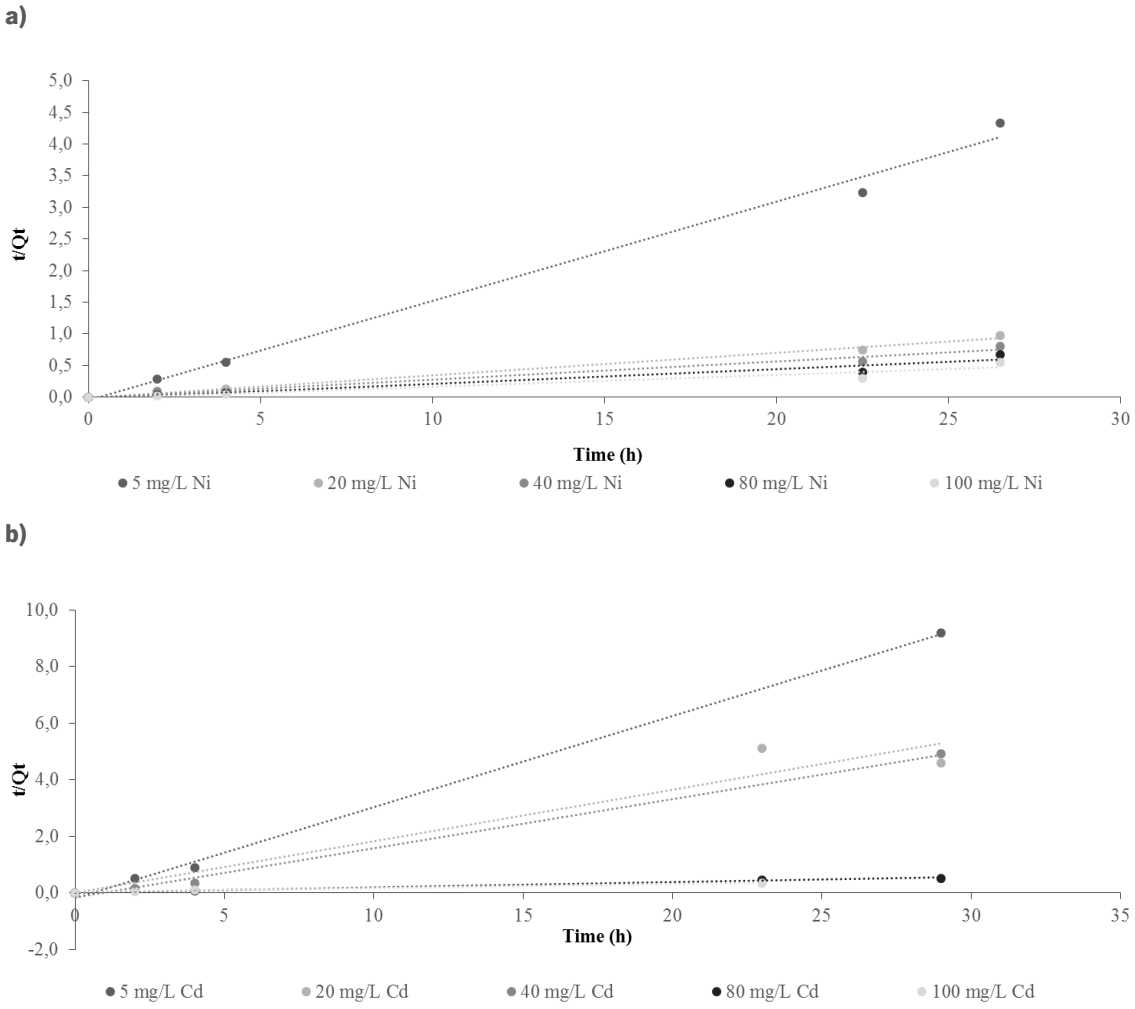

Figure 3.8. a) *Penicillium* sp. kinetic model for the sorption of **a)** Ni^{2+} (5 mg/L and 100 mg/L); **b)** Cd^{2+} (5 mg/L and 100 mg/L).

These results suggest that the growth of both fungi are positively affected by Ni^{2+} and negatively affected by Cd^{2+}, as opposite to *S. equisimilis* that is negatively affected by both metals. It is, however, extremely important to highlight that despite this sensitivity, the removal percentage, as well as the uptake obtained by *S. equisimilis* were significantly higher than those obtained with fungi.

a)

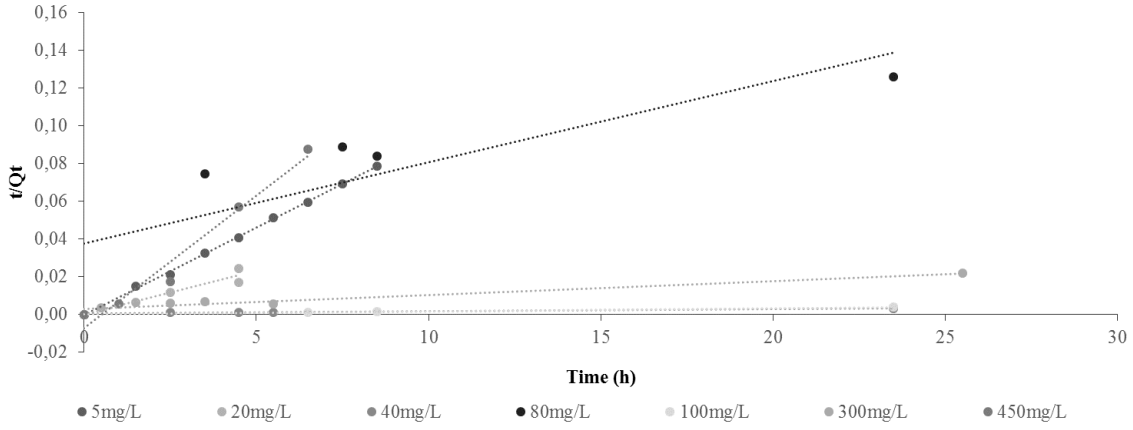

b)

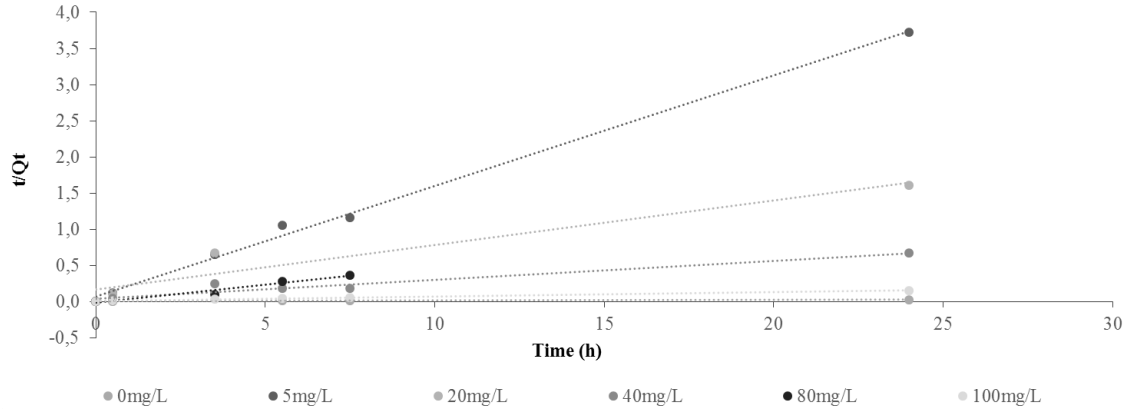

Figure 3.9. *S. equisimilis* kinetic model for the sorption of **a)** Ni^{2+} (5 mg/L and 100 mg/L); **b)** Cd^{2+} (5 mg/L and 100 mg/L).

They also suggest that an increase in the initial concentration of metal caused an increase in the uptake (Table 3.2). This may be explained by the increase of the driving force to overcome all mass transfer resistance between the aqueous and the solid phases (Çelekli and Bozkurt, 2000).

Table 3.2. Ni^{2+} and Cd^{2+} sorption percentage and uptake obtained with *Alternaria* sp., *Penicillium* sp. and *S. equisimilis* when exposed to an aqueous solution of Ni^{2+} or Cd^{2+} (5 mg/L to 100 mg/L).

			***Alternaria* sp.**		
Ni^{2+} (mg/L)	**5**	**20**	**40**	**80**	**100**
Removal (%)	71.07	73.66	69.26	75.51	75.42
Uptake (mg/g)	10.67	43.79	80.45	177.70	253.08
Cd^{2+} (mg/L)	**5**	**20**	**40**	**80**	**100**
Removal (%)	29.67	64.63	58.06	36.43	43.79
Uptake (mg/g)	3.58	29.39	45.13	56.64	90.80
			***Penicillium* sp.**		
Ni^{2+} (mg/L)	**5**	**20**	**40**	**80**	**100**
Removal (%)	70.62	70.18	49.08	34.56	33.38
Uptake (mg/g)	6.95	30.82	57.28	62.37	85.01
Cd^{2+} (mg/L)	**5**	**20**	**40**	**80**	**100**
Removal (%)	51.15	26.91	15.56	23.21	45.15
Uptake (mg/g)	6.16	12.24	12.10	56.18	140.58
			S. equisimilis		
Ni^{2+} (mg/L)	**5**	**20**	**40**	**80**	**100**
Removal (%)	87.37	79.75	79.56	61.87	82.83
Uptake (mg/g)	12.40	60.29	161.10	372.64	32.06
Cd^{2+} (mg/L)	**5**	**20**	**40**	**80**	**100**
Removal (%)	93.76	88.92	85.98	84.31	43.92
Uptake (mg/g)	7.53	26.34	53.16	89.57	154.39

Generally, under the same experimental conditions, the sorption data showed a stronger affinity of the microorganism towards Ni^{2+}. This could be due to the smaller size of the ionic radius of Ni^{2+} (Cd^{2+} (4.26 Å) > Ni^{2+} (4.04 Å)) and its higher Pauling electronegativity (Ni^{2+} (1.91) > Cd^{2+} (1.69)) (Arshadi et al. 2014).

3.3.2| Biosorption Experiments With Ni, Cd and DEK

Figure 3.10. shows the time profile of the three microorganism growth and the removal percentage (%) of diethylketone (4 g/L), Ni^{2+} and Cd^{2+} (5 mg/L). The microbial growth and the removal percentage (%) of all the pollutants, for all the concentrations tested as functions of time presented similar profiles. The biomass of *Alternaria* sp. (Figure 3.10.a) grew for a period of 25 hours, reaching a maximum concentration of 0.39 g/L, comparable to the results obtained with Ni^{2+} (2.75 g/L to 3.40 g/L) and Cd^{2+} solutions (0.56 g/L to 4.48 g/L, respectively). The data also indicates consumption of diethylketone even if the growth of *Alternaria* sp. is strongly and adversely affected by the simultaneous presence of the three pollutants. The increase of the amount of biomass during the first hours, though small, is related to the use of diethylketone in the cell growth and maintenance, while its decline may be associated with the depletion of the carbon source (diethylketone) and formation of hazardous conditions, such as accumulation of Ni^{2+} and/or Cd^{2+} on the surface and intracellular space of the microbial culture, which may lead to the death of the culture. At this stage of decline, the removal of all three pollutants cannot occur through any biologically active processes (biodegradation, bioaccumulation, etc.) and therefore processes such as sorption are favored. Table 3.3 shows that, as the initial metal concentration increases, the uptake of Ni^{2+} and Cd^{2+} increase, reaching its maximum value for the highest concentration of metal (from 0.08 mg/g to 11.32 mg/g for Ni^{2+} and from 0.08 mg/g to 8.50 mg/g for Cd^{2+}). However, the removal percentage of both metals tends to decrease (from 98.38 % to 43.79 % for Ni^{2+} and from 98.27 % to 32.88 % for Cd^{2+}). This behavior can be explained by some small variations in the initial concentration of the inoculum employed (± 20 %) and by the increasing metal concentration itself. At a lower concentration, the ratio between the initial number of moles of metal ions and the available surface area is smaller and consequently, the fractional sorption becomes independent of the initial concentration. However, at higher concentrations, the available sites for sorption become short compared to the number of

moles of metal ions present and therefore, the metal sorption percentage becomes dependent upon the initial metal ion concentration.

a)

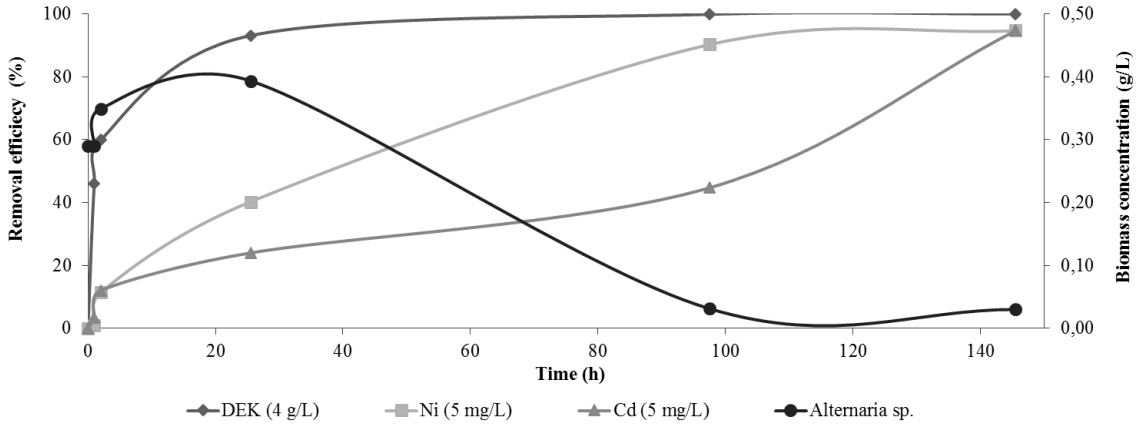

b)

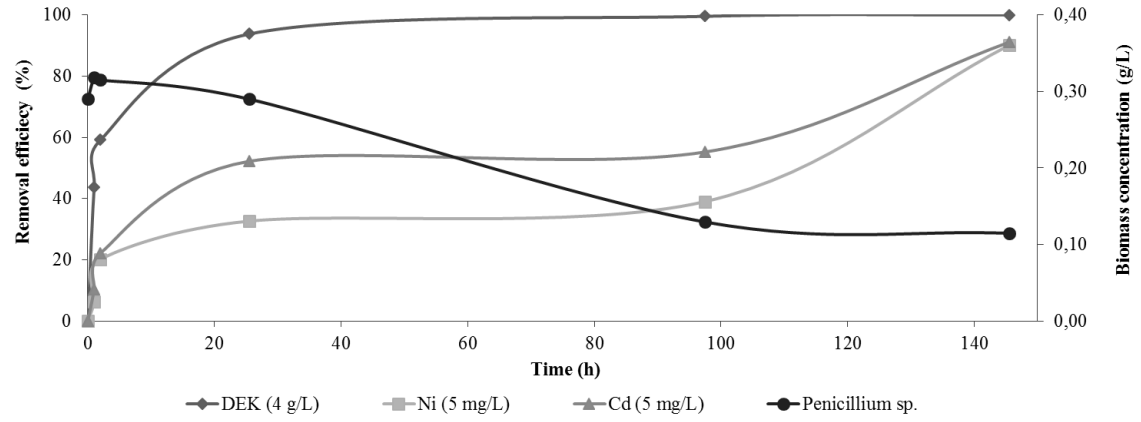

Figure 3.10. Biomass concentration (8 g/L) and removal efficiency (%) as function of time, for an initial concentration of 4 g/L of diethylketone and 5 mg/L of Ni^{2+} and Cd^{2+} (37°C, 150 rpm) **a)** for *Alternaria* sp.; **b)** for *Penicillium* sp. and **c)** for *S. equisimilis*.

c)

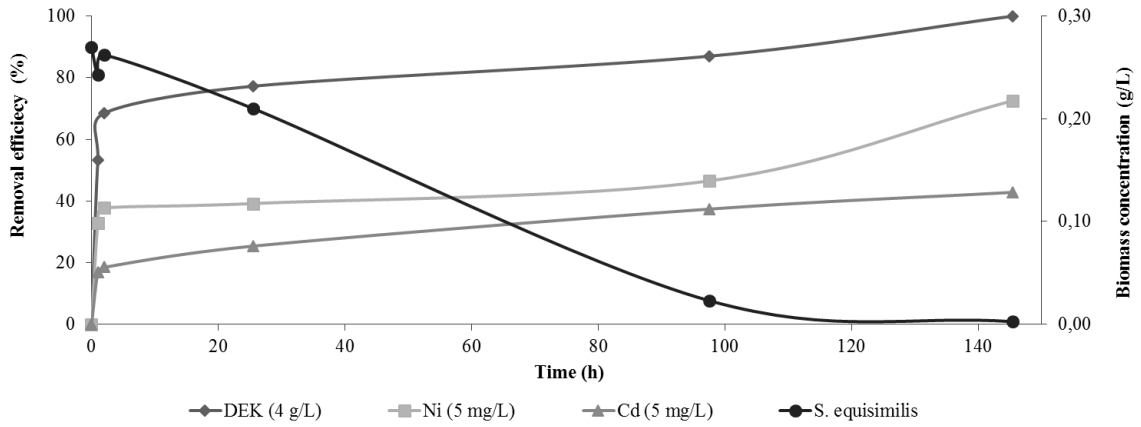

Figure 3.10. Biomass concentration (8 g/L) and removal efficiency (%) as function of time, for an initial concentration of 4 g/L of diethylketone and 5 mg/L of Ni^{2+} and Cd^{2+} (37°C, 150 rpm) **a)** for *Alternaria* sp.; **b)** for *Penicillium* sp. and **c)** for *S. equisimilis* (cont.).

In other words, the sorption process will reach maximum efficiency faster with higher ratio between the number of moles of pollutant and the number of available sites for sorption to occur (Vijayaraghavan et al. 2006). The results obtained also indicate that *Alternaria* sp. is more sensitive towards Cd^{2+} than to Ni^{2+}. It is important to highlight that the sorption of a metal can be explained by several factors such as its ionization state, its electronegativity and by its ionic radius that can facilitate or hamper the penetration of the metal into the polymeric net around the cells. Similar results were obtained by Quintelas et al. (2009) when studying the biosorption performance of an *Escherichia coli* biofilm supported on zeolite NaY for the removal of Cr(VI), Cd(II), Fe(III) and Ni(II). These authors found that the uptake values decreases in the following order Fe(III) > Ni(II) > Cd(II) >Cr(VI).

The removal of each of the three pollutants was found to be best described by the pseudo-second order ($0.899 \leq R^2 \leq 1$ for diethylketone, $0.841 \leq R^2 \leq 0.999$ for Ni^{2+} and $0.962 \leq R^2 \leq 0.999$ for Cd^{2+}) and that the pseudo-second order constant (K_2) tended to decrease with the increase of metal concentration suggesting that the removal rate of all pollutants decreases over time, due to saturation of the active sites.

Penicillium sp., biomass grew for a short period of 2 hours and reached a maximum concentration of 0.31 g/L, a significantly lower value compared to the values achieved in the toxicity assays (3.78 g/L to 2.73 g/L), thus revealing that the microbial growth is negatively affected by the simultaneous presence of diethylketone, Ni^{2+} and Cd^{2+}. Once again, the increase of the biomass though smooth, is associated with the consumption of diethylketone and its decline can be associated with the depletion of the only carbon source (diethylketone), and the formation of toxic compounds. The uptake increases with the increase of initial metal concentration (Table 3.3), until it reaches its maximum value (from 0.09 mg/g to 13.06 mg/g for Ni^{2+} and from 0.09 mg/g to 16.79 mg/g, for Cd^{2+}). Afterwards the removal percentage of both metals tends to decrease (from 97.75 % to 47.15 % for Ni^{2+} and from 95.08 % to 60.63 % for Cd^{2+}). *Penicillium* sp. seems to be more sensitive towards Ni^{2+} than to Cd^{2+} and therefore the maximum values of removal percentage and uptake achieved are lower. Similar results were obtained by Holan and Volesky (1994) that tested the biosorption capacity of different fungal and wood biosorbents towards Cd, Ni and Pb. For all the four fungal species tested the metals were sequestered in the following decreasing order Pb > Cd > Ni. The biosorption potential of *Phanarochaete chrysosporium* towards Cu(II), Cr(III), Cd(II), Ni(II) and Pb(II) was studied by Yetis et al. (1998), who observed that the sorption capacity follows the order: Pb(II) > Cr(III) > Cu(II) = Cd(II) > Ni(II).

The results are best described by the pseudo-second order ($0.999 \leq R^2 \leq 1$ for diethylketone, $0.998 \leq R^2 \leq 1$ for Ni^{2+} and $0.999 \leq R^2 \leq 1$ for Cd^{2+}), indicating that the rate-limiting step for the sorption of diethylketone, Ni^{2+} and Cd^{2+}, is dependent on the pollutants initial concentration and on available active sites of biomass (Figure 3.10.b). The straight-line of t/Qt versus t plots show the good ability of this model to describe the kinetic data obtained for each pollutant. For each pollutant, K_2 tended to decrease with the increase of metal concentration, suggesting that the removal rate of all three pollutants decreases over time, caused by the saturation of the active sites on the biomass surface and by the development of inhibitory compounds that will promote death of the microbial culture.

S. equisimilis reached a maximum concentration of 0.27 g/L (Figure 3.10.c), a value significantly lower when compared either with the values obtained in the toxicity experiments or with the *Alternaria* sp. and *Penicillium* sp. cultures. These results indicate that not only the growth of *S. equisimilis* is adversely affected by the presence of diethylketone, Ni^{2+} and Cd^{2+}, but that *S. equisimilis* is also the most sensitive microorganism tested. The increase of the biomass during the first 2 hours, though quite small, can be related to the use of diethylketone in cell growth and maintenance, while its

decrease may be related with the depletion of diethylketone and subsequent accumulation of toxic substances, which in turn, results in cell death and terminus of the biologically active removal processes. Table 3.3 shows that the increase of initial metal concentration increases the uptake of both metals, reaching its maximum value for the highest concentration of metal (from 0.96 mg/g to 55.65 mg/g for Ni^{2+} and from 0.95 mg/g to 20.37 mg/g for Cd^{2+}). The removal percentages of Ni^{2+} and Cd^{2+} tended to decrease (from 98.37 % to 58.92 % and from 96.90 % to 22.15 %, respectively) revealing a greater sensitivity towards Cd^{2+} when compared with Ni^{2+}. Similar results were obtained by Yetis et al. (1998) and Quintelas et al. (2009). Yetis et al. (1998) studied the sorption potential of *Polyporous versicolor* regarding Cu(II), Cr(III), Cd(II), Ni(II) and Pb(II).

Once again the pseudo-second order was found to be the best model to describe the obtained results ($0.998 \leq R^2 \leq 1$ for diethylketone, $0.841 \leq R^2 \leq 1$ for Ni^{2+} and $0.962 \leq R^2 \leq 1$ for Cd^{2+}), (Figure 3.10.c). The constant K_2 tends to decrease with the increase of initial concentration of metal, suggesting that the removal rate of all three pollutants decreases over time. It is important to emphasize that for all the biosorption experiments the removal of diethylketone was found to be faster within the first hours, after which it progressively slowed down until removal figures of 100 % were reached. This behavior can be explained by the availability of the biomass and its need to consume nutrients essential to the growth.

Table 3.3. Ni^{2+}, Cd^{2+} and diethylketone sorption percentage and uptake obtained with *Alternaria* sp., *Penicillium* sp. and *S. equisimilis* when exposed to an aqueous solution of Ni^{2+}, Cd^{2+} (1 mg/L to 20 mg/L) and diethylketone (4 g/L).

***Alternaria* sp.**				
Ni^{2+} initial concentration (mg/L)	**1**	**5**	**15**	**20**
Removal (%)	98.38	94.67	36.84	43.79
Metal uptake (mg/g)	0.08	1.18	2.41	11.32
Cd^{2+} initial concentration (mg/L)	**1**	**5**	**15**	**20**
Removal (%)	98.27	94.69	48.71	32.88
Metal uptake (mg/g)	0.08	1.18	3.18	8.50
DEK removal (%)	99.10	100	100	99.89
DEK uptake (g/g)	13.91	13.79	44.11	104.55
***Penicillium* sp.**				
Ni^{2+} initial concentration (mg/L)	**1**	**5**	**15**	**20**
Removal (%)	97.75	90.09	40.80	47.15
Metal uptake (mg/g)	0.09	1.30	2.41	13.06
Cd^{2+} initial concentration (mg/L)	**1**	**5**	**15**	**20**
Removal (%)	95.08	91.10	55.26	60.63
Metal uptake (mg/g)	0.09	1.31	3.26	16.79
DEK removal (%)	100	100	100	99.93
DEK uptake (g/g)	12.58	14.75	20.28	113.23

Table 3.3. Ni^{2+}, Cd^{2+} and diethylketone sorption percentage and uptake obtained with *Alternaria* sp., *Penicillium* sp. and *S. equisimilis* when exposed to an aqueous solution of Ni^{2+}, Cd^{2+} (1 mg/L to 20 mg/L) and diethylketone (4 g/L) (cont.).

	S. *equisimilis*			
Ni^{2+} initial concentration (mg/L)	**1**	**5**	**15**	**20**
Removal (%)	98.37	72.58	58.92	60.54
Metal uptake (mg/g)	0.96	5.28	7.33	55.65
Cd^{2+} initial concentration (mg/L)	**1**	**5**	**15**	**20**
Removal (%)	96.90	42.81	42.33	22.15
Metal uptake (mg/g)	0.95	3.11	5.26	20.37
DEK removal (%)	100	99.25	100	100
DEK uptake (g/g)	28.17	39.60	57.97	67.80

After this period of time, the removal percentage decreases due to biomass saturation (Costa et al. 2012). It was also found by GC analyses that no metabolites were formed during the process of diethylketone removal, contrary to what was previously reported by Costa et al. (2015), which studied the biodegradation of diethylketone, in the absence of metals by these three microorganisms. In the studies conducted by these authors, the degradation of diethylketone led to the formation of three metabolites identified as methyl acetate, ethyl acetate and 2-pentanone. The absence of metabolites in the current study may be related with the presence of Ni^{2+} and Cd^{2+}, which may have influenced the metabolic pathway of diethylketone employed by the biomass.

The viability tests showed that all three microorganisms were biologically inactive, even after successive subcultures in a new culture medium, thus confirming the xenobiotic effect of this mixture.

3.4| CONCLUSIONS

It was demonstrated that the growth of *Alternaria* sp. and *Penicillium* sp. is stimulated in the presence of Ni^{2+} and inhibited by initial concentrations of Cd^{2+} higher than 40 mg/L. *S. equisimilis* growth is negatively affected by both metals when exposed to concentrations higher than 5 mg/L, revealing a higher sensitivity towards these two metals. *S. equisimilis* presented the best results in terms of removal efficiency and uptake, thus presenting an advantage over the fungi. It was determined that an increase of the initial concentration of metal causes an increase in uptake and the sorption data shows a higher affinity of the three microorganism towards Ni^{2+}, that with the same experimental conditions. Although mixed solutions exercise a very negative impact on the removal processes and on the growth of the three microorganisms, the system employed is able to decontaminate aqueous solutions with relevant concentrations of Ni^{2+}, Cd^{2+} and diethylketone.

REFERENCES

Ahmady-Asbchin S. and Jafari N. 2013. Removal of nickel and zinc from single and binary metal solutions by *Sargassum angustifolium*. Water Science and Technology 68: 1384-1390.

Ahmed S., Chughtai S., Keane M.A. 1998. The removal of cadmium and lead from aqueous solution by ion exchange with Na-Y zeolites. Separation and Purification Technology 13: 57-64.

Aksu Z. 2005. Application of biosorption for the removal of organic pollutants: a review. Process Biochemistry 40: 997-1026.

Andrews J.F. 1968. A mathematical model for the continuous culture of microorganisms utilizing inhibitory substance. Biotechnology and Bioengineering 10: 707-723.

Arshadi M., Amiri M.J., Mousavi S. 2014. Kinetic, equilibrium and thermodynamic investigations of Ni(II), Cd(II), Cu(II) and Co(II) adsorption on barley straw ash. Water Resources and Industry 6: 1-17.

Brunner W., Focht D.D. 1984. Deterministic three-half-order kinetic model for microbial degradation of added carbon substrates in soil. Applied and Environmental Microbiology 47: 167-172.

Çelekli A., Bozkurt H. 2000. Bio-sorption of cadmium and nickel ions using *Spirulina platensis*: Kinetic and equilibrium studies. Desalination 275: 141-147.

Chaudhuri D., Majumder A., Misra A. K., Bandyopadhyay K. 2014. Cadmium Removal by *Lemna minor* and *Spirodela polyrhiza*. International Journal of Phytoremediation 16: 1119-1132.

Costa F., Neto M., Nicolau A., Tavares T. 2015. Biodegradation of diethylketone by *Penicillium* sp. and *Alternaria* sp. – a comparative study. Current Biochemical Engineering 1: 1-9.

Costa F., Quintelas C., Tavares T. 2014. An approach to the metabolic degradation of diethylketone (DEK) by *Streptococcus equisimilis*: Effect of DEK on the growth, biodegradation kinetics and efficiency. Ecological Engineering 70: 183-188.

Costa F., Quintelas C., Tavares T. 2012. Kinetics of biodegradation of diethylketone by *Arthrobacter viscosus*. Biodegradation 23: 81-92.

Edwards V.H. 1970. The influence of high substrate concentrations on microbial kinetics. Biotechnology and Bioengineering 12: 679-712.

Fereidouni M., Daneshi A., Younesi H. 2009. Biosorption equilibria of binary Cd(II) and Ni(II) systems onto *Saccharomyces cerevisiae* and *Ralstonia eutropha* cells: Application of response surface methodology. Journal of Hazardous Materials 168: 1437-1448.

Flores-Garnica J.G., Morales-Barrera L., Pineda-Camacho G. 2013. Biosorption of Ni(II) from aqueous solutions by *Litchi chinensis* seed. Bioresource Technology 136: 635-643.

Holan Z.R. and Volesky, B. 1994. Biosorption of Lead and Nickel by Biomass of Marine Algae. Biotechnology and Bioengineering 43: 1001-1009.

Işik M. 2008. Biosorption of Ni(II) from aqueous solutions by living and non-living ureolytic mixed culture. Colloids and Surfaces B: Biointerfaces 62: 97-104.

Khairy M., El-Safty A., Shenashen M.A., 2014. Environmental remediation and monitoring of cadmium. TrAC Trends in Analytical Chemistry 62: 56-68.

Khamis M., Jumean F., Abdo N. 2009. Speciation and removal of chromium from aqueous solution by white, yellow and red EUA sand. Journal of Hazardous Materials 169: 948–952.

Lam K-Y., Davidson D.F., Hanson R.K. 2012. High-Temperature Measurements of the Reactions of OH with a Series of Ketones: Acetone, 2-Butanone, 3-Pentanone, and 2-Pentanone. Journal of Physical Chemistry A 116: 5549-5559.

Luong J.H.T., 1987. Generalization of Monod kinetics for analysis of growth data with substrate inhibition. Biotechnology and Bioengineering 29: 242-248.

Monod, J. 1949. The growth of bacterial cultures. Annual Review of Microbiology 3: 371-394.

Morley G.F., Gadd, G.M. 1995. Sorption of toxic metals by fungi and clay minerals. Mycological Research 99: 1429-1438.

Powell E.O. 1967. The growth rate of microorganisms as function of substrate concentration. E. C.G.T., S. R.E. HMSO, London, United Kingdom.

Quintelas C., Costa F., Tavares T. 2012. Bioremoval of diethylketone by the synergistic combination of microorganisms and clays: Uptake, removal and kinetic studies. Environmental Science and Pollution Research 20: 1374-1383.

Quintelas C., Rocha Z., Silva B., Fonseca B., Figueiredo H., Tavares T. 2009. Biosorptive performance of an Escherichia coli biofilm supported on zeolite NaY for the removal of Cr(VI), Cd(II), Fe(III) and Ni(II). Chemical Engineering Journal 152: 110-115.

Raghuvanshi S., Babu B.V. 2010. Biodegradation kinetics of methyl iso-butyl ketone by acclimated mixed culture. Biodegradation 21: 31-42.

Saravanan P., Pakshirajan K., Saha P. 2009. Batch growth kinetics of an indigenous mixed microbial culture utilizing m-cresol as the sole carbon source. Journal of Hazardous Materials 162: 476-481.

Vijayaraghavan K., Palanivelu K., Velan M. 2006. Biosorption of copper (II) and cobalt (II) from aqueous solutions by crab shell particles. Bioresource Technology 97, 1411-1419.

Yetis Ü., Özcengiz G., Dilek F.B., Ergen N., Erbay A., Dölek A. 1998. Heavy metal biosorption by white-rot fungi. Water Science and Technology 38: 323-330.

CHAPTER 4

Bioremoval of diethylketone by the synergistic combination of microorganism and clays: uptake, removal and kinetic studies

This chapter focuses mainly on the study of a *Streptococcus equisimilis* biofilm in four different clays to remove diethylketone from aqueous solutions. The performance of this combined system in terms of uptake, removal efficiency and kinetics, as well as the interaction between the bacterial culture and the clays on the removal of diethylketone is also assessed. The results obtained prove the ability of *S. equisimilis* supported on clays to efficiently remove diethylketone from aqueous solutions. The removal pathway of diethylketone and its metabolites may be explained by the degradation of diethylketone by *S. equisimilis*, with the subsequent adsorption of the metabolites by the clays or subsequent degradation by the bacteria. Diethylketone degradation kinetics is well described by the pseudo-second order model.

This chapter is based on the following publication: Quintelas C., Costa F., Tavares T. 2012. Bioremoval of diethylketone by the synergistic combination of microorganism and clays: uptake, removal and kinetic studies. Environmental Science and Pollution Research 20: 1374-1383.

4.1| INTRODUCTION

The scientific and technological advances in addition of being responsible for the enormous progress in numerous industrial areas, are also accountable for the environmental degradation, mainly due to the discharge of untreated effluents and to the emission of toxic compounds to the atmosphere.

Ketones are release into the environment due to natural and anthropogenic sources (Aranda et al. 2004) and can be used as raw materials or intermediates and constitute waste products in the manufacturing of pharmaceutical, plastics, paints and lubricants. The intensive employment of these substances has resulted in their accumulation in aquatic and terrestrial environments (Hernandez et al. 2002).

The traditional treatment processes used for the elimination of volatile organic compounds such as thermal degradation, oxidation, with or without flame (Gasnot et al. 2000), biofiltration (Chou and Li 2010), adsorption on granular activated carbon, GAC (Buburuzan et al. 2010) and air-stripping (Kungsanant etal. 2008) are in general very expensive. Therefore, the application of microorganisms to decontaminate aqueous solutions containing ketone has been used as a cost-effective alternative.

Previous works have proven that bacteria is able to successfully bind to metals and some hazardous compounds, such as phenol, chlorophenol, *o*-cresol, hexavalent chromium and triethylamine (Quintelas et al. 2006; Quintelas et al. 2008; Quintelas et al. 2009a; Quintelas et al. 2010; Cai et al. 2011). The behaviour of *Arthrobacter viscosus* to remove diethylketone from aqueous systems was previously studied and revealed that this bacterium is able to completely remove initial concentration of diethylketone ranging between 0.8 g/L and 3.9 g/L (Costa et al. 2012).

The use of natural adsorbents such as clays has attracted much attention, due to their high cation exchange capacity, large surface area and competitive price. Zhang et al. (2010) studied the sorption and desorption of carbamazepine from water by smectite clays and Li et al. (2010) adsorbed tetracycline on kaolinite clay.

Clay materials can be modified using a variety of chemical and/or physical treatments to achieve the desired surface properties in order to obtain a better immobilisation of contaminants (Sarkar et al. 2010) or it can be combined with microorganisms, aiming an efficient removal of hazardous compounds. The interaction between microorganism and clays for the removal of hazardous

substances was investigated by several authors. Froehner et al. (2009a) improved the biodegradation of naphthalene and anthracene using modified vermiculite mixed with soil. Ohnuki et al. (2009) reported the reduction of Pu(VI) to a less hazardous Pu(IV) by a mixture of *Bacillus subtilis* and kaolinite clays, whereas Chen et al. (2009) determined the ability of living and non-living *Pseudomonas putida* CZ1 cells, goethite, kaolinite, smectite and manganite clays and their composites to accumulate copper and zinc from a liquid medium and elucidated the role of microbes in the mobility of metals. Quintelas et al. (2009b) assessed the removal of Cd(II), Cr(VI), Fe(III) and Ni(II) from aqueous solutions by an *Escherichia coli* biofilm supported into kaolinite.

The modelling of the equilibrium data is crucial for industrial applications of a biosorption process since it allows the comparison between different biomaterials under different operational conditions. On the other hand, the knowledge on the adsorption rate is important for designing and upscaling batch treatment systems.

This work aims the development of a technology that combines properties of bacteria and clays as removers of hazardous compounds, applicable to the treatment of aqueous solutions contaminated with solvents. Batch assays were performed to investigate the biosorption behaviour of *Streptococcus equisimilis* and of four different clays mixed with those bacteria in the treatment of diethylketone aqueous solutions. The effect of the initial concentration of the xenobiotic on the performance of the bacteria and the effect of the mass of clay on the performance of *S. equisimilis* mixed with four different clays were studied. The kinetic results were analysed by pseudo-first and pseudo-second order models. The comparison between the behaviour of S*. equisimilis and S. equisimilis* supported on four different clays was accomplished.

4.2| MATERIAL AND METHODS

4.2.1| Organisms, Culture Media and Chemicals Preparation

Streptococcus equisimilis (CECT 926) was obtained from the Spanish Type Culture Collection - University of Valencia. Diethylketone solutions were prepared by diluting diethylketone (Acros Organics) in distilled and sterilized water. The clays used were kaolinite, bentonite, sepiolite and vermiculite. Vermiculite was obtained from Sigma-Aldrich and has an average particle diameter of

0.45 mm, a Brunauer-Emmett-Teller (BET) surface area of 39 m^2/g. Bentonite was collected in Alentejo (Portugal) and presents an average particle diameter of 0.2 mm, a BET surface area of 11.9 m^2/g and a porosity of 11%. Kaolinite was obtained from Minas de Barqueiros, S.A (Apúlia, Portugal) and presents an average particle diameter of 2.37 μm, a BET surface area of 1.37 m^2/g and a porosity of 45.5 %. Sepiolite was obtained from Tolsa, S.A. (Spain) and has an average particle diameter of 0.58 mm, a BET surface area of 108m^2/g and a porosity of 49%.

4.2.2| Biodegradation of Diethylketone by *Streptococcus equisimilis* – Uptake and Removal Efficiency

The biodegradation of different initial concentrations of diethylketone by a culture of *S. equisimilis* in suspension was assessed through batch experiments conducted as 37°C and 150 rpm. The experiments were performed in batch mode, in 0.25 L Erlenmeyers flasks, containing 0.15 L of diethylketone solution (0.2 g/L, 0.35 g/L and 0.7 g/L) and 15 mL of suspended biomass (~ 0.3 g/L).

4.2.3| Degradation of Diethylketone by *Streptococcus equisimilis* Mixed With Clays– Uptake and Removal Efficiency

The ability of four different clays mixed with *S. equisimilis* to remove diethylketone from aqueous solutions was evaluated through batch experiments, performed at 37°C and 150 rpm. The experiments were conducted in 0.25L Erlenmeyers flasks, containing 0.15 L of diethylketone solution (1 g/L), different masses of clay (0.1 g, 0.25 g, 0.5 g, 0.75 g, 1 g and 1.5 g) and 15 mL of suspended biomass (~ 0.3 g/L). All the clays were previously sterilized at 121°C for 20 minutes, before used. Previous studies were conducted to determine the time requires for equilibrium to be achieved (15 days). The supernatant was analysed by gas chromatography (GC) to determine diethylketone concentration through time.

All the experiments were performed in duplicate and the results presented are an average of both experiments. The relative standard deviation and relative error of the experimental measurements were less than 2 % and 5 % respectively.

4.2.5| Analytical Methods

4.2.5.1| Gas Chromatography (GC)

The GC employed herein was a Chrompack CP 9001, equipped with a flame ionization detector (FID). The separations were performed using a TRB-Wax capillary column (30 m x 0.32 mm x 0.25 μm). The operating conditions were as follows: the column was held initially at 50 °C, then heated at 10 °C/minute to 100 °C, held at 100 °C for 4 minute then heated again at 40 °C/minute to 200 °C and finally held at 200 °C for 2 minutes. The temperatures of injector and detector were maintained at 250 °C. Nitrogen was used as a carrier gas at a flow rate of 30 mL/minute and the injections were made in the split mode with a split ratio of 1:14. Under these conditions, the retention time for ketone was 2.2 minutes.

4.2.5| Data Modelling

4.2.5.1| Diethylketone Degradation Kinetics

The experimental procedure performed to determine the degradation kinetics (pseudo-first and pseudo-second order kinetic model) of diethylketone are similar to the experimental procedures described in the previous sections. However in these experiments samples of 0.3 mL were collected from the duplicated Erlenmeyers flaks at different time intervals and analysed by GC (see Chapter 2, section 2.2.7.2).

4.3| RESULTS AND DISCUSSION

4.3.1| Biodegradation of Diethylketone by *Streptococcus equisimilis* – Uptake and Removal Efficiency

The C/C_0 profile obtained for all the initial concentrations of diethylketone tested is very similar and present a steady decrease in C/C_0 with time (Figure 4.1). After 400 hours, the removal of diethylketone is almost complete. The degradation of harmful compounds, such as diethylketone to less harmful compounds by microorganisms can occur through fixation by the functional groups

present on the biomass surface or by metabolic activities. The principle agents responsible for the degradation of organic compounds are enzymes. *Streptococcus* species are known to produce enzymes such as N-acetylglucosaminidase, serine proteinase, NAD-glycohydrolase, cysteine proteinase, arginine deiminase and AND-ribosyltransferase (Collin and Olsém, 2003) responsible for the degradation of hazardous compounds.

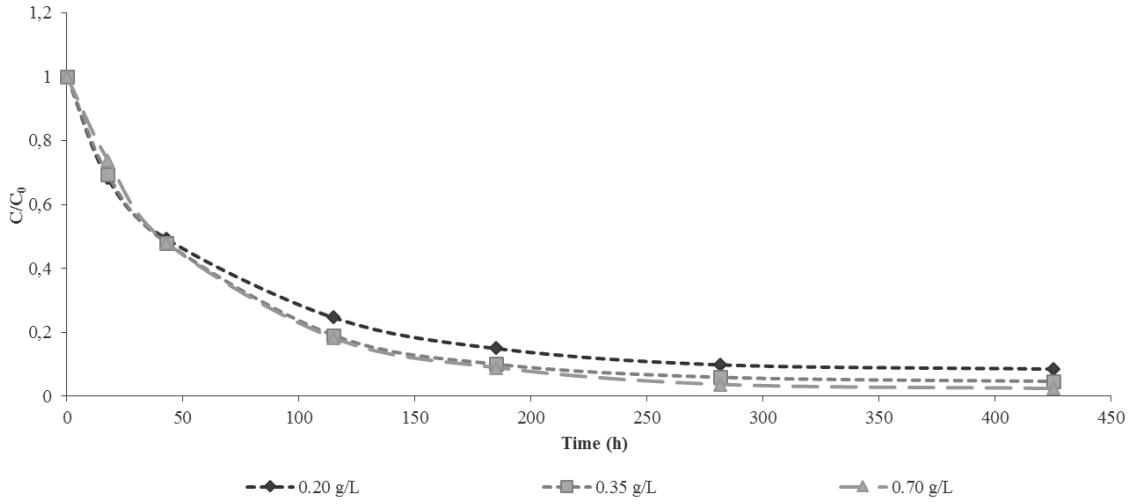

Figure 4.1. Ratio between residual and initial solvent concentration (C/C_0) versus time (in hours) for the experiments conducted only with *S. equisimilis*.

Table 4.1 Solvent uptake (mg/g) and removal efficiency (%) obtained with *S. equisimilis* (37 °C, 150 rpm, diethylketone initial concentration of 0.2 g/L, 0.35 g/l and 0.7 g/L).

Initial concentration (g/L)	Uptake (mg/g)	Removal efficiency (%)
0.2	0.17	91.4
0.35	0.33	95.4
0.7	0.68	97.7

In the present experimental work, several non-identified metabolites (intermediates) were found during the experiments, with the formation of chromatographic peaks different of diethylketone peak. At the end of the experiments, the chromatographic peaks belonging to these metabolites were found to disappear, suggesting that diethylketone degradation occurs in parallel with the degradation of diethylketone metabolites and with the adsorption performed by the functional groups present on the microbial surface.

The carbonyl group present on the ketones structure is polar as a consequence of the higher electronegativity of the oxygen centre compared to the one of carbonyl carbon and, for that reason, ketones are nucleophilic in the oxygen and electrophilic in the carbon. As the carbonyl group interacts with water by hydrogen bonding, ketones are hydrogen bond acceptors usually originating compounds with hydroxyl groups.According to van der Mei et al. (1996), the main functional groups present on *Streptococcus* sp. are amide I and amide II, with absorption bands at 1653 cm^{-1} and 1541 cm^{-1} respectively, phosphate bands at 1237 cm^{-1} and sugar bands at 1070 cm^{-1} next to hydrocarbon absorption bands in the wavelength region between 3000 cm^{-1} and 2800 cm^{-1}. Some of these groups are responsible for the adsorption of diethylketone or its metabolites and contribute to its removal. As it could be seen in Table 4.1 the removal of diethylketone ranges from 91 % to 98 %.

4.3.2| Degradation of Diethylketone by *Streptococcus equisimilis* Supported on Clays– Uptake and Removal Efficiency

Figure 4.2 shows that the ratio between residual and initial diethylketone concentration (C/C_0) as a function of time presents similar profiles for all the clays tested and for all the masses of tested. The removal of diethylketone by the suspended bacteria mixed with clays presents a typical adsorption kinetics that comprises two phases: the initial and very fast phase mainly constituted by a surface process and a second phase that is dependent mostly on the microbial metabolism.The results obtained present slightly differences on the removal efficiency and performance between the four different clays, tested with *S. equisimilis* (Table 4.2). It is possible to observe from Table 4.2 that as the mass of clay increase, the uptake of diethylketone, defined as the mass of solvent over the mass of sorbent, decreases. The values of uptakes and removal efficiency were found to be very similar, for all the masses of clay tested. However, when vermiculite is used, the removal of diethylketone is slightly faster.

a)

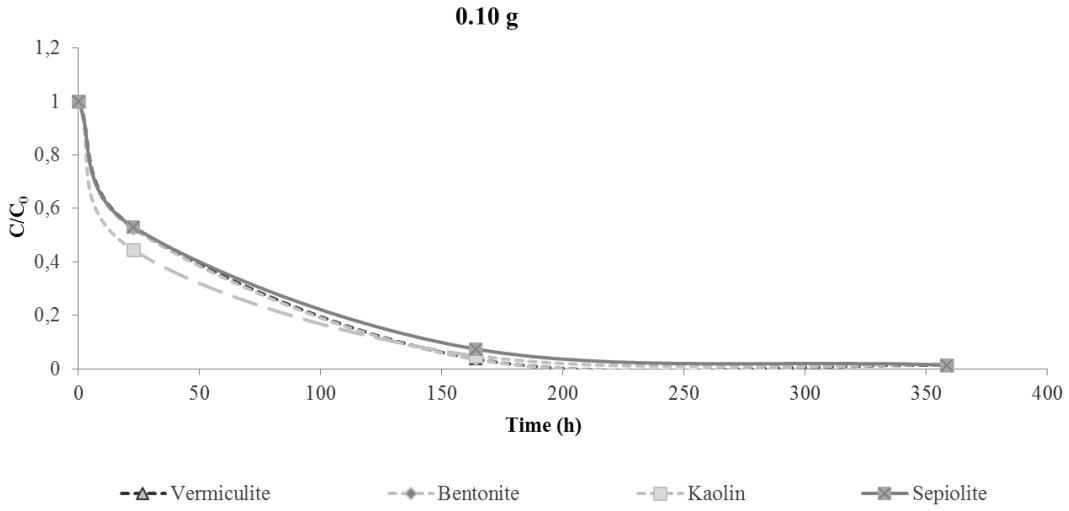

b)

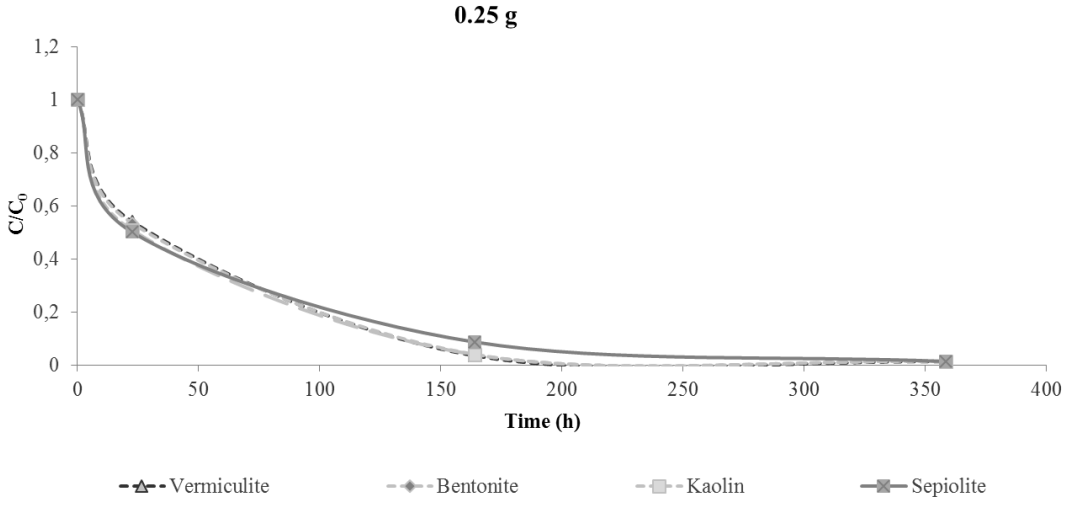

c)

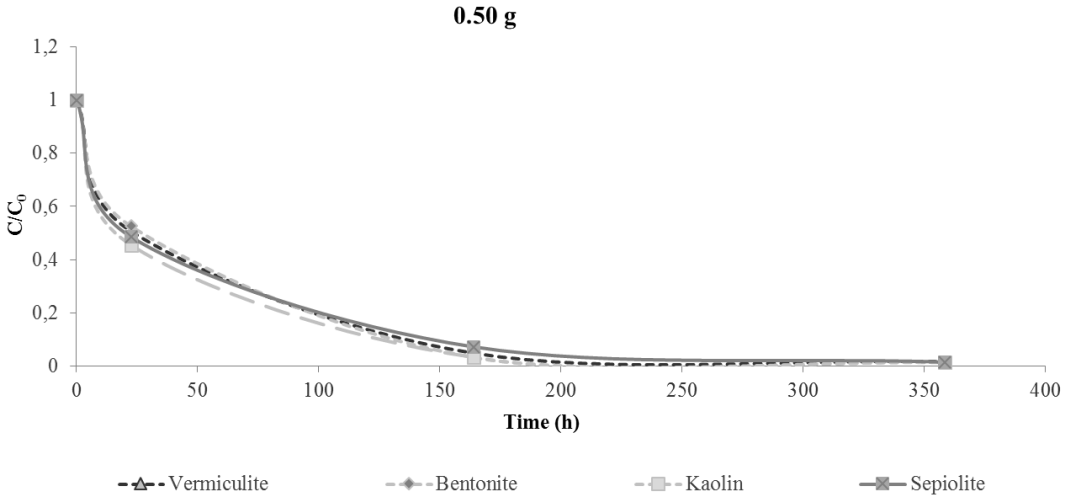

Figure 4.2. Ration between residual and initial solvent concentration (C/C_0) as a function of contact time, for clay masses of **a)** 0.1 g; **b)** 0.25 g; **c)** 0.5 g; **d)** 0.75 g; **e)** 1.0 g and **f)** 1.5 g.

d)

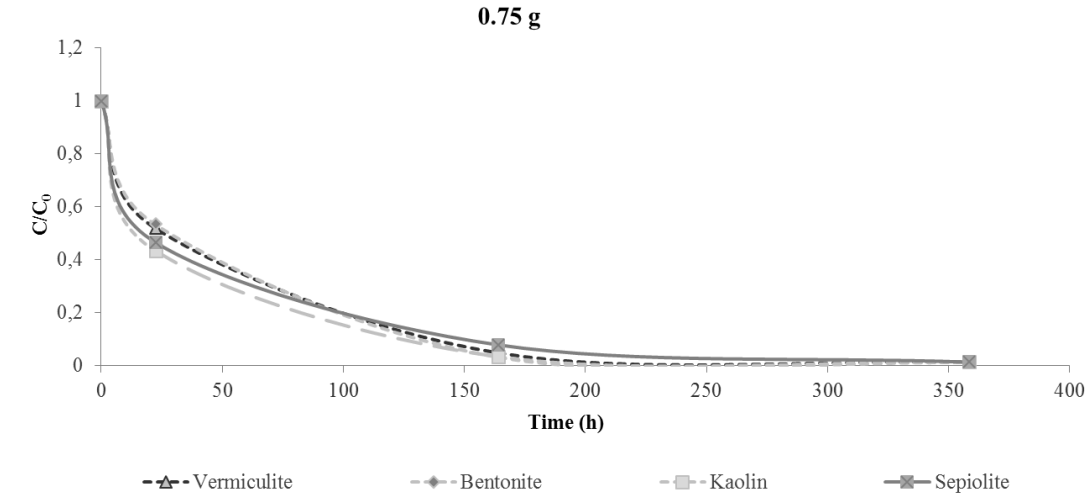

e)

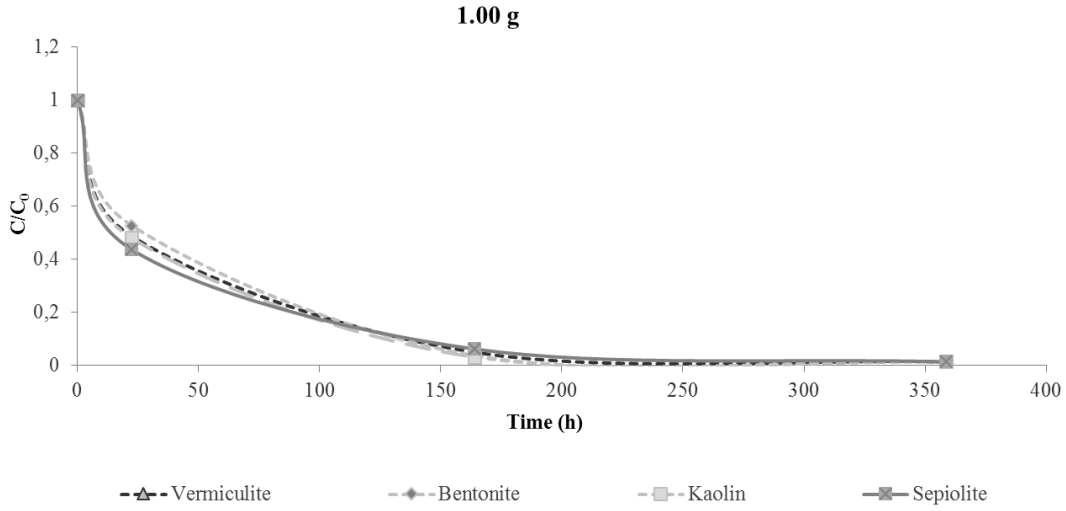

f)

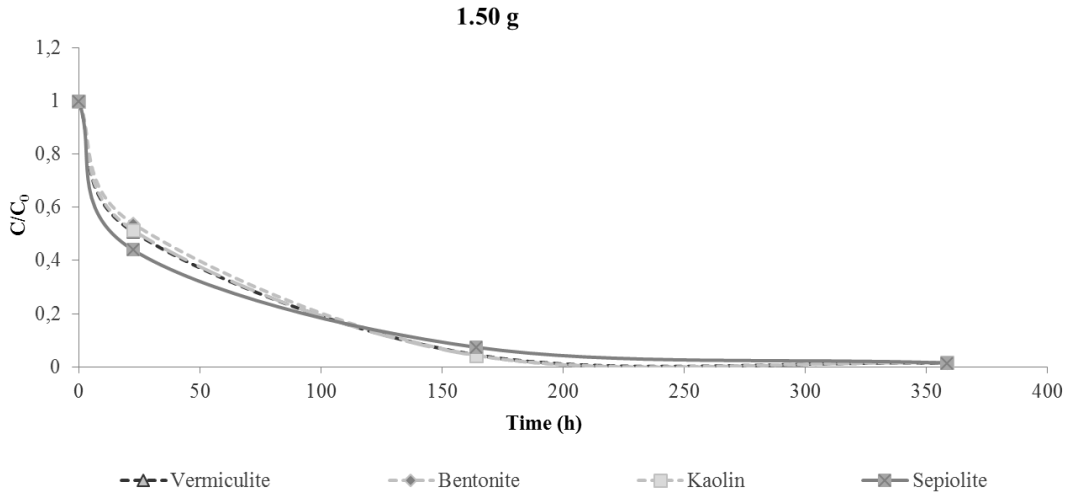

Figure 4.2. Ration between residual and initial solvent concentration (C/C_0) as a function of contact time, for clay masses of **a)** 0.1 g; **b)** 0.25 g; **c)** 0.5 g; **d)** 0.75 g; **e)** 1.0 g and **f)** 1.5 g. (cont.).

Table 4.2 Solvent uptake (mg/g) and removal efficiency (%) obtained with *S. equisimilis* mixed with different masses of clay (37 °C, 150 rpm, diethylketone initial concentration of 1 g/L).

System	Mass (g)	0.1	0.25	0.50	0.75	1.00	1.50
Vermiculite + *S. equisimilis*	Uptake (mg/g)	1.67	0.67	0.33	0.22	0.17	0.11
	Removal (%)	98.6	98.6	98.5	98.6	98.6	98.6
Bentonite + *S. equisimilis*	Uptake (mg/g)	1.66	0.67	0.33	0.22	0.17	0.11
	Removal (%)	98.6	98.5	98.6	98.6	98.6	98.6
Kaolinite + *S. equisimilis*	Uptake (mg/g)	1.67	0.67	0.33	0.22	0.17	0.11
	Removal (%)	98.6	98.6	98.6	98.6	98.6	98.6
Sepiolite + *S. equisimilis*	Uptake (mg/g)	1.67	0.67	0.33	0.22	0.17	0.11
	Removal (%)	98.6	98.6	98.6	98.6	98.6	98.6

Chen et al. (2009) also discover that the use of clays combined with *Pseudomonas putida* increases the removal of cooper and zinc. These authors sustain that microorganisms are often intimately intermixed with mineral phases, as clays, to form complex, highly hydrated, high surface area composite materials through attractive van der Waals interactions, hydrogen bonding or ion bridging. Furthermore, the surface properties of these composite materials can differ dramatically from those of pure bacterial and from mineral surfaces, mainly in terms of surface charge, double-layer properties, number of reactive sites and potential metal-binding affinity. Morley and Gadd (1995) reported that the use of mixtures of fungal biomass and montmorillonite presented a reduced uptake of metals, depressed below calculated values by up to 37 % at pH 4, probably due to masking of exchange sites. Mixtures of kaolinite and fungal biomass showed no reduction in metal uptake as the values obtained were similar to those obtained with the individual components. Bacteria, due to their small size, may avoid the masking of exchange sites.

As mentioned above and in section 4.1 there are many functional groups on the *S. equisimilis* cell walls and on clays that can coordinate with diethylketone. Results presented by Quintelas et al. (2011) showed that the main changes on the functional groups present on clays surface, such as

vermiculite, bentonite, kaolinite and sepiolite, that can be accountable for the sorption processes are the OH deformations, the SiO stretching and the -OH stretching.

The diethylketone removal mechanism proposed for this system is similar to the one previously presented (bacteria degrade the diethylketone to simpler products which are adsorbed by the functional groups present on the bacterial cell walls or on the clays' surface).

4.3.3| Diethylketone Removal Kinetics Modelling

According to Froehner et al. (2009b), several steps such as mass transfer of solute from solution to the boundary film, diffusion of solute through the boundary film and sorption of solute onto sites may control the kinetics of the adsorption phenomena on clays. Some of these steps are fast, such as sorption onto sites and others are slow, depending on some parameters like agitation and surface homogeneity. Numerous models can be employed to describe the overall mechanisms of diethylketone degradation, by *S. equisimilis* itself or supported on clays. The experimental kinetic data obtained herein were fitted by pseudo-first and pseudo-second order models for the experiments conducted only with biomass and are presented in Table 4.3, whereas the results obtained for the assays conducted with biomass supported with clays are presented in Table 4.4.

Table 4.3 Pseudo-first order and pseudo-second order kinetic models describing the removal of diethylketone by *S. equisimilis* at different initial diethylketone concentrations

Initial concentration (g/L)	q_e exp (mg/g)	q_e cal (mg/g)	K_2	R^2
0.2	0.17	0.19	0.14	0.999
0.35	0.33	0.36	0.07	0.999
0.7	0.68	0.77	0.02	0.997

The predicted equilibrium capacity values are in agreement with the experimental ones when using the pseudo-first order model, for initial diethylketone concentrations of 0.70 g/L and when using the

pseudo-second order model for initial diethylketone concentrations of 0.20 g/L and 0.35 g/L (Table 4.3). The correlation coefficients were always higher than 0.994, for the pseudo-second order model, whereas for the pseudo-first order model, the correlation coefficients ranged between 0.860 and 1.000, Table 4.4, suggesting the insufficiency of the model to fit the kinetic data for the conditions of the assay. The pseudo-first order kinetic model assumes that the reaction rate is restricted only by one step of sorption on a single class of sites and that all sites are time dependent (Fonseca et al. 2009). Pseudo-second order kinetic model assumes that the rate limiting step of the process may be chemisorption (Kumar et al. 2011), involving valence forces through the sharing or exchange of electrons between the biomass/ biomass supported on clays and diethylketone, complexation, coordination and/or chelation (Suazo-Madrid et al. 2011).

Table 4.4. Comparison between the pseudo-first order and the pseudo-second order kinetic models for the biodegradation of diethylketone by *S. equisimilis* supported on different clays at various masses of adsorbent (1 g/L of diethylketone).

Vermiculite + *S. equisimilis*						
Mass (g/L)	**Pseudo-first order**			**Pseudo-second order**		
	q_e cal (mg/g)	**$K_{1.1}$**	**R^2**	**q_e cal (mg/g)**	**K_2**	**R^2**
0.10	1.21	$7.00x10^{-3}$	0.971	1.72	$4.8x10^{2}$	0.996
0.25	0.46	$6.20x10^{-3}$	0.943	0.69	$11.5x10^{2}$	0.995
0.50	0.30	$9.70x10^{-3}$	0.997	0.34	$25.9x10^{2}$	0.997
0.75	0.20	$9.40x10^{-3}$	0.998	0.23	$36.4x10^{2}$	0.996
1.00	0.11	$4.6x10^{-3}$	0.918	0.17	$54.7x10^{2}$	0.997
1.50	0.10	$9.80x10^{-3}$	0.998	0.11	$76.7x10^{2}$	0.997

Table 4.4. Comparison between the pseudo-first order and the pseudo-second order kinetic models for the biodegradation of diethylketone by *S. equisimilis* supported on different clays at various masses of adsorbent (1 g/L of diethylketone) (cont.).

Bentonite + *S. equisimilis*						
Mass (g/L)	**Pseudo-first order**			**Pseudo-second order**		
	q_e cal (mg/g)	**$K_{1.1}$**	**R^2**	**q_e cal (mg/g)**	**K_2**	**R^2**
0.10	1.57	1.1×10^{-2}	0.999	1.72	4.9×10^{-2}	0.996
0.25	0.46	6.1×10^{-3}	0.950	0.69	1.2×10^{-2}	0.996
0.50	0.33	1.2×10^{-2}	1.000	0.34	2.5×10^{-2}	0.996
0.75	0.22	1.2×10^{-2}	0.999	0.23	3.6×10^{-2}	0.996
1.00	0.11	4.7×10^{-3}	0.886	0.17	4.9×10^{-2}	0.996
1.50	0.10	1.0×10^{-2}	0.999	0.11	6.9×10^{-2}	0.995
Kaolinite + *S. equisimilis*						
Mass (g/L)	**Pseudo-first order**			**Pseudo-second order**		
	q_e cal (mg/g)	**$K_{1.1}$**	**R^2**	**q_e cal (mg/g)**	**K_2**	**R^2**
0.10	1.20	6.9×10^{-3}	0.986	1.70	6.5×10^{-2}	0.998
0.25	0.45	6.2×10^{-3}	0.950	0.69	1.3×10^{-1}	0.997
0.50	0.31	1.3×10^{-2}	0.999	0.34	3.3×10^{-1}	0.998
0.75	0.19	1.1×10^{-2}	0.996	0.23	5.3×10^{-1}	0.998
1.00	0.10	4.6×10^{-3}	0.863	0.17	5.9×10^{-1}	0.997
1.50	0.10	1.0×10^{-2}	0.999	0.11	7.7×10^{-1}	0.996

Table 4.4. Comparison between the pseudo-first order and the pseudo-second order kinetic models for the biodegradation of diethylketone by *S. equisimilis* supported on different clays at various masses of adsorbent (1 g/L of diethylketone) (cont.).

Sepiolite + *S. equisimilis*						
Mass (g/L)	Pseudo-first order			Pseudo-second order		
	q_e cal (mg/g)	$K_{1.1}$	R^2	q_e cal (mg/g)	K_2	R^2
0.10	1.45	$6.9x10^{-3}$	0.998	1.72	$4.3x10^{-2}$	0.996
0.25	0.55	$6.0x10^{-3}$	0.995	0.68	$1.2x10^{-1}$	0.996
0.50	0.28	$7.6x10^{-3}$	0.987	0.34	$2.6x10^{-1}$	0.997
0.75	0.18	$7.1x10^{-3}$	0.979	0.23	$4.0x10^{-1}$	0.997
1.00	0.11	$4.5x10^{-3}$	0.938	0.17	$6.3x10^{-1}$	0.998
1.50	0.09	$7.4x10^{-3}$	0.976	0.11	$8.9x10^{-1}$	0.998

Ofomaja (2010) and Wu et al. (2009) studied the relationship between pseudo-second order parameters and biosorption performance. These authors established a relationship, described as the approaching equilibrium factor (R_w), between the pseudo-second order model constants and the characteristics kinetic curve. This approaching equilibrium factor (R_w) is defined as:

$$R_w = 1 / (1 + K_2 qetref) \quad (4.1)$$

In here tref is the longest operation time (based on kinetic experiments), qe and K_2 correspond respectively to the equilibrium uptake and to the pseudo-second order constant. Wu et al. (2009) refer to four different situations depending on the R_w value:

1. $R_w = 1$, type of kinetic curve: linear, not approaching equilibrium; biosorption is ineffective as equilibrium cannot be reached.

2. $1 > R_w > 0.1$, type of kinetic curve: slightly curved, approaching equilibrium;

3. $0.1 > R_w > 0.01$, type of kinetic curve: largely curved, well approaching equilibrium;

4. R_w < 0.01, type of kinetic curve: pseudo-rectangular, drastically approaching equilibrium.

When R_w = 1 as in the first situation, biosorption is ineffective as equilibrium cannot be reached.

In the present work, the values for R_w were found to range between 0.022 and 0.036 for *S. equisimilis* mixed with clays, for the decontamination of aqueous solutions with an initial concentration of 1 g/L of diethylketone. These values are situated between 0.1 and 0.01, which means that the kinetic curve is largely curved with a good approach to equilibrium confirming the good performance of the system used.

4.4| CONCLUSIONS

It was demonstrated that *S. equisimilis* by itself or by interacting with vermiculite, bentonite, kaolinite and sepiolite clays, is able to remove efficiently diethylketone from aqueous solutions. Almost complete removal of diethylketone was achieved when using *S. equisimilis* supported on clays, with removal percentages of approximately 98 % to 99 %. One possible mechanism to explain the obtained results is that diethylketone is degraded by *S. equisimilis* and the resulting metabolites may be adsorbed by the functional groups present on the cell wall and/or on the clay surfaces. Diethylketone degradation kinetics were found to be well described by the pseudo-second order model and an approaching equilibrium factor (R_w) was used to establish a relationship between pseudo-second order parameters and the biological treatment.

REFERENCES

Aranda A., de Mera Y.D., Rodríguez A., Morales L., Martínez E. (2004. Kinetic study of the gas-phase reactions of Cl radicals with 3- pentanone and 3-hexanone. Journal of Physical Chemistry A 108: 7027–7031.

Buburuzan A.M., Macoveanu M., Cojocaru C., Catrinescu C. 2010. Experimental design to optimise the removal efficiency of *o*- xylene from gaseous flux by adsorption. Journal of Environmental Protection and Ecology 11: 623–634.

Cai T., Chen L., Ren Q., Cai S., Zhang J. 2011. The biodegradation pathway of triethylamine and its biodegradation by immobilized *Arthrobacter protophormiae* cells. Journal of Hazardous Materials 186: 59–66

Chen X., Hu S., Shen C., Dou C., Shi J., Chen Y. 2009. Interaction of *Pseudomonas putida* CZ1 with clays and ability of the composite to immobilize copper and zinc from solution. Bioresource Technology 100: 330–337.

Chou M-S., Li S-C. 2010. Elimination of methyl ethyl ketone in air streams by a biofilter packed with fern chips. Environmental Engineering Science 27: 679–687.

Collin M., Olsén A. 2003. Extracellular enzymes with immunomodulating activities: variations on a theme in *Streptococcus pyogenes*. Infection and Immunity 71: 2983–2992

Costa F., Quintelas C., Tavares T. 2012. Kinetics of biodegradation of diethylketone by *Arthrobacter viscosus*. Biodegradation 23: 81–92.

Eubanks E.F., Forney F.W., Larson A.D. 1974. Purification and characterization of the nocardial acetylesterase involved in 2-butanone degradation. Journal of Bacteriology 120: 1133–1143.

Fonseca B., Maio H., Quintelas C., Teixeira A., Tavares T. 2009. Retention of Cr(VI) and Pb(II) on a loamy sand soil: kinetics, equilibria and breakthrough. Chemical Engineering Journal 152: 212–219.

Froehner S, Martins RF, Furukawa W, Errera MR (2009b) Water remediation by adsorption of phenol onto hydrophobic modified clay. Water, Air, & Soil Pollution 199: 107–113.

Froehner S., Cardoso da Luz E., Maceno M. 2009a. Enhanced biodegradation of naphthalene and anthracene by modified vermiculite mixed with soil. Water, Air, & Soil Pollution 202: 169–177.

Gasnot L., Decottignies V., Turbieza A., Pauwels J.F. 2000. Experimental and kinetic analysis of the thermal degradation of the methylethylketone in methane/air flames UMR CNRS 8522. Combustion Science and Technology 161: 1–25.

Hernandez R., Zappi M., Colucci J., Jones R. 2002. Comparing the performance of various advanced oxidation processes for treatment of acetone contaminated water. Journal of Hazardous Materials 92: 33–50.

Kim Y-M., Jung S-H., Chung Y-H., Yu C-B., Rhee I-K. 2008. Cloning and characterization of a cyclohexanone monooxygenase gene from *Arthrobacter* sp. L661. Biotechnology and Bioprocess Engineering 13: 40–47.

Kumar P.S., Ramalingam S., Sathishkumar K. 2011. Removal of methylene blue dye from aqueous solution by activated carbon pre- pared from cashew nut shell as a new low-cost adsorbent. Korean Journal of Chemical Engineering 28: 149–155.

Kungsanant S., Kitiyanan B., Rirksomboon T., Osuwan S., Scamehorn J.F. 2008. Toluene removal from nonionic surfactant coacervate phase solutions by vacuum stripping. Separation and Purification Technology 63: 370– 378.

Lameiras S., Quintelas C., Tavares M.T. 2008. Biosorption of Cr(VI) using a bacterial biofilm supported on granular activated carbon and on zeolite. Bioresource Technology 99: 801–806.

Li Z., Schulz L., Ackley C., Fenske N. 2010. Adsorption of tetracycline on kaolinite with pH-dependent surface charges. Journal of Colloid and Interface Science 351: 254–260.

Meganathan R., Ensign J.C. 1976. Stability of enzymes in starving *Arthrobacter crystallopoietes*. Journal of General Microbiology 94: 90–96.

Morley G.F., Gadd G.M. 1995. Sorption of toxic metals by fungi and clay minerals. Mycological Research 99: 1429–1438.

Ofomaja A.E. 2010. Biosorption studies of Cu(II) onto Mansonia sawdust: process design to minimize biosorbent dose and contact time. Reactive and Functional Polymers 70: 879–889.

Ohnuki T., Yoshida T., Ozaki T., Kozai N., Sakamoto F., Nankawa T., Suzuki Y., Francis A.J. 2009. Modeling of the interaction of Pu(VI) with the mixture of microorganism and clay. Journal of Nuclear Science and Technology 46: 55–59.

Park Y.C., Shaffer C., Bennett G.N. 2009. Microbial formation of esters. Applied Microbiology and Biotechnology 85: 13–25.

Quintelas C., Fernandes B., Castro J., Figueiredo H., Tavares T. 2008. Biosorption of Cr(VI) by three different bacterial species supported on granular activated carbon—a comparative study. Journal of Hazardous Materials 153: 799–809.

Quintelas C., Figueiredo H., Tavares T. 2011. The effect of clay treatment on remediation of diethylketone contaminated wastewater: uptake, equilibrium and kinetic studies. Journal of Hazardous Materials 186: 1241–1248.

Quintelas C., Fonseca B., Silva B., Figueiredo H., Tavares T. 2009a. Treatment of chromium(VI) solutions in a pilot-scale bioreactor through a biofilm of *Arthrobacter viscosus* supported on GAC. Bioresource Technology 100: 220–226.

Quintelas C., Rocha Z., Silva B., Fonseca B., Figueiredo H., Tavares T. 2009b. Removal of Cd(II), Cr(VI), Fe(III) and Ni(II) from aqueous solutions by an *E. coli* biofilm supported on kaolin. Chemical Engineering Journal 149: 319–324.

Quintelas C., Silva B., Figueiredo H., Tavares T. 2010. Removal of organic compounds by a biofilm supported on GAC: modelling of batch and column data. Biodegradation 21: 379–392.

Quintelas C., Sousa E., Silva F., Neto S., Tavares T. 2006. Competitive biosorption of ortho-cresol, phenol, chlorophenol and chromium (VI) from aqueous solution by a bacterial biofilm supported on granular activated carbon. Process Biochemistry 41: 2087–2091.

Sarkar B., Xi Y., Megharaj M., Krishnamurti G.S.R., Rajarathnam D., Naidu R. 2010. Remediation of hexavalent chromium through adsorption by bentonite based Arquad® 2HT-75 organoclays. Journal of Hazardous Materials 183: 87–97.

Suazo-Madrid A., Morales-Barrera L., Aranda-Garcia E., Cristiani- Urbina E. 2011. Nickel(II) biosorption by *Rhodotorula glutinis*. Journal of Indusrial Microbiology & Biotechnology 38: 51–64.

van der Mei H.C., Naumann D., Busscher H.J. 1996. Grouping of *Streptococcus mitis* strains grown on different growth media by FT-IR. Infrared Physics & Technology 37: 561–564.

Werner L., Latzko F., Hampel W. 1993. Spraydrying of yeast-lytic enzymes from *Arthrobacter* sp. Biotechnology Techniques 7: 663–666.

Wu F-C., Tseng R-L., Huang S-C., Juang R-S. 2009. Characteristics of pseudo-second-order kinetic model for liquid-phase adsorption: a mini-review. Journal of Chemical Engineering 151: 1–9.

Zhang W., Ding Y., Boyd S.A., Teppen B.J., Li H. 2010. Sorption and desorption of carbamazepine from water by smectite clays. Chemosphere 81: 954–960.

CHAPTER 5

Biosorption of nickel and cadmium in the presence of diethylketone by a *Streptococcus equisimilis* biofilm supported on vermiculite

This chapter focuses on the study of the capacity of a *Streptococcus equisimilis* biofilm supported on vermiculite to decontaminate aqueous solutions containing diethylketone, nickel and/or cadmium. The interaction between the sorbent matrices and the different sorbates, individually and in binary combinations, was also assessed. *Streptococcus equisimilis* growth was found to be inhibited for high concentrations of Ni^{2+} and for small concentrations of Cd^{2+}. Vermiculite by itself was found to efficiently sorb Ni^{2+} and Cd^{2+}. When Ni^{2+} and diethylketone are mixed, the sorption values were found to be higher suggesting a synergetic interaction between these two pollutants, whereas when diethylketone and Cd^{2+} are mixed, the sorption of diethylketone was found to decrease significantly, revealing a negative effect of Cd^{2+} over the retention of diethylketone. The presence of a *S. equisimilis* biofilm supported on vermiculite, was found to increase the biosorption efficiency of all pollutants tested.

This chapter is based on the following submitted publication: Costa F., Tavares T. 2016. Biosorption of nickel and cadmium in the presence of diethylketone by *a Streptococcus equisimilis* biofilm supported on vermiculite.

5.1| INTRODUCTION

Water and soil contamination by hazardous substances is as previous reported, one of the most important environmental problems of nowadays (Montagnolli et al. 2009). Many of these substances comprise heavy metals, polyaromatic hydrocarbons and volatile organic compounds that are harmful and toxic to humans due to their carcinogenic, mutagenic and toxic properties, their ability to produce hazardous intermediates and to persist in the environment (Volesky 1990; Vieira et al. 2010; Costa et al. 2012). Some of these substances are hardly degraded in nature and can easily be bio-accumulate via food chain in living tissues, triggering numerous diseases and health disorders (Srivastava et al. 2006; Quin et al. 2012; Chaudhuri et al. 2014).

Activities such as tanneries, jewellery, refinery, mining, electroplating, electronics, battery manufacture, smelting of metalliferous ores, textile, petrochemical and fine chemistry are responsible for the production and discharge of wastewater contaminated with metals causing serious environmental problems (Ahmed et al. 1998; Chopra and Pathak 2010; Kumar et al.2011, Merrikhpour and Jalali 2013). Within the several metals that are currently of high concern and environmental impact, nickel (Ni) and cadmium (Cd) have been the focus of several studies due to its intensive use and release into the environment and due to its harmful effects on living-beings (Ahmed et al. 1998; Suazo-Madrid et al. 2011; Chaudhuri et al. 2014).

Diethylketone is a simple symmetrical dialkyl ketone that is naturally produced and released to nature by plants, fruits (http://pubchem.ncbi.nlm.nih.gov/, http://toxnet.nlm.nih.gov/index.html) and by several industries (paint, plastic, food and pharmaceutical industries) (Lam et al. 2012; Quintelas et al. 2012). Exposure to this ketone may provoke dizziness, tachycardia, fainting and even cause coma or death in cases of prolonged exposure.

The widespread usage and release of these compounds into the environment resulted in their accumulation in nature. In order to control, minimize and prevent pollution as well as to protect and improve the quality of the environment, stricter environmental laws were enacted in most countries (Morlett-Chávez et al. 2010; Quintelas et al. 2012; Ahmady-Asbchin and Jafari 2013).

Some of the techniques usually employed to remove metals include reverse osmosis, chemical precipitation (Kumar et al. 2012, Qin et al. 2012; Hadi et al. 2013), adsorption and ion exchange (Vieira et al. 2010), whereas the techniques used to degrade organic solvents may comprise

oxidation, thermal degradation (Sahoo et al. 2010; Costa et al. 2012), condensation and incineration (Raghuvanshi, and Babu 2010). Several studies prove that among all these techniques, the biological processes are quite promising (Chen et al. 2000, Marseaut et al. 2004; Sar et al. 2004) and present some advantages such as low maintenance costs, high efficiency and eco-friendly character (Araújo and Teixeira, 1997; Sar et al. 1999, Çelekli and Bozkurt 2011). Besides their efficiency, biological techniques do not generate solid wastes and do not produce nitrogen oxides, which would require a secondary treatment (Raghuvanshi, and Babu 2010; Sahoo et al. 2010; Costa et al. 2012).

The use of a clay-microorganisms joint system (Çelekli and Bozkurt 2011; Quintelas et al. 2012) to remove pollutants from wastewater has proven its efficiency and has numerous advantages (Morlett-Chávez et al. 2010) since it combines the adsorption capacity of the clay: excellent physical and chemical stability, large specific surface area and high cation exchange capacity (Quintelas et al. 2012), with the microorganisms ability to degrade, fix and/or entrap pollutants from the aquatic environment, a consequence of the presence of numerous chemical groups (chitin acetamides, phosphate, amino, carboxylic groups, nucleic acids and proteins) on the biomass surface (Yin et al. 2011; Costa et al. 2012). Sorption tests with and without biofilm aim to test and corroborate the importance of the biofilm for the treatment of water contaminated with organic and inorganic compounds.

The aim of this work comprises the development of an environment-friendly technology for the treatment of singular and binary pollutants solutions containing Ni^{2+} plus diethylketone or Cd^{2+} plus diethylketone. Though these two types of pollutants (metals and ketones) appear together in the wastewater of different industries such as metal refining (Dobson and Burgess, 2007) and paint manufacturing (EPA 1993), there are very few published works regarding the simultaneous treatment of these two types of pollutants.

5.2| MATERIALS AND METHODS

5.2.1| Bacteria Strain and Vermiculite – Sorbents Properties

The bacteria strain used in the present study, *Streptococcus equisimilis*, was acquired from the Spanish Type Culture Collection, from the University of Valencia, with reference CECT 926. The

vermiculite, purchased from Sigma-Aldrich, presents a BET surface area of 39 m^2/g, an average particle diameter of 8.45 mm and a porosity of 10 %. In the present study, vermiculite was used as sorbent as well as a support for the bacterial biofilm development and establishment.

5.2.2| Culture Medium and Chemicals Preparation

Brain Heart Infusion (Oxoid CM1135) culture medium, previously sterilized for 20 minutes at 121 °C was used for the bacteria growth. Diethylketone was purchased from Acros Organics (98 % pure) and diluted in sterilized distilled water. Individual stock solutions of 1 g/L of nickel ($NiCl_2 \bullet 6H_2O$, Carlo Erba Reagents) and 1 g/L of cadmium ($CdSO_4 \bullet 8/3H_2O$, Riedel-de-Haën) were prepared by dissolving an appropriate amount of metal in 1 L of sterilized distilled water. The multi-element ICP quality control standard solution was purchased from CHEM Lab (QCS-03) (15E).

The range of concentrations of Ni^{2+} and Cd^{2+} was obtained by dilution of the respective stock solution and varied between 5 mg/L and 450 mg/L for Ni^{2+} and between 5 mg/L and 100 mg/L for Cd^{2+}. The concentration of diethylketone used in all the experimental studies was 3 g/L.

5.2.3| Assessment of the Effect of the Initial Concentration of Metal on the Microbial Growth

1 L Erlenmeyer flasks containing 0.5 L of sterilized Brain Heart Infusion culture medium were inoculated with a pure culture of *Streptococcus equisimilis* and left in an incubator for 24 hours at 150 rpm and 37 °C. The toxicity experiments were conducted in 0.250 L Erlenmeyer flasks containing 0.125 -L of sterilized Brain Heart Infusion (BHI) culture medium and Ni^{2+} (5 mg/L to 450 mg/L) or Cd^{2+} (5 mg/L to 100 mg/L). These Erlenmeyer flasks were subsequently inoculated with 10 mL of the previous culture and incubated in an orbital shaker (150 rpm) at 37°C for several hours. Samples were collected at different time intervals, centrifuged at 1300 rpm (Eppendorf MiniSpin 9056) for 10 minutes. The resuspended pellet was used to quantify the biomass concentration by optical density (OD). The supernatant was used to quantify the concentration of metal by ICP-OES analysis.

A blank, containing only culture medium and bacteria was used to assess the standard growth of *Streptococcus equisimilis*. The toxicity of diethylketone towards *S. equisimilis* is reported in Costa et al. (2014).

5.2.4| Singular and Binary Sorption Experiments

Singular and binary sorption experiments conducted with vermiculite acting as the only sorbent were performed and aimed to evaluate the sorption capacity of vermiculite towards diethylketone, Ni^{2+} and Cd^{2+} individually and mixed, and also to assess the interaction between the different sorbates and the sorbent. These experiments were designed to evaluate the retention efficiency of vermiculite and compare it with the retention efficiency of a biofilm supported on that very vermiculite.

5.2.4.1| Diethylketone Sorption on Vermiculite – Singular Sorption Experiments

Diethylketone sorption experiments were performed in 1 L Erlenmeyer flasks containing 0.425 L of diethylketone solution (3 g/L) and different masses of vermiculite (0.085 g to 40 g). The Erlenmeyer flasks were incubated in an orbital shaker (150 rpm) at 37°C until equilibrium was reached. Former experiments were conducted in order to determine the required time for equilibrium to be reached (90 hours). Samples of 1 mL were collected at different time intervals and centrifuged at 13400 rpm for 10 minutes. The supernatant was analysed by gas chromatography (GC) so that the time course of diethylketone concentration might be determined. A blank containing only an aqueous solution of diethylketone was used to assess any eventual sorption by the Erlenmeyer flasks walls.

5.2.4.2| Metal Sorption on Vermiculite – Singular Sorption Experiments

Ni and Cd sorption assays were accomplished with 1 L Erlenmeyer flasks containing 0.425 L of the metal solution (450 mg/L for Ni^{2+} and 100 mg/L for Cd^{2+}) and different masses of vermiculite (5 g, 7.5 g, 20 g and 40 g). The Erlenmeyer flasks were kept in an incubator with orbital shaker (150 rpm) at 37°C until equilibrium was reached. Previous experiments indicated the required time for

equilibrium to be reached (15 hours for Ni^{2+} and 10 hours for Cd^{2+}). Samples of 1 mL were periodically collected and centrifuged for 10 minutes at 13400 rpm. The supernatant was analyzed to quantify the concentration of metal through time, by ICP-OES analysis. A blank containing an aqueous solution of metal (Ni^{2+} or Cd^{2+}) was used to assess any eventual sorption by the Erlenmeyer flasks walls.

5.2.4.3| Diethylketone and Metal Sorption on Vermiculite – Binary Sorption Experiments

The binary experiments were conducted in 1 L Erlenmeyer flasks with a working volume of 0.425 L containing 3 g/L of diethylketone, 450 mg/L of Ni^{2+} or 100 mg/L of Cd^{2+} and different quantities of vermiculite (5 g, 7.5 g, 20 g and 40 g). The Erlenmeyer flasks were incubated in an orbital shaker (150 rpm) at 37°C until equilibrium was reached. The required time for equilibrium to be reached (20 hours for Ni^{2+} and diethylketone, 17 hours for Cd^{2+} and diethylketone) was previously determined. Samples were collected at different time intervals and centrifuged for 10 minutes at 13400 rpm. The supernatant was analysed to follow the time course of the concentrations of diethylketone and metal, by GC and ICP-OES analysis, respectively. A blank containing an aqueous solution of metal (Ni^{2+} or Cd^{2+}) and diethylketone was used to determine any sorption by the Erlenmeyer flasks walls or the interactions between the sorbates. The sorption of diethylketone by the Erlenmeyer flasks walls was determined in previous assays and found to be negligible.

5.2.5| Biosorption Experiments

The biosorption experiments were performed in 2 L Erlenmeyer flasks containing 0.850 L of working volume. Each Erlenmeyer flask contained of 5 g to 6 g of *Streptococcus equisimilis* biomass, vermiculite (0.085 g to 40 g), diethylketone (3 g/L) and Ni^{2+} (450 mg/L) or Cd^{2+} (100 mg/L). All flasks were incubated in an orbital shaker (150 rpm) at 37 °C until equilibrium was reached. Previous experiments were performed in order to determine the time needed for the equilibrium to be reached for the assays conducted with Ni^{2+} and diethylketone (165 hours for diethylketone and 100 hours for Ni^{2+}) and for the assays conducted with Cd^{2+} and diethylketone, (192.5 hours for 7.5 g and 10 g and 309.5 hours for the remaining masses of vermiculite for diethylketone and 100 hours for Cd^{2+}). At

different time intervals, 1 mL samples were collected and centrifuged at 13400 rpm for 10 minutes. The supernatant was used to determine the variation of the concentration of metal (Ni^{2+} or Cd^{2+}) and of diethylketone through time, by ICP-OES and GC analysis, respectively. A blank, containing only metal, diethylketone and vermiculite was used to isolate the influence of the biomass on the sorption process.

All experiments were performed under sterile conditions, in duplicate, with pH monitoring. The results represent the average of those duplicates and have relative standard deviation and relative errors inferior to 2 % and 5 %, respectively.

5.2.6| Analytical Methods

5.2.6.1| Gas Chromatography (GC)

The concentration of diethylketone in aqueous samples was measured using a GC-MS Varian 4000, equipped with a flame ionization detector (FID), with mass spectrometry (MS) and a ZB-WAXplus column (30 m x 0.53 mm x 1.0 µm). The column was initially held at a temperature 50 °C, then heated at 3 °C/minute to 100 °C, held at 100 °C for 4 minutes, then heated again at 40 °C/minute to 150 °C and finally held at 150 °C for 2 minutes. The temperature of injector and detector was maintained at 250 °C. Nitrogen was used as the carrier gas at a flow rate of 4 mL/min and the injections were performed in the split mode with a split ratio of 1:10. Under these conditions, the retention time for diethylketone is 5.6 minutes.

5.2.6.2| Inductively Coupled Plasma Optical Emission Spectrometry (ICP-OES)

The concentration of nickel and cadmium in aqueous samples was measured by an ICP-OES (Optima 8000, PerkinElmer). The operating conditions were as follows: RF power: 1300 W; argon plasma flow of 8 L/minute; auxiliary gas flow of 0.2 L/minute; nebulizer gas flow of 0.5 L/minute; radial plasma view, for Ni^{2+} and axial plasma view for Cd^{2+}; wavelength of 221.648 nm for Ni^{2+} and 226.502 nm for Cd^{2+}. All the calibration solutions were prepared from a stock solution of Ni^{2+} (1 g/L) and Cd^{2+} (1 g/L) as mentioned in section 5.2.2. All the samples were acidified with nitric acid before being

analysed. The instrument response was periodically checked with the multi-element ICP QC standard solution (CHEM LAB) and with a blank (HNO_3 5 %).

5.2.7| Data Modelling

5.2.7.1| Growth and Removal Kinetics Models

Five growth kinetic models using MATLAB software were tested in order to describe the growth of the biomass, when exposed to different concentrations of Ni^{2+} and Cd^{2+}. The tested models were Monod (Monod 1949), Powell (Powell 1967), Haldane (Andrews 1968), Luong (Luong et al. 1987), Edwards (Edwards 1970) and Gompertz (Zwietering et al. 1990, Fan et al. 2004, Wang and Gu, 2005) (see Chapter 2, section 2.2.7.1). The zero order, pseudo-first order and pseudo-second order models were tested in order to understand, at the experimental conditions, the sorption kinetics of all three pollutants (see Chapter 2, section 2.2.7.2).

5.2.7.2| Sorption Isotherms Models

The equilibrium of the sorption process is described by the distribution of metal ions between the liquid phase and the solid sorbent phase and is usually modelled by adsorption isotherms. In the present study, the adsorption isotherms tested to describe the equilibrium relationship between the pollutants and the solid phase, were the Langmuir (Langmuir, 1918), Freundlich (Freundlich, 1906), Dubinin-Radushkevich (D-R) (Saravanan et al. 2009; Kishore et al. 2013) and BET models (Brunauer, 1938)

Langmuir model

The Langmuir model was initially developed with studies of gas adsorption on activated carbon based on the following assumptions: a) each of the active surface site can only accommodate one adsorbed entity; b) adsorbed entities are bound to the surface at fixed locations; c) the maximum adsorption corresponds to the saturation of the monolayer on the adsorbent surface; d) the adsorption energy

is identical in all active sites and independent presence or absence of adsorbed species in the vicinity (equivalent to considering the same heat of adsorption for all active sites of the surface and the same equilibrium constant KL).

The Langmuir model is useful in describing the adsorption equilibrium in wastewater treatment systems, even if the assumptions listed above are not verified.

A general form of the Langmuir model equation is:

$$q_e = (q_{max} b C_e)/(1+bC_e) \quad (5.1)$$

where q_e is the equilibrium metal sorption capacity (mg/g), C_e is the equilibrium solute concentration in solution (mg/L), q_{max} represents the maximum sorption capacity (monolayer capacity) (mg/g), b represents the Langmuir constants related to and to the bonding energy of adsorption, respectively (L/mg) (Langmuir, 1918).

Freundlich model

The Freundlich model was obtained by assuming that adsorption occurs in heterogeneous surfaces, that is, the active sites have different affinities for the metal ion. The model is represented by the Freundlich equation:

$$q_e = K_f C_e^{1/n} \quad (5.2)$$

where once again q_e is the equilibrium metal sorption capacity (mg/g), C_e is the equilibrium solute concentration in solution (mg/L). K_f is the biosorption equilibrium constant, representative of the sorption capacity and n is a constant indicative of biosorption intensity (Freundlich, 1906).

The Langmuir and the Freundlich models do not incorporate the effects of any external variable environmental factors, although they are capable of describing many biosorption isotherms in most cases.

Dubinin- Radushkevich (D-R) model

The Dubinin-Radushkevich (D-R) states that the characteristic curve of adsorption is related to with the porous structure of the sorbent. This model can be represented by the following equation:

$$q_e=q_D \exp(-B_D [RT \ln(1+1/C_e)]^2) \quad (5.3)$$

Once again qe is the equilibrium metal sorption capacity (mg/g), C_e is the equilibrium solute concentration in solution (mg/L) and q_{max} represents the maximum sorption capacity (monolayer capacity) (mg/g). q_D denotes the theoretical saturation capacity of the monolayer (mg/g), B_D is related to the mean free energy of sorption per gram of the sorbate as it is transferred to the surface of the solid from infinite distance in the solution (mol^2/J^2), R denotes the universal gas constant, T the temperature (K)

BET model

The BET model describes the multi-layer adsorption at the adsorbent surface and assumes that the Langmuir isotherm applies to each layer. This model can be described by the following equation:

$$q_e = q_e=(B\times C_e \times q_{max} / ((C_S-C_e) \times [1+B-1) \times (C_e / C_s)] \quad (5.4)$$

where once again q_e is the equilibrium metal sorption capacity (mg/g), C_e is the equilibrium solute concentration in solution (mg/L) and q_{max} represents the maximum sorption capacity (monolayer capacity) (mg/g). C_S correspond to the saturation concentration of the adsorbed component, B is the BET constant and indicates the energy of interaction between the solute and the adsorbent surface (Brunauer et al. 1938).

5.3| RESULTS AND DISCUSSION

5.3.1| Effect of the Concentration of Metal on the Microbial Growth

After exposure of the biomass to different concentrations of Ni^{2+} (5 mg/L to 450 mg/L), it was observed that the duration of the lag phase is similar, regardless of the initial concentration of Ni^{2+} used, Figure 5.1. For concentrations lower than 100 mg/L, the specific growth rate tends to increase with the increase of Ni^{2+} concentration and is higher than the specific growth rate obtained for the control, whereas for higher concentrations this rate decreases to values closer to the control value. These results suggest that the microbial culture requires the same time to undergo intracellular changes in an effort to adapt to a set of new environment conditions no matter the xenobiotic concentration and that there is a positive stimulation by Ni^{2+} on the growth of the bacterium for concentrations lower than 100 mg/L.

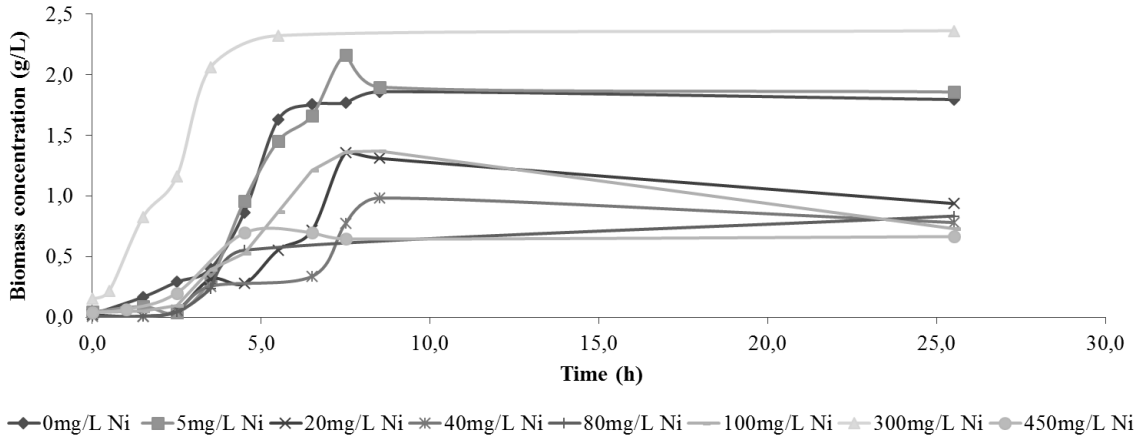

Figure 5.1. Biomass concentration of *S. equisimilis* (g/L) versus time (h) for different initial concentrations of Ni^{2+}.

The uptake and percentage of Ni^{2+} sorbed were found to depend on the initial concentration of nickel (Figure 5.2). In terms of biosorption percentages, for the range of concentrations between 5 mg/L and 80 mg/L inclusive, there were no significant changes (less than 10 %). Nevertheless, the biosorption percentage decreased sharply for Ni^{2+} concentrations higher than 80 mg/L, reaching values lower than 45 %. There was a 30 fold increase of the uptake with the increase of the initial concentration, for the range between 5 mg/L and 80 mg/L inclusive. These results can be explained

by the saturation of the sorption sites when increasing the concentration of Ni^{2+} and by the decreasing of active uptake by the bacteria due to the inhibitory effect of the metal. This behaviour was also observed by other authors (Kara and Kara 2005; Chaudhuri et al. 2014).

It was observed that for all the concentrations of Ni^{2+} tested, the pH did not suffer significant variations, ranging from pH 7.09 to 6.89. Since Ni^{2+} starts to precipitates in the form of $Ni(OH)_2$ at pH of 7.6, it is possible to infer that the decrease of N^{2+} concentration occurs not by Ni^{2+} precipitation (Espinoza et al. 2012), but by biological processes such as biosorption. These processes can occur due to the chemical bonds formed between the ion metal and the functional groups present in the bacteria surface (phosphate, carbohydrate, amide I and amide II) (Costa et al. 2014). It is important to highlight the importance of pH monitoring in order to determine not only the speciation of the metallic elements, but also to avoid any misreading of the actual concentration of metal present in solution.

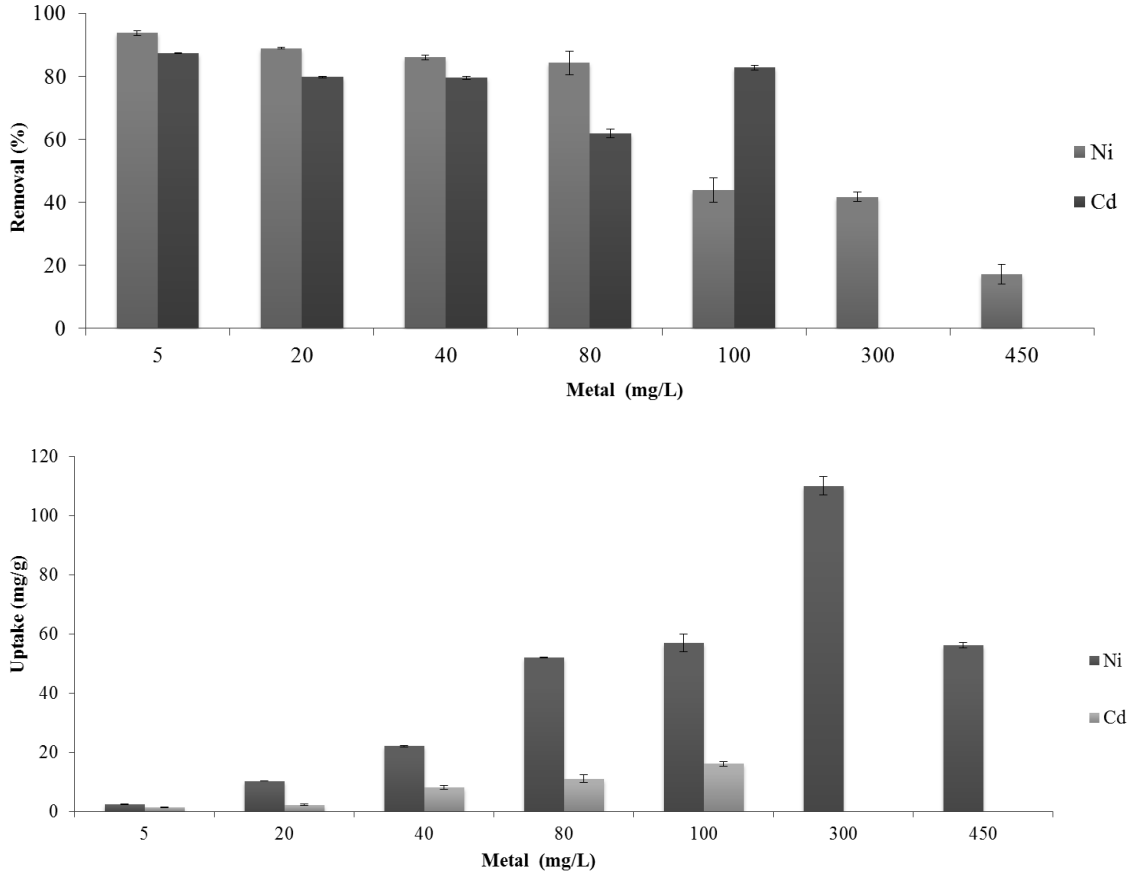

Figure 5.2. Removal (%) and uptake (mg/g) for the different initial concentrations of Ni^{2+} and Cd^{2+}.

The impact of different concentrations of Cd^{2+} on the biofilm growth is presented in Figure 5.3. The duration of the lag phase is similar for the initial concentrations tested that ranged between 5 mg/L to 80 mg/L, indicating that the culture needs the same time to endure intracellular changes in an effort to adapt itself to a new environment and to reach the exponential phase. For an initial concentration of 100 mg/L of Cd^{2+} the lag phase is significantly longer revealing that the culture needs more time to adapt to these hazardous conditions. Although the maximum concentration of biomass achieved starts to decrease for initial concentrations of Cd^{2+} higher than 5 mg/L, the specific growth rate only starts to decrease (about 25 %) for initial concentrations higher than 20 mg/L.

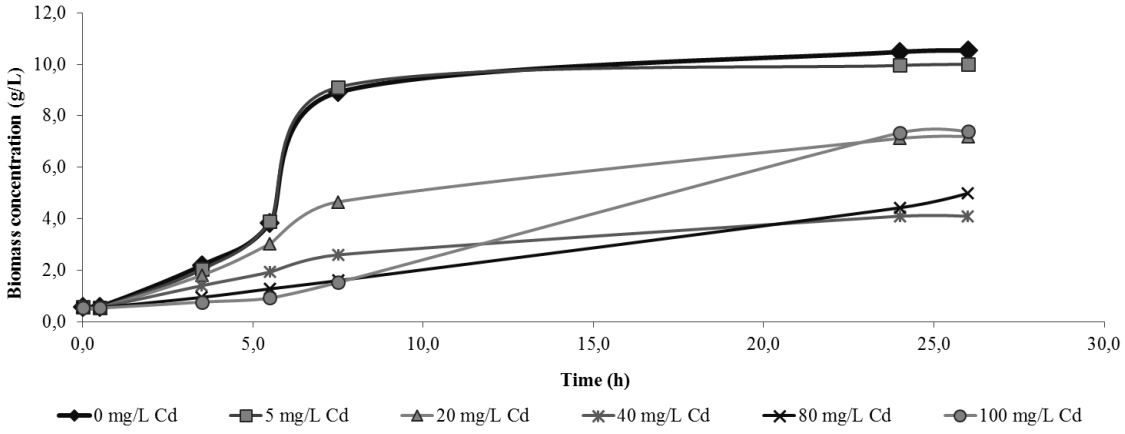

Figure 5.3. Biomass concentration of *S. equisimilis* (g/L) versus time (h) for different initial concentrations of Cd^{2+}.

Chaudhuri et al. (2014) investigated the adsorption of cadmium by *Lemna minor* and *Spirodela polyrhiza* and verified that for concentrations higher than 0.89 mg/L and 1.46 mg/L, respectively, the growth of half of those cultures was inhibited. These results show that *Lemna minor* is more susceptible to cadmium toxicity than *Spirodela polyrhiz*a.

The concentration of Cd^{2+} was also found to decrease as the initial concentration of metal increases, with the exception of the highest concentration tested (Figure 5.2). When exposed to an initial cadmium concentration of 5 mg/L, 20 mg/L, 40 mg/L, 80 mg/L and 100 mg/L, the suspended bacteria retained respectively 87.38 %, 79.75 %, 79.56 %, 61.87 % and 72.56 % of Cd^{2+}. Similar observations were reported by Kara and Kara (2005) and Chaudhuri et al. (2014) while removing

cadmium from wastewater with different biomass cultures. It is important to highlight that despite of the sensibility of the bacteria towards cadmium, the amount of initial cadmium retained was always higher than 60 %.

In these assays it was observed that for all the concentrations of Cd^{2+} tested, the pH ranged from pH 6.05 to 6.98. Since Cd^{2+} starts to precipitates as CdS for pH higher than 8, it is possible to discard the removal of Cd^{2+} by its precipitation and to attribute it to biological processes, such as biosorption. The increase of the pH values results in an increase of the hydroxyl groups and other anionic functional groups. This makes the bacterial surface to become more negatively charged, and consequently the number of electrostatic repulsion decreases and the number of electrostatic attraction increases, resulting in an increase of metal sorption (Badawy et al. 2010).

5.3.1.1| Growth and Biosorption Kinetics Modelling

Since growth is the result of anabolic and catabolic enzymatic processes, the use of a substrate or cofactor in the microbial growth, as well as the production/removal of metabolites can be quantitatively described by growth kinetics models. The specific growth rate (μ) of a population of microorganisms can be related to the substrate concentration (S) by a set of empirically derived rate laws. Monod and Powell models may be disregarded, as they do not take in consideration any inhibitory effect, which was verified to be exerted by both metals. The growth and sorption kinetic modelling are presented in Table 5.1 and Table 5.2, and are discussed below. This may be due to the fact that the substrate consumed for maintenance at the beginning of the experiments, when the biomass concentration is small, may be considered negligible.

However, it cannot be considered negligible with the course of the experiments (Fan et al. 2004). The existence of an inflection point makes sigmoid curves inappropriate for describing the exponential growth phase of microorganisms (Baty et al. 2004). The kinetic parameters of the Edward model (μ_{max}, K_s, K_1 and K) were obtained as 0.78 h^{-1}, 0.17 g/L, 492.20 g/L and $1.41x10^{15}$ mg/L. The high value obtained for K corroborates the inability of the Haldane model to properly describe the obtained data (Raghuvanshi and Babu, 2010). The coefficient of determination (R^2=0.970) indicates that the Edward model explains the microbial growth better than the Haldane and Luong counterparts. The kinetic parameters of the Edward model (μ_{max}, K_s, K_1 and K) were

obtained as 0.78 h^{-1}, 0.17 g/L, 492.20 g/L and $1.41x10^{15}$ mg/L. The high value obtained for K corroborates the inability of the Haldane model to properly describe the obtained data (Raghuvanshi and Babu, 2010). The coefficient of determination (R^2=0.970) indicates that the Edward model explains the microbial growth better than the Haldane and Luong counterparts.

Table 5.1. Monod, Powell, Haldane, Luong and Edwards growth kinetic parameters for *S. equisimilis* in the presence of Ni^{2+} and $Cd.^{2+}$

Ni^{2+}								
Model	**μ_{max}(h^{-1})**	**K_s (g/L)**	**K_i (g/L)**	**K**	**S_m (g/L)**	**m**	**n**	**R^2**
Monod	0.83	0.52	-	-	-	-	-	0.514
Powell	0.80	0.24	-	-	-	$5.12x10^{-5}$	-	0.493
Haldane	0.89	0.88	$-5.81x10^{21}$	-	-	-	-	0.558
Luong	1.81	12.04	-	-	$5.00x10^{15}$	-	$1.42x10^{13}$	0.872
Edward	0.78	0.17	492.20	$1.41x10^{15}$	-	-	-	0.970
Cd^{2+}								
Model	**μ_{max}(h^{-1})**	**K_s (g/L)**	**K_i (g/L)**	**K**	**S_m (g/L)**	**m**	**n**	**R^2**
Monod	0.37	-12.68	-	-	-	-	-	0.999
Powell	0.38	-13.08	-	-	-	-0.04	-	0.999
Haldane	0.44	0.84	36.44	-	-	-	-	0.939
Luong	1.31	2.89	-	-	$-2.97x10^{16}$	-	$-3.93x10^{14}$	0.760
Edwards	3.53	16.25	10.69	$6.75x10^{21}$	-	-	-	0.860

The kinetic parameters obtained with the Gompertz model (A, g/L; μ_{max}, h^{-1}; λ, h) for all the concentrations are presented in Table 5.2. Although the values obtained for R^2 (> 0.850) suggest that this model can also describe properly the experimental data, it does not comprise a parameter related with cellular maintenance. The sorption kinetic model that best describes Ni^{2+} sorption, for

initial concentrations of Ni^{2+} of 5 mg/L, 20 mg/L, 40 mg/L, 100 mg/L, 300 mg/L and 450 mg/L[1], is the pseudo-second order (R^2 > 0.915, Figure 5.4.a) meaning that under these experimental conditions the rate-limiting step for Ni^{2+} sorption is dependent on the initial concentration metal and on the concentration of biomass, since a higher concentration of biomass means a higher number of actives sites available for sorption and higher concentrations of metal means a higher number of molecules for a fixed number of active sites. For the assays conducted with 80 mg/L of Ni^2, the results are best described by the zero order model (R^2=0.970).

Table 5.2. Gompertz growth kinetic parameters for *S. equisimilis* in the presence of different initial concentrations of Ni^{2+} and Cd^{2+}.

Parameters	A (g/L)		μ_{max} (h^{-1})		λ (h)		R^2	
	Ni^{2+}	Cd^{2+}	Ni^{2+}	Cd^{2+}	Ni^{2+}	Cd^{2+}	Ni^{2+}	Cd^{2+}
0 mg/L	1.84	10.65	0.89	-1.57	2.92	2.86	0.975	0.972
5 mg/L	1.95	11.49	0.95	-1.62	3.12	3.07	0.985	0.953
20 mg/L	1.19	8.56	0.66	-0.90	3.51	0.46	0.871	0.957
40 mg/L	0.89	4.17	0.77	0.62	5.37	-1.33	0.893	0.998
80 mg/L	0.44	8.11	1.69	0.49	3.39	-0.28	0.920	0.998
100 mg/L	1.17	12.37	0.71	-0.68	2.74	3.90	0.859	0.996
300 mg/L	2.69	-	0.92	-	1.39	-	0.979	-
450 mg/L	3.11	-	4.85	-	2.45	-	0.987	-

Regarding Cd^{2+} assays, the microbial growth kinetic parameters for the Haldane model (μ_{max}, K_S and K_I) were respectively 0.44 h^{-1}, 0.84 g/L and 36.44 g/L (Table 5.1). The obtained values for the self-inhibition constant (K_I), the substrate affinity constant (K_S), associated with the coefficient of determination (R^2=0.939) suggest that the culture under study is not very sensitive to substrate inhibition and that this model is able to describe the data properly. The kinetic parameters of the Luong model ($\mu_{m,ax}$ K_S, S_m and n) were determined, respectively, as 1.31 h^{-1}, 2.89 g/L, -2.97x10^{16} g/L

and -3.93x10^{14}. The meaningless negative values of such parameters as well as the coefficient of determination (R^2=0.760) show that this model does not describe properly the experimental data. Although unexpected, this misfitting may be explained by several starting assumptions such as: no existence of lag phase and growth inhibition, due to the depletion of the substrate rather than to the formation of toxic intermediates (Costa et al. 2012). The Edward parameters (μ_{max}, K_s, K_1 and K) were respectively 3.53 h^{-1}, 16.25 g/L, 10.69 g/L and 6.75x10^{21} mg/L. the coefficient of determination (R^2=0.860) indicates that this model describes the microbial growth better than the Luong model. The Edward model considers 1) the formation of toxic intermediates or by-products, 2) the changing activity of one or more enzymes, 3) the dissociation of one or more enzymes and 4) the formation of metabolic aggregates that can lead to the growth and substrate inhibition (Costa et al. 2012). Being more realistic, these assumptions explain the good fitting of this model. The kinetic parameters obtained with the Gompertz model (A, μ_{max}, λ) for all the concentrations of Cd^{2+} tested are presented in Table 5.2. The high values of R^2 (> 0.950) suggest that this model is able to fit the data properly. However, as mentioned above the nonexistence of a maintenance parameter and the existence of an inflection point make the Gompertz model inappropriate to describe the exponential growth phase of these microorganisms (Baty et al. 2004).

The model that best describes the sorption of Cd^{2+} by the suspended bacteria for all the concentrations tested, is the pseudo second-order model (R^2 > 0.927, Figure 5.4.b). The K_2 constant decreases with the increase of cadmium concentration, indicating that the sorption rate of Cd^{2+} decreases over time. Similar findings were reported by Çelekli et al. (2011) for the adsorption of Cd^{2+} on *Spirulina platensis*.

a)

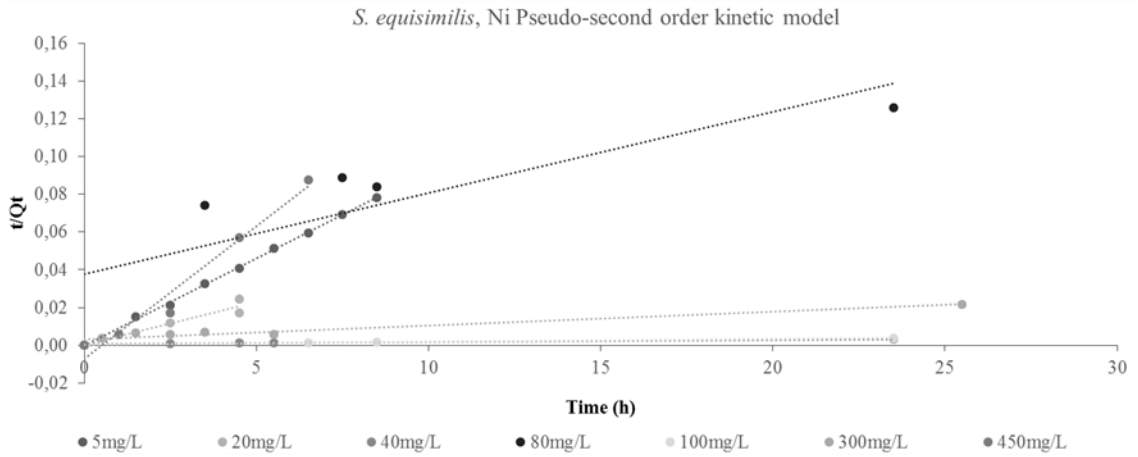

b)

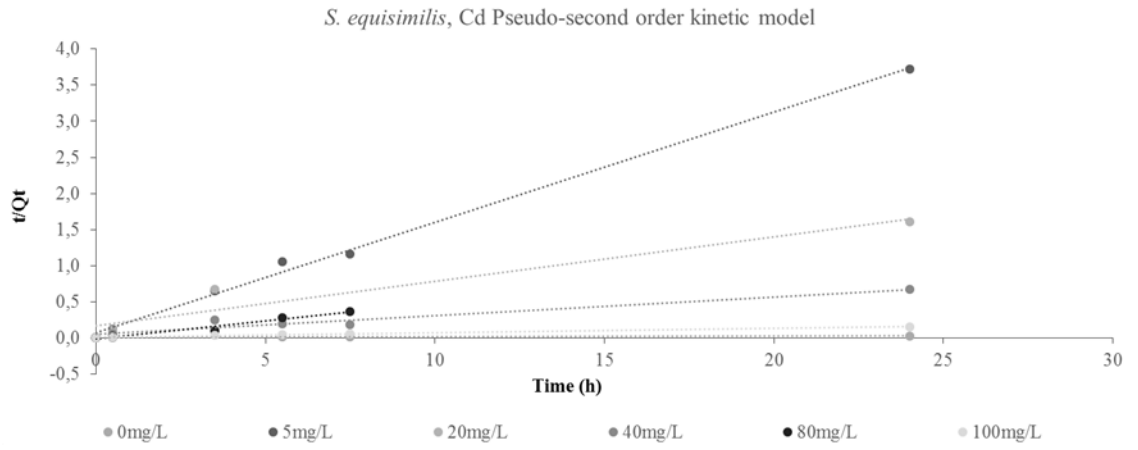

Figure 5.4. Kinetics models for **a)** Ni^{2+} sorption by *S. equisimilis* exposed to initial concentrations between 5 mg/L and 450 mg/L; **b)** Cd^{2+} sorption by *S. equisimilis* exposed to initial concentrations between 5 mg/L and 100 mg/L (cont.).

5.3.2| Singular and Binary Sorption Experiments

5.3.2.1| Diethylketone Sorption on Vermiculite – Singular Sorption Experiments

The adsorption of diethylketone (3 g/L) by different masses of vermiculite (0.085 g to 40 g) (Figure 5.5) showed similar profiles: initially it is rapid due to the high availability of surface adsorption sites, but it gradually becomes slower over time, due to the gradual occupation of those same sites.

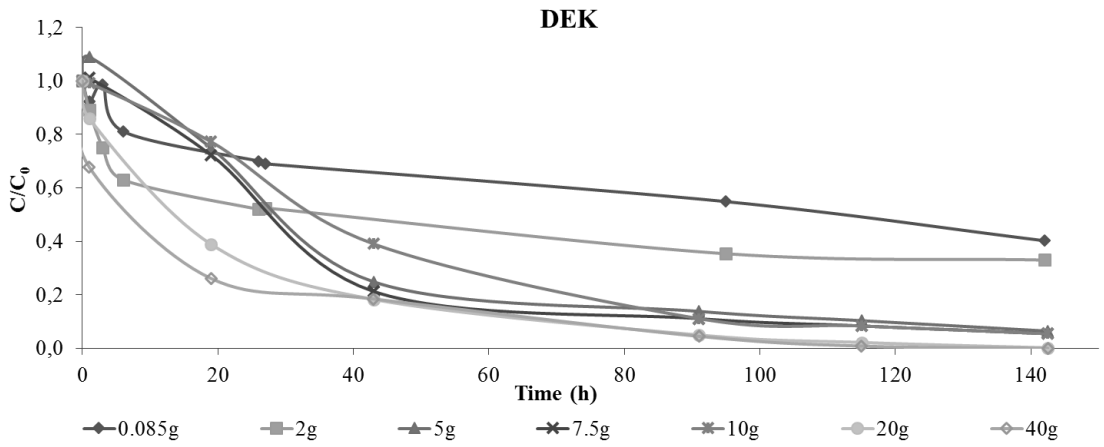

Figure 5.5. Ratio between residual and initial concentration (C/C_0) of diethylketone versus time.

The results showed that as the mass of vermiculite increases, the percentage of diethylketone sorbed by the clay also increases, being almost complete for the assays conducted with 5 g, 7.5 g and 10 g of vermiculite (sorption percentage higher than 92 %, and complete for vermiculite masses of 20 g and 40 g), but the sorption itself is also faster (about 5 times faster). Several other authors also observed this behaviour and explained it as a result of an increased surface area, which consequently translates into a greater number of sites available for adsorption (Quintelas et al. 2011).

DEK Sorption by Vermiculite - Kinetic Modelling

The experimental results referred above are well described by the pseudo-second ($0.947 \leq R^2 \leq 0.999$) and pseudo-first order ($0.913 \leq R^2 \leq 0.996$) kinetic models. The K_2 constant tends to increase with the increase of vermiculite dose, indicating that the sorption rate of diethylketone increases over time (Table 5.3), which can be explained by the increased number of active sites available for sorption.

The relation between the pseudo-second order parameters and the adsorption performance was studied by several authors (Wu et al. 2009; Ofomaja 2010), who established an approaching equilibrium factor (Rw) between the pseudo-second order constants and the characteristic kinetic curve. This approaching equilibrium factor is defined as:

$$Rw=1 / (1 + K_2 qetref) \quad (5.5)$$

In here tref is the longest operation time (based on kinetic experiments), qe and K_2 correspond respectively to the equilibrium uptake and to the pseudo-second order constant. Wu et al. (2009) refer to four different situations depending on the Rw value:

1. Rw=1, type of kinetic curve: linear, not approaching equilibrium; biosorption is ineffective as equilibrium cannot be reached.

2. 1>Rw>0.1, type of kinetic curve: slightly curved, approaching equilibrium;

3. 0.1>Rw>0.01, type of kinetic curve: largely curved, well approaching equilibrium;

4. Rw<0.01, type of kinetic curve: pseudo-rectangular, drastically approaching equilibrium.

The Rw factor was found to range between 0.004 and 0.090 for all the vermiculite masses, with the exception of the assay conducted with 5 g of vermiculite (Rw=0.120). These results suggest that the kinetic curve is well approaching equilibrium, confirming the good performance of the system.

Table 5.3. Fitting parameters for pseudo-second order kinetic model for diethylketone singular sorption assays.

Singular sorption assays	Vermiculite (g)	Pseudo-second order	
		K_2	R^2
DEK	0.085	5.00×10^{-7}	0.947
	2	8.18×10^{-3}	0.996
	5	8.85×10^{-5}	0.913
	7.5	1.36×10^{-4}	0.977
	10	2.81×10^{-4}	0.993
	20	2.06×10^{-3}	0.994
	40	6.80×10^{-3}	0.996

DEK Sorption by Vermiculite - Equilibria Modelling

The parameters for the adsorption equilibria of diethylketone by vermiculite are listed in Table 5.4, along with the linear regression coefficients. According to Raman and Jackson (1963) and Quintelas et al. (2011) vermiculite has a heterogeneous surface and its structure consists of overlayed tetrahedral-octahedral-tetrahedral sheets (2:1 layer). The R^2 values obtained for the BET and Freundlich isotherm models are close to unity, as opposed to the R^2 value obtained for the Langmuir and D-R models. The BET parameter C_S indicates the saturation concentration of the solute (C_S=0.43 mg l^{-1}) whereas the constant B relates the energy of interaction with the surface (B=0.76). The energy of adsorption (E_D) may be calculated by the following equation:

$$E_D = 1 / (2B_D)^{1/2} \quad (5.6)$$

Here, B_D is an isotherm constant related to the mean free energy of adsorption per mole of adsorbate (mol^2/J^2). For values of E_D is < 8 kJ/mol, the adsorption process is physical in nature; if it ranges between 8 kJ/mol and 16 kJ/mol, the adsorption mechanism is governed by chemical ion-exchanges processes. If E_D is > 16 kJ/mol the adsorption mechanism may be dominated by particle diffusion. The obtained value of E_D is lower than 8 kJ/mol, suggesting that the adsorption process is physical in nature. Similar results were obtained by Ouadjenia-Marouf et al. (2013).

Table 5.4. Adsorption equilibria for diethylketone

Model	Langmuir	Freundlich	D-R	BET
q_{max} (mg/g)	499.80	-	-	-0.17
b (L/mg)	$1.57x10^{-4}$	-	-	-
K_f	-	$1.43x10^{-1}$	-	-
n	-	1.48	-	-
q_D (mg/g)	-	-	0.09	-
B_D (mol^2/J^2)	-	-	-0.03	-
B	-	-	-	0.76
C_s (mg/L)	-	-	-	0.43
R^2	0.887	0.896	0.847	0.999

Morphological changes in the vermiculite surface were detected at the end of the experiments and confirmed by SEM (Leica Cambridge S360), Figure 5.6. Exposure to diethylketone made the vermiculite surface more glazed, polished and with broken and worn leaves, and this may result from the eventual chemical stress performed by diethylketone over the vermiculite surface.

a) **b)**

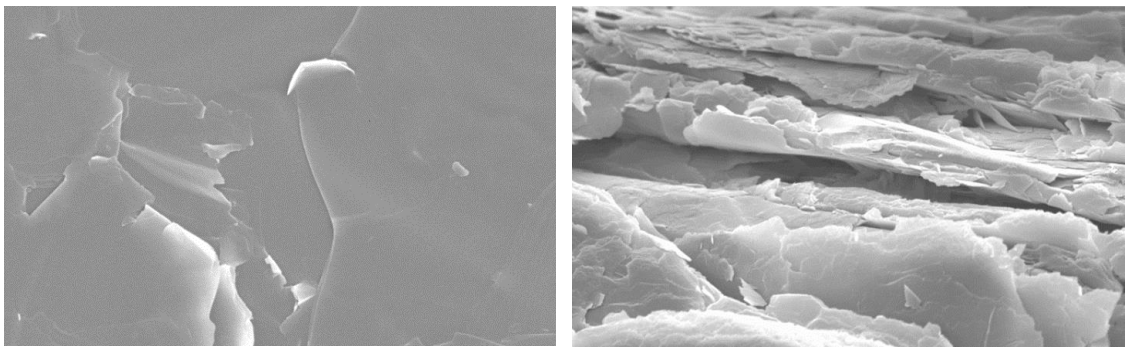

Figure 5.6. SEM images with an amplification of 3000 x of **a)** vermiculite exposed to distilled water; **b)** vermiculite exposed to diethylketone (3 g/L) after 120 hours.

5.3.2.2| Nickel Sorption on Vermiculite – Singular Sorption Experiments

The experimental results of the singular sorption assays with Ni^{2+} and vermiculite allowed inferring that the sorption process is initially rapid due to the high availability of surface adsorption sites, but it becomes gradually slower through time, due to the gradual occupation of those same sites. It was found that despite the uptake decreases as the mass of vermiculite employed increases (from 24.69 mg/g to 4.78 mg/g), the percentage of Ni^{2+} sorbed increases, reaching a maximum value of 100 % for vermiculite quantities higher than 7.5 g. This can be due to the increase of surface area available, which is translated into a higher number of active sites available for sorption. Vermiculite can adsorb heavy metals by two distinct mechanisms: production of inner-sphere complexes through $Si\text{-}O^-$ and $Al\text{-}O^-$ groups at the vermiculite particle edges and cation exchange at the planar site, resulting from the interaction between ion metals and the out-sphere complexes, that present a negative permanent charge. Since both of these mechanisms are pH-dependent and pH is able to change the vermiculite surface properties and the metal speciation, is possible to infer that in aqueous solutions, the pH plays an important and crucial role in the control of cationic adsorption. (Badawy et al. 2010).

In these experiments, it was found that the pH ranged from 7.39 to 6.14, that the vermiculite point of zero charge is 2 pH and Ni^{2+} precipitates in the form of $Ni(OH)_2$ at a pH higher than 7.6. These results allow to conclude that the decrease on Ni^{2+} concentration is due to sorption processes between Ni^{2+} and the functional groups (Si-O-Si, H-O-H, CO and OH) present on the vermiculite surface (Espinoza et a. 2012).

Nickel Sorption by Vermiculite - Kinetics Modelling

The results obtained are best described by the pseudo-second order kinetic model (Table 5.5). The behaviour of the K_2 constant was unexpected, since it decreased for the assays with 5 g to 7.5 g of vermiculite, and then increased for bigger vermiculite masses and decreases again, suggesting that the sorption rate oscillates through time and with the mass of sorbent employed (Plazinski et al. 2013). The negative values obtained for K_0 and $K_{1.1}$ exclude the zero-order and the pseudo-first order kinetic models to describe the experimental data.

Table 5.5. Fitting parameters for pseudo-second order kinetic model for Ni^{2+} singular sorption assays.

Singular sorption assays	Vermiculite (g)	Pseudo-second order	
		K_2	R^2
Ni^{2+}	5	$2.35x10^{-1}$	0.999
	7.5	$6.39x10^{-2}$	0.998
	20	$6.05x10^{-1}$	0.985
	40	$8.59x10^{-2}$	0.973

In these assays the R_w factor was found to range between 0.005 and 0.087 indicating that the kinetic curve is largely curved with a good approach to equilibrium, confirming the good performance of the system. In this set of experiments no significant changes on the vermiculite surface were detected by SEM observations (data not shown).

5.3.2.3| Cadmium Sorption on Vermiculite – Singular Sorption Experiments

The singularsorption assays with Cd^{2+} revealed that the sorption process is initially rapid due to the high availability of surface adsorption sites, but it becomes gradually slower through time, due to the gradual occupation of those same sites. It was also possible to conclude that the percentage of Cd^{2+} sorbed increases as the quantity of vermiculite increases, reaching a maximum value of 95.40 % for vermiculite masses of 40 g.

In these experiments the pH ranged from 7.23 to 5.78. As previously mentioned, the vermiculite point of zero charge is 2 and Cd^{2+} precipitates at a pH higher than 8, so it is possible to conclude that sorption processes are responsible for the decrease of Cd^{2+} through time, and therefore to discard, once again, that the decrease of Cd^{2+} concentration occurs by precipitation processes.

Cadmium Sorption by Vermiculite - Kinetics Modelling

The pseudo-second order model describes properly the results achieved (Table 5.6). The K_2 constant tends to increase as the mass of vermiculite employed increases and this may be justified by the increased number of actives sites available for sorption. The values obtained for K_0 and $K_{1.1}$ allow the exclusion of the zero-order and the pseudo-first order kinetic models.

In these assays the R_w factor was found to range between 0.009 and 0.091 indicating that the kinetic curve is well approaching equilibrium, confirming the good performance of the system. Once again, there were no significant changes detected by SEM observations on the vermiculite surface (data not shown).

Table 5.6. Fitting parameters for pseudo-second order kinetic model for Cd^{2+} singular sorption assays.

Singular sorption assays	Vermiculite (g)	Pseudo-second order	
		K_2	R^2
Cd^{2+}	5	$5.12x10^{-3}$	0.999
	7.5	$4.26x10^{-1}$	0.999
	20	$2.46x10^{-1}$	0.931
	40	$5.88x10^{-1}$	0.991

5.3.2.4| Diethylketone and Metal Sorption on Vermiculite – Binary Sorption Experiments

5.3.2.4.1| Diethylketone and Nickel Sorption on Vermiculite

The simultaneous adsorption of diethylketone and Ni^{2+}, when exposed to different quantities of sorbent, showed that for all the quantities of vermiculite tested, a complete sorption of diethylketone was achieved within the first 8 hours to 24 hours, whereas for Ni^{2+} as mass of vermiculite increased Ni^{2+} sorption also increased, reaching a maximum value of 100 % and 98.69 %, respectively, for 7.5 g and 40 g of vermiculite within 8 hours after the beginning of the experiment.

According to Srivastava et al. (2006) a mixture of different adsorbates may exhibit three possible types of behaviour:

1. Non-interaction (the mixture has no effect on the adsorption of each of the adsorbates);

2. Synergism (the mixture increases the adsorption of each individual adsorbate);

3. Antagonism (the mixture decreases the adsorption of each individual adsorbate).

Comparing these results with the results obtained in the assays conducted with vermiculite and only one sorbate, it is possible to infer that not only the sorption of both sorbates is faster (about 5 times faster) when mixed, but it also presents higher maximum sorption values, suggesting the existence of a synergetic effect between these two sorbates. The pH was found to range between 7.24 and 6.26. Comparing these results with the ones obtained in the singular sorption experiments, conducted with Ni^{2+} and vermiculite, it is also possible to conclude that pH varied similarly and that the process responsible for the decrease of Ni^{2+} concentration is biosorption.

It is possible to observe that the sorption of both pollutants is best described by the pseudo-second order kinetic model ($0.978 \leq R^2 \leq 0.999$ for diethylketone and $0.955 \leq R^2 \leq 0.998$ for Ni^{2+}) (Table 5.7). It was possible to observe that as the mass of vermiculite increases, the pseudo-second order constants (K_2) for diethylketone and for Ni^{2+} tend to decrease, indicating that the sorption rate of diethylketone and Ni^{2+} decreases over time. This behaviour can be explained by the saturation of the active sites available on the surface of the mineral clay and by the competition between these two pollutants for the same active sites.

In these assays the R_w factor was found to range between 0.006 and 0.029 for diethylketone and between 0.034 and 0.095 for Ni^{2+}, indicating that the kinetic curve is largely curved with a good approach to equilibrium, endorsing the good performance of the system.

Table 5.7. Fitting parameters for pseudo-second order kinetic model for diethylketone and nickel binary sorption assays.

DEK and Ni^{2+} binary assays	Vermiculite (g)	Pseudo-second order	
		K_2	R^2
DEK	5	37.63	0.999
	7.5	12.12	0.978
	20	$2.28x10^{-2}$	0.996
	40	$-9.75x10^{-1}$	0.985
Ni^{2+}	5	$1.00x10^{-1}$	0.998
	7.5	$4.31x10^{-2}$	0.955
	20	$1.69x10^{-2}$	0.976
	40	$2.05x10^{-1}$	0.992

5.3.2.4.2| Diethylketone and Cadmium Sorption on Vermiculite

When mixed and exposed to different quantities of vermiculite, diethylketone and Cd^{2+} present different behaviours. An increase on the mass of vermiculite lead to a decrease on the percentage of diethylketone sorbed (from 43.56 % to 23.75 %) whereas the sorption percentage of Cd^{2+} tends to increase reaching a maximum value of 100 % for 20 g and 40 g of vermiculite. These results suggest that the sorption of diethylketone is negatively affected by the presence of Cd^{2+}. Comparing these results with the ones obtained with the singular sorbates assays it is possible to establish an antagonistic behaviour between these pollutants. This antagonistic behaviour can be explained by the competition between both sorbates for the available sites on the surface of the clay and it is not due to pH variation since this is similar in both experiments, the vermiculite point of zero charge is 2, and Cd^{2+} precipitates as sulphide at a pH higher than 8.

Diethylketone and Cadmium Sorption by Vermiculite - Kinetic Modelling

Table 5.8 summarizes the kinetic parameters obtained for the pseudo-second order model, which best describes the experimental data for both pollutants. For both pollutants, the pseudo-second order constant K_2 increases with the increase of the mass of vermiculite suggesting that adsorption rate of diethylketone and Cd^{2+} increases over time. The negative values obtained for K_0 and $K_{1.1}$ constants exclude the zero-order and the pseudo-first order kinetic models to describe the experimental data. Similar results were obtained by Vieira et al. (2010), Çelekli and Bozkurt (2011) and Chaudhuri et al. (2014).

The R_w factor was found to range between 0.004 and 0.167 for diethylketone and between 0.009 and 0.017 for Cd^{2+} indicating that the kinetic curve is largely curved with a good approach to equilibrium, validating the good performance of the system.

Table 5.8. Fitting parameters for pseudo-second order kinetic model for diethylketone and cadmium binary sorption assays.

DEK and Cd binary assays	Vermiculite (g)	Pseudo-second order	
		K_2	R^2
DEK	5	$1.57x10^{-3}$	0.660
	7.5	$7.70x10^{-3}$	0.967
	20	$6.28x10^{-2}$	0.994
	40	$9.92x10^{-1}$	0.999
Cd^{2+}	5	$9.06x10^{-1}$	0.999
	7.5	4.68	0.999
	20	24.75	1
	40	$5.60x10^{14}$	1

5.3.3| Biosorption Experiments

The adsorption process is generally defined as the physical/chemical accumulation of the sorbate (ions) onto the surface of the sorbent. The distribution of the sorbate onto the sorbent surface is usually expressed in terms of adsorption isotherms whereby the sorbate is sequestered by the sorbent through several mechanisms and is in equilibrium with its residual left free solution. In order to establish the most appropriate correlation between the adsorbates and the adsorbents several isotherm models were tested: Langmuir, Freundlich, Dubinin-Radushkevich (D-R) and BET. The mechanistic path of these processes can be deduced from various kinetic models such as zero-order, pseudo-first order and pseudo-second order.

5.3.3.1| Biosorption Experiments With Diethylketone and Ni

Concentrated biomass of *S. equisimilis* (circa 5 g/L), diethylketone (3 mg/L), Ni^{2+} (450 mg/L) and vermiculite (0.085 g to 40 g) were used in the biosorption assays. The ratios between residual and initial concentration of diethylketone and of Ni^{2+} (C/C_0) as functions of time are presented in Figure 5.7.a. It is possible to observe that as the mass of vermiculite increases, the C/C_0 ratio for diethylketone reaches near 0 for all the assays, with the exception of the experiments with 0.085 g and 10 g of vermiculite. For Ni^{2+}, the C/C_0 ratio is slightly higher (~ 0.2), with the exception of the assay with 10 g of vermiculite, in which a sorption percentage of 97.37 % was obtained (about 9 times higher than the results obtained for 0.085 g vermiculite).

Figure 5.7.b shows that the maximum sorption percentage of diethylketone achieved does not increase significantly with the increase of the vermiculite mass. The maximum sorption percentage of diethylketone was obtained with 40 g of vermiculite, and is about 1.25 times the sorption percentage obtained with 7.5 g and 10 g (77.90 % and 80.07 %).

This behaviour although unexpected, may be related with the fact that 1) when the environmental conditions become unfavourable, the biofilm can act as clumps or as single colonies (Kesaano and Sims, 2014) and 2) the biofilm formed is composed by a single bacterial species. In general, a multiple species biofilm presents an enriched diversity and functionalities which are translated in an enhanced potential for degradation of toxic compounds (Burmølle et al. 2014).

In these experiments the pH was found to range between 5.66 and 6.20. Taking into account the vermiculite point of zero charge and the pH at which Ni^{2+} precipitates as hydroxide, the results obtained allow to discard the hypothesis that precipitation might be responsible for the decrease of Ni^{2+} concentration (Espinoza et al. 2012). Once again, the increase of pH results in a decrease of protons and in an increase of hydroxyl groups and other anionic functional groups. The increase of anionic groups in solution will make the surface of the biofilm and of the vermiculite to become negatively charged and consequently the number of electrostatic attraction increase, resulting in an increase of metal sorption (Badawy et al. 2010).

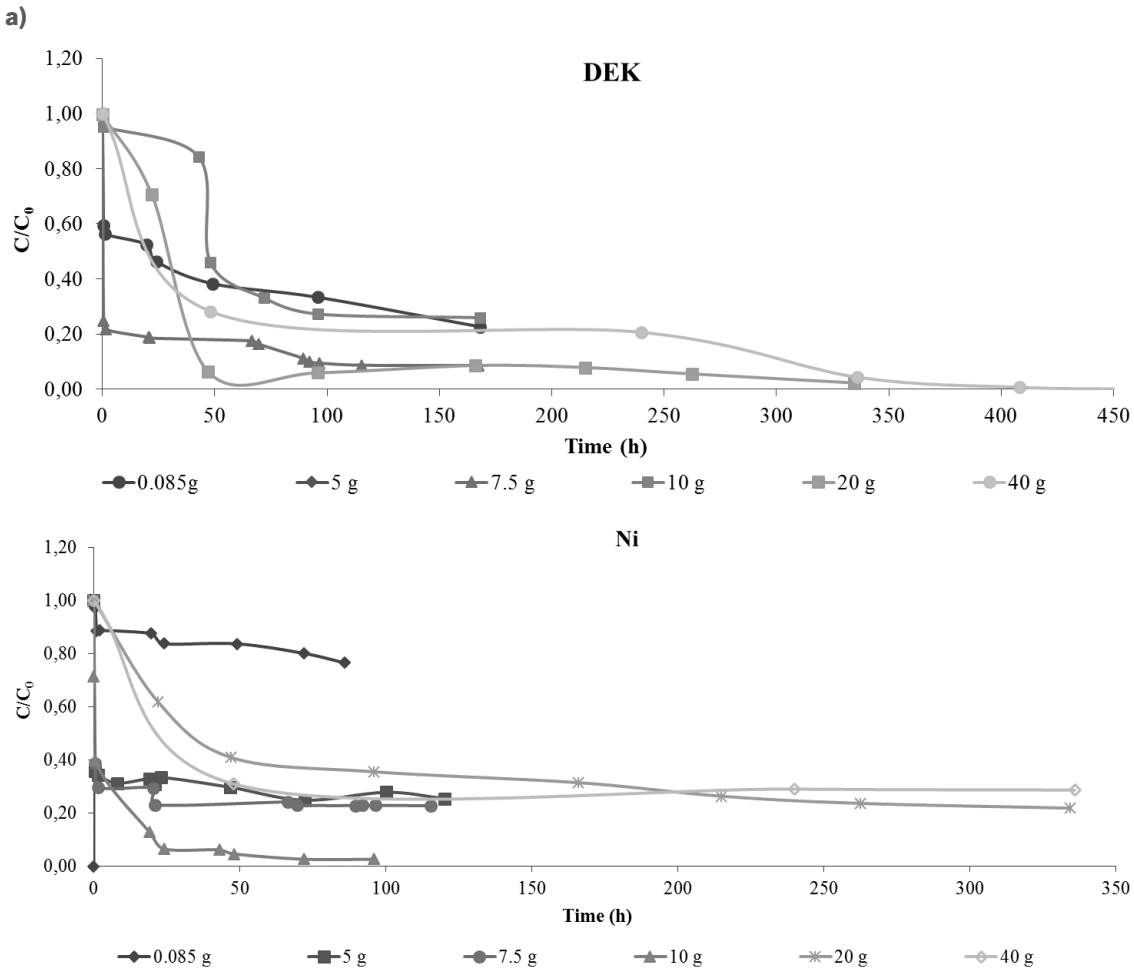

Figure 5.7. a) Ratio between residual and initial concentration (C/C_0) of DEK and of Ni^{2+} versus time for different vermiculite masses for the biosorption/biodegradation assays conducted with diethylketone and Ni^{2+}; **b)** Sorption percentage of diethylketone and Ni^{2+} using a biofilm of *S. equisimilis* supported on different masses of vermiculite.

b)

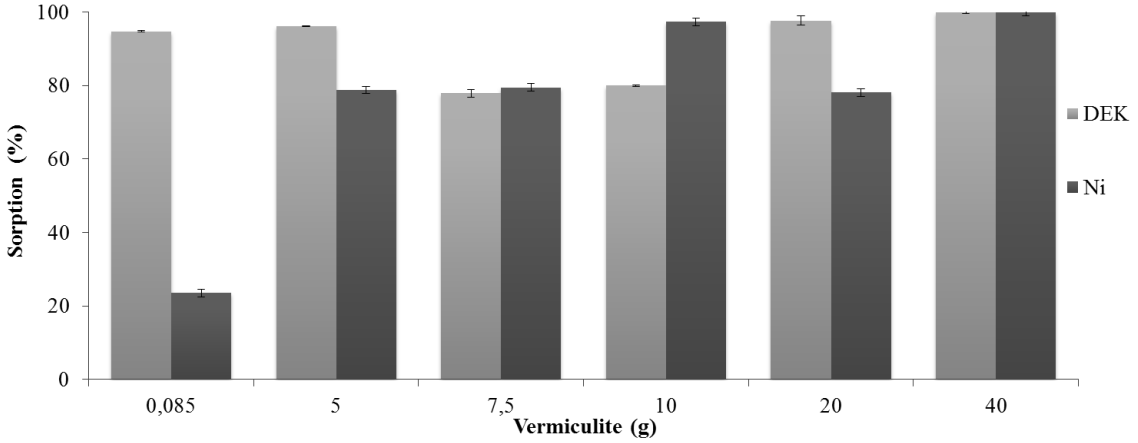

Figure 5.7. a) Ratio between residual and initial concentration (C/C_0) of DEK and of Ni^{2+} versus time for different vermiculite masses for the biosorption/biodegradation assays conducted with diethylketone and Ni^{2+}; **b)** Sorption percentage of diethylketone and Ni^{2+} using a biofilm of *S. equisimilis* supported on different masses of vermiculite (cont.).

Table 5.9 shows that the uptake of both pollutants decreases as the sorbent mass (vermiculite and biomass) increases. These results ought to be clarified since the surface area available for the biofilm formation and for the retention of both pollutants increases.

Table 5.9. Diethylketone and metal uptake and sorption percentage obtained with *S. equisimilis* (~5 g/L) supported on different masses of vermiculite and exposed to an aqueous solution of diethylketone and nickel and diethylketone and cadmium.

	Ni^{2+}		DEK	
Clay (g)	**Uptake (mg/g)**	**Sorption (%)**	**Uptake (mg/g)**	**Sorption (%)**
0.085	904.01	12.56	23470.00	94.80
5	59.08	78.79	477.34	96.18
7.5	40.08	79.50	191.20	77.90
10	37.19	97.37	204.85	80.07
20	14.76	97.04	125.04	97.73
40	9.56	100.00	63.96	100
	Cd^{2+}		DEK	
Clay (g)	**Uptake (mg/g)**	**Sorption (%)**	**Uptake (mg/g)**	**Sorption (%)**
0.085	218.67	20.95	15678.96	42.38
5	11.38	66.95	1843.58	49.73
7.5	9.76	72.27	307.77	73.97
10	7.26	85.37	214.73	94.32
20	3.14	86.16	121.55	95.02
40	2.10	98.85	63.67	99.53

Figure 5.8.a illustrates the existence of a biofilm of *S. equisimilis* supported on 5 g of vermiculite and exposed to an aqueous solution of diethylketone and Ni^{2+}, 170 hours after the start of the experiment.

a) **b)**

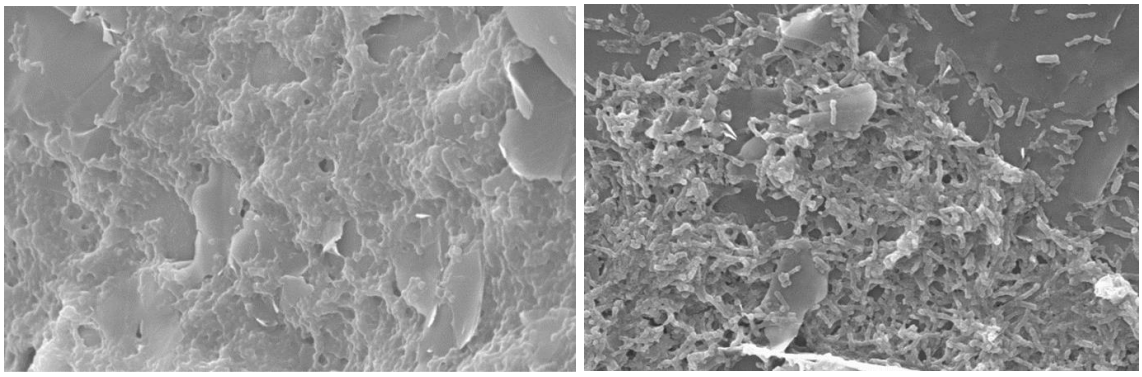

Figure 5.8. SEM images with an amplification of 3000 x of **a)** a *Streptococcus equisimilis* biofilm supported on vermiculite (5 g) and exposed to an aqueous solution of diethylketone (3 g/L) and Ni^{2+} (450 mg/L), 170 hours after the beginning of the experiment**; b)** a *Streptococcus equisimilis* biofilm supported on vermiculite (0.085 g) and exposed to an aqueous solution of diethylketone (3 g/L) and Cd^{2+} (100 mg/L), 339.5 hours after the beginning of the experiment.

These observations validate the ability of this microorganism to grow in hazardous conditions, which is an advantage in treating contaminated wastewater.

Biosorption Kinetic Modelling

For both Ni^{2+} and diethylketone and for all the masses of vermiculite tested, the results are best fitted by the pseudo-second order ($0.873 < R^2 \leq 0.999$ for diethylketone and $0.977 < R^2 \leq 0.999$, for Ni^{2+}, Figure 5.9.a).

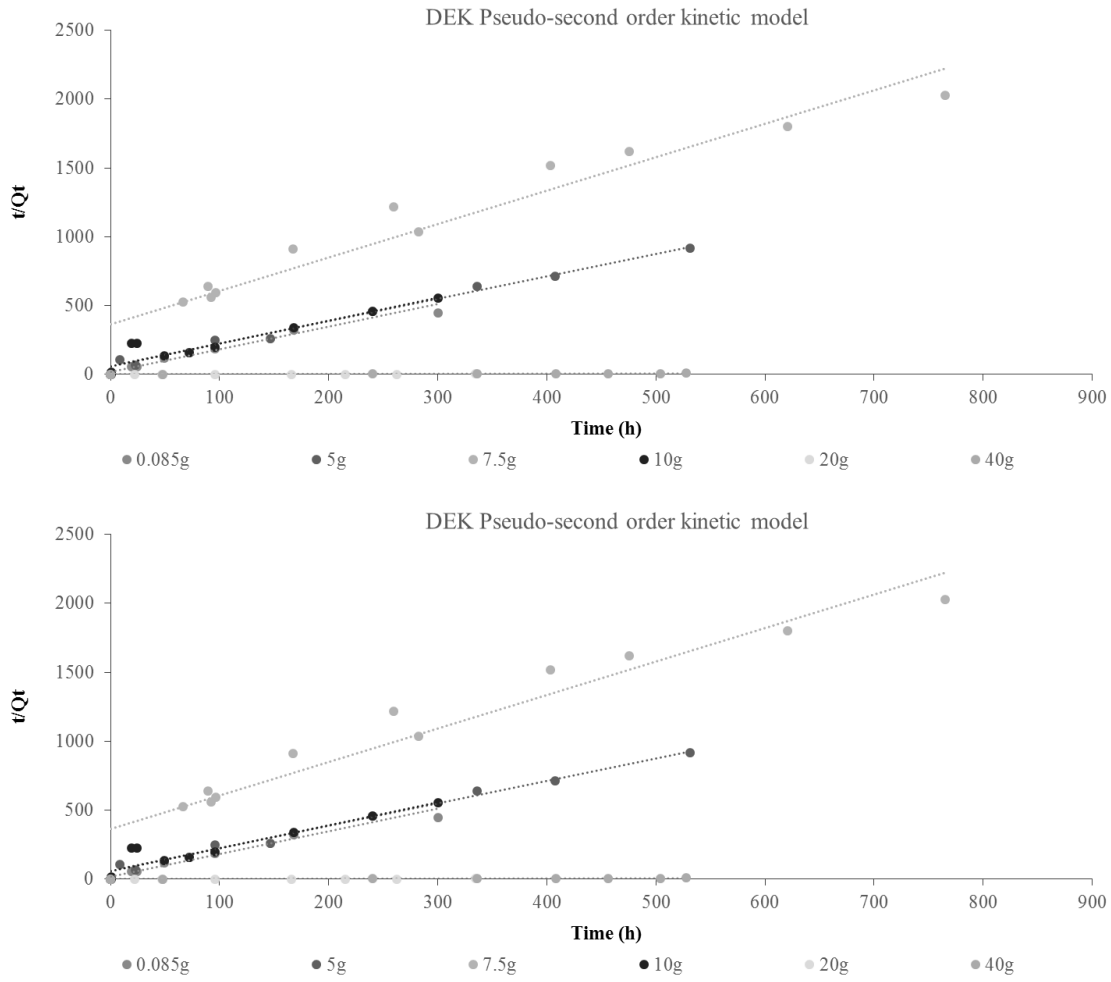

Figure 5.9. Comparison between the experimental results and those predicted by different models for diethylketone and Ni^{2+} biosorption, at 37 °C using *S. equisimilis* supported on vermiculite kinetics.

The pseudo-second order model assumes that the rate limiting step of the process is chemisorption (Quintelas et al, 2011), involving valence forces through the sharing or exchange of electrons between the biomass or the biomass mixed with mineral clay and diethylketone or Ni^{2+}, through complexation, coordination and/or chelation (Ahmady-Asbchin and Jafari, 2013). For diethylketone, the pseudo-second order K_2 constant tends to decrease with the increase of the mass of vermiculite, suggesting that the sorption rate of diethylketone decreases over time. For Ni^{2+}, this constant tends to increase for vermiculite masses lower than 10 g and decreases for vermiculite masses higher than 7.5 g. These results suggest that the biosorption rate of diethylketone and Ni^{2+} is influenced by the mass of sorbate and by the microbial activity (biofilm growth, development and maturation), which

can be translated into an increased need for nutrients and production of toxic metabolites as a consequence of the metabolic activity.

Biosorption Equilibria Modelling

The Langmuir, Freundlich, BET and Dubinin-Radushkevich (D-R) models were fitted to several experimental adsorption isotherms. Parameters are presented in Table 5.10 and the fitting is shown in Figure 5.10 The best fit for the biosorption of diethylketone was obtained with the Freundlich model (R^2=0.999), followed by the Langmuir model (R^2=0.964). The Freundlich isotherm is based on multilayer adsorption with interaction between the adsorbed molecules. This model is suitable for heterogeneous surfaces, with a uniform energy distribution and reversible adsorption and suggests that the adsorption energy decreases exponentially on saturation of the adsorption sites of a surface (Kishore et al. 2013). The values obtained for K_f and n were respectively 160409 mg/g and 0.05 and indicate the high maximum adsorption capacity of the system and that the adsorption is favourable and cooperative (1/n > 1) (Dada et al. 2012). The values obtained for q_D and B_D with the Dubinin-Radushkevich model and the values obtained for B and C_S with the BET model eliminate these models from consideration.

Table 5.10 Adsorption equilibria for the different biosorption experiments.

Model	Parameter	Experiment		Experiment	
		DEK	Ni^{2+}	DEK	Cd^{2+}
Langmuir	q_{max} (mg/g)	17562	$8.96x10^{9}$	0.36	10.62
	b (L/mg)	$2.16x10^{-4}$	$2.77x10^{7}$	9.97	$4.87x10^{-1}$
	R_L	0.17	$4.03x10^{-18}$	$2.79x10^{-4}$	$1.39x10^{-1}$
	R^2	0.964	0.735	0.989	0.930
Freundlich	K_f	160409	$1.05x10^{-5}$	0.30	$1.01x10^{-6}$
	n	0.05	0.32	3.70	$2.28x10^{-1}$
	R^2	0.999	0.995	0.979	0.994
D-R	q_D (mg/g)	$1.31x10^{-4}$	21.80	0.137	5.05
	B_D (mol^2/J^2)	$-2.73x10^{1}$	$-3.08x10^{-5}$	-0.22	$-6.10x10^{-4}$
	R^2	0.999	0.997	0.484	0.998
BET	q_{max} (mg/g)	0.12	$3.33x10^{6}$	0.14	37.30
	B	$-5.55x10^{20}$	$-3.01x10^{22}$	-1.96	$6.51x10^{14}$
	C_s (mg/L)	-0.67	$3.67x10^{2}$	-0.05	$-1.77x10^{16}$
	R^2	0.999	0.998	0.999	0.956

The results achieved for the biosorption equilibrium of Ni^{2+} are best fitted by the Freundlich isotherm. The values obtained for K_f and n were respectively $1.05x10^{-5}$ mg/g and 0.32, indicating that the maximum sorption capacity of this system is lower for Ni^{2+} than for diethylketone and that the sorption process is favourable and cooperative ($1/n > 1$). The small value obtained for the correlation coefficient (R^2) for the Langmuir model associated with the value obtained for B_D with the Dubinin-Radushkevich model and the values obtained for B and C_S with the BET model eliminate the consideration of these models.

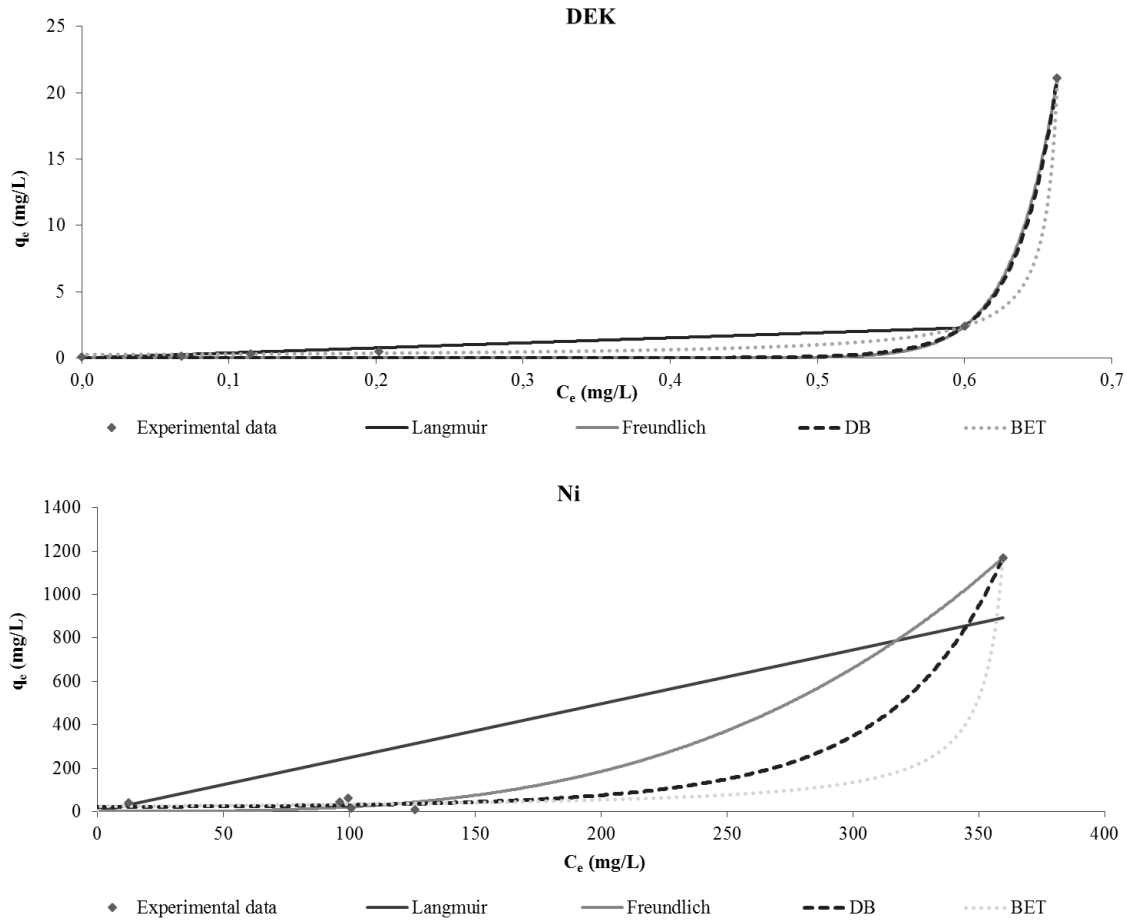

Figure 5.10. Comparison between the experimental results and those predicted by different models for diethylketone and Ni^{2+} biosorption, at 37 °C using *S. equisimilis* supported on vermiculite isothermic equilibria.

5.3.3.2| Biosorption Experiments with Diethylketone and Cd

Biosorption assays were carried out using a biofilm of *S. equisimilis* supported on vermiculite (0.085 g to 40 g) and in contact with an aqueous solution of Cd^{2+} (100 mg/L) and diethylketone (3 g/L). The ratio between residual and initial concentration of diethylketone (C/C_0) as a function of time is shown in Figure 5.11.a. Two distant profiles were observed: for vermiculite masses higher than 0.085 g there is an initial and very fast phase, mainly controlled by the rapid surface saturation followed by a second phase which depends mostly on the microorganism metabolism. For 0.085 g of vermiculite the sorption/biodegradation of diethylketone is not as notorious or fast, presenting only one phase.

The ratio between residual and initial concentration of Cd^{2+} (C/C_0) as a function of time allowed concluding that as the mass of vermiculite increases, the Cd^{2+} C/C_0 ratio decreases (Figure 5.11.a), reaching zero for the experiments conducted with 40 g of vermiculite. From Figure 5.11.a two distinct profiles were detected: for masses higher than 0.085 g of vermiculite, the sorption of Cd^{2+} presents also two distinct phases: an initial and very fast phase mainly dominated by the rapid surface saturation, followed by a slower and metabolism dependent phase (Quintelas et al. 2012).

In Figure 5.11.b it is observable that the maximum sorption percentage of diethylketone (99.53 %) achieved increases significantly with the increase of the vermiculite mass. The maximum sorption percentage of Cd^{2+} was obtained for 40 g of vermiculite, and it is about 2.3 times higher than the results obtained for 0.085 g and 10 g. It is possible to observe that for Cd^{2+} as the mass of sorbent increased, the percentage of Cd^{2+} sorbed also increased, reaching a maximum value of 98.85 % for the assays conducted with 40 g of sorbent.

The pH was found to range from 6.15 to 5.58, which according to the vermiculite point of zero charge and the pH at which Cd^{2+} precipitates as sulphide, allow to conclude that biological processes, such as biosorption, are responsible for the decrease of Cd^{2+} concentration over time, instead of precipitation.

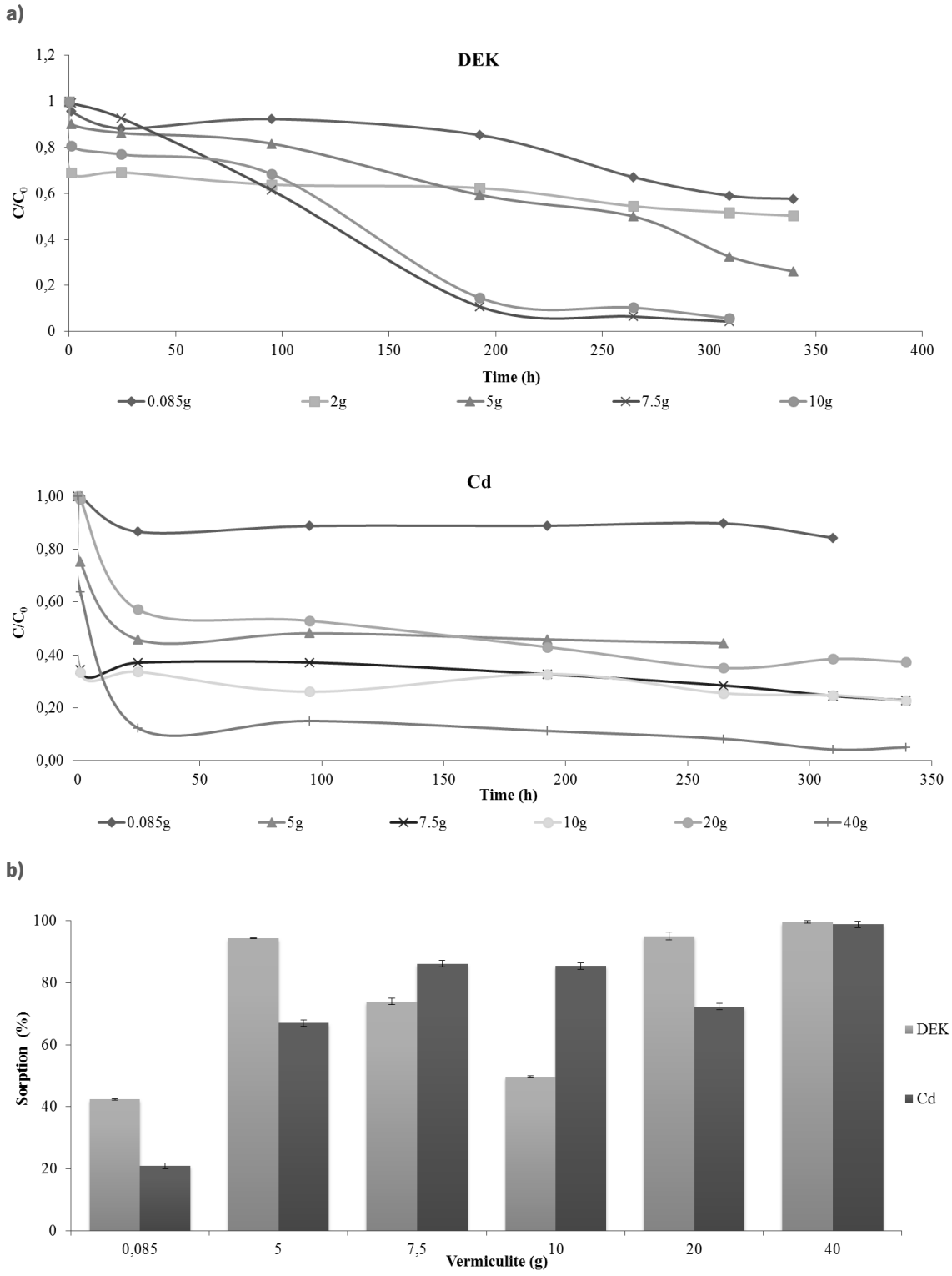

Figure 5.11. a) Ratio between residual and initial concentration (C/C_0) of DEK and Cd^{2+} versus time for different vermiculite masses for the biosorption/biodegradation assays conducted with diethylketone and Cd^{2+}; **b)** Sorption percentage of diethylketone and Cd^{2+} using a biofilm of *S. equisimilis* supported on different masses of vermiculite.

Table 5.9 shows that as the mass of the sorbent increases, the sorption percentage of diethylketone and Cd^{2+} increases whereas their uptake decreases. This behaviour was expected since the surface area available for the biofilm formation and for the retention of both pollutants also increases. Figure 5.8.b illustrates the presence of a *S. equisimilis* biofilm supported on 0.085 g of vermiculite, only three hours after the start of the experiment and after 339.5 hours. These results corroborate, once again, the ability of this microorganism to grow in toxic conditions, which is an advantage in treating contaminated wastewater.

Biosorption Kinetic Modelling

For both pollutants and for all the quantities of vermiculite employed, experimental data is best described by the pseudo-second order model ($0.933 < R^2 \leq 1$ for diethylketone and $0.815 < R^2 \leq 0.999$ for Cd^{2+}), (Figure 5.12). This model assumes that the rate limiting step of the process is chemisorption (Kumar et al. 2011) involving valence forces through the sharing or exchange of electrons between the biomass and the biomass mixed with mineral clays and diethylketone /Cd, complexation, coordination and/or chelation (Quintelas et al. 2012). For both pollutants the K_2 constant increases for the assays conducted with 0.085 g to 5 g of vermiculite and then it decreases for the assays conducted with 5 g to 10 g of vermiculite, increasing again for the assays conducted with 10 g to 40 g of vermiculite. The zero order and pseudo-first order models do not fit the experimental data obtained for both sorbates, for the quantities of vermiculite tested.

These results indicate that the competition for the actives sites of the sorbents surface is generally dominated by diethylketone, most likely due to its transformation into other organic compounds that will compete with Cd for the active sites available and will be used as a carbon source for the microorganism and on the other hand due to the toxicity of Cd^{2+}.

In this set of experiments, the R_w factor ranged between 0 and 0.08 for Cd^{2+} and between 0 and 0.097 for diethylketone indicating that the kinetic curve is largely curved, well approaching equilibrium, confirming the good performance of the system.

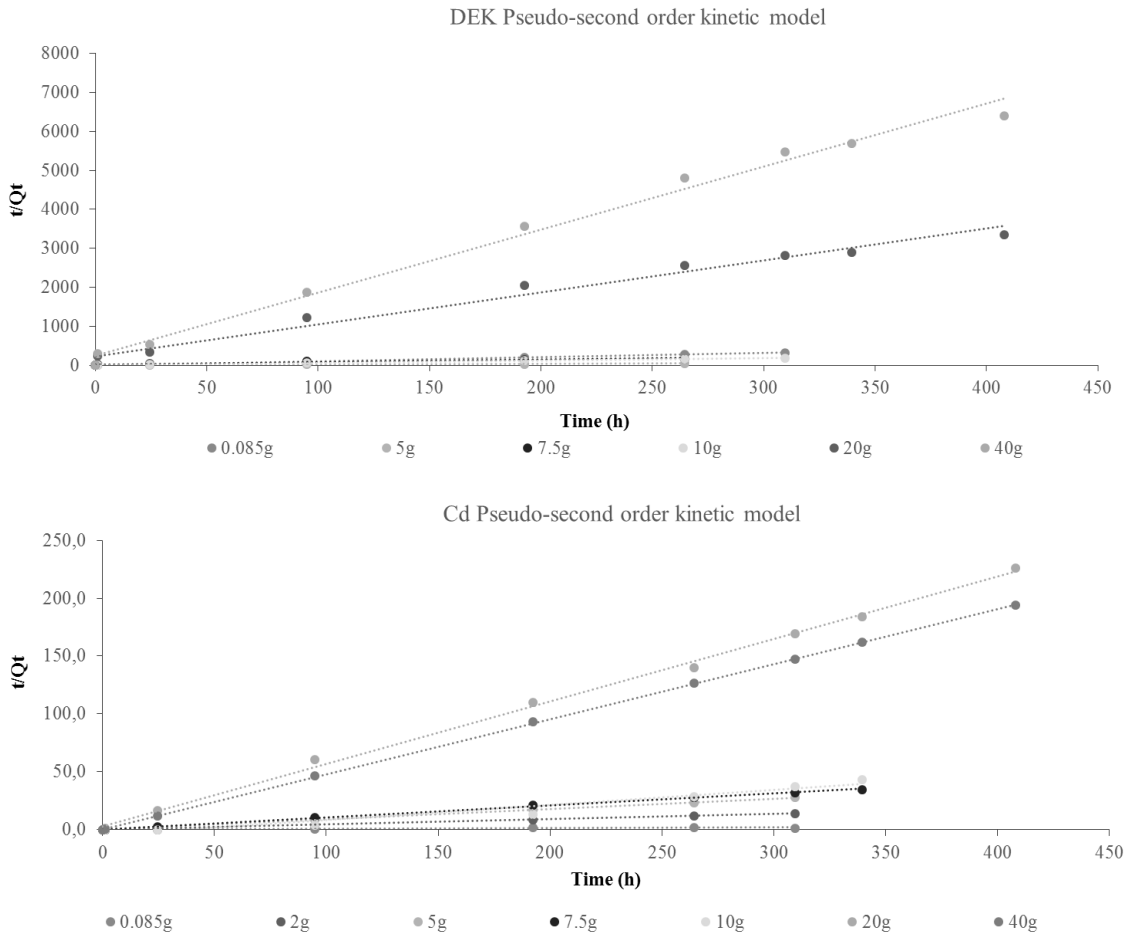

Figure 5.12. Comparison between the experimental results and those predicted by different models for diethylketone and Cd^{2+} biosorption, at 37 °C using *S. equisimilis* supported on vermiculite kinetics.

Biosorption Equilibria Modelling

Langmuir, Freundlich, BET and D-R models were fitted to several experimental adsorption isotherms and the parameters are listed in Table 5.10, while the fitting quality of the different models is shown in Figure 5.13 The best fit for diethylketone was obtained with the Langmuir model (R^2=0.989). This isotherm describes quantitatively the formation of a monolayer of adsorbate on the outer surface of the adsorbent, assuming that after that no additional adsorption occurs. The values obtained for q_{max}, b and R_L were respectively 0.36 mg/g, 9.97 L/mg and $2.79x10^{-4}$, respectively, and indicate that the sorption of diethylketone favourable ($0<R_L<1$). For Cd^{2+}, the best fit was obtained with the Freundlich isotherm model (R^2=0.994). The values obtained for K_f and n were respectively $1.01x10^{-6}$ mg/g and $2.28x10^{-1}$ showing the high adsorption capacity of the system and that the adsorption is favourable

and cooperative (1/n > 1) (Dada et al. 2012). The small value obtained for the R^2 with the D-R model and the negative value obtained for B and C_S with the BET model, forces to disregard these models.

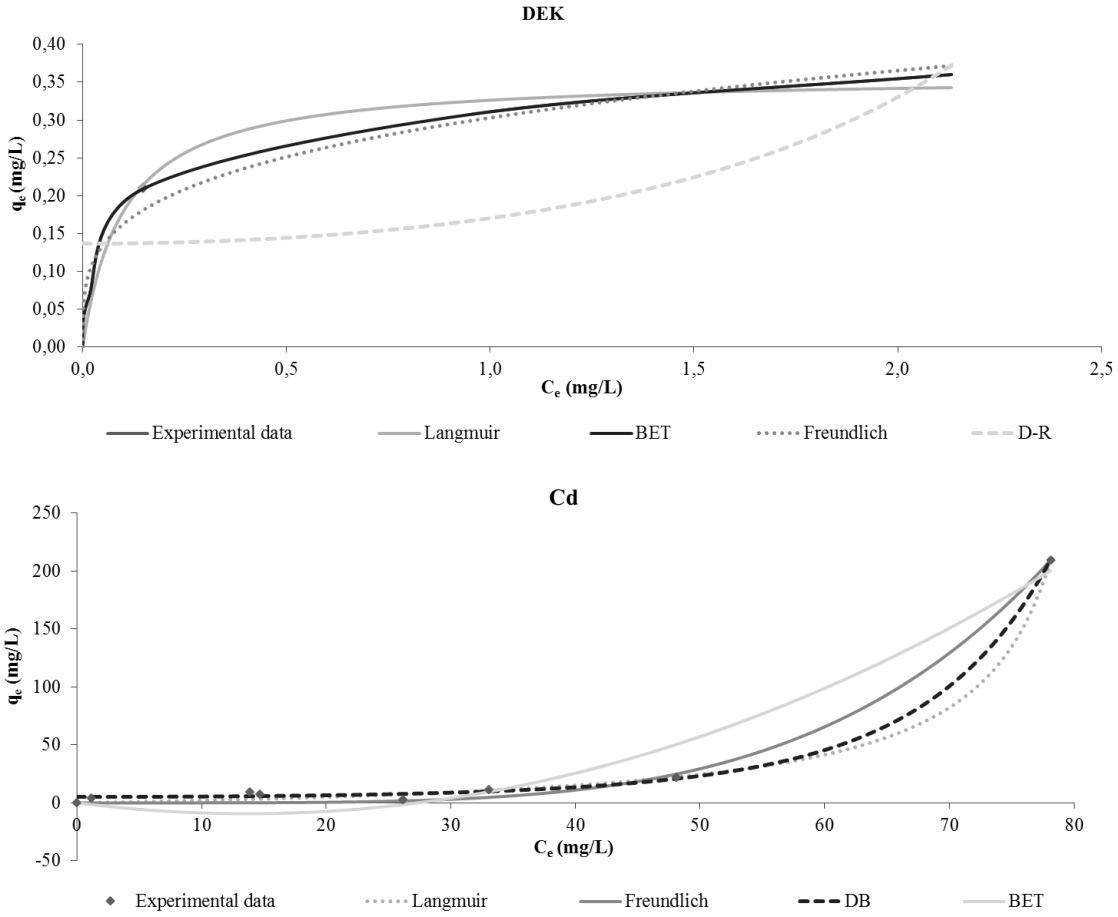

Figure 5.13. Comparison between the experimental results and those predicted by different models for diethylketone and Cd biosorption, at 37 °C using *S. equisimilis* supported on vermiculite isothermic equilibria.

5.3.4| Identification of DEK By-Products

During the biosorption experiments several intermediates were detected by the GC analyses of the aqueous solution (Figure 5.14).

a) **b)**

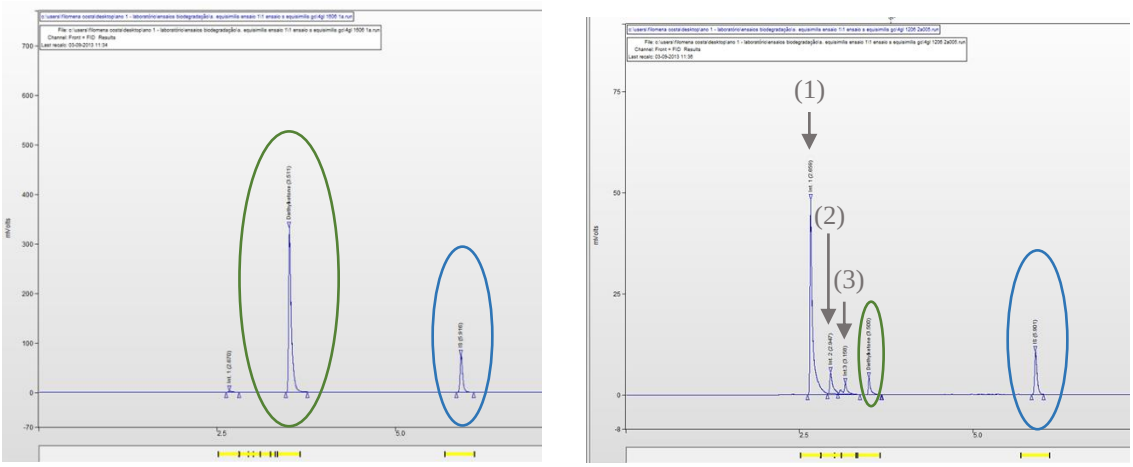

Figure 5.14. Example of a chromatogram from one of the biodegradation assays with *Streptococcus equisimilis*, at 150 rpm and an initial diethylketone concentration of 3 g/L **a**) Concentration of diethylketone at the beginning of the test; **b**) Concentration of diethylketone after 5 days accompanied by formation of several intermediates, (1)- methyl acetate; (2) ethyl acetate and (3) 2-pentanone.

These metabolites were identified as 2-pentanone, methyl-acetate and ethyl-acetate and disappeared during the experiment, meaning that these same compounds were subject to biomass degradation/sorption. The presence and subsequent identification of the metabolites formed, allowed an approach to the metabolic degradation pathway of diethylketone by *S. equisimilis*. The classic metabolic degradation pathway of ketones was well described by Nielson and Allard (2009) and takes place by carboxylation followed by hydrolysis.

Although the presence of 2-pentanone only represents a change on the carbon atom where the ketone group is attached to, the presence of compounds with lower number of carbons than diethylketone (methyl-acetate and ethyl-acetate) corroborate the existence of a biodegradation

process. Diethylketone is firstly transformed in ethyl-acetate and posteriorly transformed in methyl-acetate. As mentioned above, all the metabolites are completely consumed by the biomass.

5.4| CONCLUSIONS

In the present study it was found that *S. equisimilis* is negatively affected by concentrations higher than 80 mg/L of Ni^{2+} and 5 mg/L of Cd^{2+} and that when vermiculite acts as the only sorbent it is able to efficiently sorb Ni^{2+} and Cd^{2+}. When Ni^{2+} and diethylketone are mixed, the sorption values are higher suggesting a synergetic interaction between these two pollutants, whereas when diethylketone and Cd^{2+} are mixed, the sorption of diethylketone decreases significantly, revealing a negative effect of Cd^{2+} over the retention of diethylketone. The results obtained with the biosorption experiments suggest that the presence of the biofilm may be an advantage in this type of treatment, with a general increase in terms of sorption efficiency and can be explained by the presence of functional surface groups on the biofilm, that may implement the substrate molecules adsorption and eventually promote the biodegradation of diethylketone and by the increase of the available sites for sorption.

REFERENCES

Ahmady-Asbchin S., Jafari N. 2013. Removal of nickel and zinc from single and binary metal solutions by *Sargassum angustifollium*. Water Science & Technology 68: 1384-1390.

Ahmed S., Chughtai S., Keane MA. 1998. The removal of cadmium and lead from aqueous solution by ion exchange with Na-Y zeolites. Separation and Purification Technology 13: 57-64.

Andrews J.F. 1968. A mathematical model for the continuous culture of microorganisms utilizing inhibitory substance. Biotechnology and Bioengineering 10:707-723.

Araújo M.M., Teixeira J.A. 1997. Trivalent chromium sorption on alginate beads. International Biodeterioration & Biodegradation 40: 63-74

Badawy N.A., El-Bayaa A.A. and Abd AlKhalik E. 2010. Vermiculite as an exchanger for copper(II) and Cr(III) ions kinetic studies. Ionics 16: 733-739.

Baty F., Delignette-Muller M-L. 2004. Estimating the bacterial lag time: which model, which precision?. International Journal of Food Microbiology 91: 261-277.

Burmølle M., Ren D., Djarnsholt T., Sørensen S.J. 2014. Interactions in multispecies biofilms: do they actually matter?. Trends in Microbiology 22: 84-91.

Çelekli A., Bozkurt H. 2011. Bio-sorption of cadmium and nickel ions using *Spirulina platensis*: Kinetic and equilibrium studies. Desalination 275: 141-147.

Chaudhuri D., Majumder A., Misra A.K., Bandyopadhyay K. 2014. Cadmium Removal by *Lemna minor* and *Spirodela polyrhiza*. International Journal of Phytoremediation 16: 1119-1132.

Chen B-Y., Utgikar V.P. Harmon, S.M. Tabak H.H. Bishop D.F., Govind R. 2000. Studies on biosorption of zinc(II) and copper(II) on *Desulfovibrio desulfuricans*. International Biodeterioration & Biodegradation 46: 11-18.

Chopra A.K., Pathak C, 2010. Biosorption technology for removal of metallic pollutants – An overview. Journal of Applied and Natural Science 2: 318-329.

Costa F., Quintelas C., Tavares T. 2012. Kinetics of biodegradation of diethylketone by *Arthrobacter viscosus*. Biodegradation 23: 81-92.

Costa F., Quintelas C., Tavares T. 2014. An approach to the metabolic degradation of diethylketone (DEK) by *Streptococcus equisimilis*: Effect of DEK on the growth, biodegradation kinetics and efficiency. Ecological Engineering 70: 183-188.

Dada A.O., Olalekan A.P., Olatunya A.M., Dada O. 2012. Langmuir, Freundlich, Temkin and Dubinin–Radushkevich Isotherms Studies of Equilibrium Sorption of Zn^{2+} Unto Phosphoric Acid Modified Rice Husk. IOSR Journal of Applied Chemistry 3: 38-45.

Dbson R.S., Burgess J.E. 2007. Biological treatment of precious metal refinery wastewater: A review. Minerals Engineering 20: 519-532.

Edwards V.H. 1970. The influence of high substrate concentrations on microbial kinetics. Biotechnology and Bioengineering 12: 679-712.

Espinozo E., Escudero R., Tavera F.J. 2012. Waste water Treatment by Precipitating Copper, Lead and Nickel Species. Research Journal of Recent Sciences 1: 1-6.

Fan Y.Z., Wang Y.Y., Qiao P-Y., Gu J-D. 2004. Optimization of phthalic acid batch biodegradation and the use of modified Richards model for modelling degradation. International Biodeterioration & Biodegradation 53: 57–63.

Hadi P., Barford J., McKay G. 2013. Synergistic effect in the simultaneous removal of binary cobalt-nickel heavy metals from effluents by a novel e-waste-derived material. Chemical Engineering Journal 228: 140-146.

Kara Y., Kara I. 2005. Removal of cadmium from water using duckweed (*Lemna trisulca* L.). International Journal of Agriculture & Biology 7: 660-662.

Kesaano M., Sims R, 2014. Algae biofilm based technology or wastewater treatment. Algal Research 5: 231-240

Kishore G., Sree P., Krishna D. 2013. Industrial wastes as adsorbents for the removal of chromium from waste water: A review. International Journal of Chemical Science 11: 1371-1384.

Kumar R., Bhatia D., Singh R., Rani S., Bishnoi N.R. 20111. Sorption of heavy metals from electroplating effluent using immobilized biomass *Trichoderma viride* in a continuous packed-bed column. International Biodeterioration & Biodegradation 65: 1133-1139

Kumar R., Bhatia D., Singh R., Rani S., Bishnoi N.R. 2012.Metal tolerance and sequestration of Ni(II), Zn(II) and Cr(VI) ions from simulated and electroplating wastewater in batch process: Kinetics and equilibrium study. International Biodeterioration & Biodegradation 66: 82-90

Lam K-Y., Davidson F.F., Hanson R.K. 2012, High-Temperature Measurements of the Reactions of OH with a Series of Ketones: Acetone, 2-Butanone, 3-Pentanone, and 2-Pentanone. The Journal of Physical Chemistry A 116: 5549-5559.

Luong J.H.T. 1987. Generalization of Monod kinetics for analysis of growth data with substrate inhibition. Biotechnology and Bioengineering 29: 242-248.

Marseaut S., Debourg A., Dostálek P., Votruba J., Kuncová G., Tobin J.M. 2004. A silica matrix biosorbent of cadmium. International Biodeterioration & Biodegradation 54: 209-214,

Merrikhpour H., Jalali M. 2013. Sorption processes of natural Iranian bentonite exchanged with Cd^{2+}, Cu^{2+}, Ni^{2+}, and Pb^{2+} cations. Chemical Engineering Communications 200: 1645-1665.

Monod. J. 1949. The growth of bacterial cultures. Annual Review of Microbiology 3: 371-394.

Montagnolli R.N., Lopes P.R.M., Bidoia E.D. 2009. Applied models to biodegradation kinetics of lubricant and vegetable oils in wastewater. International Biodeterioration & Biodegradation 63: 297-305.

Morlett-Chávez J.A., Ascacio-Martínez J.A., Rivas-Estilla A.M., Velásquez-Vadillo J.F., Haskins W.E., Barrera-Saldaña H.A., Acuña-Askar K. 2010. Kinetics of BTEX biodegradation by a microbial consortium acclimatized to unleaded gasoline and bacterial strains isolated from it. . International Biodeterioration & Biodegradation 64: 581-587.

Nielsen A., Allard A.S. 2009. Chemistry of organic pollutants In: Environmental and Ecological Chemistry (Vol 1). EOLSS, pp. 1–424.

Ofomaja A.E. 2010. Biosorption studies of Cu (II) onto Mansonia sawdust: process design to minimize biosorbent dose and contact time. Reactive and Functional Polymers 70: 879–889.

Ouadjenia-Marouf F., Marouf R., Schott J., Yahiaoui A. 2013. Removal of Cu(II), Cd(II) and Cr(II) ions from aqueous solution by dam silt. Arabian Journal of Chemistry 6: 401-406.

Plazinski W., Dziuba J., Rudzinski W. 2013. Modeling of sorption kinetics: the pseudo-second order equation and the sorbate intraparticle diffusivity. Adsorption 19: 1055-1064.

Powell E.O. 1967. The growth rate of microorganisms as function of substrate concentration, E. C.G.T., S. R.E. HMSO, London, United Kigndom.

Qin B., Luo H., Liu G., Zhang R., Chen S., Hou Y., Luo Y. 2012. Nickel ion removal from wastewater using the microbial electrolysis cell. Bioresource Technology 121: 458-461.

Quintelas C., Costa F., Tavares T. 2012. Bioremoval of diethylketone by the synergistic combination of microorganisms and clays: Uptake, removal and kinetic studies. Environmental Science and Pollution Research 20: 1374-1383.

Quintelas C., Figueiredo H., Tavares, T. 2011. The effect of clay treatment on remediation of diethylketone contaminated wastewater: Uptake, equilibrium and kinetic studies. Journal of Hazardous Materials 186: 1241-1248.

Raghuvanshi S., Babu B.V. 2010. Biodegradation kinetics of methyl iso-butyl ketone by acclimated mixed culture. Biodegradation 21: 31-42.

Raman K.V.V., Jackson M.L. 1963. Vermiculite surface morphology. Clay and Clay Minerals 12: 434-429.

Sahoo N.K., Pakshirajan K., Ghosh P.K. 2010. Enhancing the biodegradation of 4-chlorophenol by *Arthrobacter* chlorophenolicus A6 via medium development. International Biodeterioration & Biodegradation 64: 474-480.

Sar P., Kazy S.K., Asthana R.K., Singh S.P. 1999. Metal adsorption and desorption by lyophilized *Pseudomonas aeruginosa*. International Biodeterioration & Biodegradation 44: 101-110,

Sar P., Kazy S.K., Souza S.F.D. 2004. Radionuclide remediation using a bacterial biosorbent. International Biodeterioration & Biodegradation 54: 193-202.

Saravanan P., Pakshirajan K., Saha P. 2009. Batch growth kinetics of an indigenous mixed microbial culture utilizing *m*-cresol as the sole carbon source. Journal of Hazardous Materials 162: 476-481.

Srivastava V.M., Mall I.D., Mishra I.M. 2006. Equilibrium modelling of single and binary adsorption of cadmium and nickel onto bagasse fly ash. Chemical Engineering Journal 117: 79-91.

Suazo-Madrid A., Morales-Barrera L., Aranda-Garcia E., Cristiani-Urbina E. 2011. Nickel (II) biosorption by *Rhodotorula glutinis*. Journal of Industrial Microbiology & Biotechnology 38: 51-64.

Vieira M.G.A., Neto A.F.A., Gimenes M.L., Silva M.G.C. 2010. Sorption of kinetics and equilibrium for the removal of nickel ions from aqueous phase on calcined Bofe bentonite clay. Journal of Hazardous Materials 177: 362-371.

Volesky B. 1990. Biosorption of heavy metals. CRC press, Boca Raton, Ann Arbor, Boston.

Wang Y. L., Gu J.D. 2005. Influence of temperature, salinity and pH on the growth of environmental isolates of Aeromonas and Vibrio species isolated from Mai Po and the Inner Deep Bay Nature Reserve Ramsar site of Hong Kong. Journal of Basic Microbiology 45: 83–93.

Wu F-C., Tseng R-L., Huang S-C., Juang R-S. 2009. Characteristics of pseudo-second-order kinetic model for liquid-phase adsorption: a mini-review. Chemical Engineering Journal 151: 1-9.

Yin Y., Hu Y., Xiong F. 2011.Sorption of Cu(II) and Cd(II) by extracellular polymeric substances (EPS) from *Aspergillus fumigates*. International Biodeterioration & Biodegradation 65: 1012-1018.

Zwietering M.H., Jongenburger I., Rombouts F.M. and Van't Riet K. 1990. Modeling of the bacterial growth curve. Applied and Environmental Microbiology 56: 1875-1881.

WEB REFERENCES

http://pubchem.ncbi.nlm.nih.gov/

http://toxnet.nlm.nih.gov/index.html

CHAPTER 6

Pilot scale sorption studies of diethylketone in the presence of Cd and Ni

The effect of pH on the sorption capacity of vermiculite towards cadmium and nickel was tested in batch systems and it was shown that the sorption percentages increase with increasing the mass of vermiculite and with increasing the initial pH. Maximum sorption percentages were obtained for a pH of 8 and 4 g of vermiculite (86.5 % for Cd^{2+} and 86.1 % for Ni^{2+}, for solutions with 100 mg/L of metal). As a consequence, it was possible to establish a range of optimal pH for biosorption processes, by combining the so determined optimal sorption pH of vermiculite with the optimal growth pH of *Streptococcus equisimilis*, a bacterium used to treat contaminated water. Pilot-scale experiments with a *S. equisimilis* biofilm supported on vermiculite were conducted in close loop aiming the treatment of large volumes of diethylketone aqueous solutions, eventually containing Cd^{2+} or Ni^{2+}. These experiments proved the excellent capacity of this joint system to simultaneously biodegrade diethylketone and biosorb Cd^{2+} or Ni^{2+}. The removal percentage and the uptake increase through time, even with the replacement of the initial solution by new ones. The breakthrough curves that best describe the results achieved for Cd^{2+} and Ni^{2+} are respectively, the Adams-Bohart model and the Yoon and Nelson model.

This chapter is based on the following submitted publication: Costa F., Tavares T. 2016. Pilot scale sorption studies of diethylketone in the presence of Cd and Ni.

6.1| INTRODUCTION

Water contamination has become a serious threat to society due to the rapid and growing industrialization, the increasing use of modern agricultural practices, the severe exploitation of natural resources and the illegal discharges of wastewater (Fonseca et al. 2009; Murthy et al. 2012; Bhuvaneshwari and Sivasubramanian, 2014). These practices introduce hazardous and persistent substances like organic and metallic compounds in the environment, which tend to accumulate and deteriorate the different environmental matrices (Murthy et al. 2012). This problem has been receiving substantial attention, especially since it was established that aquatic organisms can readily incorporate (adsorb, bio-accumulate or biodegrade) those contaminants, which may then enter directly into the human food chain (Meena et al. 2005). On a small scale, both organic and inorganic contaminants can safely be removed from any water body and thus not affecting the aquatic communities. However, on a larger scale, the aquatic system is unable, in due time, to effectively remove the contaminants present, being thus severely hampered (Bhuvaneshwari and Sivasubramanian, 2014). In this context, the study of processes able to efficiently and effectively treat wastewater is of utmost importance, as well as the understanding of the contaminants migration between phases and the factors affecting such phenomena (Fonseca et al. 2009).

Industries such as petrol and petrochemical, electronics, paints, pharmaceuticals and food processing use ketones as solvents, polymer precursors or intermediates in their processes. One such example is diethylketone, also known as 3-pentone. The release of diethylketone into the environment constitutes a threat to living beings since it is persistent in water, soil and air, it has high mobility and it can form toxic and phototoxic intermediates (Costa et al. 2015).

Cadmium and nickel are two metals commonly found in wastewater from different industries like printing, electronic devices manufacturing, paints, dyes, oil refining, pulp and paper, fertilizers, steels, pesticides (Ogbodu et al. 2015), jewellery, tanneries, mining, batteries, textile, petrochemical and fine chemistry, chemicals (Ahmed et al. 1998; Chopra and Pathak, 2010; Merrikhpour and Jalali, 2013) and health care products (Tam et al. 1989), causing serious environmental and health problems. Cadmium is irritant to the respiratory system and it is able to cause anaemia, to affect the action of enzymes, hampering respiration, photosynthesis, transpiration and chlorosis (Ahmed et al. 1998), to cause cancer, to promote infertility and serious health problems in different organs. Nickel

is considered a carcinogenic element, capable of causing several types of acute and chronic symptoms and illnesses (Suazo-Madri et al. 2011).

Techniques such as adsorption on granular activated carbon (GAC), air-stripping, oxidation with or without flame, thermal degradation, condensation and incineration, chemical precipitation, reverse osmosis and ion exchange (Qin et al. 2012; Hadi et al. 2013) are used to remove organic solvents and heavy metal from wastewater. These techniques present however, several drawbacks like the emission of nitrogen gases (NO_x), which requires the application of a secondary treatment, with a consequent increase of operational costs and production of contaminated solid wastes, reduced efficiency, excessive usage of chemicals and high operational, maintenance and equipment costs (Raghuvanshi and Babu, 2010; Costa et al. 2012).

In recent years, several studies have demonstrated that biological processes such as biosorption and biodegradation, present numerous advantages over the conventional methods mentioned above. These biological processes do have an eco-friendly character since they do not generate solid wastes and nitrogen oxides, they present high efficiency and they reduce maintenance and operational costs (Araújo and Teixeira, 1997; Çelekli and Bozkurt 2011; Costa et al. 2012)

Volatile organic compounds and heavy metals are expected to be among the high diversity of contaminants present in industrial and domestic effluents (Amor et al. 2001; Azeez et al. 2013). Several studies concerning the decontamination of such effluents and its optimization have been conducted and became of major importance and relevance not only for environment rehabilitation, but also aiming its economics sustainability.

A joint system was used in this study that combines the properties of clays and microorganisms to improve the removal of different kind of pollutants from aqueous solutions. The use of joint systems to treat wastewater has proven their efficiency, since they combine the sorption capacity of the clay besides its high cation exchange capacity, large specific surface area, excellent chemical and physical stability (Quintelas et al. 2012), with the microorganism ability to biodegrade, fix and/or entrap contaminants, due to the existence of enzymes and the presence of several functional groups on the biomass surface (chitin acetamides, phosphate, amino, carboxylic groups, nucleic acids and proteins) (Yin et al. 2011; Costa et al. 2012).

The main goal of the present chapter comprises the development of an environmental-friendly technology capable to decontaminate multicomponent systems containing diethylketone, eventually with nickel or cadmium. Metals and ketones appear together in wastewater (EPA 1993; Dobson and Burgess, 2007), but there are very few published works regarding the simultaneous removal of these two types of contaminants.

6.2| MATERIALS AND METHODS

6.2.1| Bacteria Strain and Vermiculite

The bacterium used was *Streptococcus equisimilis* and it was acquired from the Spanish Type Culture Collection, from the University of Valencia (reference CECT 926). *Streptococcus equisimilis* was grown in sterilized Brain Heart Infusion (Oxoid CM1135) culture medium at 37° C, 150 rpm, for several days.

Vermiculite is a hydrated magnesium aluminium silicate purchased from Sigma-Aldrich and it was used as a support for the bacterial biofilm establishment and development. It has a BET surface area of 39 m^2/g, an average particle diameter of 8.45 mm and a porosity of 10%.

6.2.2| Chemicals Preparation

Diethylketone was purchased from Acros Organics (98% pure) and diluted in sterilized distilled water. Individual stock solutions of 1 g/L of cadmium ($CdSO_4 \cdot 8/3H_2O$, Riedel-de-Haën) and 1 g/L of nickel ($NiCl_2 \cdot 6H_2O$, Carlo Erba Reagents) were prepared by dissolving an accurately weighed amount of metal in sterilized distilled and deionized water. The multi-element ICP quality control standard solution was purchased from CHEM Lab (QCS-03) (15E). In all the experiments, the concentration of cadmium and nickel was 100 mg/L and it was obtained by dilution of the respective stock solution.

Previous experiments conducted at lab-scale in batch mode to evaluate the effect of concentrations of diethylketone, Cd^{2+} or Ni^{2+}, on singular or multi-component solutions on the growth of *S. equisimilis* and on the sorption capacity of *S. equisimilis*, vermiculite and a *S. equisimilis* biofilm supported on

vermiculite are reported by our team in Quintelas et al. (2011), Quintelas et. (2012), Costa et al. (2014); Costa et al. (2016 a,b).

6.2.3| The Effect of pH on the Sorption of Ni and Cd by Vermiculite - Lab Scale Experiments

These experiments were conducted in 1 L Erlenmeyer flasks with a working volume of 0.425 L containing 100 mg/L of $Cd^{2+}$and of Ni^{2+}, different doses of vermiculite (0.1 g, 2.05 g and 4 g) and different initial pH values (3, 5.5 and 8). The Erlenmeyer flasks were incubated in an orbital shaker (150 rpm) at 37°C until equilibrium was reached. The required time for equilibrium to be reached (24 hours for Cd^{2+} and Ni^{2+}) was previously determined. At pre-establish time intervals samples were collected and centrifuged at 1300 rpm (Eppendorf MiniSpin 9056) for 10 minutes. The supernatant was analysed by ICP-OES in order to determine the concentrations of $Cd^{2+}$and Ni^{2+} through time. A blank containing just an aqueous solution of Cd^{2+} and Ni^{2+} was used to assess any sorption by the Erlenmeyer flasks walls or the interactions between the two metals.

6.2.4| Biodegradation of Diethylketone and Biosorption of Cd^{2+}or Ni^{2+} by a Biofilm Ssupported in Vermiculite in Open Systems – Pilot Scale Experiments

A compact polycarbonate acrylic column of 22.7 L with an internal diameter of 17 cm and a total height of 100 cm was used as a bioreactor in the pilot scale experiments. A maximum packing fraction of 1/3 of the bioreactor was filled with vermiculite (700 g). An Erlenmeyer flask (2 L) containing 1 L of Brain Heart Infusion culture medium previously sterilized at 121°C for 20 minutes, was inoculated with *S. equisimilis* and incubated in an orbital shaker for 24 hours at 37°C and 150 rpm. The Erlenmeyer flask was capped with a cotton stopper in order to allow passive aeration. The inoculum culture was then transferred to the bioreactor setup and was pumped upwards at a flow rate of 250 mL/minute, during 5 days with total recirculation, in order to allow the biomass to attach to the vermiculite and form a well-developed biofilm. Once the biofilm was formed, the bed was washed out and a 40 L solution (S_1) containing 7.5 g/L of diethylketone and 100 mg/L of metal (Cd^{2+} or Ni^{2+}) was continuously pumped upwards through the bioreactor with a constant flow rate of 25 mL/minute. For the pilot scale experiments performed with Ni^{2+} the solution S_1 was replaced by a

new solutions (S_2 and S_3) that also contained diethylketone (7.5 g/L) and Ni^{2+} (100 mg/L) (Figure 6.1). At the end of the experiment only diethylketone was added to the solution S_3 (S_4). For the experiments performed with Cd^{2+}, the solution S_1 was replaced by new solutions (S_2 and S_3) that also contained diethylketone (7.5 g/L) and Cd^{2+} (100 mg/L).

At pre-established time intervals, samples of the effluent (8 mL) were taken, centrifuged at 1300 rpm (Eppendorf MiniSpin 9056) for 10 minutes and the aqueous phase was analysed by GC-MS and by ICP-OES in order to determine respectively the concentration of diethylketone and metals through time. At the end, the bioreactor was washed out and samples of the effluent and of the vermiculite were inoculated in Petri plates with Brain Heart Infusion culture medium, in order to determine and evaluate the metabolic activity of the bacteria. The pH was also monitored.

a) **b)**

Figure 6.1. Pilot scale installation for **a)** the growth and formation of the *S. equisimilis* biofilm on vermiculite at room temperature; **b)** biodegradation and biosorption assays of diethylketone and Ni^{2+} or diethylketone and Cd^{2+}.

6.2.5 |Analytical Methods

6.2.5.1| Gas Chromatography (GC)

A GC-MS Varian 4000, equipped with a flame ionization detector (FID), mass spectrometry (MS) and a ZB-WAXplus column (30 m x 0.53 mm x 1.0 µm) was used to determine the concentration of diethylketone in samples. The column was initially held at a temperature 50 °C, then heated at 3 °C/minute to 100 °C, held at 100 °C for 4 minutes, then heated again at 40 °C/minute to 150 °C and finally held at 150 °C for 2 minutes. The temperature of injector and detector were kept at 250 °C. Nitrogen was used as the carrier gas at a flow rate of 4 mL/min and the injections were performed in the split mode with a split ratio of 1:10. The retention time for diethylketone and for the internal standard (2-methyl-1-butanol) was found to be respectively 5.3 minutes and 11.3 minutes.

6.2.5.2| Inductively Coupled Plasma Optical Emission Spectrometry (ICP-OES)

An ICP-OES (Optima 8000, PerkinElmer) was used to determine the concentration of Cd^{2+} and Ni^{2+} in samples. The operating conditions were as follows: RF power: 1300 W; argon plasma flow of 8 L/minute; auxiliary gas flow of 0.2 L minute; nebulizer gas flow of 0.5 L/minute; axial plasma view; wavelength of 228.802 nm for Cd^{2+} and 221.648 nm for Ni^{2+}.

All calibration solutions were prepared from a Cd^{2+} and Ni^{2+} stock solution with a concentration of 1 g/L. All the samples were acidified with concentrated nitric acid (HNO_3 69 %) and filtered before being analysed.

The instrument response was periodically checked with the multi-element ICP QC standard solution (CHEM LAB) and with a blank (HNO_3 5 %).

6.2.5.4| Characterization of Sorbents by FTIR, XRD and SEM

To determine the functional groups involved in the biosorption of diethylketone, $Cd^{2+}$and Ni^{2+} an infrared spectra of the sorbents, with and without previous contact with the pollutants, were obtained using a Fourier Transform Infrared Spectrometer (FTIR BOMEM MB 104). For the FTIR analyses, the

sorbents were centrifuged and dried for 24 h at 60°C. Then, 10 mg of sorbent was encapsulated in 100 mg of KBr (Riedel) in order to obtain a translucent sample disk. Background correction for atmospheric air was used for each spectrum. The resolution was 4 cm^{-1} and minimums of 30 scans were conducted for each spectrum with the range between 500 and 4000 wavenumbers.

The X-ray diffraction (XRD) analyses were performed using a Philips PW1710 diffractometer. Scans were taken at room temperature in a 2 range between 5 and 60ªC, using Cu K radiation.

Scanning Electron Microscopy (SEM) observations of the sorbents, with and without previous contact with diethylketone, $Cd^{2+}$and Ni^{2+}, were performed on Leica Cambridge S360 to observe any morphological changes on the sorbents properties.

6.2.5.5| Data Modelling

6.2.5.5.1| Removal Kinetics Modelling

The sorption kinetics of all contaminants (Cd^{2+}, Ni^{2+} and diethylketone) were analysed using the linearized form of four different kinetic models: the zero order, pseudo-first order, pseudo-second order and three-half order (Brunner and Focht, 1984; Khamis et al. 2009; Saravanan et al. 2009) (see Chapter 2, section 2.2.7.1).

6.2.5.5.2| Sorption Isotherms Modelling

The equilibrium of sorption processes is usually described by the distribution of contaminants between the liquid phase and the solid sorbent phase and is usually modelled by adsorption isotherms. Langmuir, Freundlich, Dubinin-Radushkevich (D-R) and BET models (Saravanan et al. 2009; Kishore et al. 2013) were used to describe the equilibrium relationship between the solutions and the solid phase (see Chapter 5, section 5.28).

6.2.5.5.3| Breakthrough Curves Modelling

One of the criteria for a successful design of a fixed-bed column system for adsorption processes is the prediction of the breakthrough curve (concentration–time profile). Adams–Bohart, Wolborska and Yoon and Nelson models (Bohart and Adams, 1920; Yoon and Nelson, 1984; Wolborska 1989) were used to predict the breakthrough curves.

The Adams-Bohart model

The Adams-Bohart model (1920) is based on the surface reaction theory and assumes that equilibrium is not instantaneous, thus the rate of adsorption is proportional to the residual capacity of the sorbent and to the concentration of the sorbing species. The mass transfer rate can be described by the following equations:

$$\partial q / \partial t = -k_{AB} q C_b \quad (6.1)$$

$$\partial C_b / \partial Z = (k_{AB} / U_0)\, q C_b \quad (6.2)$$

where k_{AB} is the kinetic constant (L/mg·h), q is the concentration of sorbate in the solid phase, (mg/L), C_b denotes the sorbate concentration in solution inside the column (mg/L), Z is the bed depth of column (cm) and U_0 is the linear velocity of influent (cm/h) . This differential equation system can be solved if two assumptions are made: $t \rightarrow \infty$ and $q \rightarrow N_0$ (N_0 represents the maximum sorption capacity per unit of volume of column sorbent).

After the differential equation system is solved, the linearized form of the Adams-Bohart model is obtained:

$$\ln (C_t / C_0) = k_{AB} C_0 t - k_{AB} N_0 (Z / U_0) \quad (6.3)$$

where C_0 and C_t denote, respectively, the influent and effluent sorbate concentration (mg/L) at time t. The experimental values of N_0 and k_{AB} are obtained from the intercept and slope of the linear plot of $\ln (C_t / C_0)$ versus t for a given flow rate and bed height.

The Wolborska model

The Wolborska model is based on several mass transfer equations, namely the diffusion mechanisms, for low concentrations range of breakthrough curve. The mass transfer in fixed-bed systems may be expressed by the following equations:

$$\partial C_b\, \partial t + U_0\, (\partial C_b / \partial Z) + (\partial q / \partial t) = D\, (\partial^2 C_b / \partial^2 Z) \quad (6.4)$$

$$\partial q\, \partial t = -\, v\, (\partial q / \partial Z) = \beta_a\, (C_b - C_{S.1}) \quad (6.5)$$

where again C_b is the sorbate concentration in solution inside the column (mg/L), U_0 denotes the linear velocity of influent (cm/h), Z the bed depth of column (cm), D the axial diffusion coefficient (cm^2/h), v the interstitial velocity (cm/h), β_a the kinetic coefficient of the external mass transfer (h^{-1}) and $C_{S.1}$ the solute concentration at the solid/liquid interface (mg/L). Taking into account that $C_{S.1} \ll C_b$, $v \ll U_0$ and that the axial diffusion is considered negligible: $D \longrightarrow 0$ when $t \longrightarrow 0$, the solution of this differential equation system is approximated to the following equation:

$$\ln C / C_0 = (\beta_a C_0 / N_0)\, t - (\beta_a Z / U_0) \quad (6.6)$$

with

$$\beta_a = U_0^2 / 2D \sqrt{((1 + 4\beta_0 D/U_0^2) - 1)} \quad (6.7)$$

where β_0 is the external mass transfer coefficient with a negligible axial dispersion coefficient D. Wolborska noticed that in short beds or at high flow rates of solution through the bed, the axial diffusion was negligible and $\beta_a = \beta_0$. The migration velocity of the steady-state front is determined from Wicke's law:

$$v = (U_0 C_0) / (N_0 + C_0) \quad (6.8)$$

N_0 is the maximum sorption capacity per unit of volume of column sorbent used in the Adams-Bohart model. Equation 6.8 defines that the Wolborska model is equivalent to the equation Adams-Bohart model if $k_{AB} = \beta_a / N_0$.

The Yoon and Nelson model

Yoon and Nelson (1984) proposed a relatively simple model to describe the sorption process and the sorbates breakthrough in active carbon, since it does not require information about the characteristics of the systems used (type of sorbent and physical properties of the sorption bed for example). This model assumes that the rate of decrease in the probability of adsorption of each sorbate molecule is proportional to the probability of the sorbate sorption and the sorbate breakthrough on the sorbent. It can be expressed by the following equation:

$$\ln [C/(C_0-C)] = k_{YN} t - \tau k_{YN} \quad (6.9)$$

where k_{YN} is the kinetic coefficient (h^{-1}), τ the time needed (h) to reach 50 % of the sorbate breakthrough and t is the sampling time (h). The k_{YN} and τ parameters can be obtained from the slope and intercept of the linear plot of ln [C/ (C_0-C)] versus t.

6.3| RESULTS AND DISCUSSION

The effect of concentrations of diethylketone, Cd^{2+} and Ni^{2+}, in singular and in multi-component solutions, on the growth of *S. equisimilis* and on the sorption capacity of *S. equisimilis*, of vermiculite and of a *S. equisimilis* biofilm supported on vermiculite was previously established at lab-scale and batch mode by our team as described in Quintelas et al. (2011), Quintelas et. (2012), Costa et al. (2014); Costa et al. (2016 a,b). Briefly, the relevant results for the present study were the following:

- *S. equisimilis* growth starts to be inhibited for concentrations of diethylketone, $Cd^{2+}$and Ni^{2+} higher than 3.2 g/L, 80 mg/L and 5 mg/L, respectively;
- Sorption experiments conducted with vermiculite, diethylketone, Cd^{2+}or Ni^{2+} (singular sorbat solutions) achieved maximum sorption percentages of 92 %, 100 % and 95.4 %, respectively. In these experiments the sorption percentages tended to increase with the increase on the mass of vermiculite employed;
- Sorption experiments conducted with vermiculite, diethylketone and Cd^{2+}or Ni^{2+} (binary sorbat solutions) attained maximum sorption percentages of 43.6 % for diethylketone and 100 % for Cd^{2+} and complete sorption of both sorbates for the assays performed with diethylketone and Ni^{2+};

- Biosorptions experiments conducted at lab-scale in batch mode, using a *S. equisimilis* culture suspended in an aqueous solutions containing diethylketone and different concentrations of $Cd^{2+}$and Ni^{2+} reveal the complete removal of diethylketone. The maximum removal percentage of Cd^{2+}, 96.9 % and of Ni^{2+}, 98.4 %, tended to decrease with the increase of the initial concentration of metal;
- Biosorptions experiments conducted at lab-scale in batch mode using a *S. equisimilis* biofilm supported into different masses of vermiculite lead to removal percentages (biodegradation and biosorption/or sorption) higher than 97 % for all the contaminants for all the systems (diethylketone and Cd^{2+} and diethylketone and Ni^{2+}).

6.3.1| The Effect of pH on the Sorption of Cd and Ni by Vermiculite - Lab Scale Experiments

In these set of assays the concentrations of metals (Cd^{2+} and Ni^{2+}) were kept constant, whereas the amount of vermiculite employed and the value of the initial pH varied, from 0.1 g to 4 g for mass of vermiculite and from 3 to 8 for pH. It was observed that as the mass of vermiculite employed increased, the sorption percentage of Cd^{2+} and of Ni^{2+} tended to increase as well, whereas the uptake tended to decrease, Table 6.1.

For Cd^{2+}, the maximum removal percentages and uptake values achieved were respectively 86.5 % and 367.8 mg/g (pH 8), whereas for Ni^{2+} the maximum removal percentages and uptake values obtained were 86.1 % and 365.9 mg/g (pH 8). On the other hand, the maximum sorption percentage and uptake tend to increase when increasing the initial pH for the same mass of vermiculite. The concentration of H^{+} on the surface sites decreases and the concentration of OH^{-} increases, leading the clay surface to become negatively charged resulting in a significant decrease of electrostatic repulsion and thus in an increase of metal sorption (Badawy et al. 2010).

Since the point of zero charge of vermiculite is 2 and the pH at which Ni^{2+} and Cd^{2+} start to precipitate in the form of nickel hydroxide and cadmium sulphide, is respectively 7.6 and 8, it is possible to conclude that at pH 3 and 5.5, the decrease on the concentration of metals is due to sorption processes between each metal and the functional groups present on the vermiculite surface (Si-O-Si, H-O-H, CO and OH, for example) and not due to precipitation processes (Espinoza et a. 2012). For the assays conducted at pH 8 no precipitation was observed, allowing the authors to assume

that under these experimental conditions the decrease on Ni^{2+} and Cd^{2+} concentration is still due to sorption processes and not to precipitation.

It is concluded that the optimal pH to decontaminate aqueous solutions containing Ni^{2+} and Cd^{2+} by vermiculite sorption lies between 6 and 8.

Table 6.1. Sorption efficiency (%) and uptake (mg/g) of different masses of vermiculite when exposed to an aqueous solution containing Ni^{2+} and Cd^{2+} (100 mg/L) at different initial pH values.

pH 3				
	Ni^{2+}		**Cd^{2+}**	
Vermiculite (g)	**Sorption (%)**	**Uptake (mg/g)**	**Sorption (%)**	**Uptake (mg/g)**
0.1	11.70	49.71	7.81	33.21
2.05	44.17	9.16	18.08	3.75
4	70.17	7.46	46.28	4.92
pH 5.5				
Vermiculite (g)	**Sorption (%)**	**Uptake (mg/g)**	**Sorption (%)**	**Uptake (mg/g)**
0.1	47.16	292.27	44.15	196.97
2.05	54.12	9.78	45.21	9.37
4	68.86	5.75	46.35	4.69
pH 8				
Vermiculite (g)	**Sorption (%)**	**Uptake (mg/g)**	**Sorption (%)**	**Uptake (mg/g)**
0.1	76.57	365.91	63.04	367.77
2.05	85.26	14.94	73.21	15.18
4	86.10	9.06	86.53	6.69

Sorption Kinetic Modelling

The kinetic model that best describes the results obtained for Ni^{2+} and Cd^{2+} sorption, for all the initial pH tested is the pseudo-second order model (pH 3, $R^2 > 0.982$ for Ni^{2+} and $R^2 > 0.940$ for Cd^{2+}, pH 5.5, $R^2 > 0.971$ for Ni^{2+} and $R^2 > 0.933$ for Cd^{2+}, pH 8, $R^2 > 0.903$ for Ni^{2+} and $R^2 > 0.863$ for Cd^{2+}), Figure 6. 2. The behaviour of the pseudo-second constant (K_2) for Ni^{2+} and for Cd (except at pH 5.5) was unexpected since it increases with the increase of the vermiculite mass from 0.1 g to 2.05 g and then starts to decrease. This suggests that the sorption rate oscillates through time and with the mass of sorbent employed (Plazinski et al. 2013).

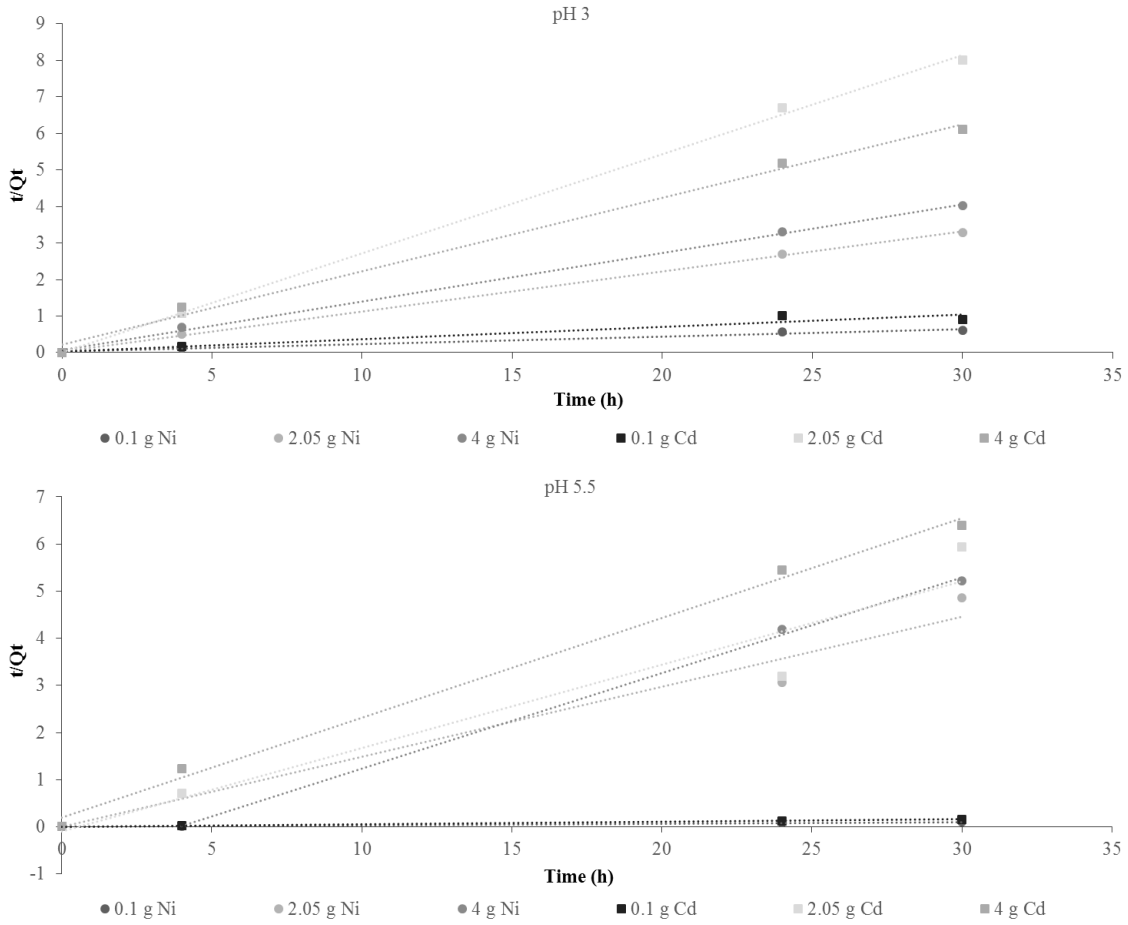

Figure 6.2. Kinetics modelling of the sorption of Ni^{2+} and Cd^{2+} (100 mg/L) by vermiculite (0.1 g, 2.05 g and 4 g) when exposed at lab-scale to an initial pH of 3, 5.5 and 8.

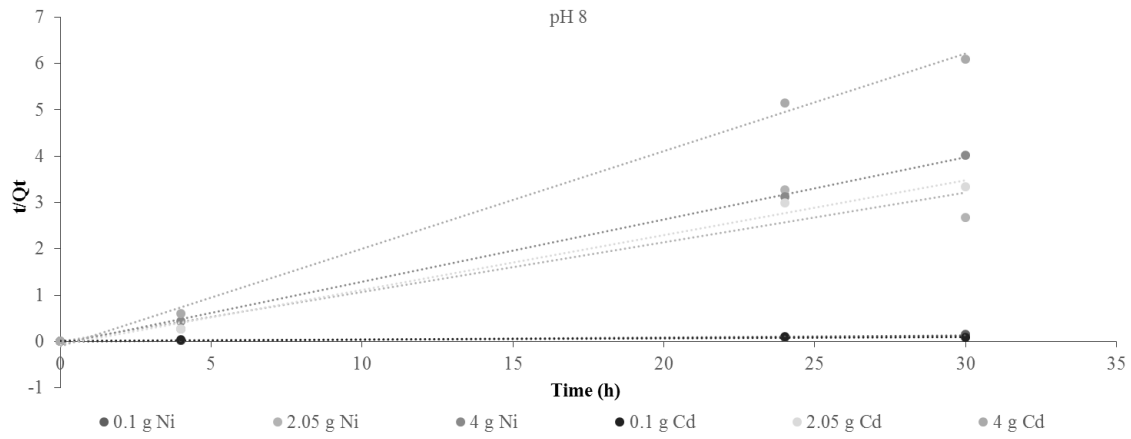

Figure 6.2. Kinetics modelling of the sorption of Ni^{2+} and Cd^{2+} (100 mg/L) by vermiculite (0.1 g, 2.05 g and 4 g) when exposed at lab-scale to an initial pH of 3, 5.5 and 8 (cont.).

6.3.2| Biodegradation of Diethylketone and Biosorption of Cd^{2+} by a Biofilm Supported in Vermiculite in Open Systems – Pilot Scale Experiments

Figure 6.3 shows that the removal (biosorption and/or biodegradation) of diethylketone, as well as the sorption of Cd^{2+} are continuous through time and tend to increase after the replacement of the solution S_1 by the solutions S_2 and S_3. This may be due to microbial growth that besides increasing the substrate consumption (need for growth and cellular maintenance) it also increases the number of actives sites of the biofilm, used for Cd^{2+} sorption, hampering the saturation of actives sites, either of the biomass and of the vermiculite. For diethylketone, the maximum removal percentages and uptake values obtained were 98.2 % and 421.0 mg/g, whereas for Cd^{2+} the maximum removal percentages and uptake values achieved were 87.6 % and 5.0 mg/g. From Figure 6.3 and Table 6.2 is possible to observe that the removal percentage achieved for Cd^{2+} is lower that the removal percentage obtained for diethylketone, which correspond to removal of 393.9 mol of Cd^{2+} and 25383.2 mol of diethylketone.

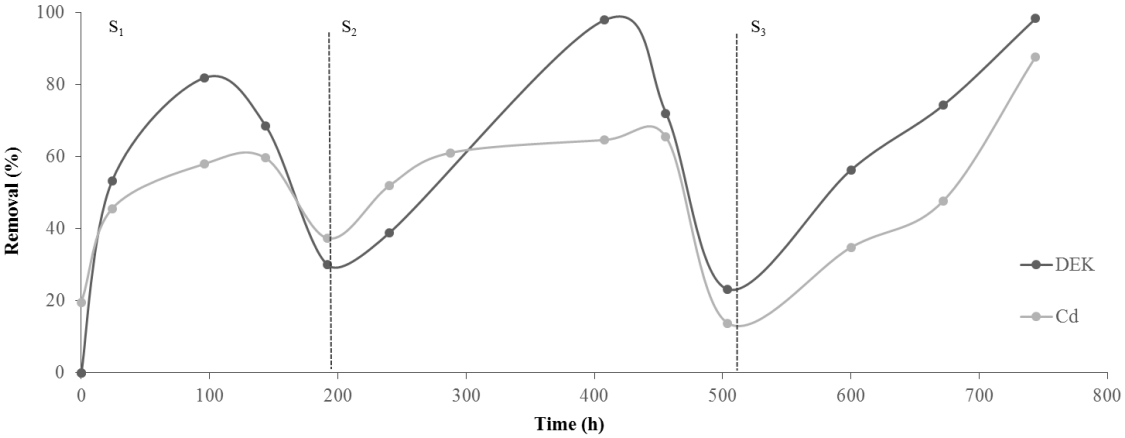

Figure 6.3. Removal performance (%) by a *Streptococcus equisimilis* biofilm supported on vermiculite for diethylketone (7.5 g/L) and Cd^{2+} (100 mg/L), at pilot plant scale.

Table 6.2. Biosorption performance of the bioreactor column for diethylketone (7.5 g/L) and for Cd^{2+} or Ni^{2+} (100 mg/L).

Maximum biosorption efficiency (%)					
Time (h)	**DEK**	**Cd^{2+}**	**Time (h)**	**DEK**	**Ni^{2+}**
S_1 (0 h – 192 h)	81.830	59.470	S_1 (0 h – 309.5 h)	46.948	33.641
S_2 (192 h – 504h)	97.854	65.266	S_2 (309.5 h – 767.5 h)	50.250	57.612
S_3 (504 h – 744 h)	98.236	87.640	S_3 (767.5 h – 1199.5 h)	50.770	38.498
-	-	-	S_4 (1199.5 h – 1942 h)	64.743	51.370
-	-	-	S_4 - end (1942 h – 2374 h)	87.310	67.819

These results may be explained because diethylketone can either be entrapped by the biofilm or by the vermiculite, but it can also suffer biodegradation by the biofilm. Meena et al. (2005) studied the removal of several heavy metals from aqueous solutions using carbon aerogel as an adsorbent. These authors obtained Cd removal percentages of about 65 %, 72 %, 80 % and 95 % for carbon aerogel adsorbent doses of 5 g/L, 8 g/L, 10 g/L and 12 g/L respectively and an initial concentration of 3 mg/L. Quintelas et al. (2009) studied the removal of Cd, Cr, Fe and Ni from aqueous solutions using a *E. coli* biofilm supported on kaolin and for similar initial concentrations of Cd obtained a

maximum removal percentage of 71.3 %. When comparing the results obtained by these authors, with the results obtained herein it is possible corroborate the good performance and capacity of these systems to simultaneously decontaminate aqueous solutions contaminated with Cd^{2+} and diethylketone.

The pH was found to freely range between 6 and 7, which according to results obtained previously, is within the optimal range for the sorption of these two metals by vermiculite and is close to the optimum pH for the growth of *S. equisimilis* (7.4). This presents a significant advantage since no adjustment of pH is required. At the end of the pilot scale experiments, viability tests were conducted and revealed that *the S. equisimilis* biofilm present biological activity, which is an important advantage in the treatment of wastewater using microorganisms, since they the microbial culture resistance allows not only the continuous removal of the pollutants (organic or mineral) due to the biological active and/or inactive mechanisms, which results in the unsaturation on the biomass biodegradation and sorption capacity.

Breakthrough Curves Modelling

Predicted and experimental breakthrough curves are shown in Figure 6.4 and all the calculated parameters are shown in Table 6.3.

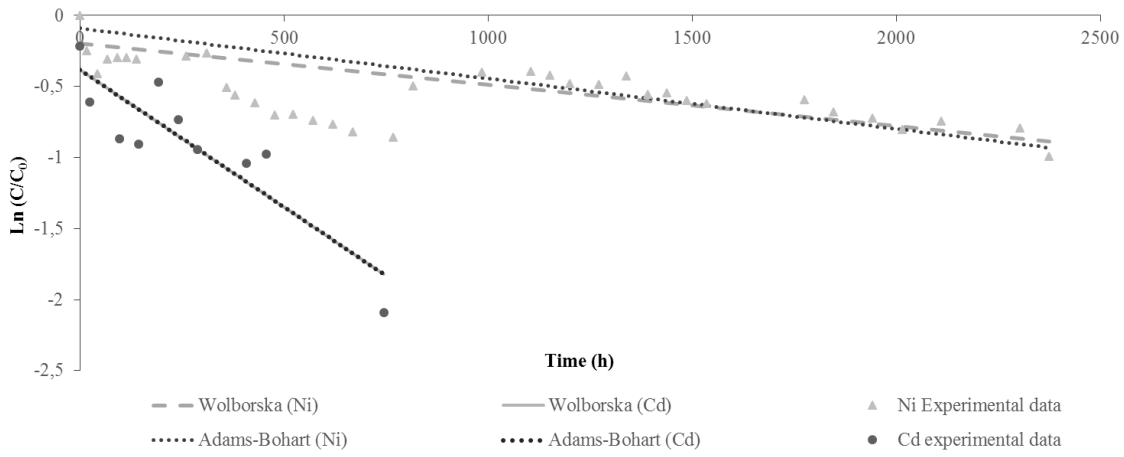

Figure 6.4. Predicted and experimental breakthrough curves for Cd^{2+} and Ni^{2} at pilot-scale.

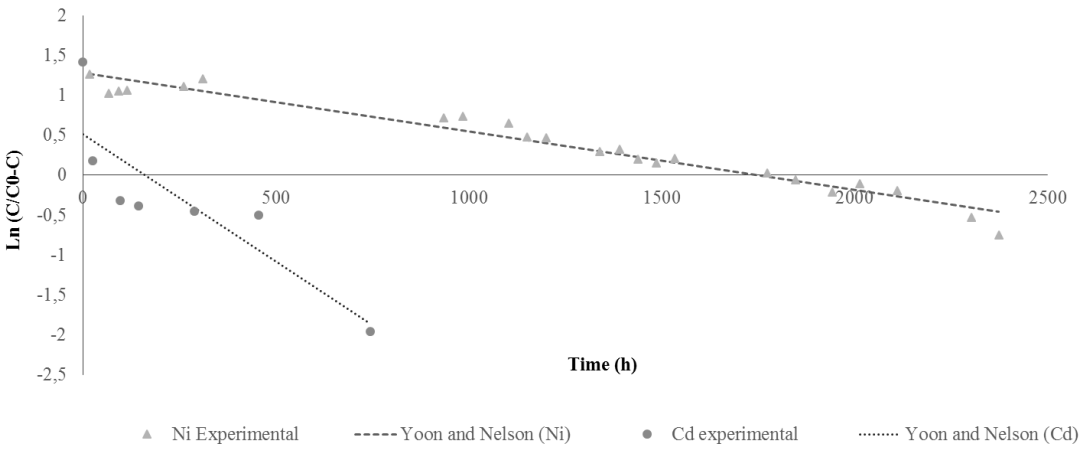

Figure 6.4. Predicted and experimental breakthrough curves for Cd^{2+} and Ni^{2} at pilot-scale (cont.).

The results obtained for diethylketone are properly described by any of the models employed (R^2 < 0.750, data not shown). The experimental results obtained for Cd^{2+} are best described by the Adams-Bohart model (R^2 > 0.800) and the predicted k_{AB} values for Cd^{2+} are presented in Table 6.3.

Table 6.3. Breakthrough parameters obtained for the pilot-scale experiments.

Metal	Adams-Bohart			Wolborska			Wolborska	
	k_{AB} (L/mgh)	N_0 (mg/L)	R^2	β_o (h^{-1})	R^2	k_{YN} (h^{-1})	τ (h)	R^2
Cd^{2+}	9.953e-5	1.906	0.809	-1.446e-3	0.784	-3.189e-3	160	0.740
Ni^{2+}	-1.186e-3	1.429	0.907	6.420e-5	0.850	7.34e-4	1751	0.955

6.3.3| Biodegradation of Diethylketone and Biosorption Ni^{2+} by a Biofilm Supported in Vermiculite in Open Systems – Pilot Scale Experiments

It is possible to observe in Figure 6.5 that the removal of diethylketone is continuous and tends to increase through time (Table 6.2), whereas the percentage of Ni^{2+} sorbed, despite increasing after replacing the solution S_3 (composed by 7.5 g/L of diethylketone and 100 mg/L of Ni^{2+}) with solution

S_4 (composed 7.5 g/L of diethylketone), its sorption efficiency is lower. The decrease on Ni^{2+} sorption may be explained by the saturation of the active presents present on the biomass surface, not only by the addition of diethylketone, but also by the continuous formation of by-products, such as methyl acetate and ethyl acetate (Costa et al. 2014), which may be used also as carbon sources or sorbed by the cells, competing therefore with Ni^{2+}. The maximum removal percentages and uptake values obtained for diethylketone were respectively 87.3 % and 379.0 mg/g, whereas for Ni^{2+} the maximum removal percentages and uptake values achieved were 67.8 % and 3.9 mg/g.

It is observable that diethylketone uptake increases continuously through time, probably as a result from the combined action of biodegradation and biosorption processes. Ni^{2+} uptake also increases continuously through time, and this may be explained by the conjugation of sorption processes, realized both by the bacteria and by the vermiculite, with Ni^{2+} continuous bioaccumulation by the bacteria, whose growth increases through time. Meena et al. (2005) performed different assays on the removal of Ni^{2+}, among other metals, from aqueous solutions using different masses of carbon aerogel as adsorbent.

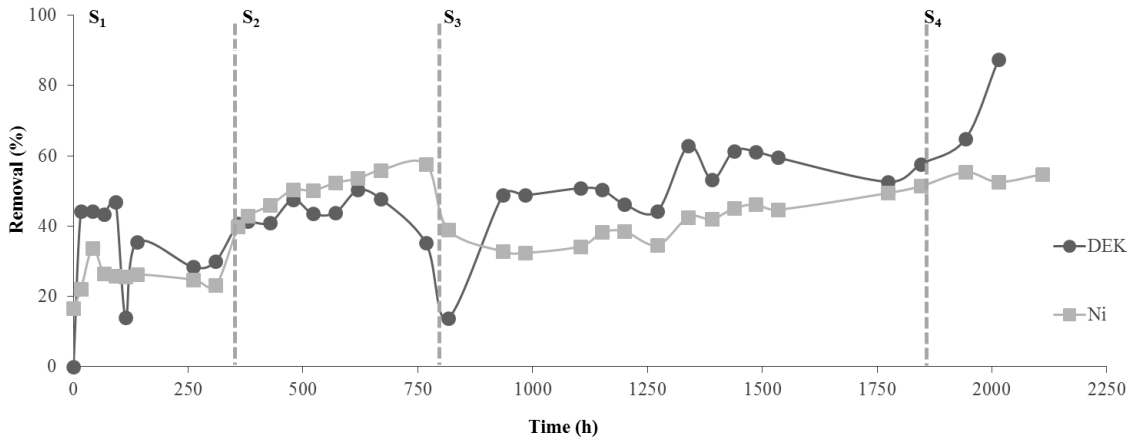

Figure 6.5. Removal percentage of diethylketone and Ni^{2+} at pilot plant scale by a biofilm of *S. equisimilis* supported into vermiculite. S_1 – Solution with Ni^{2+} (100 mg/L) and diethylketone (7.5 g/L); S_2 – replacement of the solution S_1 for a fresh, similar one; S_3 – replacement of the solution S_2 for a fresh, similar one; S_4 – addition of diethylketone (7.5 g/L) to the solution S_3.

These authors obtained Ni^{2+} removal percentages of 50 %, 60 %, 65 % and 80 % for adsorbent masses of 5 g/L, 8 g/L, 10 g/L and 12 g/L, respectively, and an initial concentration of Ni^{2+}equal to 3 mg/L. Comparing these results with those described herein, it is possible to infer that apart from the higher removal percentages, the initial concentration of Ni^{2+} is also superior (150 fold), which reveals and corroborate the good performance and capacity of this system to decontaminate Ni^{2+} and diethylketone aqueous solutions.

The pH ranged between 6 and 7, which as mentioned above is in the optimal pH range for the sorption of the two metals by vermiculite and close to the optimum pH for the growth of the biofilm (7.4).

After exposure to S_1, S_2, S_3 and S_4 solutions the column was washed out and different samples of supported biofilm were inoculated in Petri dishes containing fresh culture medium. The growth of *S. equisimilis* revealed to be fast and may be related to the fact that when in the form of biofilm, *S. equisimilis* developed accessible pathways for the substrate and protection mechanisms against hazardous compounds due to the development of a polymeric matrix that acts as a diffusion barrier, increasing the resistance of the cells against toxic substances. This is an important advantage in the treatment of wastewater using microorganisms.

Breakthrough Curves Modelling

Predicted and experimental breakthrough curves are shown in Figure 6.4 and all the calculated parameters are shown in Table 6.3. The results obtained for diethylketone are well described by any of the models employed ($R^2 < 0.750$, data not shown). The experimental results obtained for Ni^{2+} are best described by the Yoon and Nelson model ($R^2 > 0.950$) and the predicted τ values for Ni^{2+} are presented in Table 6.3.

6.3.4| FTIR, XRD and SEM Analyses

FTIR spectra of unloaded and loaded vermiculite with diethylketone and of *S. equisimilis* biomass in suspension and supported, eventually loaded with diethylketone and Cd^{2+}or Ni^{2+}, in the range of 500

cm^{-1} to 4000 cm^{-1} were taken to confirm the presence of functional groups that are usually responsible for the sorption processes and are shown in Figure 6.6.

Vermiculite shows a number of sorption peaks, reflecting the complex nature of the mineral clays. The band at 1000 cm^{-1} of the unloaded vermiculite, denotes the Si–O–Si stretching, whereas the band at 1635 cm^{-1} represents the H–O–H in absorbed water bending (Covelo et al. 2007) and the band at 3400 cm^{-1} represents the OH functional group stretching vibration (Comte et al. 2006). Some of these band signals were also identified by several other authors (Omoike and Chorover, 2004; Eboigboduin and Biggs, 2008) on clays and were found to correspond to surface functional groups responsible for the sorption of hazardous compounds (Van der Mei et al. 1996; Volesky, 2007). Vermiculite shows a number of sorption peaks, reflecting the complex nature of the mineral clays. The band at 1000 cm^{-1} of the unloaded vermiculite, denotes the Si–O–Si stretching, whereas the band at 1635 cm^{-1} represents the H–O–H in absorbed water bending (Covelo et al. 2007) and the band at 3400 cm^{-1} represents the OH functional group stretching vibration (Comte et al. 2006). Some of these band signals were also identified by several other authors (Omoike and Chorover, 2004; Eboigboduin and Biggs, 2008) on clays and were found to correspond to surface functional groups responsible for the sorption of hazardous compounds (Van der Mei et al. 1996; Volesky, 2007).

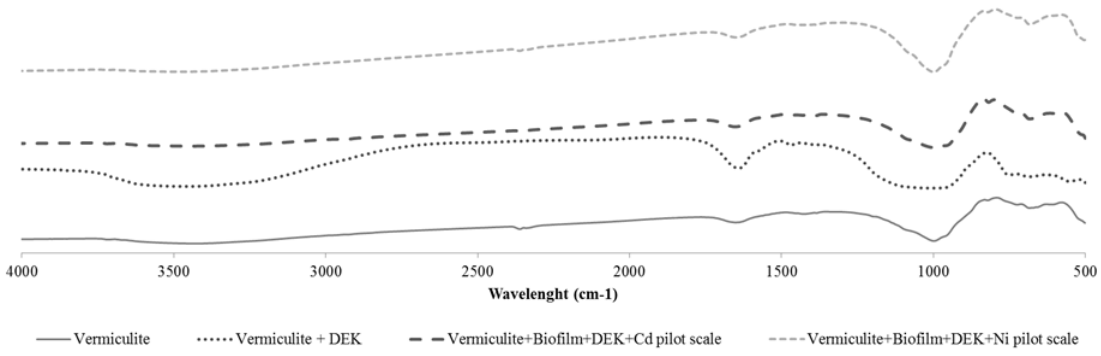

Figure 6.6. FTIR spectra of different samples: vermiculite unloaded, vermiculite exposed to diethylketone (7.5 g/L), *Streptococcus equisimilis* biofilm supported on vermiculite, loaded with diethylketone (7.5g/L) and 100 mg/L of either Cd^{2+}or Ni^{2+}.

These functional groups can interact with the different contaminants used in the present work. Samples of vermiculite exposed to diethylketone and samples of *S. equisimilis* biofilm exposed to diethylketone (7.5 g/L) and Cd^{2+} or Ni^{2+} (100 mg/L) reveal numerous modifications either on the intensity, on the shape of the peaks and on the disappearance and/or formation of new peaks. After exposure to diethylketone, bands at 1400 cm^{-1} and at 2400 cm^{-1} corresponding respectively to C-H bending (-CH3) and to C≡C and/or C≡N stretching, suffer important changes, specifically the first band that disappeared and the second one presenting higher intensity and different shape. The intensity of the bands detected at 675 cm^{-1}, 1000 cm^{-1}, 1650 cm^{-1}, and 3500 cm^{-1} and corresponding respectively to C-OH stretching vibrations, Si–O–Si stretching, C═O stretching groups and to the hydroxyl functional group stretching vibration (-OH), was found to decrease significantly. All these modifications may be explained by the interaction and involvement of the different functional groups present on the sorbent surface with the functional groups (C═O) of diethylketone. Bands at 2300 cm^{-1} and at 3500 cm^{-1} were found to disappear on the samples analysed containing *S. equisimilis* biofilm supported into vermiculite and exposed to diethylketone and to Cd^{2+} or Ni^{2+}. According to Volesky (2007) the main functional groups responsible for biosorption processes are the imidazole, phosphodiester, amide, sulfonate, hydroxyl, carboxyl, phosphonate, and carbonyl groups. Some of these functional groups (phosphate bands at 1237 cm^{-1} and carbohydrate bands at 1070 cm^{-1} next to hydrocarbon sorption bands in the wavelength region between 3000 cm^{-1} and 2800 cm^{-1}) (Van der Mei et al. 1996) are present on the surface of *Streptococcus* sp. and are responsible for the biosorption and biodegradation of hazardous substances like diethylketone (Costa et al. 2014).

The XRD patterns of different samples (unloaded and loaded vermiculite with diethylketone, and *S. equisimilis* biomass in suspension and supported, eventually loaded with diethylketone and Cd^{2+}or Ni^{2+} were recorded at 2θ range between 5 and 60°C and some representative patterns are presented in Figure 6.7. The sample of unloaded vermiculite and the sample of vermiculite loaded with diethylketone exhibited the typical pattern of clays, with no evident change in the position of the diffraction peaks for clays after exposure to diethylketone. This similarity between the two diffractograms suggests a similar crystallinity of vermiculite before and after being exposed to diethylketone, revealing that no significant structural modification in the vermiculite occurred. Nonetheless, the samples containing *S. equisimilis* biofilm supported into vermiculite exposed either to diethylketone and Cd^{2+} or diethylketone and Ni^{2+} presented several changes not only on the position

of the diffraction peaks but also in their intensity. These changes are an evidence of the extensive actions on the vermiculite structure.

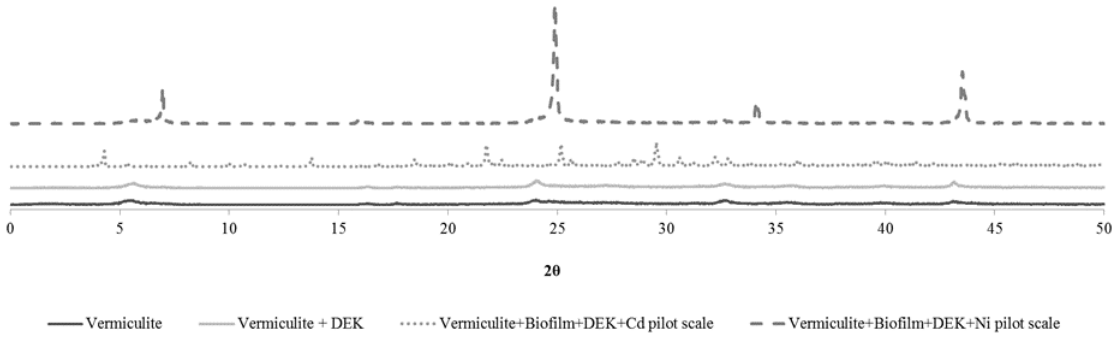

Figure 6.7. XRD patterns of original and recovered vermiculite.

Samples of vermiculite without contact to diethylketone, Cd^{2+} and Ni^{2+} and samples containing *S. equisimilis* biofilm supported in vermiculite, were analysed by SEM. SEM analyses confirm the exposure of vermiculite to diethylketone, Cd^{2+} and Ni^{2+} that makes the vermiculite surface more glazed and polished, with broken and worn leaves and the presence of a well-developed biofilm (Figure 6.8).

Numerous white incrustations were observable on the surface of the sorbent, which according to Sharma et al. (2008) represent the binding of the metal ions to the surface of biomass and are a proof of the biosorption of the metal by the biofilm. Analogous evidences were also found in previous works conducted by Quintelas et al. (2011).

The biofilm formation and development was evident, as well as the formation of some uncharacterized composite that remained attached to the column and presented a white color (Figure 6.9).

a) **b)**

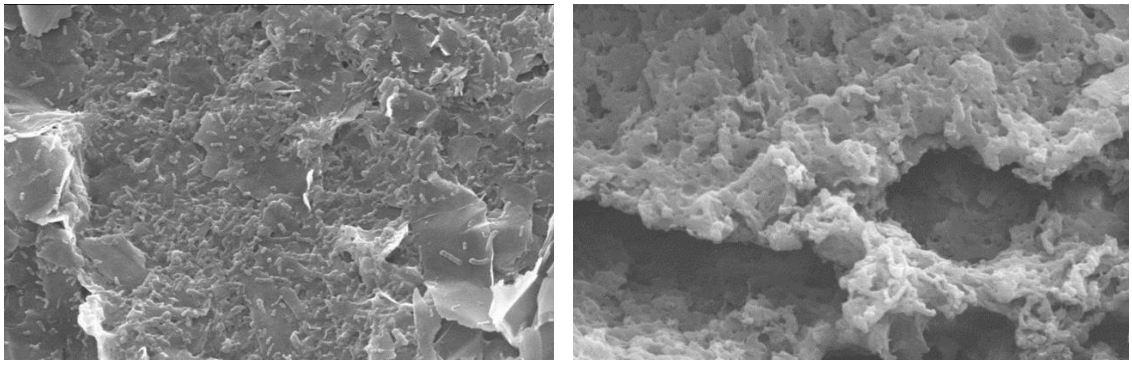

Figure 6.8. SEM images of *Streptococcus equisimilis* supported on vermiculite (700 g) and exposed to diethylketone (7.5g/L) and **a)** 100 mg/L of Cd^{2} for 744 hours, with an amplification of 3000x; **b)** 100 mg/L of Ni^{2} for 2374 hours, with an amplification of 3000x;

a) **b)** **c)**

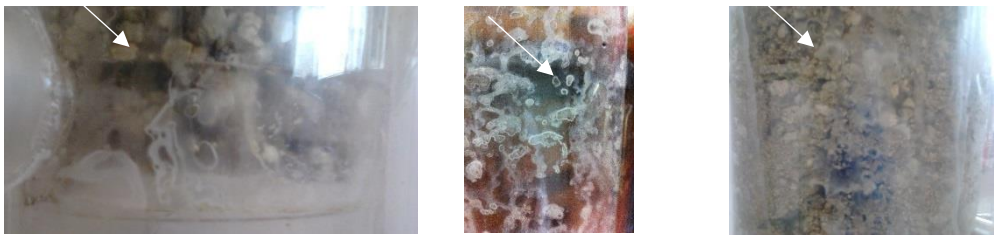

Figure 6.9. Evidences of *S. equisimilis* biofilm formation and the development of a white and rigid composite that remained attached to the column and presented a white color (white arrows) in the pilot-scale systems when using the pollutants **a)** diethylketone (7.5 g/L) and Ni^{2+} (100 mg/L) after 8 days of operation; **b)** diethylketone (7.5 g/L) and Ni^{2+} (100 mg/L) at the end of the experiments (2374 hours of operation) and **c)** diethylketone (7.5 g/L) and Cd^{+} (100 mg/L) at the end of the experiments (744 hours of operation).

Although this white and rigid composite was analysed by SEM and XRD it was not possible to conclude until the present time its composition, but it is the authors' opinion that it may correspond to exopolysaccharides produced by the biofilm, when exposed to both pollutants in order to control the pollutant diffusion rate into the biofilm.

6.4| CONCLUSIONS

Although the maximum sorption percentages for $Cd^{2+}$and Ni^{2+} were achieved at pH 8 for 4 g of vermiculite, the optimal pH was set between pH 6 and pH 7 due to the optimum pH for the growth of *S. equisimilis*. The pilot scale assays have proven the system to be able to remove efficiently and continuously sorbates from binary solutions containing high concentrations of diethylketone and heavy metals (Cd^{2+}or Ni^{2+}) without adjusting the pH. The experiments conducted at pilot scale demonstrated the excellent capacity of bacteria and clay joint system to simultaneously biodegrade diethylketone and biosorb Cd^{2+}or Ni^{2+}. The removal percentage and the uptake increase through time, even after replacing the initial solution by new solutions. The results achieved for Cd^{2+} and Ni^{2+} were found to be best described, respectively by the Adams-Bohart model and Yoon and Nelson model. The FTIR and SEM analyses allowed to prove the existence of a well and established biofilm, with functional groups recognized as responsible for the sorption of hazardous substances. The XRD analyses demonstrated that the exposure of vermiculite (with or without biofilm) to diethylketone and Cd^{2+} or Ni^{2+} alters significantly the structure of vermiculite.

REFERENCES

Ahmed S., Chughtai S., Keane M.A. 1998. The removal of cadmium and lead from aqueous solution by ion exchange with Na-Y zeolites. Separation and Purification Technology 13: 57-64.

Amor L., Kennes C., Veiga M.C. 2001. Kinetics of inhibition in the biodegradation of monoaromatic hydrocarbons in presence of heavy metals. Bioresource Technology 72: 181-185.

Araújo M.M., Teixeira J.A. 1997. Trivalent chromium sorption on alginate beads. International Biodeterioration & Biodegradation 40: 63-74

Azeez L., Adeoye M.D., Lawal A.T., Idris Z.A., Majolagbe T.A., Agbaogun B.K.O., Olaogur M.A. 2013. Assessment of volatile organic compounds and heavy metals concentrations in some Nigerian-made cosmetics. Analytical Chemistry: An Indian Journal 12: 443-483.

Badawy N.A., El-Bayaa A.A., Abd AlKhalik E. 2010. Vermiculite as an exchanger for copper(II) and Cr(III) ions kinetic studies. Ionics 16. 733-739.

Bhuvaneshwari S., Sivasubramanian V. 2014. Equilibrium, Kinetics, and Breakthrough Studies for Adsorption of Cr(VI) on Chitosan. Chemical Engineering Communications 201: 834-854.

Bohart G.S., Adams E.Q. 1920. Some aspects of the behaviour of charcoal with respect to chlorine. Journal of the American Chemical Society 42. 523-529

Brunner W., Focht D.D. 1984. Deterministic three-half-order kinetic model for microbial degradation of added carbon substrates in soil. Applied and Environmental Microbiology 47: 167-172.

Çelekli A., Bozkurt H. 2011. Bio-sorption of cadmium and nickel ions using *Spirulina platensis*: Kinetic and equilibrium studies. Desalination 275: 141-147.

Chopra A.K., Pathak C. 2010. Biosorption technology for removal of metallic pollutants – An overview. Journal of Applied and Natural Science 2: 318-329.

Comte S., Guibaud G., Baudu M. 2006. Biosoprtion properties of extracellular polymeric substances (EPS) resulting from activated sludge according to their type: soluble or bound. Process Biochemistry 41: 815-823.

Costa F., Neto M., Nicolau A., Tavares T. 2015. Biodegradation of Diethylketone by *Penicillium* sp. and *Alternaria* sp. – A Comparative Study Biodegradation of Diethylketone by Fungi. Current Biochemical Engineering 2. 81-89.

Costa F., Quintelas C., Tavares T. 2012. Kinetics of biodegradation of diethylketone by *Arthrobacter viscosus*. Biodegradation 23. 81-92.

Costa F., Quintelas C., Tavares T. 2014. An approach to the metabolic degradation of diethylketone (DEK) by *Streptococcus equisimilis*: Effect of DEK on the growth, biodegradation kinetics and efficiency. Ecological Engineering 70: 183-188.

Costa F., Tavares T. 2016a. Biosorption of nickel and cadmium in the presence of diethylketone by a *Streptococcus equisimilis* biofilm supported on vermiculite. (submitted).

Costa F., Tavares T. 2016b. Bioremoval of Ni and Cd in the presence of diethylketone by fungi and by bacteria – A comparative study. (submitted).

Covelo E.F., Vega F.A., Andrade M.L. 2007. Competitive sorption and desorption of heavy metals by individual soil components. Journal of Hazardous Materials 140. 308-315.

Dbson R.S., Burgess J.E. 2007. Biological treatment of precious metal refinery wastewater: A review. Minerals Engineering 20. 519-532.

Eboigboduin K.E., Biggs C.A. 2008. Characterization of the extracellular polymeric substances produced by Escheria coli using infrared spectroscopic, proteomic and aggregation studies. Biomacromolecules 9: 686-695.

Espinozo E., Escudero R., Tavera F.J. 2012. Waste water Treatment by Precipitating Copper, Lead and Nickel Species. Research Journal of Recent Sciences 1: 1-6.

Fonseca B., Maio H., Quintelas C., Teixeira A., Tavares T.2009. Retention of Cr(VI) and Pb(II) on a loamy sand soil Kinetics, equilibria and breakthrough. Chemical Engineering Journal 152: 212-219.

Hadi P., Barford J., McKay G. 2013. Synergistic effect in the simultaneous removal of binary cobalt-nickel heavy metals from effluents by a novel e-waste-derived material. Chemical Engineering Journal 228: 140-146.

Khamis M., Jumean F., Abdo N. 2009. Speciation and removal of chromium from aqueous solution by white, yellow and red EUA sand. Journal of Hazardous Materials 169: 948–952.

Kishore G., Sree P., Krishna D. 2013. Industrial wastes as adsorbents for the removal of chromium from waste water: A review. International Journal of Chemical Science 11: 1371-1384.

Lam K-Y., Davidson D.F., Hanson R.K. 2012. High-Temperature Measurements of the Reactions of OH with a Series of Ketones: Acetone, 2-Butanone, 3-Pentanone, and 2-Pentanone. Journal of Physical Chemistry A 116: 5549-5559.

Meena A.K., Mishra G.K., Rai P.K., Rajagopal C., Naga P.N. 2005. Removal of heavy metals from aqueous solutiOns using carbon aerogel as an adsorbent. Journal of Hazardous Materials 122: 161-70.

Merrikhpour H., Jalali M. 2013. Sorption processes of natural Iranian bentonite exchanged with Cd^{2+}, Cu^{2+}, Ni^{2+}, and Pb^{2+} cations, Chemical Engineering Communications 200: 1645-1665.

Murthy S., Bali G., Sarangi S.K. 2012. Biosorption of Lead by Bacillus cereus Isolated from Industrial Effluents. British Biotechnology Journal 2: 73-84.

Ogbodu R.O., Omorogie M.O., Unuabonah E., Babalola J.O. Biosorption of heavy metals from aqueous solutions by *Parkia biglobosa* biomass: Equilibrium, kinetics, and thermodynamic studies. Environmental Process &. Sustainable Energy 34: 1694-1704.

Omoike A., Chorover J. 2004. Spectroscopy study of extracellular polymeric substances from *Bacillus subtillis*: aqueous chemistry and adsorption effects. Biomacromolecules 5: 1219-1230.

Plazinski W., Dziuba J., Rudzinski W. 2013. Modeling of sorption kinetics: the pseudo-second order equation and the sorbate intraparticle diffusivity. Adsorption 19. 1055-1064.

Qin B., Luo H., Liu G., Zhang R., Chen S., Hou Y., Luo Y. 2012. Nickel ion removal from wastewater using the microbial electrolysis cell. Bioresource Technology 121: 458-461.

Quintelas C., Costa F., Tavares T.2012. Bioremoval of diethylketone by the synergistic combination of microorganisms and clays: Uptake, removal and kinetic studies. Environmental Science and Pollution Research 20: 1374-1383.

Quintelas C., Figueiredo H., Tavares T. 2011. The effect of clay treatment on remediation of diethylketone contaminated wastewater: Uptake, equilibrium and kinetic studies. Journal of Hazardous Materials 186: 1241-1248.

Raghuvanshi S., Babu B.V. 2010. Biodegradation kinetics of methyl iso-butyl ketone by acclimated mixed culture. Biodegradation 21: 31-42

Saravanan P., Pakshirajan K., Saha P. Batch growth kinetics of an indigenous mixed microbial culture utilizing *m*-cresol as the sole carbon source. Journal of Hazardous Materials 162: 476-481.

Sharma M., Kaushik A., Somvir B.K., Kamra A. 2008. Sequestration of chromium by exopolysaccharides of Nostoc and Gloeocapsa from dilute aqueous solutions. Journal of Hazardous Materials 157: 315–318.

Tam N.F.Y., Wong Y.S., Wong M.H. 1989. Effects of acidity on acute toxicity of aluminium-waste and aluminium-contaminated soil. Hydrobiology 188/189: 385-395.

Van der Mei H.C., Naumann D., Busscher H.J. 1996. Grouping of Streptococcus mitis strains grown on different growth media by FT-IR. Infrared Physics & Technology 37: 561–564.

Volesky B. 2007. Biosorption and me. Water Research 41: 4017-1029.

Wolborska A. 1989. Adsorption on activated carbon of *p*-nitrophenol from aqueous solution. *Water Research* 23: 85–91.

Yin Y., Hu Y., Xiong F. 2011. Sorption of Cu(II) and Cd(II) by extracellular polymeric substances (EPS) from *Aspergillus fumigates*. International Biodeterioration & Biodegradation 65: 1012-1018.

Yoon Y.H., Nelson J.H. 1984. Application of gas adsorption kinetics II. A theoretical model for respirator cartridge service life. American Industrial Hygiene Association Journal 45: 509-516

CHAPTER 7

Sorption studies of diethylketone in the presence of Al^{3+}, Cd^{2+}, Ni^{2+} and Mn^{2+}, from lab-scale to pilot scale: kinetics and equilibrium modeling

This chapter focuses on assessing the ability of a *Streptococcus equisimilis* biofilm supported in vermiculite to biodegrade diethylketone, in the presence of different metals (Al^{3+}, Cd^{2+}, Ni^{2+} and Mn^{2+}), at lab and pilot scale. These experiments aim to mimic the microbial behaviour of *S. equisimilis* when exposed to complex solutions, such as real effluents The results obtained were characterized by diffraction analysis (XRD), chemical analysis (ICP-OES and GC), spectroscopic method (FTIR) and microscopic analyses (SEM). At lab and pilot scale it was proven the excellent capacity of the *S. equisimilis* and vermiculite joint-system to biodegrade high concentrations of diethylketone in the presence of high concentrations of Al^{3+}, Cd^{2+}, Ni^{2+} and Mn^{2+}. With the exception Al^{3+}, the uptake for all metals employed increased as the initial concentration of each metal in the mixed solution increased.

This chapter is based on the following submitted publication: Costa F., Tavares T. 2016. Sorption studies of diethylketone in the presence of Al^{3+}, Cd^{2+}, Ni^{2+} and Mn^{2+}, from lab-scale to pilot scale: kinetics and equilibrium modelling.

7.1| INTRODUCTION

One of the environment subjects of greatest importance and concern relates to the pollution of aquatic and terrestrial systems with metals and volatile organic compounds and its consequences on life and ecology (Ogbodu et al. 2015). This is particularly challenging since in addition of not being biodegradable, metals tend to be accumulate in living organisms and in living tissues via food chain, generating numerous diseases and health disorders (Ibrahim et al. 2013). Metals can enhance and/or increase the toxic and inhibitory effects on the microbial growth and can enter the environment through aqueous effluents from different industries such as dyes, fertilizers, steels, electronic devices manufacturing, pesticides, printing, oil refining, paints, pulp and paper (Ogbodu et al. 2015) jewellery, textile, batteries, petrochemical and fine chemistry, mining, tanneries, chemicals production, (Ahmed et al. 1998) and health care products (Azeez et al. 2013). Toxic metals such as aluminium (Al^{3+}), cadmium (Cd^{2+}), nickel (Ni^{2+}) and manganese (Mn^{2+}) are among the most common metal pollutants present in soil and water (Tam et al. 1989). Although toxic when present in high concentrations, metals such as nickel and manganese are required for the functioning of several cellular enzymes (co-factors, also known as essential metals or micro-nutrients) such as urease and hydrogenase, manganese superoxide dismutase, pyruvate carboxylase and for the activation of others enzymes such as kinases, decarboxylases, transferases and hydrolases.

Ni release into the environment can occur from biogenic sources such as windblown, dust and volcanic eruptions. However, the majority of its release comes from the burning of residual and fuel oils from metal refining, municipal incineration, steel production and coal production (Bennet 1984). Ni is considered a carcinogenic element, able to cause several kinds of acute and chronic health disorders such as skin dermatitis, chest pain, lungs and kidney damage, nausea, pulmonary fibrosis, renal edema, cyanosis and extreme weakness (Suazo-Madrid et al. 2011). Manganese and manganese compounds are employed mainly in the manufacture of steel and iron alloys, batteries, glass and fireworks. They are also used as oxidants for cleaning, bleaching and disinfection purposes and in fertilizers, varnish and fungicides (ATSDR 2000).

Exposure to manganese may occur either orally or by inhalation and can onset serious toxic responses. Usually, the initial symptoms are headache, disorientation, anxiety, insomnia, memory loss and lethargy. With continued exposure, these symptoms can develop and lead to motor

disturbances, tremors and difficulty in walking (hydratechnm.org). Aluminium and cadmium on the other hand do, not present any biological activity or function (nonessential metals).

Aluminium can be used in an extensive variety of industries (aircraft, automotive and construction, as a structural material), products (cooking utensils, food packaging, metal alloys, pigments, paints, heat resistant fibbers, pharmaceutical and personal care products) and compounds (food additives, antacids, antiperspirants) (ATSDR 1992). Exposure to aluminium may affect particularly people with kidney disorders, since they have less capacity to remove this metal from their body. Although the health effects of aluminium on humans are not definitive and perceived, the Joint Food and Agriculture Organization and the World Health Organization Expert Committee on Food Additives lowered the allowable intake of aluminium in 2006, from 7 mg/Kg body weight to 1 mg/Kg body weight per week (Bondy 2016).

Ccadmium is employed in six major classes: Ni-Cd batteries, cadmium pigments, cadmium stabilizers, cadmium coatings, cadmium alloys and cadmium electronic compounds such as cadmium telluride (CdTe) (http://www.cadmium.org). Exposure to cadmium may affect the action of enzymes, hampering respiration, photosynthesis, transpiration and chlorosis (Ahmed et al. 1998), cause cancer, lead to infertility and promote severe health problems in different organs. Cadmium presents also high mobility in soil, high solubility in water and extreme toxicity, even at low concentration (Ibrahim et al. 2013).

Volatile organic compounds such as ketones are usually released into the atmosphere by biogenic and anthropogenic sources. Diethylketone, also known as 3-pentanone, is naturally produced and released into nature by plants, fruits (http://pubchem.ncbi.nlm.nih.gov/, http://toxnet.nlm.nih.gov/index.html) and produced industrially to be used as solvent or polymer precursor (Lam et al. 2012), as an intermediate in the synthesis of pharmaceuticals, cosmetics, flavors and pesticides (Quintelas et al. 2012). Besides reacting with OH radicals promoting the formation of ozone and other components of the photochemical smog in urban areas (Lam et al. 2012) diethylketone is persistent in water, soil and air and presents high mobility (www.cdc.gov) and ability to form toxic and phototoxic intermediates (Costa et al. 2012). Exposure to diethylketone may cause, according to the Occupational Safety and Health Hazards (OSHA) of United States Department Labor, skin and eyes irritation, coughing and sneezing. Prolonged exposure may cause shortness of breath, tachycardia, faintness, nausea, coma and even death.

There are countless studies on metal and organic solvents removal from wastewater. Techniques such as chemical precipitation, reverse osmosis, ion exchange, adsorption on granular activated carbon (GAC), condensation, thermal degradation, oxidation and incineration (Costa et al. 2015). Studies conducted by numerous authors over the last few years, have demonstrated that biological processes present several advantages over the traditional methods mentioned above. The biological processes present reduced maintenance and operation costs, high efficiency and eco-friendly character since they do not produce solid wastes and nitrogen oxides, which would require a secondary treatment (Costa et al. 2012).

Since some contaminated systems can contain simultaneously metals and volatile organic compounds (Azeez et al, 2013), the studies concerning the decontamination of this kind of systems and its subsequent optimization become of major importance and relevance not only for environment rehabilitation, but also aiming its economics sustainability.

In this study, a joint system was used that combines the properties of clays and microorganisms to enhance the removal of different kind of pollutants from aqueous solutions. This joint system combines the sorption capacity of the clay, providing excellent physical and chemical stability, large specific surface area, high cation exchange capacity (Quintelas et al. 2012) with the ability of the microorganisms to degrade, fix and/or entrap pollutants, due of the presence of several functional groups on the biomass surface (Costa et al. 2012). The main goal of the present work comprises the development of an environment-friendly technology able to treat multicomponent systems, containing diethylketone, aluminium, cadmium, nickel and manganese. Although these two types of pollutants (metals and ketones) appear together in the wastewater of different industries such as metal refining (Dobson and Burges 2007) and paint manufacturing (EPA 1993), the knowledge regarding simultaneous treatment of water containing these pollutants is once again rather scarce.

7.2| MATERIALS AND METHODS

7.2.1| Bacteria Strain and Vermiculite

Streptococcus equisimilis was obtained from the Spanish Type Culture Collection, at the University of Valencia, with the following reference CECT 926. The vermiculite was purchased from Sigma-

Aldrich and presents a BET surface area of 39 m^2/g, an average particle diameter of 8.45 mm and a porosity of 10%. In the present study, the bacterial biofilm was developed and established on the vermiculite.

7.2.2| Culture and Chemicals Properties

Streptococcus equisimilis was grown in sterilized Brain Heart Infusion (Oxoid CM1135) culture medium at 37° C, 150 rpm, for several days. Diethylketone was purchased from Acros Organics (98% pure) and diluted in sterilized distilled water. Individual stock solutions of 1 g/L of aluminium ($Al(OH)_3$, Merck), 1 g/L of nickel ($NiCl_2 \bullet 6H_2O$, Carlo Erba Reagents), 1 g/L of cadmium ($CdSO_4 \bullet 8/3H_2O$, Riedel-de-Haën) and 1 g/L of manganese ($MnSO_4 \bullet H_2O$, Panreac) were prepared by dissolving an accurately weighed amount of metal compound in sterilized distilled and deionized water. The multi-element ICP quality control standard solution was purchased from CHEM Lab (QCS-03) (15E). The range of concentrations of each ion, Al^{3+}, Cd^{2+}, Ni^{2+} and Mn^{2+}, was obtained by dilution of the respective stock solution and varied between 5 mg/L and 100 mg/L.

7.2.3| Lab Scale Experiments – Biosorption in Batch Systems

Erlenmeyer flasks (1 L) containing 0.5 L of sterilized Brain Heart Infusion culture medium, were inoculated with a pure culture of *S. equisimilis* and left to grow in an incubator for 24 hours at 150 rpm and 37 °C (Culture X). After this period, 250 mL of Culture X was transferred to 1 L of a new sterilized Brain Heart Infusion culture medium and left to grow on an incubator for 48 hours at 150 rpm and 37 °C (Culture Y). The lab scale biosorption experiments were conducted in 0.250 L Erlenmeyer flasks containing 0.125 L of sterilized Brain Heart Infusion culture medium, 4 g/L of diethylketone and 5 mg/L to 100 mg/L of Al^{3+}, Cd^{2+}, Ni^{2+} and Mn^{2+}. These Erlenmeyer flasks were inoculated with 10 mL of the culture Y and incubated under orbital shaking (150 rpm) at 37°C for several days. At pre-establish times intervals samples were collected and centrifuged at 1300 rpm (Eppendorf MiniSpin 9056) for 10 minutes. The supernatant was analyzed by ICP-OES and GC-MS in order to quantify respectively the concentration of heavy metals and diethylketone. Two blanks were used. One containing only diethylketone and bacteria, and other containing 4 g/L of

diethylketone and 5 mg/L of Al^{3+}, Cd^{2+}, Ni^{2+} and Mn^{2+}. The first blank was used to assess the growth of the bacteria whereas the second blank assessed the eventual interaction between the different pollutants and the Erlenmeyer's walls. At the end of the experiments, samples were collected and inoculated in Petri dishes in order to confirm the metabolic activity of the bacteria. The pH along the assays was also monitored.

7.2.4| Pilot Scale Experiments – Biosorption in Open Systems

The pilot scale experiments were conducted in a compact polycarbonate acrylic bioreactor of 22.7 L, with an internal diameter of 17 cm and a total height of 100 cm. One third of the bioreactor was filled with vermiculite (700 g). For the biofilm development, a *S. equisimilis* culture was grown in an Erlenmeyer flask (2 L) containing 1 L of Brain Heart Infusion culture medium, previously sterilized at 121°C for 20 minutes. The Erlenmeyer flask was inoculated with *S. equisimilis*, incubated in orbital shaker for 24 hours at 37°C and 150 rpm and capped with cotton stoppers in order to allow a passive aeration. The inoculum culture was transferred to the bioreactor setup and recirculated upwards at a flow rate of 250 mL/min during 5 days in order to allow the biomass to attach to the vermiculite and form a well-developed biofilm. Once the biofilm was formed, the bed was washed out and a 40 L solution containing 100 mg/L of each metal (Al^{3+}, Cd^{2+}, Ni^{2+} and Mn^{2+}) and 7.5 g/L of diethylketone (that acted as carbon source) was continuously pumped upwards through the bioreactor with a constant flow rate of 25 mL/min. Periodically, diethylketone was added to the working solution in order to continuously supply a carbon source to the biofilm and also to infer about its impact on the metals sorption. At pre-established time intervals, samples of the effluent were taken, centrifuged at 1300 rpm (Eppendorf MiniSpin 9056) for 10 minutes and the aqueous phase was analyzed by GC-MS and by ICP-OES in order to assess respectively the concentration of diethylketone and heavy metals through time. At the end, the bioreactor was washed out and samples of the effluent and of the vermiculite were inoculated in Petri dishes with Brain Heart Infusion culture medium, in order to confirm the metabolic activity of the bacteria. The pH was also measured.

7.2.5| Analytical Methods

7.2.5.1| Gas Chromatography (GC)

A GC-MS Varian 4000, equipped with a flame ionization detector (FID), mass spectrometry (MS) and a ZB-WAXplus column (30 m x 0.53 mm x 1.0 µm) was used to determine the concentration of diethylketone in distinct samples. The column was initially held at a temperature 50 °C, then heated at a rate of 3 °C/minute until it reached 100 °C, then held at 100 °C for 4 minutes, heated again at a rate of 40 °C/minute to 150 °C and finally held at 150 °C for 2 minutes. The temperature of the injector and detector were kept at 250 °C. Nitrogen was used as the carrier gas at a flow rate of 4 mL/min and the injections were performed in the split mode with a split ratio of 1:10. The concentration of diethylketone was determined by comparing the areas of the peak of the internal standard (2-methyl-1-butanol) to the areas and retention time of the peaks appearing in the samples taken during the experiments. The retention time for diethylketone and for the internal standard was found to be respectively 5.3 minutes and 11.3 minutes.

7.2.5.2| Inductively Coupled Plasma Optical Emission Spectrometry (ICP-OES)

An ICP-OES (Optima 8000, PerkinElmer) was used to measure the concentration of Al^{3+}, Cd^{2+}, Ni^{2+} and Mn^{2+} through time for the lab and pilot scale experiments. The operating conditions were as follows: 1300 W of RF power, argon plasma flow of 8 L/minute, auxiliary gas flow of 0.2 L/minute, nebulizer gas flow of 0.5 L/minute, axial plasma view and wavelength of 309.271 nm for Al^{3+}, 228.802 nm for Cd^{2+}, 221.648 nm for Ni^{2+} and 257.610 nm for Mn^{2+}. All the calibration solutions were prepared from a multi-element Al^{3+}, Cd^{2+}, Ni^{2+} and Mn^{2+} stock solution with a concentration of 1 g/L for each metal. All the samples were acidified with concentrated nitric acid (HNO_3 69%) and filtered before being analyzed. The instrument response was periodically checked with the multi-element ICP QC standard solution (CHEM LAB) and with a blank (HNO_3 5%).

7.2.5.3| Characterization of Sorbents by FTIR, XRD and SEM Analyses

To identify the functional groups involved in the biosorption of diethylketone, Al^{3+}, Cd^{2+}, Ni^{2+} and Mn^{2+} by the sorbents, an infrared spectra of the sorbents, with and without previous contact with the pollutants, were obtained using a Fourier Transform Infrared Spectrometer (FTIR BOMEM MB 104). For the FTIR analyses, the sorbents were centrifuged and dried for 24 h at 60°C. Then, 10 mg of each sorbent was encapsulated in 100 mg of KBr (Riedel) in order to obtain a translucent sample disk. Background correction for atmospheric air was used for each spectrum. The resolution was 4 cm^{-1} and a minimum of 30 scans was conducted for each spectrum with a range between 500 and 4000 wavenumbers.

The XRD analyses were performed using a Philips PW1710 diffractometer. Scans were taken at room temperature in a 2 range between 5 and 60 ◦ C, using Cu K radiation.

Scanning Electron Microscopy (SEM) of the sorbents with and without previous contact with diethylketone, Al^{3+}, Cd^{2+}, Ni^{2+} and Mn^{2+} was performed on Leica Cambridge S360 to observe any morphological changes on the sorbents surfaces.

7.2.6| Data modelling

7.2.6.1| Sorption Kinetic Models

The phenomena involved in biodegradation and/or biosorption processes are of utmost importance because they provide an understanding of the time dynamics of sorption processes and how they determine the chemical reaction, as well as the mass transfer and diffusion processes. These phenomena can differ significantly from open, semi-closed and closed systems, even when all the remaining conditions are kept equal. For a better understanding of diethylketone, Al^{3+}, Cd^{2+}, Ni^{2+} and Mn^{2+} removal kinetics by *S. equisimilis* (lab scale experiments) and by *S. equisimilis* biofilm supported on vermiculite (pilot scale experiments), the experimental results were fitted by the pseudo-first order and pseudo-second models reported in the literature (Kishore et al. 2013) (see Chapter 2, section 2.2.7.1).

7.2.6.2| Breakthrough Curves Modelling

One of the prerequisites for a successful design of a fixed-bed column system for the removal of organic compounds and/or heavy metals in aqueous solution is the prediction of the concentration–time profile or breakthrough curve. In this study the Adams–Bohart, Wolborska and Yoon and Nelson models were used to describe the breakthrough curves (Yoon and Nelson 1984; Wolborska 1989; Bohart and Adams 1920) (see Chapter 6, section 6.2.5.3).

7.3| RESULTS AND DISCUSSION

7.3.1| Lab Scale Experiments – Biosorption in Batch Systems

In these set of experiments the initial concentration of diethylketone was kept constant (4 g/L), whereas the initial concentration of Al^{3+}, Cd^{2+}, Ni^{2+} and Mn^{2+} has increased from 5 mg/L to 100 mg/L. Percentages of diethylketone biodegradation and/or sorption higher than 95% were reached in 74 h, for the control containing just diethylketone and biomass. The same diethylketone removal percentage was achieved in solutions with initial concentrations of Al^{3+}, Cd^{2+}, Ni^{2+} and Mn^{2+} between 5 mg/L to 40 mg/L in 4 h and in 0.5 h, for initial concentrations of the same ions between 80 mg/L and 100 mg/L, (Figure 7.1). These results suggest that, as the initial concentration of metals increases, the time required to achieve biodegradation and/ or sorption percentages of diethylketone higher than 95 % decreases significantly, meaning that the increase of the initial concentration of the metals accelerates the complete degradation and/ or sorption of diethylketone.

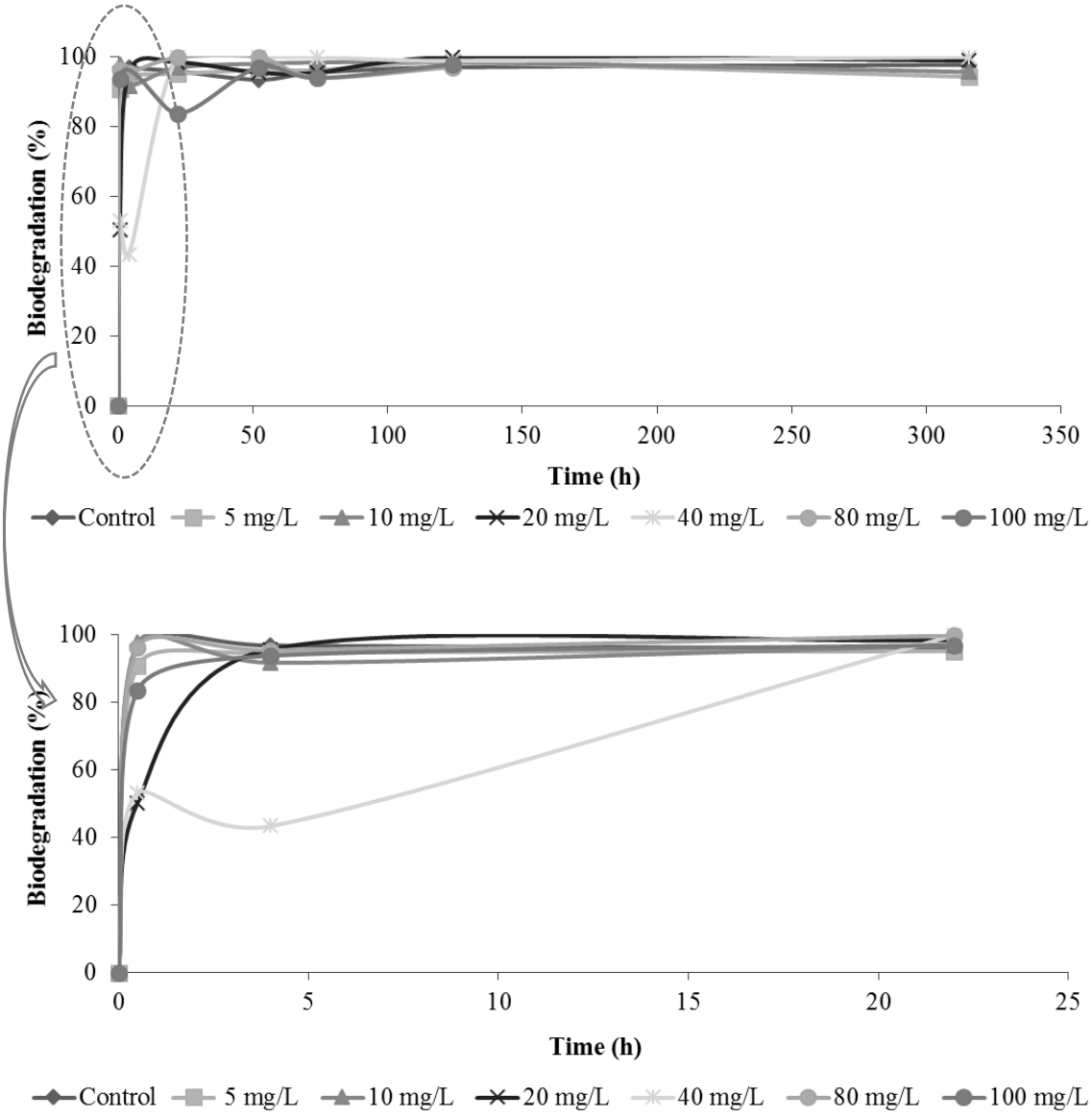

Figure 7.1. Biodegradation efficiency (%) of *Streptococcus equisimilis* for diethylketone (4 g/L) when exposed to different initial concentrations of metal ions, M.I., Al^{3+}, Cd^{2+}, Ni^{2+} and Mn^{2+} (5 mg/L to 100 mg/L).

Complete biodegradation and/ or sorption of diethylketone was obtained for the assays conducted with initial concentrations of metals equal or higher than 20 mg/L. These results may be explained by the fact that the acclimation period obtained is shorter than the ones obtained with smaller concentrations of metal, and therefore the time required by the microbial culture to achieve the same level of performance is smaller (Olaniram et al. 2013). Studies conducted by Dilek et al. (1998) and Gonzalez-Gil et al. (1999) revealed that the presence on Ni^{2+} at low concentrations is not only nontoxic respectively to the microbial growth of the activated sludge and methanogenic sludge, but actually it

enhances the microbial growth rate and metabolic activity. According to Nies (1999), the majority of microorganisms overcome the presence of heavy metals (nonessential and essential metals, at low or high concentrations) by using two different mechanisms of metals uptake. One of the mechanisms is essentially constitutively expressed and driven by the chemiosmotic gradient across the cytoplasmic membrane of the bacteria, being thus a fast and unspecified mechanism. The other mechanism is used only by the microbial culture in specific circumstances (starvation or special metabolic conditions, for example), and uses ATP hydrolysis, as a way of obtaining energy. It is an inducible, very specific and slower mechanism than the first one described herein (Ji and Silver 1995). However, when exposed to high concentrations of metals (nonessential metals included), some microorganisms may develop a metal resistance mechanism, such as intra and extra-cellular sequestration, enzymatic detoxification, exclusion by permeability barrier and active transport efflux pumps, for example, allowing them not only to survive but also to grow in contaminated environments. It is important to highlight that in order to have a toxic or physiological effect, most metals have to enter the cell and to be present at high concentrations. The toxicity of nonessential metals may occur through ligand interactions and/or through the displacement of the essential metals from their native binding sites). The toxicity effect itself (towards the microbial growth and towards the biodegradation of organic pollutant compounds) is dependent on the amount of metal bioavailable rather than the total or even soluble metal concentration present in the system (Olaniran et al. 2013).

The biosorption profiles of Al^{3+}, Cd^{2+}, Ni^{2+} and Mn^{2+} are quite different from each other (Figure 7.2) and from diethylketone.

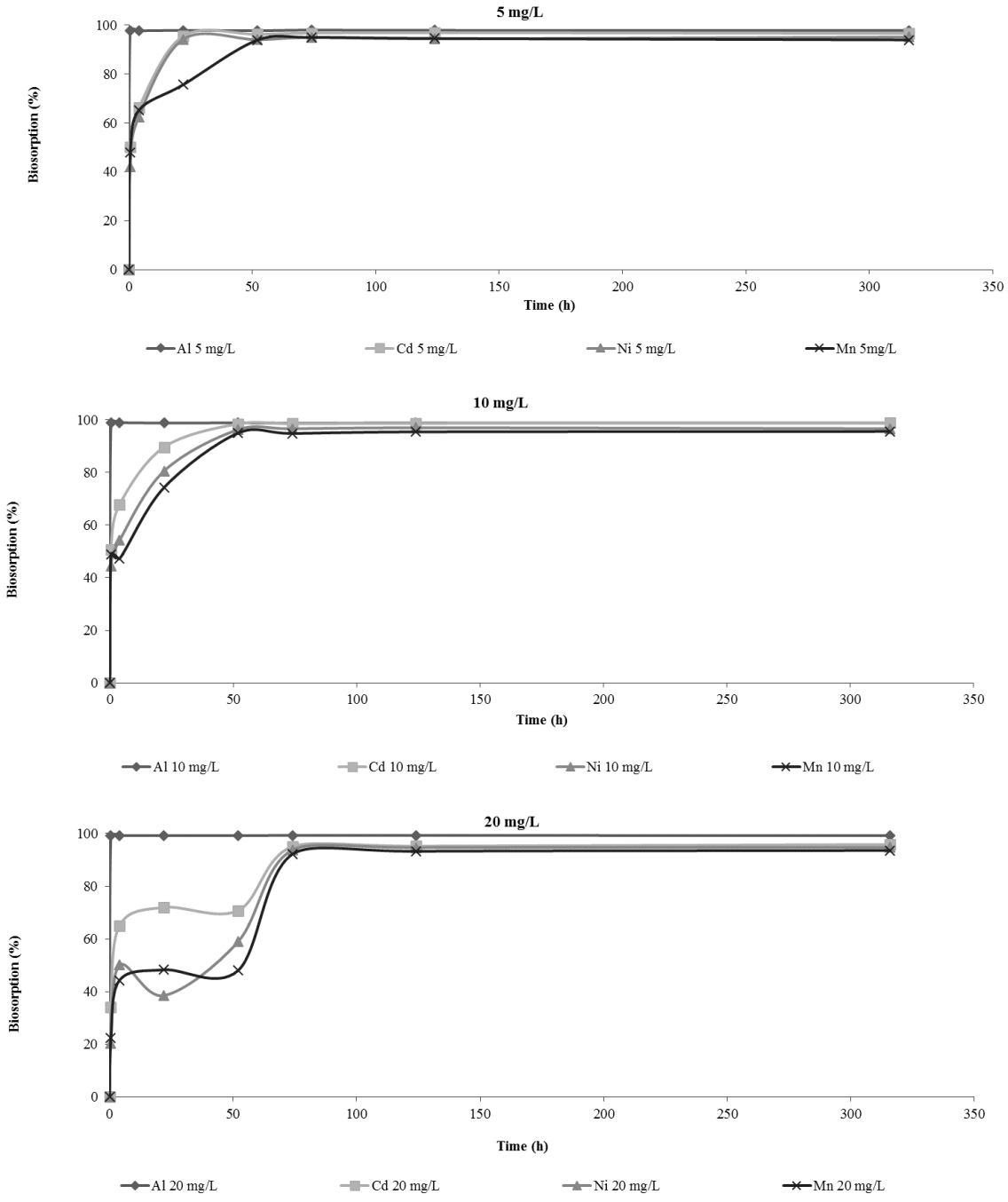

Figure 7.2. Biosorption efficiency (%) of *Streptococcus equisimilis* for Al^{3+}, Cd^{2+}, Ni^{2+} and Mn^{2+} (5 mg/L to 100 mg/L) when exposed to diethylketone (4 g/L).

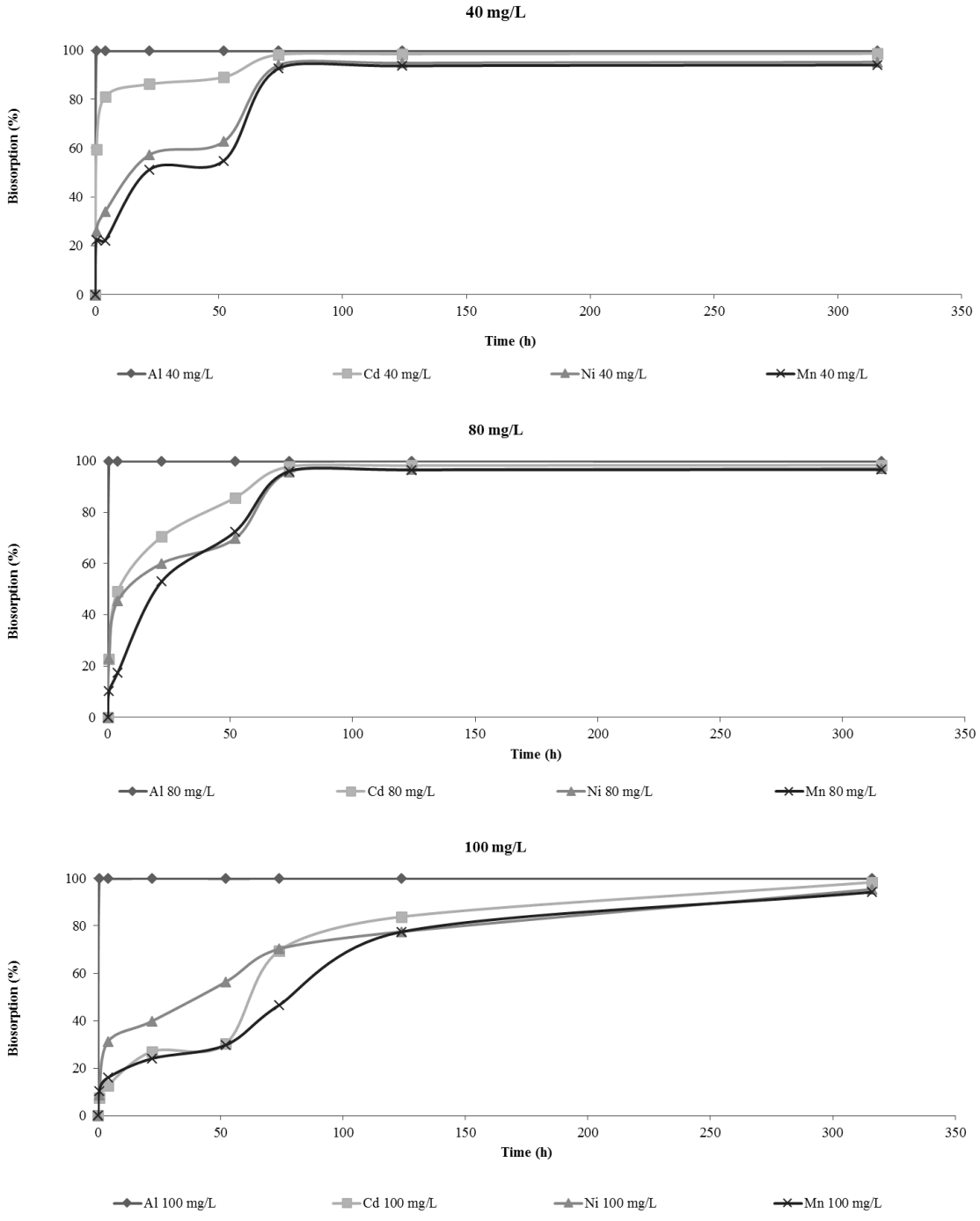

Figure 7.2. Biosorption efficiency (%) of *Streptococcus equisimilis* for Al^{3+}, Cd^{2+}, Ni^{2+} and Mn^{2+} (5 mg/L to 100 mg/L) when exposed to diethylketone (4 g/L) (cont.).

For initial concentrations of Al^{3+}, Cd^{2+}, Ni^{2+} and Mn^{2+} ranging between 5 mg/L and 80 mg/L the biosorption efficiency (%) was found to follow the following sequence $Al^{3+} > Cd^{2+} \geq Ni^{2+} \geq Mn^{2+}$, whereas for the experiments conducted with an initial concentration 100 mg/L of Al^{3+}, Cd^{2+}, Ni^{2+} and Mn^{2+} the biosorption efficiency (%) was found to follow the following sequence $Al^{3+} > Ni^{2+} > Cd^{2+} > Mn^{2+}$. The affinity of microbial culture for a metal can be explained by the affinity between the metal cations and the negative charge of the cellular surface. Considering Pauling electronegativity, Ni^{2+} (1.91 Pauling) has a higher electronegativity than Cd^{2+} (1.69 Pauling), Al (1.61 Pauling) and Mn (1.55 Pauling). Despite their electronegativity and oxidation state, the reduced ionic radius of Al^{3+} and Ni^{2+} enhance their penetration into the surface of the cell membrane, contributing thus to the overall results obtained. It is possible to observe that the essential metals (Ni^{2+}, Mn^{2+}) present lower biosorption performances, which according to the literature is unexpected. This behaviour may be justified with the difference between the relative size of the ionic radius and the active sites of the biomass but also by the fact that many divalent heavy metal cations are structurally very similar, allowing the replacement of some essential cation metals for nonessential ones. In terms of uptake, with the exception of Al^{3+}, all the metals showed an increase of uptake with the increase of the initial concentration of each metal in the mixed solution and similar uptake profiles (Table 7.1). The results obtained with Al^{3+} could be explained by a reduced bioavailability of the metal in solution (Olaniran et al. 2013). The use of mathematical models to describe the dynamics of the sorption processes is very important not only for the design of an operational control of the sorption process, but also because it is very helpful for the scale up and process optimization, allowing the description of the behaviour of the sorption processes operating under different conditions.

Table 7.1. Maximum and minimum uptake for different initial concentrations of Al^{3+}, Cd^{2+}, Ni^{2+} and Mn^{2+} for the lab-scale experiments.

Metal concentration (mg/L)		**5**	**10**	**20**	**40**	**80**	**100**
Al^{3+}	Time (h)	0.74	0.50	0.74	316	124	22
	Maximum uptake (mg/g)	0.97	0.96	0.95	0.96	0.98	0.96
Cd^{2+}	Time (h	124	52	74	74	316	316
	Maximum uptake (mg/g)	1.62	3.2	6.39	13.15	26.24	32.77
Ni^{2+}	Time (h	22	52	74	74	74	316
	Maximum uptake (mg/g)	1.59	3.23	6.32	12.97	25.86	31.79
Mn^{2+}	Time (h	74	52	74	74	316	316
	Maximum uptake (mg/g)	1.58	3.19	6.24	12.53	25.74	31.39

7.3.1.1| Batch Systems Biodegradation and Sorption Kinetic Modelling

The experimental results obtained for all the concentrations and for all the pollutants used in these assays were found to be best described by the pseudo-second order kinetic model (Figure 7.3, Table 7.2).

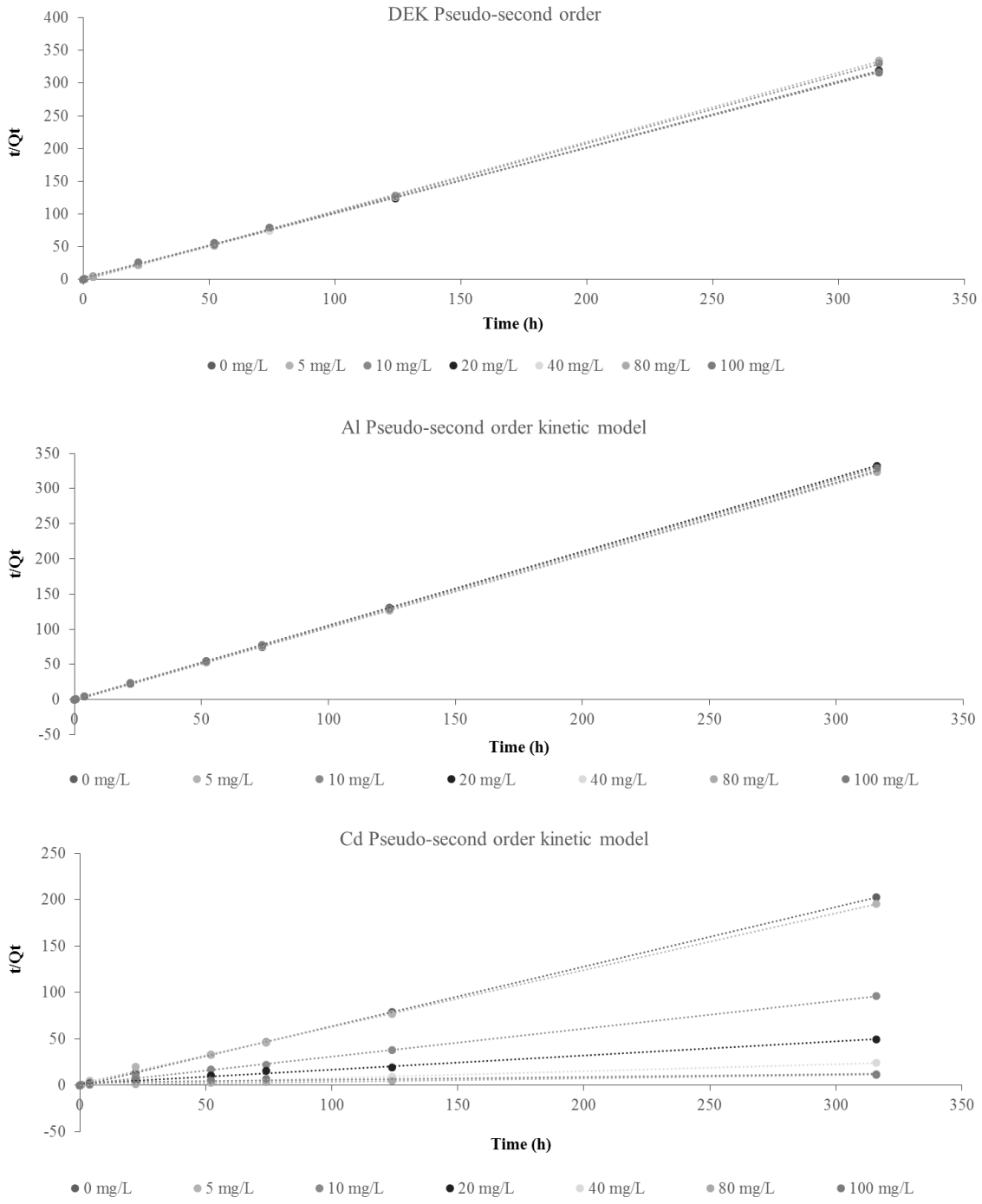

Figure 7.3. Kinetics model for diethylketone (DEK) and aluminium (Al), cadmium (Cd), nickel (Ni) and manganese (Mn) for the biosorption experiments conducted at lab-scale with *Streptococcus equisimilis*, when exposed to diethylketone (4 g/L) and Al^{3+}, Cd^{2+}, Ni^{2+} and Mn^{2+} (5 mg/L to 100 mg/L).

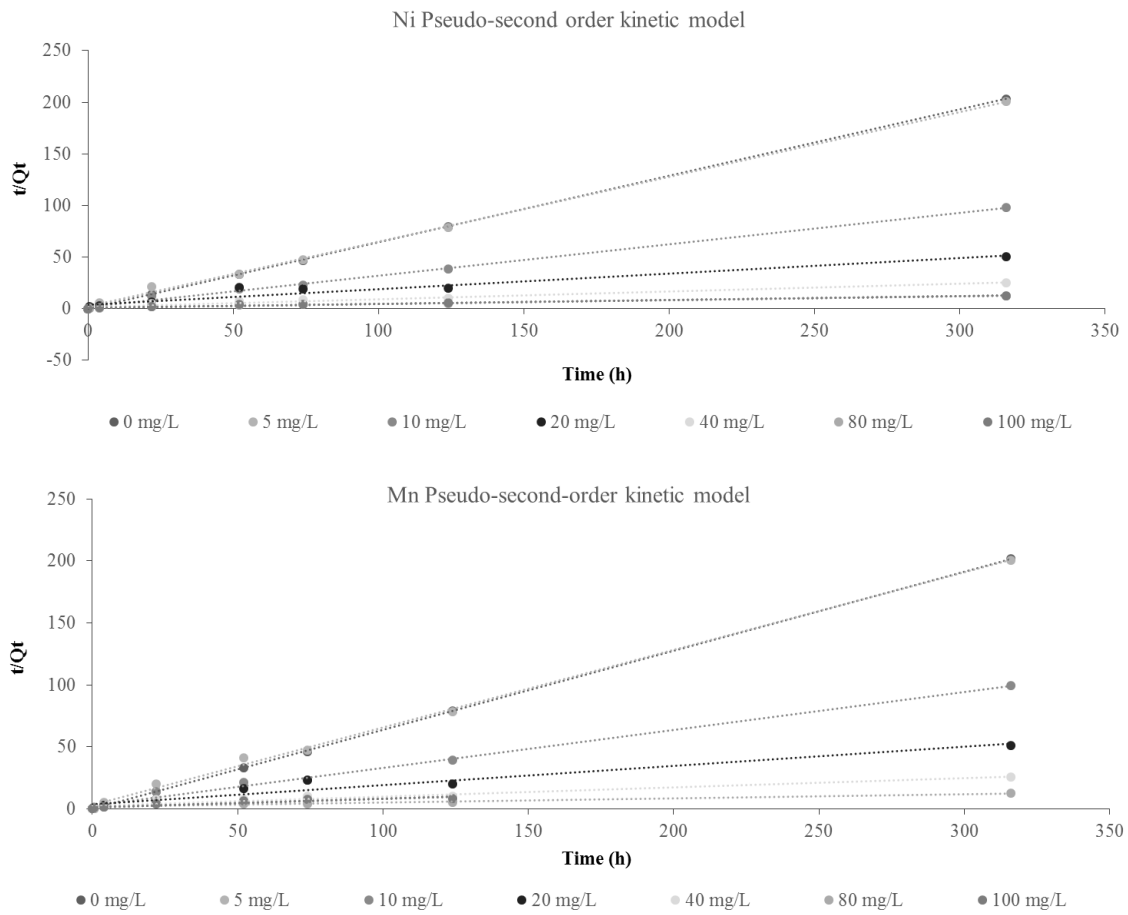

Figure 7.3. Kinetics model for diethylketone (DEK) and aluminium (al), cadmium (Cd), nickel (Ni) and manganese (Mn) for the biosorption experiments conducted at lab-scale with *Streptococcus equisimilis*, when exposed to diethylketone (4 g/L) and Al^{3+}, Cd^{2+}, Ni^{2+} and Mn^{2+} (5 mg/L to 100 mg/L) (cont.).

For diethylketone, the K_2 constant increases with the increase of metal concentration, reaching its maximum value for 40 mg/L. For initial concentrations of metal higher than 40 mg/L, the K_2 constant stars to decrease, suggesting that for the range of metals with an initial concentration between 5 mg/L and 40 mg/L inclusive, the biodegradation and/or sorption rate of diethylketone by *S. equisimilis* increases over time, whereas for higher initial concentration of metal it decreases. This behaviour may be explained by to the saturation of the active sites on the biomass surface, as well as by the development of an inhibitory effect on the cellular growth. For aluminium, the K_2 constant increased with the increase of initial metal concentration, until an initial concentration of 80 mg/L was used, indicating that the biosorption rate increases through time. For initial concentrations higher than 80 mg/L the K_2 constant decreases, revealing that for initial concentrations higher than 80

mg/L, the biosorption rate decreases. For cadmium, the K_2 constant decreases with the increase of metal concentration, until a maximum value of 80 mg/L. These results suggest that for the range of metals with an initial concentration between 5 mg/L and 80 mg/L inclusive, the sorption rate of Cd^{2+} by *S. equisimilis* decreases over time. For nickel and manganese, the K_2 constant decreases with the increase of metal concentration, suggesting that, as the initial concentration of metals increase, the sorption rate of Ni^{2+} and Mn^{2+} by *S. equisimilis* decreases over time. These results can be justified by the saturation of the active sites on the cell surface, by the competition between the different metals and by their bioavailability to the microbial culture.

Table 7.2. Fitting parameters for pseudo-second order kinetic model obtained for diethylketone, Al^{3+}, Cd^{2+}, Ni^{2+} and Mn^{2+} for the lab-scale experiments.

System	Pollutant	Pseudo-second order	
		K_2	R^2
Control	DEK	4.009	0.999
	Al^{3+}	-4.320	0.999
	Cd^{2+}	1.598	1
	Ni^{2+}	-1.390	1
	Mn^{2+}	-1.587	1
***S. equisimilis*, 4 g//L DEK, 5 mg/L Al^{3+}, Cd^{2+}, Ni^{2+}, Mn^{2}**	DEK	1.361	0.999
	Al^{3+}	28.952	1
	Cd^{2+}	0.219	0.999
	Ni^{2+}	0.204	1
	Mn^{2+}	0.138	0.998
***S. equisimilis*, 4 g//L DEK, 10 mg/L Al^{3+}, Cd^{2+}, Ni^{2+}, Mn^{2}**	DEK	1.406	0.999
	Al^{3+}	78.588	1
	Cd^{2+}	0.088	0.999
	Ni^{2+}	0.052	0.999
	Mn^{2+}	0.043	0.994
***S. equisimilis*, 4 g//L DEK, 20 mg/L Al^{3+}, Cd^{2+}, Ni^{2+}, Mn^{2}**	DEK	2.747	0.999
	Al^{3+}	51.637	1
	Cd^{2+}	0.016	0.993
	Ni^{2+}	0.006	0.937
	Mn^{2+}	0.006	0.940

Table 7.2. Fitting parameters for pseudo-second order kinetic model obtained for diethylketone, Al^{3+}, Cd^{2+}, Ni^{2+} and Mn^{2+} for the lab-scale experiments (cont.).

System	Pollutant	Pseudo-second order	
		K_2	R^2
***S. equisimilis*, 4 g//L DEK, 40 mg/L Al^{3+}, Cd^{2+}, Ni^{2+}, Mn^{2}**	DEK	5.215	1
	Al^{3+}	111.813	1
	Cd^{2+}	0.018	0.999
	Ni^{2+}	0.004	0.972
	Mn^{2+}	0.002	0.930
***S. equisimilis*, 4 g//L DEK, 80 mg/L Al^{3+}, Cd^{2+}, Ni^{2+}, Mn^{2}**	DEK	1.110	0.999
	Al^{3+}	190.001	1
	Cd^{2+}	0.003	0.994
	Ni^{2+}	0.002	0.984
	Mn^{2+}	0.001	0.903
S. equisimilis, 4 g//L DEK, 100 mg/L Al^{3+}, Cd^{2+}, Ni^{2+}, Mn^{2}	DEK	0.450	0.999
	Al^{3+}	116.40	1
	Cd^{2+}	0.299	0.748
	Ni^{2+}	0.001	0.976
	Mn^{2+}	0.003	0.840

Viability tests were conducted at the end of the experiments and showed that the metabolic activity of *S. equisimilis* was adversely affected, since the number of colonies obtained were very small and only after several inoculations, the microbial growth presented a similar profile to the one obtained without the addition of diethylketone, Al^{3+}, Cd^{2+}, Ni^{2+} and Mn^{2+} in the culture medium. During all the experiments the pH ranged between 4 and 4.5.

7.3.2| Pilot Scale Experiments – Biosorption Studies in Open Systems

Pilot-scale experiments were conducted in a bioreactor column with a work solution volume of 40 L, with an initial concentration of diethylketone of 7.5 g/L, 100 mg/L of Al^{3+}, Cd^{2+}, Ni^{2+} and Mn^{2+} and 700 g of vermiculite. As previously mentioned, diethylketone was added to the working solution at different moments in order to continuously supply a carbon source to the system and also to infer about its impact on the metal sorption. It was found that for all the pollutants studied, the sorption percentage tends to increase through time and it follows the sorption order: diethylketone > Al^{3+} > $Cd^{2+} \approx Ni^{2+}$ > Mn^{2+} (Table 7.3).

Table 7.3. Biosorption performance of the bioreactor column for diethylketone (7.5 g/L) and for Al^{3+}, Cd^{2+}, Ni^{2+} and Mn^{2+} (100 mg/L).

Time (h)	Biosorption efficiency (%)				
	DEK	**Al^{3+}**	**Cd^{2+}**	**Ni^{2+}**	**Mn^{2+}**
1st period – 528 h	93.04	99.47	16.93	31.75	26.68
2nd period – 1992 h	100	98.85	36.88	44.43	47.81
3rd period – 2928 h	100	99.85	41.75	49.03	52.03

The results obtained for Al^{3+} can be justified by the small ionic radius (0.50 Å) that facilitates its sorption by the cell surface and its penetration into the intracellular space. The results obtained for Cd^{2+} and Ni^{2+} are very similar, which is unexpected since Ni^{2+} has a smaller ionic radius (0.78 Å) and a higher electronegativity (1.91 Pauling) than Cd (0.97 Å, 1.69 Pauling). These results may be explained by their bioavailability and structural similarity that can trigger the substitution of Ni^{2+} uptake by Cd^{2+} by the cell enzymes. The reduced sorption obtained for Mn^{2+} may be due to the ionic radius of Mn^{2+} (0.80Å) combined with its reduced electronegativity (1.55 Pauling), considering the small porosity of vermiculite. It was also observed that the complete sorption and /or biodegradation of diethylketone (that act as the carbon source), was reached and that after each addition of diethylketone to the system, the sorption of each metal gradually increased (Figure 7.4). This behaviour may be explained by a state of carbon depletion, which after being overcome, led to a

positive stimulus not only for the development of the biofilm but also for the decontamination of the mixed solution. The time required to achieve sorption and /or biodegradation percentages of diethylketone equal or higher than 95 % was higher than in the lab scale experiments (168 h, 192 h and 408 h). This can be justified by the increase of the acclimation period, by the open system operation with continuous feeding, and by the formation of nonspecific metallic complex compounds within the cell, that increase their toxic and inhibitory effects, thus affecting the overall bacterial metabolism. During the pilot scale experiments the pH ranged between 4 and 5.

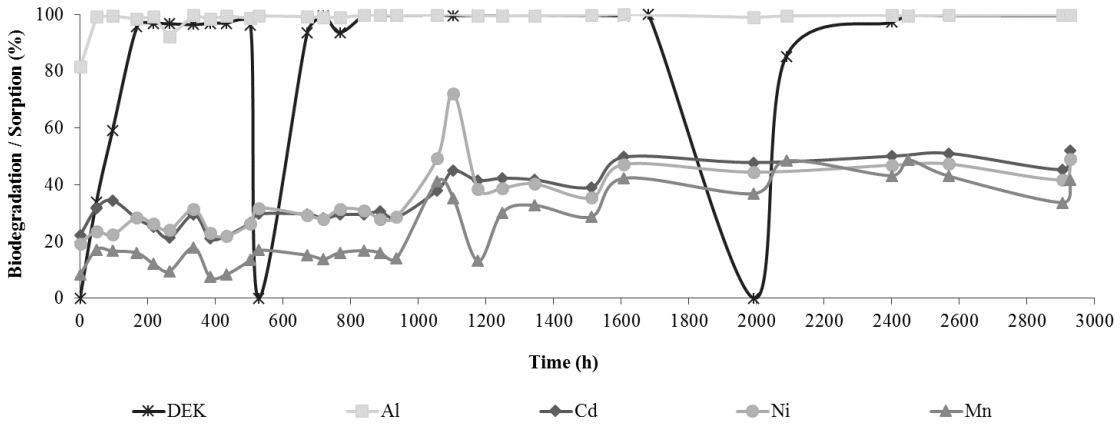

Figure 7.4. Biodegradation and sorption performance (%) of *Streptococcus equisimilis* biofilm supported on vermiculite for diethylketone (7.5 g/L) when exposed to initial concentrations of 100 mg/L of Al^{3+}, Cd^{2+}, Ni^{2+} and Mn^{2+}.

Viability tests were conducted at the end of the experiments and revealed that the *S. equisimilis* biofilm presented a normal biological activity after the first inoculation. *S. equisimilis* in the form of biofilm seems to be more resistant to the toxic effects of high concentrations of Al^{3+}, Cd^{2+}, Ni^{2+} and Mn^{2+}, when compared to the bacteria in suspension (Lab scale experiments – biosorption in batch systems section). These results are in agreement with the literature, since the biofilm community offers several benefits such as easy access to substrate (Comte et al. 2006), protection against hazardous compounds due to the polymeric matrix that compose the biofilm and that acts as a diffusion barrier, increasing the resistance of the cells against toxic substances and/or environmental conditions (Covelo et al. 2007).

7.3.2.1| Breakthrough Curves Modelling

Breakthrough curves are essential for industrial application of biosorption and/or biodegradation process since they provide essential information regarding the behaviour of a column sorption process in the treatment of solutions of hazardous pollutants. The breakthrough point is defined as the pre-established saturation concentration accepted for the outflow of the system. Three breakthrough modelling equations have been tested in the present study: Adams-Bohart, Wolborska and Yoon and Nelson models. The Adam–Bohart and Wolborska models were applied to the experimental results in order to obtain a description of the initial part of the breakthrough curve. This approach was focused on the estimation of characteristic parameters such as the kinetic constant (k_{AB}) and the maximum absorption capacity (N_0) of the Adam–Bohart model and the kinetic coefficient of the external mass transfer (β_a) of the Wolborska model. The values of N_0, k_{AB} and β_a were calculated from the ln (C/C_0) versus t plot. In short fixed-bed column systems or in fixed-bed column systems with high flow rates, the axial diffusion is negligible, therefore if $k_{AB} \approx \beta_a / N_0$ and the Wolborska model approaches the Adams-Bohart model. The Yoon and Nelson model was used to investigate the breakthrough behaviour of the pollutants with the *S. equisimilis* biofilm in a column bioreactor. The value of k_{YN} and τ were determined from the ln [($C/(C_0-C)$] versus t plot. All the calculated breakthrough parameters are presented in Table 7.4. and the predicted and experimental breakthrough curves are shown in Figure 7.5.

Table 7.4. Breakthrough curves parameters obtained for the pilot-scale experiments.

Metal	Adams-Bohart			Wolborska		Yoon and Nelson		
	k_{AB} (L/ mg h)	N_0 (mg/L)	R^2	β_a (h^{-1})	R^2	k_{YN} (h^{-1})	τ (h)	R^2
Cd^{2+}	2.21e-5	-352194	0.895	-6.17e-5	0.889	-6.20e-4	2102	0.866
Ni^{2+}	1.04e-5	57671	0.902	-1.51e-3	0.891	-1.05e-3	2177	0.892
Mn^{2+}	1.58e-5	-236951	0.868	3.63e-3	0.884	-4.83-4	2547	0.866

The results obtained for diethylketone and for Al^{3+} are not properly described by any of the models employed (R^2 < 0.750, data not shown). For Cd^{2+} the experimental results are best described by the Adams-Bohart and Wolborska models (R^2 > 0.889), whereas for Ni^{2+} the data is best described by the Yoon and Nelson model (R^2 > 0.870). For the Yoon and Nelson model, the predicted τ values for the metals (Table 7.4) were found to be very similar to the experimental values (2400 h for Cd, 2568 h for Ni^{2+} and 2088 h for Mn^{2+}). For Mn^{2+} the results are best fitted by the Wolborska model (R^2 > 0.867).

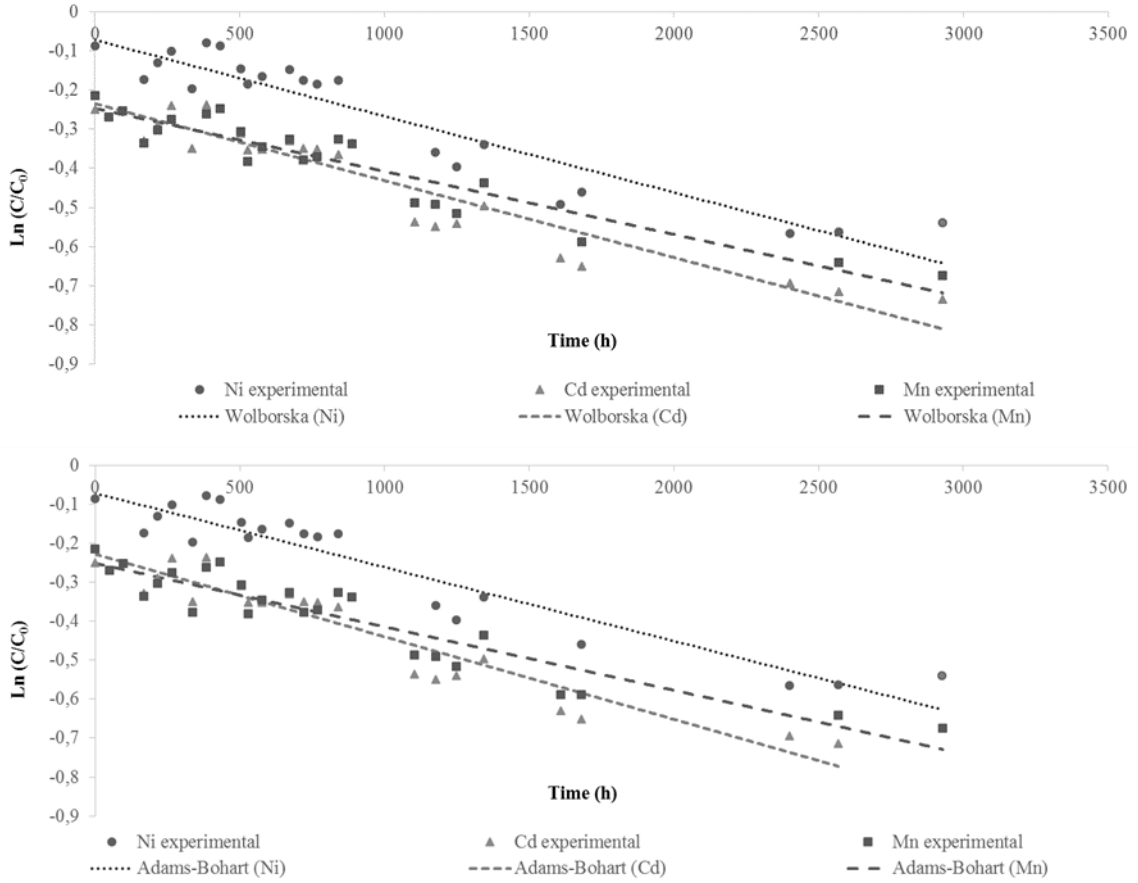

Figure 7.5. Predicted and experimental breakthrough curves for cadmium, manganese and nickel at pilot-scale.

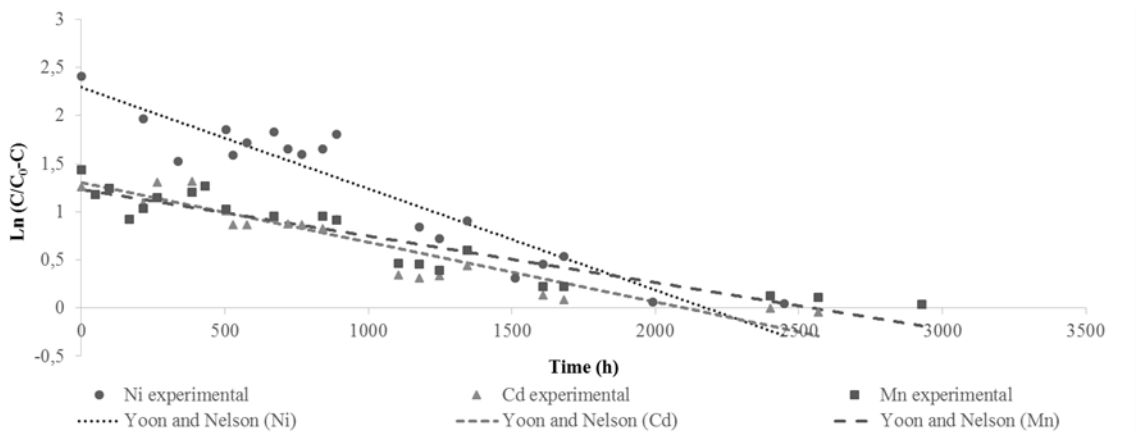

Figure 7.5. Predicted and experimental breakthrough curves for cadmium, manganese and nickel at pilot-scale (cont.).

7.3.3| FTIR, XRD and SEM Analyses

FTIR spectra of unloaded and loaded vermiculite with diethylketone, and of *S. equisimilis* biomass in suspension and supported, eventually loaded with diethylketone and Al^{3+}, Cd^{2+}, Ni^{2+} and Mn^{2+}, in the range of 500 cm^{-1} to 4000 cm^{-1} were taken to confirm the presence of functional groups that are commonly responsible for the sorption processes and are presented in Figure 7.6.a. It is possible to observe that vermiculite exhibits a number of sorption peaks, reflecting the complex nature of the clays. For the unloaded vermiculite, the band at 1000 cm^{-1} represents the Si–O–Si stretching, whereas the band at 1635 cm^{-1} is for H–O–H in absorbed water bending (Covelo et al. 2007) and the band at 3400 cm^{-1} represents the OH functional group stretching vibration. Some of these band signals were also detected by several other authors (Omoike and Chorover 2004) on clays and were found to correspond to surface functional groups responsible for the sorption of toxic substances Do˘ gan et al. 2008). These groups may interact with the different type of pollutants used in the present study. Samples of vermiculite exposed to diethylketone and samples of *S. equisimilis* biofilm supported into vermiculite and exposed to 7.5 g/L of diethylketone and 100 mg/L of Al^{3+}, Cd^{2+}, Ni^{2+} and Mn^{2+} reveal several changes on the intensity and /or on the shape of the peaks and the disappearance/formation of new peaks. After interaction with diethylketone, bands at 1400 cm^{-1} and at 2400 cm^{-1} corresponding respectively to C-H bending (-CH_3) and to C≡C and/or C≡N stretching, suffer significant changes, namely the first band, which disappeared and the second one presented higher intensity and different shape. For the bands detected at 675 cm^{-1}, 1000 cm^{-1}, 1650 cm^{-1}, and 3500 cm^{-1} and corresponding respectively to C-OH stretching vibrations, Si–O–Si stretching, C═O

stretching groups and to the hydroxyl functional group stretching vibration (-OH), the intensity was found to decrease significantly. These changes may be due to the interaction and involvement of the functional groups present in the vermiculite surface with the functional groups of diethylketone, allowing its sorption by the clay. The samples of *S. equisimilis* biofilm supported into vermiculite and exposed to diethylketone and to the four metals reveal the disappearing of the bands at 2300 cm^{-1} and at 3500 cm^{-1}.

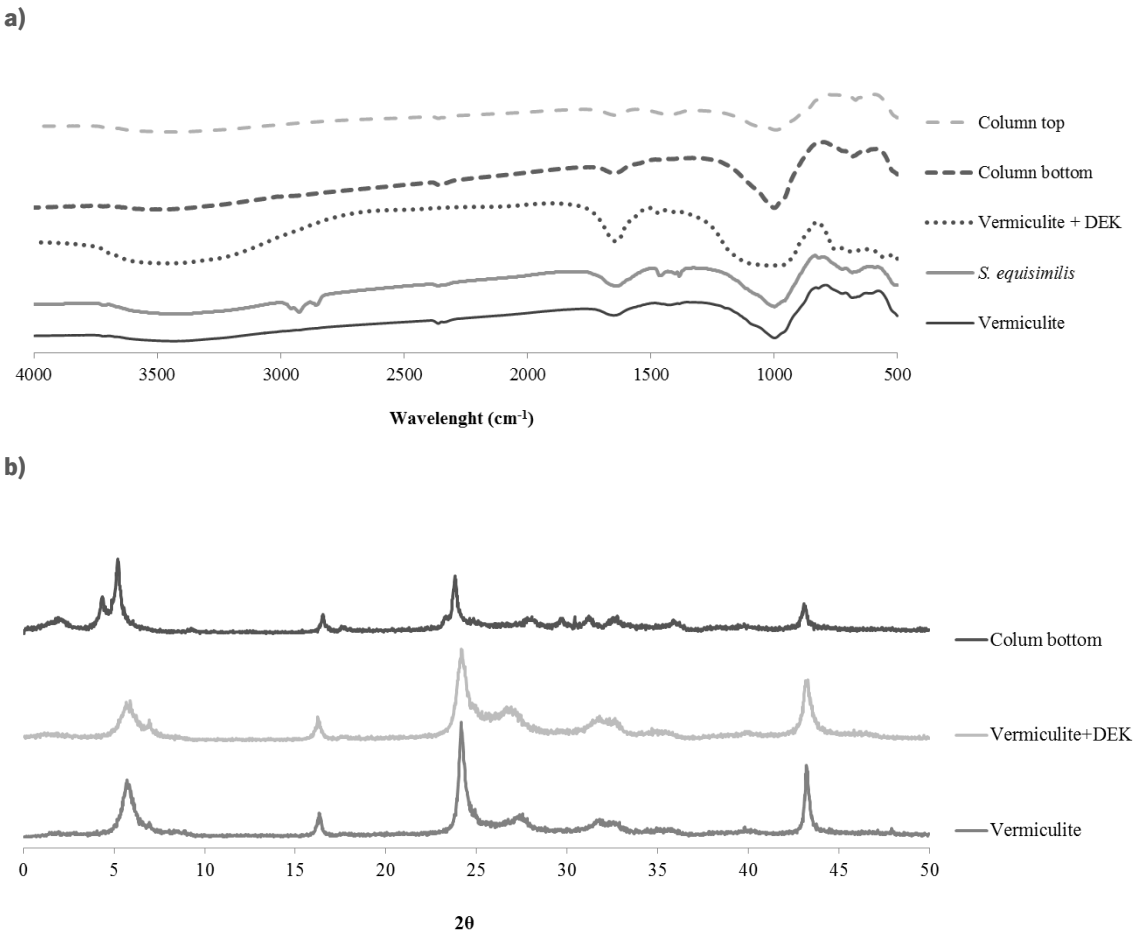

Figure 7.6. a) FTIR spectra of different samples: vermiculite unloaded, *S. equisimilis* biomass, vermiculite loaded with diethylketone and *S. equisimilis* biofilm supported on vermiculite, loaded with diethylketone (7.5 g/L) and 100 mg/L of Al^{3+}, Cd^{2+}, Ni^{2+} and Mn^{2+} (at the bottom and at the top of the bioreactor); **b)** XRD patterns of original and recovered vermiculite, **c)** SEM images of *S. equisimilis* supported on vermiculite (700 g) and exposed to diethylketone (7.5 g/L) and 100 mg/L of Al^{3+}, Cd^{2+}, Ni^{2+} and Mn^{2+} with an amplification of 1000x **c.1)** at the middle of the bioreactor and **c.2)** at the bottom of the bioreactor. The white incrustations (black arrows) correspond to the binding of metal ions on the surface of biomass and are an evidence of the biosorption of metal by the biofilm.

c.1) **c.2)**

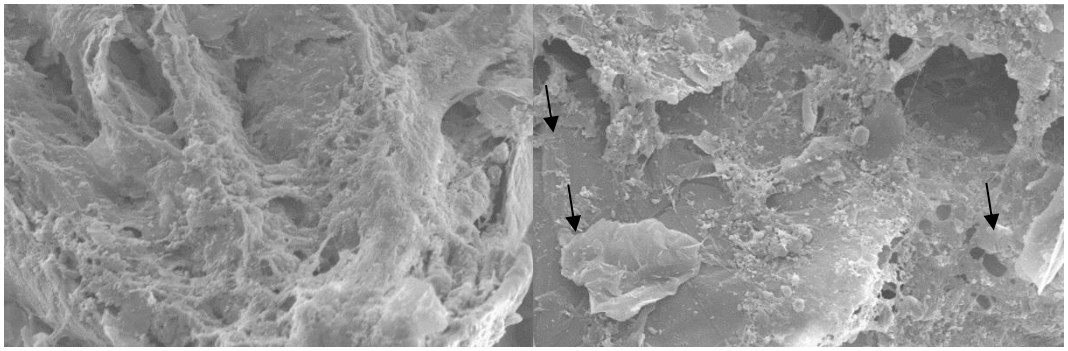

Figure 7.6. a) FTIR spectra of different samples: vermiculite unloaded, *S. equisimilis* biomass, vermiculite loaded with diethylketone and *S. equisimilis* biofilm supported on vermiculite, loaded with diethylketone (7.5 g/L) and 100 mg/L of Al^{3+}, Cd^{2+}, Ni^{2+} and Mn^{2+} (at the bottom and at the top of the bioreactor); **b)** XRD patterns of original and recovered vermiculite, **c)** SEM images of *S. equisimilis* supported on vermiculite (700 g) and exposed to diethylketone (7.5 g/L) and 100 mg/L of Al^{3+}, Cd^{2+}, Ni^{2+} and Mn^{2+} with an amplification of 1000x **c.1)** at the middle of the bioreactor and **c.2)** at the bottom of the bioreactor. The white incrustations (black arrows) correspond to the binding of metal ions on the surface of biomass and are an evidence of the biosorption of metal by the biofilm (cont.).

For the sample collected at the top of the bioreactor column, the intensity of all peaks are significantly lower when compared to the peaks obtained only with vermiculite, whereas for the samples collected at the bottom of the bioreactor column they presented peaks with higher intensity and with different shapes. These results may support the idea that the biomass present at the bottom of the column is exposed to higher concentrations of metals and diethylketone, whereas the biomass present at the top of the column is exposed to a lower concentration of these pollutants and therefore reduced toxicity, as the upwards circulation in the bioreactor leads to a higher sorption by the settled vermiculite and/or vermiculite biomass. These changes may be explained by the interaction of the functional groups of the different pollutants present in the solution. According to Volesky (2007) the main functional groups responsible for sorption processes are the phosphodiester, phosphonate, sulfonate, imidazole, hydroxyl, amide, carboxyl and carbonyl groups. Some of these functional groups (phosphate bands at 1237 cm^{-1} and carbohydrate bands at 1070 cm^{-1} next to hydrocarbon sorption bands in the wavelength region between 3000 cm^{-1} and 2800 cm^{-1}) (Van der Mei et al. 1996) are known to be present on the Streptococcus sp. surface and to be responsible for the biosorption and biodegradation of toxic compounds such as diethylketone (Costa et al. 2014).

The powder XRD diffraction patterns of different samples (unloaded and loaded vermiculite with diethylketone, and *S. equisimilis* biomass in suspension and supported, eventually loaded with diethylketone and Al^{3+}, Cd^{2+}, Ni^{2+} and Mn^{2+}) were recorded at 2θ range between 5 and 60°C and some representative patterns are presented in Figure 7.6.b. The sample of vermiculite (unloaded) and the sample of vermiculite loaded with diethylketone exhibited the typical pattern of clays, with no obvious change in the position of the diffraction lines for clays after contact with diethylketone and with *S. equisimilis* biomass, diethylketone and Al^{3+}, Cd^{2+}, Ni^{2+} and Mn^{2}, although some loss of the diffraction peaks are observed. This similarity between the diffractograms indicates a comparative crystallinity of vermiculite after the loading with diethylketone and that this process does not promote any significant structural modification in the clays. Nonetheless, the samples of vermiculite loaded with the *S. equisimilis* biomass, diethylketone and the four heavy metals present several changes not only on the position of the diffraction lines but also in their intensity. These changes are an evidence of the extensive damage on the vermiculite structure and were observable at SEM.

At the end of the experiment, the biofilm was analysed by SEM and it was possible to confirm the presence of a well-developed biofilm (Figure 7.6.c) and a more glazed, polished surface, with broken and worn leaves of vermiculite. Several white incrustations are observable on the surface (black arrows). According to Sharma et al. (2008) these incrustations represent the binding of metal ions on the surface of biomass and are an evidence of the biosorption of metal by the biofilm. Similar evidences were found in previous works conducted by Quintelas et al. (2011). These results corroborate the sorption of metals and biodegradation/sorption of diethylketone by the joint-system used in this work.

7.4| CONCLUSION

It was demonstrated that *S. equisimilis* is able to efficiently biodegrade high concentrations of diethylketone in the presence of heavy metals (Al^{3+} > Cd^{2+} > Ni^{2+} > Mn^{2+}). At pilot scale it was found that the biodegradation of diethylketone was complete and that the metal uptake, with the exception of Al^{3+}increase through time and with the renewing of the contaminated solutions. FTIR, SEM and XRD analyses allow to confirm the sorption of metals and diethylketone by the biomass and/or vermiculite surface. These results prove the excellent capacity of this system to simultaneously treat solutions containing ketone and heavy metals.

REFERENCES

Ahmed S., Chughtai S., Keane M.A. 1998. The removal of cadmium and lead from aqueous solution by ion exchange with Na-Y zeolites. Separation and Purification Technology 13: 57-64.

ATSDR. 1992. Toxicological profile for aluminium. Atlanta, GA, US Department of Health and Human Services, Public Health Service, Agency for Toxic Substances and Disease Registry.

ATSDR. 2000. Toxicological profile for manganese. Atlanta, GA, US Department of Health and Human Services, Public Health Service, Agency for Toxic Substances and Disease Registry.

Awwad A.M., Salem N.M. 2014. Kinetics and thermodynamics of Cd(II) biosorption onto loquat (*Eribotrya japonica*) leaves. Journal of Saudi Chemical Society 18: 486-493.

Azeez L., Adeoye M.D., Lawal A.T., Idris Z.A., Majolagbe T.A., Agbaogun B.K.O., Olaogur M.A. 2013. Assessment of volatile organic compounds and heavy metals concentrations in some Nigerian-made cosmetics. Analytical Chemistry Indian Journal 12: 443-483.

Bennett, B.G. 1984. Environmental nickel pathways in man In: Nickel in the human environment. Proceedings of a joint symposium. IARC scientific publication no. 53. Lyon, France: International Agency for Research on Cancer, pp. 487-495.

Bohart G.S., Adams E.Q. 1920. Some aspects of the behaviour of charcoal with respect to chlorine. Journal of the American Chemical Society 42: 523-529.

Bondy S.C. 2016. Low levels of aluminum can lead to behavioral and morphological changes associated with Alzheimer's disease and age-related neurodegeneration. Neurotoxicology 52: 222-229.

Comte S., Guibaud G., Baudu M. 2006. Biosorption properties of extracellular polymeric substances (EPS) resulting from activated sludge according to their type: soluble or bound. Process Biochemistry 41: 815-823.

Costa F., Neto M., Nicolau A., Tavares T. 2015. Biodegradation of Diethylketone by *Penicillium* sp. and *Alternaria* sp. – A Comparative Study. Current of Biochemical Engineering 2: 81-89.

Costa F., Quintelas C., Tavares T. 2012. Kinetics of biodegradation of diethylketone by *Arthrobacter viscosus*. Biodegradation 23: 81-92.

Costa F., Quintelas C., Tavares T. 2014. An approach to the metabolic degradation of diethylketone (DEK) by *Streptococcus equisimilis*: Effect of DEK on the growth, biodegradation kinetics and efficiency. Ecological Engineering 70: 183-188.

Covelo E.F., Veja F.A., Andrade M.L. 2007. Competitive sorption and desorption of heavy metals by individual soil components. Journal of Hazardous Materials 140: 308-315.

Dilek F.B., Gokcay C.F., Yetis U. 1998. Combined effects of Ni(II) and Cr(VI) on activated sludge. Water Research 2: 303-312.

Do˘gan M., Turhan Y., Alkan M, Namli H., Turan P., Demirbas Ö. 2008. Functionalized sepiolite for heavy metal ions adsorption. Desalination 230: 248–268.

Dobson R.S., Burgess J.E. 2007. Biological treatment of precious metal refinery wastewater: A review. Minerals Engineering 20: 519-532.

Gonzalez-Gil G., Kleerebezem R., Lettinga G. 1999. Effects of nickel and cobalt on kinetics of metanol conversion by methanogenic slugde as assessed by on-line CH_4 monitoring. Applied and Environmental Microbiology 65: 1789-1793.

Ibrahim W.M., Mutawie H.H. 2013. Bioremoval of heavy metals from industrial effluent by fixed-bed column of red macroalgae. Toxicology and Industrial Health 29: 38-42.

Ji G., Silver S. 1995. Bacterial resistance mechanisms for heavy metals of environmental concern. Journal of Industrial Microbiology 14:61–75.

Kishore G., Sree P., Krishna D. 2013. Industrial wastes as adsorbents for the removal of chromium from waste water: A review. International Journal of Chemical Sciences 11: 1371-1384.

Lam K-Y., Davidson F.F., Hanson R.K. 2012. High-Temperature Measurements of the Reactions of OH with a Series of Ketones: Acetone, 2-Butanone, 3-Pentanone, and 2-Pentanone. The Journal of Physical Chemistry A 116: 5549-5559.

Nies D.H. 1999. Microbial heavy metal resistance. Applied and Environmental Microbiology. 51: 730–750.

Ogbodu R.O., Omorogie M.O., Unuabonah E., Babalola J.O. 2015. Biosorption of heavy metals from aqueous solutions by *Parkia biglobosa* biomass: Equilibrium, kinetics, and thermodynamic studies. Environmental Progress & Sustainable Energy 34: 1694-1704.

Olaniran A.O., Balgobind A., Pillay B. 2013. Bioavailability of Heavy Metals in Soil: Impact on Microbial Biodegradation of Organic Compounds and Possible Improvement Strategies International Journal of Molecular Sciences 14: 10197-10228.

Omoike A., Chorover J. 2004. Spectroscopy study of extracellular polymeric substances from *Bacillus subtillis*: aqueous chemistry and adsorption effects. Biomacromolecules 5: 1219-1230.

Quintelas C., Costa F., Tavares T. 2012. Bioremoval of diethylketone by the synergistic combination of microorganisms and clays: Uptake, removal and kinetic studies. Environmental Science Pollution Research 20: 1374-1383.

Quintelas C., Figueiredo H., Tavares T. 2011. The effect of clay treatment on remediation of diethylketone contaminated wastewater: Uptake, equilibrium and kinetics studies. Journal of Hazardous Materials 186: 1241-1248.

Sharma M., Kaushik A., Somvir B.K., Kamra A. 2008. Sequestration of chromium by exopolysaccharides of Nostoc and Gloeocapsa from dilute aqueous solutions. Journal of Hazardous Materials 157: 315–318.

Suazo-Madrid A., Morales-Barrera L., Aranda-Garcia E., Cristiani-Urbina E. 2011. Nickel (II) biosorption by *Rhodotorula glutinis*. Journal of Industrial Microbiology & Biotechnology 38: 51-64.

Tam N.F.Y., Wong Y.S., Wong M.H. 1989. Effects of acidity on acute toxicity of aluminium-waste and aluminium-contaminated soil. Hydrobiology 188/189: 385-395.

Van der Mei H.C., Naumann D., Busscher H.J. 1996. Grouping of *Streptococcus mitis* strains grown on different growth media by FT-IR. Infrared Physics & Technology 37: 561–564.

Volesky B. 2007. Biosorption and me. Water Research 41: 4017-1029.

Wolborska A. 1989. Adsorption on activated carbon of *p*-nitrophenol from aqueous solution. Water Research 23: 85–91.

Wolborska A., Pustelnik P. 1996. A simplified method for determination of the break-through time of an adsorbent layer. Water Research 30: 2643–2650.

Yoon Y.H., Nelson J.H. 1984. Application of gas adsorption kinetics II. A theoretical model for respirator cartridge service life. American Industrial Hygiene Association Journal 45: 509-516.

CHAPTER 8

Concluding Remarks and Future Perspectives

In this final chapter, a general overview of the work performed during the execution of this doctoral thesis and the most pertinent conclusions are presented. Some perspectives on the future work on biodegradation of organic compounds are proposed.

8.1| CONCLUDING REMARKS

The contamination of water systems is a serious problem that has received special attention over the past decades. In order to prevent and minimize the hazardous impacts caused by the increasing environmental pollution, several efforts have been made to develop alternative eco-friendly and low-cost technologies for the removal of volatile organic compounds and metals from water bodies. Within these technologies, biodegradation by bacterial and/or fungal biomass, as well sorption performed by the mineral clays, appear to present several advantageous solutions in comparison to the traditional techniques. These advantages are especially important for small industrial units, since they operate on tight economic resources, far from centers of technological innovation where the decontamination processes are established.

In this research work, several biological systems that have the ultimate purpose of achieving an efficient biodegradation of high volume of diethylketone solutions, with or without the presence of metals, have been proposed. For the experiments conducted only with microorganisms and diethylketone, it was demonstrated that both fungi (*Penicillium* sp. and *Alternaria* sp.) present similar biodegradation performances, being however, the biodegradation performed by *Penicillium* sp. faster than the one promoted by *Alternaria* sp. When comparing these results with published data, it is possible to observe that, for the same operational conditions, the bacterium *Streptococcus equisimilis* is capable to biodegrade relevant concentrations of diethylketone in shorter periods of time (< 60 hours) without having its growth inhibited, making this bacteria also a suitable and promising microorganism to be used in the biodegradation of diethylketone.

Since real effluents are composed by several types of pollutants such as volatile organic compounds, dyes, metals, aromatic and aliphatic compounds, it is of extreme importance to study not only the microorganism removal ability when exposed to complex solutions, but also to study the interactions between the different pollutants and to determine how the removal process of these pollutants is affected by the presence of the remaining. In this regard several sets of experiments were performed at laboratory scale and in batch mode, exposing either *Penicillium* sp., *Alternaria* sp. and *Streptococcus equisimilis* to singular (nickel or cadmium) and complex solutions (nickel, cadmium and diethylketone). In these experiments, it was possible to conclude that the growth of both fungi is enhanced by the presence of nickel and inhibited by the presence of cadmium concentrations higher than 40 mg/L, whereas *S. equisimilis* growth is strongly inhibited by the presence of both metals.

Within the microorganisms tested, *S. equisimilis* was found to present the best results in terms of removal efficiency and uptake, thus being the microorganism selected for future experiments.

In parallel with the experiments mentioned above, assays aiming to determine the efficiency and performance of a system composed by *S. equisimilis* supported on different clays (vermiculite, bentonite, kaolinite and sepiolite) to remove diethylketone from aqueous solutions, as well as to evaluate the interactions between the bacterial culture and the clays, were conducted at laboratory scale and in batch mode. The results achieved reveal that although all the combined systems are able to efficiently remove diethylketone (> 98 %) from aqueous solutions, the system combining *S. equisimilis* with vermiculite presented better results in terms of time required to achieve the same removal efficiency. The results obtained also allowed to propose a removal mechanism for diethylketone and its metabolites.

After selecting the microorganism and clay with the best performance and characteristics to treat water contaminated with high concentrations of diethylketone, several sets of experiments conducted at laboratory scale and in batch mode were performed, exposing different masses of vermiculite to singular and binary solutions containing either diethylketone, nickel and cadmium and exposing a *S. equisimilis* biofilm supported on different masses of vermiculite to binary solutions containing diethylketone and nickel or diethylketone and cadmium. These experiments allowed to infer that when vermiculite is used as the only sorbent it is able to efficiently sorb nickel and cadmium, whereas when nickel and diethylketone are mixed together the sorption of these two pollutants increase significantly, revealing a synergetic interaction, as opposite to what occurs when diethylketone and cadmium are mixed. The use of *S. equisimilis* biofilm was found as expected, to be advantageous since it increases diethylketone, nickel and cadmium removal efficiency, which may be explained by the combined occurrence of two distinct cellular processes: one dependent on cellular metabolism (biodegradation and intracellular accumulation) and the other independent of it (sorption by the biofilm, eventually also by the vermiculite surface).

As previously mentioned, the main purpose of this thesis is the development and subsequent application of a biological system able to decontaminate high volumes of water solutions. In this regard, the system previously developed at laboratory scale and in batch mode, was up-scaled to a pilot bioreactor column, with a total volume of 22.7 L which operated in continuous mode. In a first stage experiments a *S. equisimilis* biofilm supported on vermiculite was exposed to high

concentrations of binary solutions (diethylketone and nickel and diethylketone and cadmium), whereas in a second stage, with the purpose of increasing the complexity of the contaminated solution and thus mimic the composition of real effluents, a *S. equisimilis* biofilm supported on vermiculite was exposed to quinary concentrated solutions (diethylketone, aluminium, nickel, cadmium and manganese). The first set of pilot-scale experiments proved the excellent capacity of this joint system to simultaneously biodegrade diethylketone and to biosorb nickel and cadmium. Nickel and cadmium removal efficiency and uptake increase through time, even with the successive replacement of the initial solution by new ones. The second set of pilot-scale experiments prove once again the ability of this joint system not only to biodegrade continuously and completely high concentrations of diethylketone in the presence of high concentrations of aluminium, nickel, cadmium and manganese, but also to achieve, with the exception of aluminium, high uptake values that increases through time and with the renewing of diethylketone, aluminium, nickel, cadmium and manganese solutions.

It is, therefore, possible to conclude the development and subsequent application of a cost-reduced, easy maintenance and eco-friendly system able to continuously and efficiently remove high volumes of organic solvents present in complex aqueous solutions.

8.2| FUTURE PERSPECTIVES

With a theme as broad and diverse as the proposed in this thesis, there are several areas where new approaches can be developed. Several stimulating and interesting lines of research concerning the simultaneous removal of diethylketone (or other volatile organic compounds) in the presence of other chemical contaminants, such as metals should be pursued. One such line would be to investigate the ability of the system develop and described herein to treat, real effluents initially at pilot scale and secondly at industrial scale in facilities where this treatment methodology might be implemented. It would also be interesting to investigate the performance of other microbial cultures, such as yeasts and algae and other materials, such as wood waste, leaves and food waste to act as support and sorbents, to decontaminate solutions containing diethylketone, aluminium, nickel, cadmium and manganese or solutions with similar composition. It would also be interesting to evaluate the ability of these systems to be reused as well as their life cycle. Another line of research could be to study the ability of a native and mixed microbial culture present on terrestrial and aquatic matrices to treat

aqueous solutions containing similar composition as the ones used herein and to research the genetic manipulations that could enhance the biofilm properties to optimize its application on such treatment stations.